The molecular basis of thiol odorant sensitivity in the mammalian olfactory system

Thesis submitted in accordance with the requirements of the University of Liverpool for the degree of Doctor in Philosophy by Rachel Helen Spice

May 2004

ABSTRACT

This thesis is an investigation into the potential mechanisms that could explain the olfactory sensitivity to thiol compounds thought to be conserved across mammalian species. Proteomics techniques were employed as unbiased tools to search for highly conserved proteins in olfactory cilia theoretically capable of strong interactions with thiol odorants. Comparisons of the protein profiles and directed protein labelling studies of olfactory cilia from three mammalian species - the house mouse (*Mus musculus*), the rat (*Rattus norvegicus*) and the sheep (*Ovis aries*) - and respiratory cilia preparations from the rat enabled the identification of cytoskeletal proteins and olfactory receptors as potential targets for sulphydryl-mediated thiol odorant interactions. It is therefore predicted that olfactory detection of thiol odorants utilises a traditional olfactory receptor conserved across mammalian species, the observed thiol sensitivity potentially a by-product of a strong interaction between odorant and receptor.

This study also represents the first broad ranging study of the protein complement of mammalian olfactory cilia derived from the three model species. The characterisation of olfactory and respiratory cilia proteomes from multiple mammalian species has highlighted a novel family of putative pheromone binding proteins uniquely associated with mouse olfactory cilia preparations. It has also provided further evidence for the ongoing investigations of the functions of odorant-binding proteins and annexins.

ACKNOWLEDGEMENTS

I would like to take this opportunity to thank my supervisor Professor Rob Beynon for all his help and guidance, Dr. Krishna Persaud, who acted as advisor on all things of an olfactory nature and most especially Dr. Ernest Polak, without whose interest and enthusiasm this project would never have happened. I would also like to thank all of the Protein Function Group at Liverpool for their invaluable practical advice and my fond memories of my time working with them. Finally I would like to gratefully acknowledge all the assistance given to me by the technical staff at the Department of Veterinary Preclinical Science, in particular Marion Pope and Fay Cullingham.

On a less academic note I would like to thank my wonderful family for their constant love, support and embarrassing Christmas games and my boyfriend Nick, for keeping me sane during the preparation of this thesis. Final thanks go to Thierry Henry for making life as an Arsenal fan that much more enjoyable.

This work is dedicated to Grandma and Gramps who never got to see my thesis-

I miss you and I hope you're proud.

TABLE OF CONTENTS

LIST OF FIGURES

Page numbers provided refer to the immediately preceding page of text.

Chapter 1: Introduction

Chapter 2: Materials and Methods

Chapter 3: The adaptation of the olfactory cilia proteome

Chapter 4: The role of exposed cysteine residues in olfactory cilia

Chapter 5: Metalloprotein hypothesis of olfactory receptor function

Appendix

References

Chapter 1

INTRODUCTION

1.1 Chemoreception – the universal sense

Chemoreception is the most ancient of senses. It is found in various guises throughout the animal kingdom, from unicellular organisms to humans. Chemoreception informs organisms of the chemical nature of their environment, providing sensory data on the relative abundance of food, toxins and the location of potential mates. It also provides the basis for chemical communication between organisms. From the simple methyl-accepting chemotaxis proteins (MCPs) governing directional movement in *E. coli* to the complex processing of the mammalian dual olfactory systems, chemoreception is the data-mining mystery of the sensory world.

The broadest definition of chemoreception encompasses all molecular interactions involved in chemical signalling between proteins, tissues and organisms including the detection of circulating hormones by a single cell of a multicellular organism and at the molecular level, the binding of a compound to a receptor. In this thesis, chemoreception is defined as the sensory process by which an organism gains information about its external chemical environment.

In mammals there are two sensory modalities dedicated to chemoreception: gustation and olfaction, more commonly known as taste and smell respectively. The two processes are surprisingly difficult to define. Both involve interactions between molecules and sensory receptors that provide information on the chemical environment and in both, the molecular events of reception occur in an aqueous environment. The stimulatory molecules for olfaction in terrestrial organisms are volatile as opposed to the water-borne stimulants of taste receptors. However fish

have a dedicated olfactory system so this brings us no closer to a firm definition. Anatomical classification, whilst usefully defining olfaction in higher organisms, does not apply to invertebrates. Olfaction is generally the more sensitive chemoreceptive system due to its ability to detect chemicals released a greater distance from its receptors. Both Bargmann *et al.* (1993) and Eisthen (2002) used the property of detection of molecules originating from a distant source to define olfaction and the same definition will be used in this thesis.

1.2 Olfaction in higher organisms

Although there is little recognisable similarity between olfaction and the basic chemoreception process observed in unicellular organisms, the principle remains the same. An external chemical stimulus interacts with a receptor providing an organism with information about its surroundings to which it can respond appropriately. In bacteria, chemoreceptors influence tumbling frequency to steer the cell towards an attractant or away from a repellant (van Houten, 2000). In higher organisms, stimulation of the olfactory receptors of olfactory sensory neurons generates electrical signals to be transmitted to the brain for interpretation and the generation of an appropriate response.

More primitive animals rely to a greater extent on having this direct source of information and so are likely to have a larger proportion of their brain devoted to the processing of olfactory information. Ancient dependance on our sense of smell may also explain why unlike other sensory modalities, olfactory information can pass directly to regions of the cortex without being relayed through the thalamus (Carpenter, 1996). Olfaction is a sense designed to yield immediate results, vital if the odour is for example, associated with a predator.

In mammals, the molecular events of olfaction occur at the membrane of the olfactory cilia, which protrude from the dendritic terminal of olfactory receptor neurons (ORNs). The ORNs from which the cilia project, are part of the olfactory epithelium, a membranous lining of structures in the nasal cavity called the nasal turbinates. The cellular and subcellular locations of olfaction will be discussed first, before addressing the molecular events at the very start of the olfactory process.

1.3 Olfactory Cilia

The olfactory cilia are the subcellular location for the odorant-binding events in olfaction. Cilia were first observed by the Dutch microscopist Leeuwenhoek in 1675 and were later discovered in mammals by Purkinje and Valentin (Sleigh, 1962). In the olfactory system, 5-20 non-motile cilia protrude from the knob at the dendritic terminal of each ORN (Anholt, 1987; Breer, 1994; Schild and Restrepo, 1998), increasing the effective surface area of the epithelium by an estimated 240 times (Stein, 1982).

Olfactory cilia contain an enriched population of olfactory receptors (Dwyer *et al.*, 1998) and are the site for the primary molecular recognition events in olfaction. They are also enriched in the transduction proteins required for olfactory reception such as adenylyl cyclase III (Pace *et al.*, 1985), increasing their local concentration and therefore the efficiency of signalling pathways. Prior to the creation of cilia in the final stages of differentiation, ORNs do not respond to odorants with any specificity (Gesteland *et al.*, 1982; Schwob, 1992).

Cilia are also present on the ciliated cells of the nasal respiratory epithelium (Menco and Farbman, 1987). These cilia differ slightly from olfactory cilia as they are motile and therefore align themselves with cilia from neighbouring cells.

However the 9+2 microtubule arrangement characteristic of cilia is common to both olfactory and respiratory types (Farbman, 1992; Menco and Farbman, 1992).

1.4 The Olfactory Epithelium

Epithelia have evolved to serve two functions. The first is a protective role in the prevention of tissue damage via microorganisms, dehydration, surface abrasion and loss of heat. The second function is the control of exchange processes between tissues and the blood *e.g.* blood-brain barrier and liver sinusoids (Rhodin, 1974). To satisfy these varying requirements, cells on the free epithelial surface have specialised properties *e.g.* dry surfaces tend to have flat, keratinised cells to protect against mechanical injuries, respiratory surfaces commonly have ciliated cells to keep a film of moisture moving and epithelia with secretion/absorption functions have microvilli to maximise surface area (Rhodin, 1974). The mammalian nasal cavity contains two major types of epithelium: the respiratory epithelium, a columnar epithelium bearing microvillous and ciliated cells, and the olfactory epithelium. It is at the surface of the olfactory epithelium that the primary events in olfaction take place.

The olfactory epithelium lines the nasal turbinates of the nasal cavity (Figure 1.1 and 1.2). It is a pseudostratified epithelium in which all cells maintain a direct, if somewhat slender connection to the basement membrane. As shown in Figure 1.1, there are three main cell types present, olfactory receptor neurons (ORNs), sustentacular cells and basal cells (Masukawa *et al.*, 1983; Buck and Axel, 1991; Farbman, 1992; Suzuki *et al.*, 2000) and all play important roles in the maintenance of a functional olfactory epithelium.

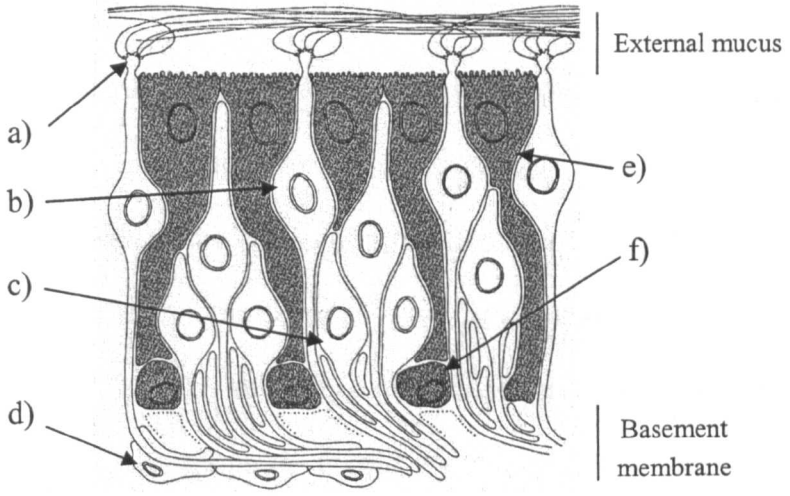

Figure 1.1 Diagram of the cross-section of the olfactory epithelium. The arrows indicate **a)** dendritic knobs of the olfactory receptor neurons from which olfactory cilia project, **b)** mature olfactory receptor neurons, **c)** developing olfactory receptor neurons, **d)** horizontal basal cells, **e)** sustentacular cells and **f)** globose basal cells. Source: Farbman, 1992.

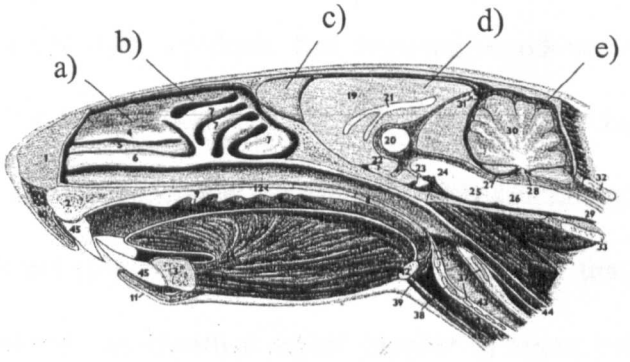

Figure 1.2 Diagram of the sagittal section of a rat head *rattus norvegicus*. The arrows indicate **a)** nasal conchae, lined with respiratory epithelium, **b)** nasal turbinates, lined with olfactory epithelium, **c)** olfactory bulb, **d)** cortex and **e)** cerebellum. Source:Popescu et al., 1992.

There are two types of basal cell in the olfactory epithelium, characterised by differing morphologies (Schwartz Levey et al, 1991; Feron et al, 1999). Globose basal cells line the basement membrane and are the stem cells responsible for the replacement of epithelial cells. Horizontal basal cells are also found at the basement membrane. The function of these cells is not clear although it has been suggested that they may penetrate the basement membrane to act as progenitor cells for the olfactory ensheathing cells of the lamina propria (Chang & Barnett, 2003)

Sustentacular cells are considered to have many putative functions including roles in mucus secretion, uptake and transport of odorants, ionic reservoir/buffer for ORNs and phagocytosis of apoptotic ORNs (Farbman, 1992; Carr *et al.*, 2001). Certainly the presence of microvilli on the apical surface of these cells would aid a secretory function (Rhodin, 1974; Reed, 1992). These cells may also be responsible for the maintenance of epithelial integrity during conditions of stress (Carr *et al.*, 2001).

ORNs are one of only two classes of neurons with nerve processes exposed to the external environment (the other class being neurons of the trigeminal system). They are bipolar neurons with dendritic tips exposed to odour molecules in the olfactory mucus, whilst their axons pass through the basement membrane of the olfactory epithelium to form synaptic connections with secondary neurons in the olfactory bulb. ORNs are responsible for odorant detection and the conversion of a receptor-binding event into an electrical signal capable of being transmitted to and interpreted by the brain to produce the sensation of smell.

The mammalian olfactory epithelium is covered in 10-30μm depth of mucus (Lancet, 1986), which prevents the tissue from drying out. As discussed later, it may also play other vital roles in olfaction via specific properties such as metal ion

content, precise pH conditions and the resident 10-100μM odorant-binding proteins (Pevsner *et al.*, 1989; Schild and Restrepo, 1998; Bear *et al.*, 2001).

1.5 Olfactory receptors

The primary event in olfaction is an interaction between an odorant and an olfactory receptor. This contact triggers a signal cascade leading ultimately to the opening of cation channels (reviewed by Schild and Restrepo, 1998) and depolarisation of the olfactory receptor neuron (Figure 1.3). The search for the identity of the olfactory receptors is the study of the primary coding mechanism of the olfactory system.

Both lipids and proteins have been considered as possible sites for odorant interaction with ORNs. Attempts to radiolabel olfactory receptors via pyrazine odorants led to the discovery of mammalian odorant-binding proteins (Pelosi *et* al., 1982; Bignetti *et* al., 1985; Pevsner *et al.*, 1985). Other research focussed on lectin-binding glycoproteins (Chen and Lancet, 1984; Chen *et al.*, 1986a; Shirley *et al.*, 1987a; Shirley *et al.*, 1987b; Fesenko, 1988), providing strong evidence for the involvement of glycosylated proteins in olfactory reception. In contrast Kurihara and co-workers attributed membrane depolarisation in response to odorant exposure to the properties of the neuronal membrane (Kashiwayanagi and Kurihara, 1985; Nomura and Kurihara, 1987).

Lancet (1986) reviewed the evidence arguing for a protein-based receptor citing the observed stereo-specificity of the olfactory system (Theimer *et al.*, 1977), alterations in electro-olfactograms (EOGs) after treatment with protein-specific reagents (Menevse *et al.*, 1978; Shirley *et al.*, 1983) and the existence of genetically based and specific anosmia as evidence for the involvement of protein receptors.

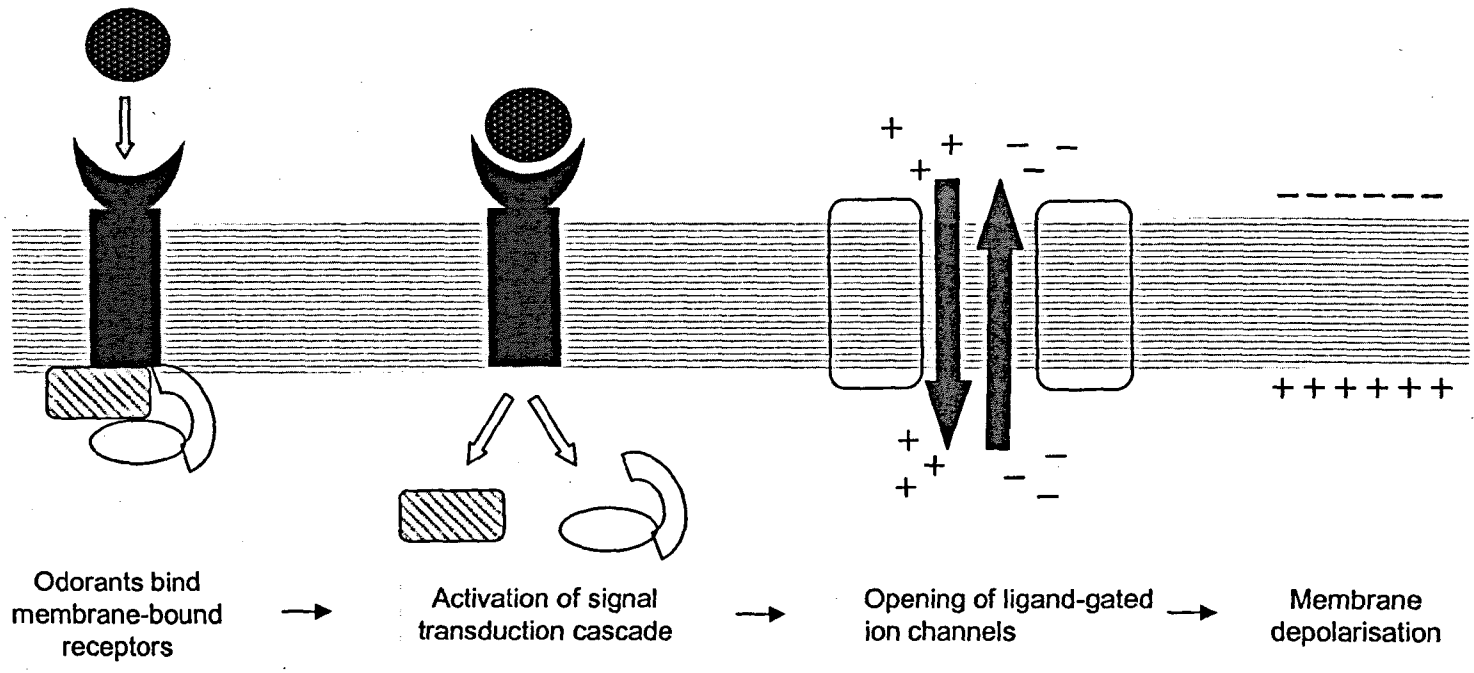

Figure 1.3 The primary molecular events of olfaction at the membrane of the olfactory cilia of olfactory receptor neurons

The binding of an odorant by a membrane-bound olfactory receptor triggers a signal transduction cascade that leads to the opening of cyclic-nucleotide gated channels allowing an influx of positively-charged calcium cations. The influx of Ca^{2+} ions activates Ca^{2+}-dependant chloride channels leading to the flow of negatively-charged out of the cell. A combination of these ion movements result in the depolarisation of the olfactory cilia membrane. If this depolarisation reaches a threshold level it triggers an action potential in the olfactory receptor neuron.

Five years later, Buck and Axel discovered the olfactory receptor protein family (Buck and Axel, 1991).

Buck and Axel based their experiments on the observations that isolated cilia preparations respond to odorants by the stimulation of an adenylate cyclase enzyme (Pace *et al.*, 1985; Sklar *et al.*, 1986), in a GTP-dependent manner; leading to the conclusion that GTP-binding proteins (G-proteins) and therefore G protein-coupled receptors are involved in the transduction pathway of odorant detection (Buck and Axel, 1991). They designed polymerase chain reaction (PCR) primers to recognise and amplify homologs of the G protein-coupled receptor family expressed in the olfactory epithelium and discovered one of the largest multigene families in the mammalian genome (Buck and Axel, 1991; Gibson and Garbers, 2000). Olfactory receptor genes comprise approximately 1% of the rodent genome (Mombaerts, 1999) and an estimated 900 genes in humans (Young and Trask, 2002). Homologous G-protein-coupled olfactory receptors have since been found in both fish (Ngai *et al.*, 1993a; Cao *et al.*, 1998) and amphibia (Freitag *et al.*, 1995).

Evidence for the localisation and function of the putative olfactory receptors was provided by *in situ* hybridisation experiments, which confirmed the expression of the putative olfactory receptor OR5 in rat ORNs (Raming *et al.*, 1993). Furthermore OR5 receptor expressed in the Sf9 insect cell line responded specifically to certain odorants. Other researchers have since provided further evidence of receptor function, again introducing putative olfactory receptor sequences into heterologous systems (Zhang *et al.*, 1997, Krautwurst *et al.*, 1998). The first proof of the function of these receptors *in vivo* used adenovirus-mediated infection to over-express a putative olfactory receptor (rat I7) in rat ORNs; over-expression resulting

in increased yet specific responses of the infected cells to the odorant, octanal (Zhao *et al.*, 1998).

Recently, Wang *et al.* have proposed the hypothesis that the olfactory receptor functions as a metalloprotein (Wang *et al.*, 2003a). This theory provides a plausible mechanism for the activation of G-proteins upon odorant binding and also an explanation of differential odorant sensitivity, based on metal-ion co-ordination capacity. This idea will be reviewed more thoroughly in Chapter 6.

1.6 Transduction mechanisms

The ultimate goal of the transduction machinery in the olfactory cilia is to convert an odorant-receptor interaction into membrane depolarisation. The basic system of receptor ⇒ G protein ⇒ effector enzyme (*e.g.* adenylyl cyclase, phosholipase C) ⇒ second messenger gated channel, generates the membrane potentials in both vertebrate and invertebrate ORNs (Hildebrand and Shepherd, 1997), although the precise mechanisms and proteins involved can vary greatly between different species and potentially even between alternative odorants and concentrations (Boekhoff *et al.*, 1990).

In the vast majority of ciliated ORNs, G protein-mediated activation of adenylyl cyclase III and the subsequent production of cAMP are required to open the cyclic-nucleotide gated (CNG) channel and initiate membrane depolarisation (Wong *et al.*, 2000, Zufall and Munger, 2001). There are however, many variations on this theme (see Table 1.1).

Seven subtypes of the G_α protein, part of the three subunits G_α, G_β and G_γ that form a multimeric G protein, have been found in the vertebrate olfactory epithelium including G_{olf}, G_q, G_i and G_0 (Schandar *et al.*, 1998). Whereas in the majority of

Transduction Proteins		Enzyme Effector	2nd Messenger	Ion Channel
G proteins	G_{olf}	Adenylyl Cyclase III	cAMP	Cyclic Nucleotide-Gated Channel
G proteins	G_i G_o G_q	Phospholipase C	IP_3	IP_3-Gated Channel
?		?	NO/CO (+cGMP?)	Cyclic Nucleotide-Gated Channel
?		Guanylyl Cyclases	cGMP	Cyclic Nucleotide-Gated Channel

Table 1.1 The transduction pathways leading to membrane depolarisation events at the olfactory cilia membrane.

neurons the activated G_{olf}-containing G proteins stimulate cAMP production via the subtype of adenylyl cyclase (AC_{III}), G protein activation in ORNs expressing the alternative G_{α} subunits G_i, G_0 and G_q leads to the stimulation of phospholipase C and the production of a different second messenger, IP_3 (Sklar *et al.*, 1986; Boekhoff *et al.*, 1990; Schild and Restrepo, 1998; Schandar *et al.*, 1998). The role of IP_3 in olfactory cilia is still debated with biochemical evidence for the involvement of this second messenger (Boekhoff *et al.*, 1990) apparently contradicted by more recent work by Wong *et al.*, (2000). It is extremely unlikely however, that an IP_3 receptor would be localised to the olfactory cilia in both the lobster (Munger *et al.*, 2000) and rat (Cunningham *et al.*, 1993) if it played no part in odorant detection. Receptors could potentially act either indirectly by modulating the cAMP-driven signal or directly influencing membrane depolarisation via Ca^{2+}-dependant channels or PKC-mediated stimulation of adenylyl cyclase (Duchamp-Viret *et al.*, 2003). The IP_3 response could also be combined with the cAMP directed response as an extra element of coding (Boekhoff *et al.*, 1990; Ronnett, 1993; Duchamp-Viret *et al.*, 2003)

If cAMP is the main player, IP_3 is unlikely to be the only member of the supporting cast. Olfactory-specific guanylyl cyclases have been found in rodents (Gibson and Garbers, 2000) and there is evidence to suggest that in a sub-population of ORNs in the mammalian olfactory system, cGMP rather than cAMP stimulates the opening of CNG channels (Juilfs *et al.*, 1997; Meyer *et al.*, 2000). Furthermore, the gaseous second messengers carbon monoxide and nitric oxide are produced upon odorant exposure and also cause CNG channel opening, possibly via the cGMP pathway (Broillet, 2002; Rawson and Gomez, 2002). Added together this means that

in the very first stages of the olfactory process there are many pathways leading to an initial membrane depolarisation.

When the CNG channel (or its IP_3 receptor equivalent) opens it enables an initial influx of Ca^{2+} ions. The Ca^{2+} ions have a role to play in the modulation of the odorant response in the cell (reviewed by Hildebrand and Shepherd, 1997) but the immediate results of the influx is the activation of Ca^{2+}-dependant chloride channels (Reisert and Matthews, 2001). This leads to an efflux of Cl^- ions, which further amplifies the membrane depolarisation. Once this depolarisation has surpassed the activation threshold for the voltage-gated Na^+ channels, an action potential is initiated (Schild and Restrepo, 1998) and an electrical signal transmitted along the axon of the ORN to the secondary neurons in the olfactory bulb. The termination of the signal is achieved by uncoupling the transduction cascade via various negative feedback loops involving kinase phosphorylation of olfactory receptors and hyperpolarising K^+ currents. (Boekhoff, 1997; Schild and Restrepo, 1998).

It must be noted that for the generation of all the discussed electrical potentials, the ion content of both the ORNs and the overlying mucus are of vital importance. The relative ion concentrations will determine the direction of current flow and in so doing control whether channel activation is stimulatory *i.e.* depolarising or inhibitory *i.e.* hyperpolarising (Schild and Restrepo, 1998).

1.7 Transmission of olfactory signals to the brain

In the mature OE, approximately 40 million ORN axonal processes penetrate the basement membrane and project through the underlying lamina propria and cribiform plate to form cranial nerve I (Stein, 1982; Carpenter, 1996). The axons terminate in the olfactory bulb, where they form globular synaptic complexes with secondary

neurons in complex structures called glomeruli (Stein, 1982; Buck and Axel, 1991; Yoshihara and Mori, 1997; Uchida *et al.*, 2000).

Mitral and tufted cells are the secondary neurons of the olfactory system (Stein, 1982). Their axons project to the numerous regions of the brain driven directly or indirectly, by olfactory stimuli (Figure 1.4). The main targets for the mitral and tufted cells are the anterior olfactory nucleus, piriform cortex, olfactory tubercle and the lateral entorhinal cortex, collectively known as the primary olfactory cortex. From these regions the neuronal pathways continue to regions of the limbic system, including the amydala and hippocampus, in addition to targets in the higher cortex (McLean and Shipley, 1992; Carpenter, 1996). The majority of neuronal pathways ultimately target the orbitofrontal cortex and it is here that the conscious perception of smell is thought to take place (Bear *et al.*, 2001).

1.8 Odour coding: Olfactory receptor neurons

1.8.1 Olfactory receptors and odorant specificity

The coding ability of the primary binding events in olfaction is determined by two key elements: the level of specificity of odorant binding and the number of different olfactory receptors that are expressed in a single ORN. Odorants are defined here as low molecular weight compounds that interact with proteins in the cilia of olfactory receptor neurons and subsequently induce a membrane depolarisation event.

The specificity of binding is governed by the olfactory receptor. As we know that the receptor is a protein with a 3D-structure rather than a specialised lipid membrane, binding specificity is implicit in the protein fold. Genetics provides evidence for the selectivity of odorant binding by the sheer numbers of different receptors that are coded for in the mammalian genome; were interactions less

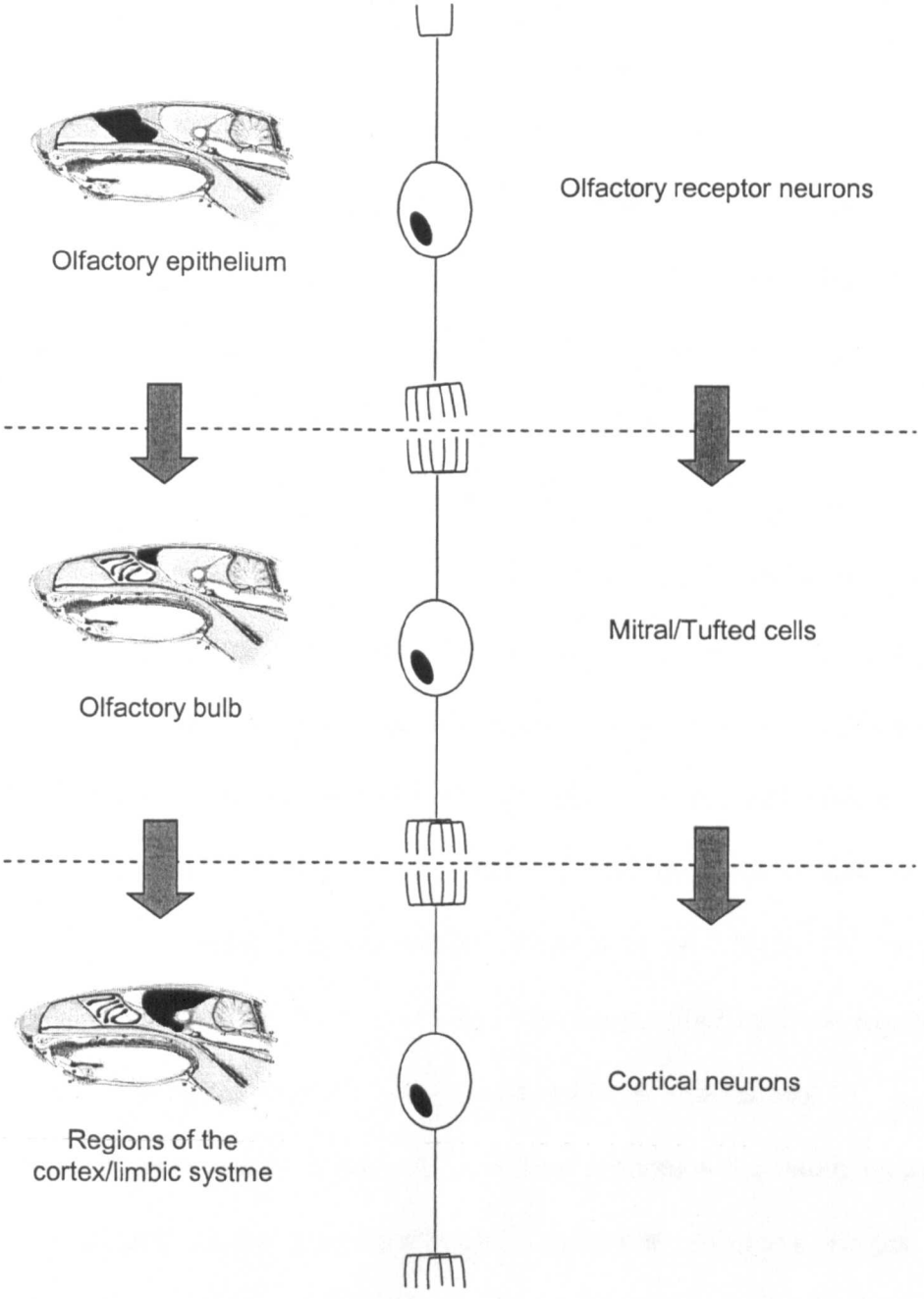

Figure 1.4 The basic neuronal/anatomical pathway of olfaction

Initial molecular events occur at the cilia membrane of the dendritic terminals of olfactory receptor neurons. Action potentials generated in the olfactory receptor neurons are transmitted to secondary neurons in the olfactory bulb called mitral/tufted cells, which form synaptic connections with neurons in selected regions of the cortex/limbic system.

specific, an estimated 1% mouse and rat genomes would not encode putative receptors (Mombaerts, 1999).

Analysis of putative receptor genes for the positive selection of residues (Singer *et al.*, 1996; Gilad *et al.*, 2000) and levels of conservation of each amino acid across different receptor families suggested that individual/small groups of residues in transmembrane regions 3, 4 and 5 control odour binding specificity (Buck and Axel, 1991; Ngai *et al.*, 1993a; Singer *et al.*, 1995; Pilpel and Lancet, 1999). Confirmation of the importance of these regions and their specific residues was provided by a site-directed mutagenesis experiment, where a single residue change from valine to isoleucine in transmembrane region 5 altered the preferential receptor binding of mouse I7 receptor from octanal to heptanal (Krautwurst *et al.*, 1998).

The binding specificity of olfactory receptors is not absolute as demonstrated by a single olfactory receptor (rat OR 5) expressed in insect Sf9 cells exhibiting significant, measurable biochemical responses to four different classes of odour compound including aldehydes and amines (Raming *et al.*, 1993). The responses varied between the odorants tested, the largest response resulting from exposure to aldehydes indicating preferential receptor binding of these compounds.

These experiments illustrate two important properties for odour binding by olfactory receptors: odour determinants and molecular receptive ranges. Each odorant has primary and secondary determinants that govern whether or not they bind to a certain receptor. The primary determinants are the nature and relative positions of any functional groups and have the largest impact on binding (Uchida *et* al., 2000). They are reinforced/moderated by the secondary features of the molecule *e.g.* length and branching patterns of the carbon chain (Uchida *et al.*, 2000; Nagao *et al.*, 2002). Individual olfactory receptors have their own molecular receptive ranges.

These are defined as the variety of odour compounds a given receptor will interact with (Uchida *et al.*, 2000) and describe the levels of specificity shown by a receptor *i.e.* capable of interactions with a group of similar odorants *versus* specificity to a single molecule.

Alternative theories of recognition, by molecular vibration (Turin, 1996) and metal ion co-ordination ability (Wang *et al.*, 2003a) have been put forward, although the 3D binding site recognising 3D chemical structures is still considered the most likely mechanism for odorant binding specificity. This does not preclude recognition by the vibrational or nucleophilic properties of an odorant but emphasises the importance of defined amino acid residues in direct interactions with multiple features of a given odorant (Singer *et al.*, 1995; Singer *et al.*, 1996; Pilpel and Lancet, 1999).

In addition to responding to a given odorant stimuli there is evidence that even at this early stage of olfaction there may be integration of odorant mixture information into the response of an ORN (Duchamp-Viret *et al.*, 2003). This adds an extra dimension to the primary coding mechanism of olfaction, where the collective signals from all ORNs will encode the odorant mixture but may not necessarily equal the sum of an odorant mixture's parts.

1.8.2 Encoding the stimulation of olfactory receptors

Experiments based on human perception rather than biochemical or electrical effects demonstrated clearly that odours that bind to the same receptors have the same perceived smell (Theimer *et al.*, 1977). Section 1.6 discussed the transduction mechanisms responsible for the generation of an action potential but the number of

receptors expressed in a neuron will ultimately determine the complexity of maintaining the identity of the receptor stimulated by an odorant.

The "one receptor, one neuron" hypothesis dictates that information about the molecular features of an odorant can be gained by monitoring which receptor neurons have been stimulated by virtue of their expressing of a single receptor protein to which the odorant can bind. This explains the existence of zone-to-zone projection, where the olfactory epithelium can be considered as four major groups of neurons with similar odorant specificities, in four broad regions of the olfactory epithelium, that project their axons to four specific zones in the olfactory bulb (Strotmann *et al.*, 1994; Vassar *et al.*, 1994; Ressler *et al.*, 1994). There is some evidence for the "one receptor, one neuron" hypothesis, at least in mouse ORNs (Vassar *et al.*, 1993; Malnic *et al.* 1999; reviewed by Mombaerts, 1999). This is provided by single cell reverse transcription PCR (RT-PCR) experiments (Chess *et al.*, 1994; Malnic *et al.* 1999) and evidence of monoallelic expression of olfactory receptors (Chess *et al.*, 1994).

The combination of olfactory receptors stimulated sends an electrical description of the odorant molecule to the olfactory bulb as shown by electro-olfactogram (EOG) recordings. These represent the summated receptor potentials of multiple neurons and change in size and temporal properties according to the individual odorant used (Menevse *et al.*, 1978; Lancet, 1986; Stein, 1982).

An alternative hypothesis is that multiple receptors are expressed by each neuron as observed in nematode chemosensory cells (Mombaerts *et al.*, 1999). This could explain the dual responses seen when odorant-stimulated mammalian ORNs appear to increase production of both IP_3 and cAMP and the apparently ligand-specific and concentration specific extents to which each second messenger is

produced (Ronnett *et al.*, 1993). It would also provide one possible mechanism by which single neurons could produce both excitatory and inhibitory currents in response to an odorant mixture (Sanhueza *et al.*, 2000). The expression of multiple receptors in ORNs has been proposed for spiny lobster and catfish (Cromarty and Derby, 1997) and subsequent single cell PCR experiments on rat ORNs demonstrated the expression of two and three different receptors in a subset of neurons (Rawson *et al.*, 2000). However the same PCR experiments also showed that the majority of ORNs express only a single olfactory receptor.

The potential presence of multiple receptors in selected neurons means that in some cases more than just the identity of the stimulated neuron must be transmitted to the higher order processing centres. The information transmitted in these cases would need to convey a) identity of ORN stimulated and b) identity of stimulated receptor. This could in theory be encoded by electrical signalling properties, where the cross talk or summation between pathways yields a specific pattern of depolarisation and repolarisation in individual ORNs, transmissible to mitral/tufted cells (Cromarty and Derby, 1997; Sanhueza *et al.*, 2000). Multiple receptor expression systems could also split ORNs into two groups: cells expressing single, broad specificity receptors for combinatorial coding and a second group expressing multiple, high-specificity receptors communicating an absolute feature of an odorant.

1.9 Odour coding: Olfactory bulb

The second level of coding in the olfactory system is provided by the olfactory bulb, a structure comprised partly of neuropil structures known as glomeruli, where ORN axons form synaptic connections with the secondary neurons of the olfactory system: the mitral/tufted cells (Ressler *et al.*, 1994; Carpenter, 1996).

ORN axons expressing a given receptor specifically target a pre-determined glomerulus in a process known as glomerular convergence (Figure 1.5). Up to several thousand ORN axons expressing a defined receptor extend their axons to glomeruli in one of only two sites out of approximately 1800 potential contact points (Vassar *et al.*, 1994; Ressler *et al.* 1994; Mombaerts *et al.*, 1996). This growth process is governed by factors including OCAM cell adhesion molecules (Uchida *et al.*, 2000), olfactory receptors (Mombaerts *et al*, 1996; Yoshihara and Mori, 1997) and ephrin-A proteins (Cutforth *et al.*, 2003); the two alternative locations forming parts of the dual sensory maps in the lateral and medial hemispheres of the olfactory bulb (Nagao *et al.*, 2002). The process of glomerular convergence has been suggested to increase odorant sensitivity by increasing the signal-to-noise ratio of electrical transmissions between the epithelial surface and the olfactory bulb (Duchamp-Viret *et al.*, 1990; Vassar *et al.*, 1994)

Duchamp-Viret *et al.* reported that at a defined odorant concentration (expressed as a fraction of saturated vapour) whilst only 5-20% ORNs appeared to be stimulated, 10-40% mitral/tufted cell population was activated (Duchamp-Viret *et al.*, 1990). This may represent evidence that a subset of ORNs in some animals is able to project axons to more than one glomerulus, as subsequently reported by Royal and Key (1999). Using the same strain of transgenic mice, the occurrences of multiple glomerular innervation was reported as <5% (Mombaerts *et al.*, 1996) and approximately 85% (Royal and Key, 1999) therefore the levels of occurence and relevance of these cases is unknown. Certainly it is a highly variable phenomenon and may partially represent system aberrations in addition to a possible alternative odour coding system.

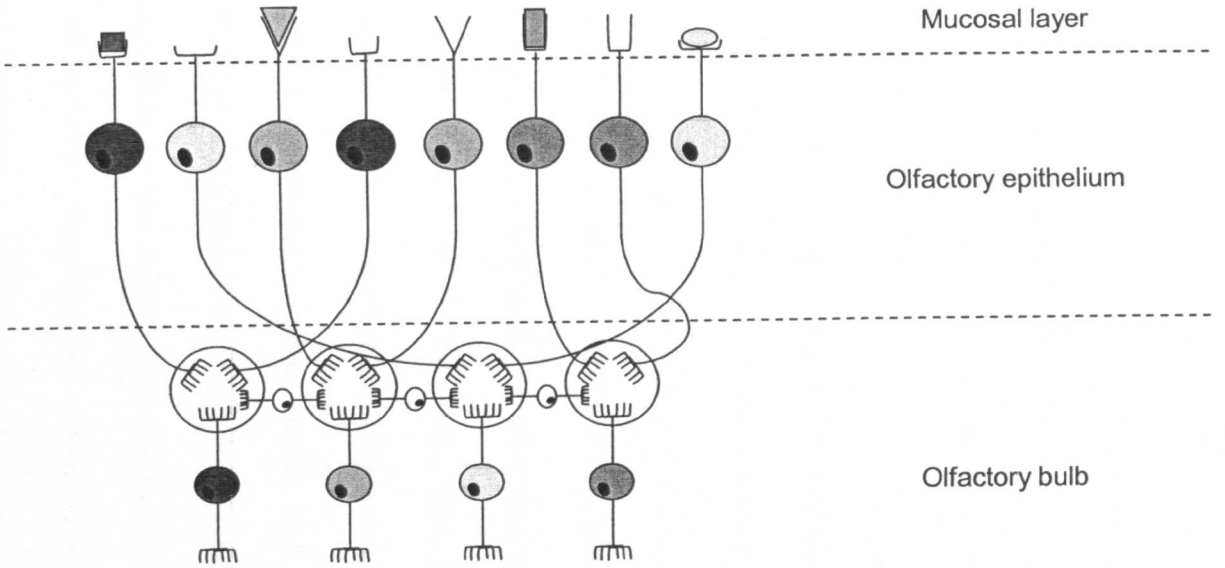

Figure 1.5 Olfactory receptor neurons form synaptic contacts with mitral-tufted cells in structures known as glomeruli

The axons of olfactory receptors innervate predetermined glomeruli in the olfactory bulb (represented by the circled areas) according to the olfactory receptor each one expresses. This process is called glomerular convergence. In side the glomerular structure olfactory receptor neurons form synaptic contacts with mitral/tufted cells and also the periglomerular cells responsible for lateral inhibition in the olfactory bulb..

In addition to the ORN axons, each glomerulus is also innervated by the primary dendrites of approximately 20 mitral/tufted cells. As these cells project a single dendrite to one glomerulus, their activity reflects the specificity of the ORNs present (Mori *et al.*, 1999). The functionality of ORN axonal convergence was demonstrated by electrophysiology experiments recording from the mitral/tufted cells, which demonstrated that cells responsive to fatty acid odorants are located in the dorsomedial region of the olfactory bulb, in contrast to cells stimulated by aldehyde compounds, which were present in both the dorsomedial and ventral regions (Imamura *et al.*, 1992).

The use of electrophysiology the activity/stimulation of the olfactory bulb has also been investigated using alternative methods such as 2-deoxyglucose uptake (Stewart *et al.*, 1979), c-fos expression (Onoda *et al.*, 1992) and optical imaging of intrinsic signals (Rubin and Katz, 1999). Patterns of glomerular activation elicited by different odorants vary significantly yet are commonly conserved between individual animals (Vassar *et al.*, 1994; Ressler *et al.*, 1994; Rubin and Katz, 1999). They are also sufficiently variable to distinguish between highly similar compounds such as phenols with substitutions at ortho-, meta- and para- positions and alternative acid/alcohol attachment positions of ester compounds (Uchida *et al.*, 2000).

These experiments demonstrate that the olfactory bulb encodes information (transmitted by ORNs) regarding the molecular features of an odorant, in its own patterns of glomerular activity. These activation patterns represent a spatial map of ORN stimulation analogous to the visual system (Hildebrand and Shepherd, 1997), which can then be transmitted via the mitral/tufted cells to selected regions of the brain. The existence of dual sensory maps in the olfactory bulb may represent two

pathways for transmitting olfactory information of differing functional significance to alternative locations in the cortex (Nagao *et al.*, 2002).

The discussion so far has assumed the olfactory bulb to be akin to a linear relay point for olfactory information to pass directly to a secondary neuron and then onto the brain. However, alongside the ORNs and mitral/tufted cells there are three other neuronal cell types in the olfactory bulb: granule cells, interneurones and periglomerular cells (Carpenter, 1996), which form synapses between neighbouring mitral/tufted cells to provide various forms of feedback and lateral inhibition (Nickell and Shipley, 1992; Yokoi *et al.*, 1995). This capacity for inhibition adds another potential influence on the coding and processing of olfactory information, for example changes in the synapses between granule and mitral/tufted cells is thought to be the basic mechanism behind olfactory/pheromonal memory (Mori *et al.*, 1999).

1.10 Odour coding: Intensity

In addition to information on the quality of an odorant, it is also important to recognise the quantity *i.e.* intensity of the scent. This is particularly true when the scent is associated with food or danger. If olfactory receptors bind only specific odorants how is this quantitative data obtained and transmitted?

Olfactory bulb experiments indicate that increasing odorant concentration results in the stimulation of additional glomeruli (Chalasonnet and Chapu, 1998; Rubin and Katz, 1999; Uchida, 2000), presumably due to an increase in the number of stimulated ORNs. The first method of achieving this increase is for larger numbers of receptor neurons to interact with the odorant. Increased odorant concentrations may allow the odorant to interact with receptor proteins that have a lower affinity than its specialised receptors.

An increase in the mean firing frequency of ORNs has been observed upon increasing stimulus intensity (Duchamp-Viret *et al.*, 2000), where an increased firing frequency may improve the chances that a weak interaction with an odorant could result in a sufficient membrane potential to generate an action potential. Such alterations also differ according to the individual odour and could be the basis for differential detection thresholds.

A third option for intensity coding in ORNs is the dual receptor system, whereby the response of a given receptor is different at high and low ligand concentration (Boekhoff *et al.*, 1990; Duchamp-Viret *et al.*, 2000). This could act by increasing the number of stimulated ORNs by the enhancement of excitatory transduction events or by the suppression of inhibitory currents. Such effects would still require receptor mediation to maintain the consistent glomerular activation patterns observed and are therefore unlikely to occur via non-specific membrane disruption or direct opening of ion channels.

The firing frequencies of the mitral/tufted cells do not appear to change upon exposure to increasing odour concentrations. This implies that the information transmitted by the olfactory bulb concerns odour quality but not necessarily quantity. However, work by other researchers has provided contrary evidence that mitral/tufted cells increase their firing frequency in response to increasing odour concentration and thus provide a potential mechanism for intensity coding (Imamura *et al.*, 1992). These differences may be as a result of the species used and experimental protocols *e.g.* recording from freely breathing anaesthetised rats (Chalasonnet and Chaput, 1998) *versus* rabbits on an artificial respirator (Imamura *et al.*, 1992). They are also likely to represent cell populations from different regions of the olfactory bulb as Chalasonnet and Chaput (1998) tested a range of odorants

including limonene, an odorant that did not stimulate the mitral/tufted cells recorded from during the experiments of Imamura *et al.* (1992). This allows the potential for different cell populations to respond differently to increased odorant concentrations depending on the individual odorant involved.

Changes in glomerular activity patterns could mean that higher concentrations may be perceived differently, consistent with the idea that concentration increases are encoded by alterations in the spatial map of glomerular activation rather than the electrical activity of the mitral/tufted cells (Pause *et al.*, 1997). These investigations also predicted that at higher concentrations, odorants may stimulate not only neurons of the olfactory system but trigerminal nerve endings. This is discussed further in Section 1.12 and could potentially mean that in the case of some odorants, the olfactory system need not have an intrinsic odour intensity coding mechanism.

Increasing the concentration of an odorant can change its qualitative perception and potentially stimulate the neurons of the trigeminal system. It may also have an effect on the perceived pleasantness of an odour. During increases in the concentration of selected chemicals, the properties of a compound can change from attractive at low concentrations to repellent at high concentration (Bargman *et al.*, 1993). This provides evidence for a link between odorant concentration and aversion. One group of volatile compounds that change in perception from attractive to highly repugnant, even at low concentrations are the thiol odorants.

1.11 Introduction to the biology of thiol compounds

The thiol group, also referred to as the sulphydryl group, comprises simply of a sulphur atom covalently linked to a hydrogen atom and many of its properties are related to the unusual chemical nature of the sulphur atom.

Sulphur is most commonly incorporated into the body via the amino acids cysteine and methionine (Torchinsky, 1981). In this form, sulphydryl groups contribute to both the stability and reactivity of proteins. Pairs of cysteine residues form disulphide linkages between regions of a single polypeptide to stabilise three-dimensional protein structure or connect two polypeptide chains *e.g.* insulin A and B chains (Branden and Tooze, 1999). Cysteine residues are also commonly found in the metal-binding sites of metalloproteins (Seebungkert and Lynch, 2001; Wang *et al.*, 2003a) and functionally important for many enzymes, as indicated by the majority of intracellular enzymes being inhibited by sulphydryl group directed reagents (Torchinsky, 1981).

One possible reason for the inclusion of cysteine residues in chemically active protein sites is the versatility of the thiol group. Sulphur is a p-block element and its properties can be compared to both oxygen (in terms of reactions participated in) and carbon (in terms of equal electronegativity). Sulphur atoms possess d-orbitals that allow sulphur to have multiple oxidation states of 2, 4 and 6 and co-ordination numbers from 0-7 (Clayden *et al.*, 2001). This variability increases the number and variety of the chemical structures it can form and allows thiol groups to participate in a wide range of reactions including alkylation, acylation, oxidation, thiol-disulphide exchange, reactions with sulphenyl halides and possibly formation of charge transfer complexes (Torchinsky, 1981), *via* both their soft nucleophilic and electrophilic

characteristics (Clayden *et al.*, 2001). Of these reactions the only one unique to thiol groups is the thiol-disulphide exchange.

The multiple reactions that sulphydryl groups are capable of can be modulated via the immediate chemical environment *e.g.* proximity to charged residues increases cysteine nucleophilicity in the active site of the plant protease papain (Friedman, 1973). Certainly in the case of papain, the variability of the pK_a of thiol groups is important, commonly around 8 but mutable from 4-10 depending on the precise environment (reviewed by Torchinsky, 1981).

1.12 Thiol odorants – sensitivity and aversion in mammals

From a biological view and of relevance to this thesis, sulphur compounds and in particular thiols smell. Sulphur compounds account for some of nature's (and man's) most illustrious stenches (Figure 1.6). The volatile products of chopped onions responsible for their characteristic odour and the lacrymatory effect are sulphoxide compounds. Propanedithiol/4-methyl-4-sulphenylpentan-2-one released from a chemical plant in Freiburg, created a stench so powerful that the entire city had to be evacuated (Clayden *et al.*, 2001) and of course nature's most infamous smell of all – skunk spray – is a mixture comprising mainly of two odorous thiol compounds: (E)-2-butene-1-thiol and 3-methyl-1-butanethiol (Andersen and Bernstein, 1975). Coincident with the aversive properties of thiol compounds, there is an incredible level of sensitivity to sulphurous compounds and especially thiol odorants. Humans can detect 1-part *tert*-butyl thiol per 50,000,000,000 parts odour labelling of natural gas (Clayden *et al.*, 2001) and in EOG recordings from the rat olfactory epithelium, measurable amplitudes were observed at odorant concentrations $<10^{-9}$M, lower than all other odorants tested (Shirley *et al.*, 1987a).

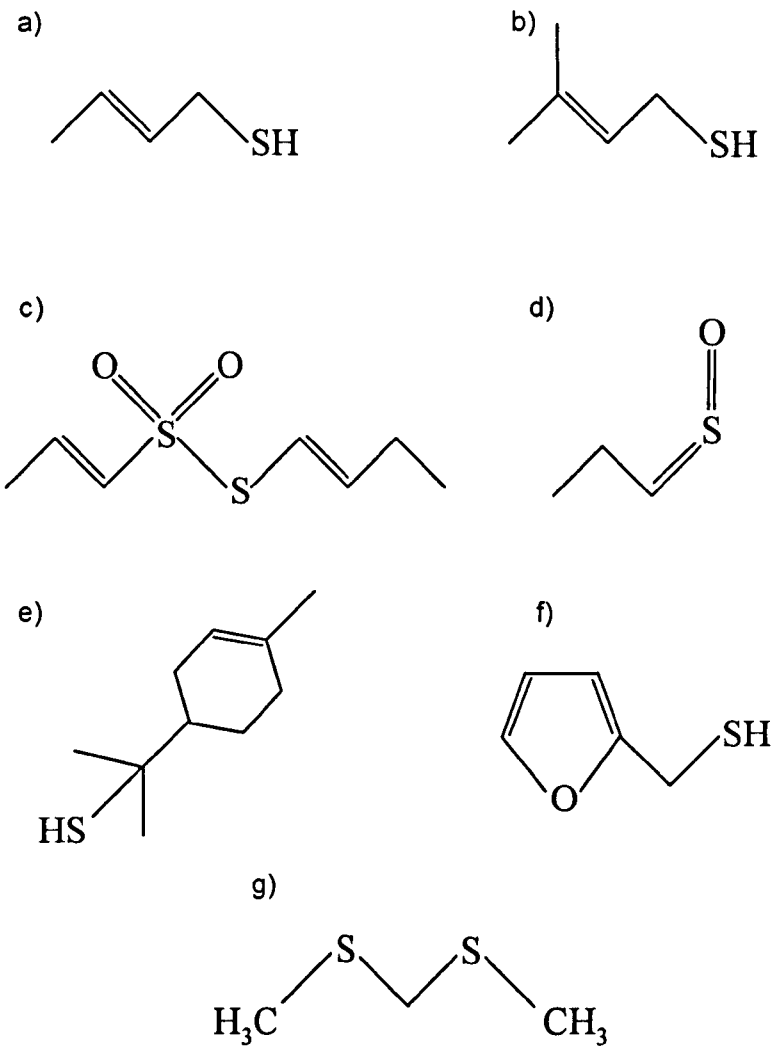

Figure 1.6 The chemical structures of several well-known sulphurous odorant compounds

a) 2-butene-1-thiol and **b)** 3-methyl-2-butene-1-thiol are the two thiol compounds responsible for the potency of skunk defensive spray. **c)** S-but-1-enyl prop-1-ene-1-sulfonothiate and **d)** 1-sulfinylpropane are the volatile compounds responsible for the odour and tear-inducing properties of raw onion respectively. **e)** 1-methyl-1-(4-methylcyclohex-3-en-1-yl)ethyl hydrosulphide is responsible for the sharp taste of grapefruit. Taste is the second of our chemoreceptive senses and is also acutely sensitive to thiols. This compound is detected at $2x10^{-5}$ parts per billion. **f)** 2-furamethanethiol is a thiol compound commonly found in coffee and **g)** 2,4-dithiapentane one constituent of the odour of truffles, detected by pigs through 1m of soil. Source: Clayden *et al.*, 2001.

During psychological studies testing the perception of pleasant *versus* unpleasant odours, many odours perceived as pleasant were common in the natural world and could therefore serve as signals that a given foodstuff was safe to consume. The reverse was true of unpleasant odours and suggested that neutral odours *e.g.* alcohols elicited little perceptual response as there appeared to be no selection criteria for recognising these odorants *i.e.* no association with danger or food (Wright, 1982). Extension of this hypothesis leads to the conclusion that sensitivity to thiol compounds is as a result of their common natural occurrence in decaying matter (unsafe for ingestion by most animals) and that this necessitates a high level of selective pressure to preserve the ability to detect these compounds. It is perhaps this pressure that has lead to the potency of thiol compounds and the sensitivity of detection in mammalian species, preserved even in the context of our own significantly reduced reliance on olfaction.

By recording brain activity and odour perception in human subjects at higher concentrations, many odours were described as "pungent" (Pause *et al.*, 1997). This suggests a possible link between increasing the response of the olfactory system to an odorant and the perception of smells as unpleasant. One hypothesis followed during this work is that aversion to an individual odorant can be the result of increased sensitivity to that compound. This would enable the level at which a smell becomes unpleasant to be lowered to concentrations that are typically encountered and is corroborated by the lowest human olfactory perception thresholds belonging to amine and thiol odorants (Wang *et al.*, 2003a), the groups of compounds that provide some of nature's worst smells of decay and sewage.

1.13 Potential mechanisms for odorant sensitivity

There are likely to be two broad mechanisms for the generation of an aversive response to an odour: aversion as a result of increased sensitivity or alternative methods of processing for a given odorant via different transduction mechanisms or the combination of two sensory input systems.

1.13.1 Olfactory receptor-mediated

There are three broad categories of methods to increase the sensitivity of an organism to a particular odorant/class of odorant: increase the affinity of receptors, increase the number of receptors or alter the efficiency of downstream signalling pathways and processing of an odorant-binding event.

One possible method to increase olfactory sensitivity to an odorant is to increase receptor affinity (Figure 1.7). In this model, an odorant that can form stronger interactions with a given receptor is far more likely to generate membrane and action potentials than those relying on weaker binding forces and thus has a greater chance of being perceived at very low concentrations. Increasing the K_d of the olfactory receptor complex would act in a similar way to increase the likelihood of inducing cellular responses in the ORN.

The existence of differential receptor affinities has been reported in experiments measuring odorant-induced of second messenger levels over a range of odour concentrations, suggesting the involvement of two independent receptor systems with low and high affinity (Boekhoff *et al.*, 1990).

The second model for increased sensitivity is to increase the number of receptors in the sensory system. Direct evidence for this comes from a behavioural test showing that increased exposure of immature ORNs to an odorant increases an

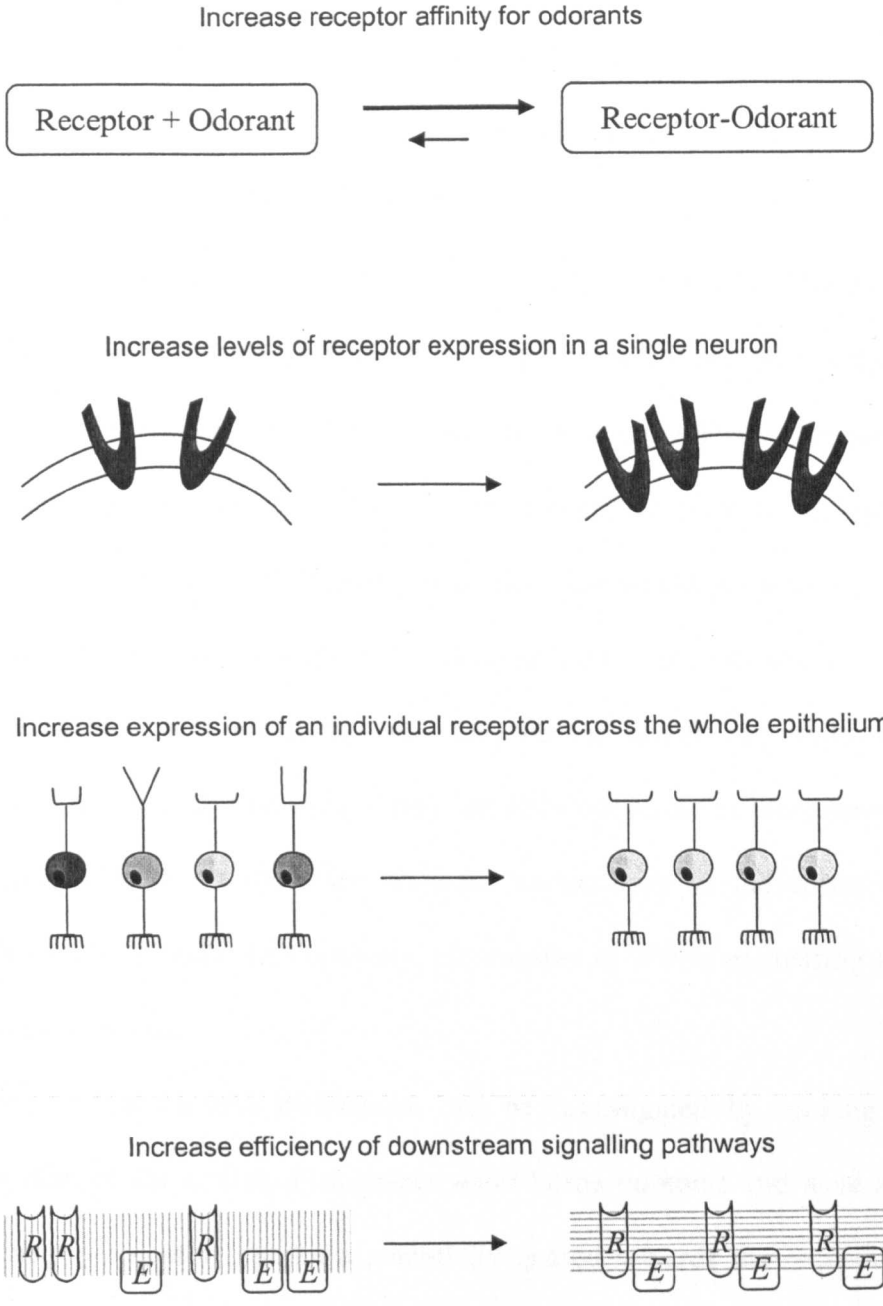

Figure 1.7 Possible mechanisms to increase odorant sensitivity of the receptor-mediated olfactory pathway

In the fourth diagram R= receptor proteins, E= effector proteins.

animal's sensitivity to that odour (Yee and Wysocki, 2001). Although a molecular mechanism could not be assigned by their work, the effects were confirmed to result from changes occurring in the olfactory epithelium independently of the olfactory bulb. Computer modelling also predicts that increasing the number of receptors for a given odorant can increase odorant sensitivity without any changes in receptor affinity (Cleland and Linster, 1999).

These mechanisms of increasing odorant sensitivity would act by increasing the chances of a freely diffusing odorant being exposed to a responsive receptor and as the number of stimulated receptors required to induce membrane depolarisation remains constant this also increases the chances of even low odorant concentrations causing ORN depolarisation. There are two models that would allow an increase in the expression levels of a given olfactory receptor. Firstly the number of olfactory receptors expressed by a given neuron could be increased. The expression of olfactory receptors in heterologous systems has shown that the overexpression of a given receptor leads to an increased response to exposure to the corresponding odorant (Zhao *et al.*, 1998). Alternatively, the number of ORNs expressing a given odorant can be increased.

The potential for this mechanism can be investigated by looking at the olfactory system of the catfish. Fish detect water-borne odorants and have a much reduced olfactory receptor repertoire potentially geared towards the reception of a smaller variety of compounds than land vertebrates (Ngai *et al.*, 1993a; Freitag *et al.*, 1995). *In situ* hybridisation evidence supports the one receptor, one neuron hypothesis suggesting that any specialisation of the olfactory system in response to limited odorant diversity is not achieved by the reduction in the number of different receptors expressed (Ngai *et al.*, 1993a). Analysis of catfish olfactory receptor

sequences shows that in contrast to the mammalian class of olfactory receptors, these sequences are far more closely related (Ngai *et al.*, 1993b). This means that while the one receptor, one neuron hypothesis holds in olfactory systems specialised towards certain classes of odorants (in this case water-borne), the receptors may adapt to have greater overlap, in effect increasing the number of receptors in the olfactory system that respond to a certain odorant.

Computer modelling also predicts that receptors could be tuned by alterations in receptor/effector coupling. In this model, modulation of effector sensitivity (for its second messenger) yields a more efficient transduction system and leaves a greater number of receptors "spare" by decreasing the receptor occupancy threshold for membrane depolarisation.

Alterations of the downstream signalling/processing in represent the third overall method of achieving sensitivity. The efficiency of signal transduction pathways can be improved if the components of the pathway *e.g.* effector enyzymes are concentrated in an area. This method of maximising sensitivity is thought to be already present in the olfactory system in the form of caveolae, a type of lipid raft acting to concentrate the key components of the signalling cascade in the membrane of olfactory cilia (Schreiber *et al.*, 2000).

In addition to increasing the efficiency of a general transduction pathway, if two independent signalling systems are acting in the same ORN there is also the choice between different pathways. Indeed it has been suggested that some putrid odours may stimulate the IP_3 transduction pathway rather than the adenylyl cyclase/cAMP mechanism (Sklar *et al.*, 1986; Boekhoff *et al.*, 1990; Fabbri *et al.*, 1995). This hypothesis may be especially pertinent to thiol odorant detection, as during experiments with sheep, thiol exposure was not shown to be a highly efficient

stimulant of adenylyl cyclase activity (Fabbri *et al.*, 1995) and bovine adenylyl cyclase appears to be strongly inhibited by exposure to 1mM dithiothreitol (Lazard *et al.*, 1989).

1.13.2 Non-olfactory receptor mediated

Non-receptor mediated mechanisms for odorant sensitivity come under two major categories: protein-based effects and lipid-based effects. These allow the odorant to bypass olfactory receptors and target other proteins to bring about neuronal depolarisation.

Concanavalin A suppresses the EOG generated by isobutylmercaptan suggesting the involvement of glycosylated proteins in the response to thiol odorants (Shirley *et al.*, 1987a), however embedded in the membrane of olfactory cilia there are proteins other than olfactory receptors capable of interactions with odorants. Perhaps the most potent of these proteins are the ion channels, which experiments have suggested can directly interact with odorants in the ORNs of rats (Sanhueza and Bacigalupo, 1999; Seebungkert and Lynch, 2001) and newts (Kawai, 1999). These effects may be neuronal-based rather than olfactory-specific (Seebungkert and Lynch, 2001) but provide a potential method for increased sensitivity to an odorant by providing an alternative binding site that again results in changes in membrane polarisation. However, many of the effects reported in the literature show inhibitory effects and thus while they may influence the precise electrical response to an odorant they are unlikely to lead to markedly greater odorant sensitivity.

Where an odorant is able to penetrate the ORN membrane there is another set of protein targets that may be influenced to produce depolarisation: the cytoskeleton. The actin cytoskeleton is known to be involved in neurite growth and synapse

formation but may also regulate ion channel activity (Maguire *et al.*, 1998). Work on whole cell currents in retinal neurons in the tiger salamander showed that disruption of the cytoskeleton enhanced whole cell K^+ currents (Maguire *et al.*, 1998), although this has not been demonstrated in mammalian neurons. Again these effects are likely to be neuronal rather than olfactory-specific but they do provide a non-receptor mediated mechanism for cell depolarisation.

In addition to protein-mediated effects it is also possible that direct interactions occur between odorants and the lipid bilayer of the olfactory cilia. Experiments performed using N-18 neuroblastoma cells, unrelated to olfactory receptor cells and therefore unlikely to express olfactory receptors, odorant exposure leads to membrane depolarisation (Kashiwayanagi and Kurihara, 1985). The same study also demonstrated that different odorants interact with alternative regions in the lipid bilayer *e.g.* fluid regions, gel regions, border regions and have differential effects on the membrane potential. These responses included depolarisation and hyperpolarisation effects and were demonstrated to be dose-dependant and independent of the external K^+ concentration. Later studies using azolectin liposomes also showed that the composition of the lipid bilayer influenced the sensitivity of the odorant responses (Nomura and Kurihara, 1987). In both studies, the odorant concentrations eliciting membrane potential changes showed good correlation with the thresholds for odorant detection in the frog olfactory system.

1.14 Role of cysteine residues in the olfactory system

Research groups studying olfaction in the 1970s were already investigating the potential role of sulphydryl groups in the olfactory system. The sulphydryl groups of cysteine residues are key factors in the creation and maintenance of the tertiary

structure of many proteins but subsequent research on the olfactory system has since highlighted additional ways in which protein sulphydryl groups can influence odorant detection.

Recent sequence analysis of the olfactory receptor genes illustrates the relative importance of cysteine residues in olfactory receptors. Olfactory receptor families are defined by 40-60% sequences homology and yet cysteine residues show >80% conservation in seven positions across all known human olfactory receptor sequences (Fuchs *et al.*, 2001). Two of these cysteine residues are found in the predicted 1st and 2nd extracellular loops of olfactory receptors and by homology with other G protein-coupled receptors in the same family are predicted to form a disulphide bond (Strader *et al.*, 1989). However, the role of cysteine residues may not be purely structural.

Cysteine residues have also been implicated in the binding site for odorant-mediated inhibition of delayed rectifier K^+ channels in amphibians and mammals (Seebungkert and Lynch, 2001). Evidence for cysteine residue involvement in odorant binding by olfactory receptors comes from many studies involving the derivatisation of cysteine residues with sulphydryl-directed reagents (Villet, 1974; Singer *et al.*, 1975; Menevse *et al.*, 1978; Shirley *et al.*, 1983). This derivatisation selectively reduces the EOG amplitude in response to certain odorants, a specific effect reduced by pre-exposure of the olfactory tissue to these odorants (Menevse *et al.*, 1978). The key cysteine residues may be involved in direct interactions with odorants or as recently proposed may be part of a metal-ion binding motif (Wang *et al.*, 2003a).

Cysteine residues are also crucial to the efficiency of the subsequent transduction systems. Bovine adenylyl cyclase is strongly inhibited by exposure to

1mM dithiothreitol (Lazard *et al.*, 1989) and the sulphydryl directed reagents iodoacetamide (IAA) and N-ethylmaleimide (NEM) have been shown to cause immediate CNG channel opening via derivatisation of intracellular thiol groups (Broillet, 2002). The cysteine residues in the latter case being of potential importance during the development/regeneration of the olfactory system (Broillet, 2002).

1.15 Application of proteomics techniques in olfactory research

The application of proteomics approaches to the search for an olfactory "receptor" for thiol odorants allows a relatively unbiased search of all proteins with the potential to interact with these compounds. There are however, a number of criteria used to define the required properties of any putative "receptor" protein. As discussed in section 1.13, the protein responsible for primary interactions with thiol compounds need not be a traditional membrane-bound protein receptor. For this reason, putative candidates for interactions with thiol odorants are referred to as thiol sensors.

The main advantage of proteomics techniques is the unbiased nature of the protein selection and identification processes. There are set criteria that must be fulfilled by any candidate thiol sensor however, these do not include the presence of extracellular domains or membrane localisation so all proteins of the cilia proteome are regarded as potential sensors. This approach is only made possible by the ability to generate a specialised preparation enriched for cilia and therefore ciliary proteins, from both the olfactory and respiratory epithelium in the nasal cavity.

The use of mass spectrometry as a tool for protein identification also allows the search to go beyond proteins without specific antibodies raised against them and thus no specific hypothesis on a detection mechanism is applied at the start of experiments. Two different types of mass spectrometry are utilised in this study:

matrix-assisted laser desorption/ionisation time of flight (MALDI-ToF) mass spectrometry and tandem mass spectrometry, identifying proteins by a peptide mass fingerprint or peptide sequence data respectively. These types of mass spectrometry and their respective data analysis methods are discussed in detail in Chapter 3 and Chapter 4.

1.16 Criteria for putative thiol sensor

The use of a broad ranging approach such as proteomics to address the mechanism of thiol odorant detection and sensitivity necessitates the definition of properties that must be exhibited by a putative thiol sensor candidate.

The ultimate requirement of any putative thiol sensor is that an interaction between it and a thiol odorant results in the generation of an action potential in the ORN. Traditional odorant receptors and signal transduction pathways could achieve this, but as discussed in section 1.13, this is not the only possible depolarisation mechanism. An alternative route, bypassing olfactory receptors may result in differential processing of the electrical signal from ORNs providing a higher order coding mechanism for aversion or may simply allow stimulate a greater number of ORNs.

As the majority of odorant detection is a specific property of the ORNs, it is assumed that any interactions involved in odorant detection occur on the surface/in the olfactory cilia. This subproteome will therefore be considered as containing candidates for putative thiol sensor proteins.

In order to be maximally effective as a chemical deterrent, thiol compounds must invoke an aversive reaction in a range of potential threats/predators. This requires that the detection mechanism should be conserved across multiple species.

To address this, three model species are used in this work: mouse, rat and sheep. The rodent species are closely related in evolutionary terms but wider levels of conservation will become apparent upon comparison with sheep cilia preparations. These three species exhibit differing dependency on olfaction according to their individual lifestyles, therefore conservation of individual/groups of proteins across the species would emphasise the importance of these molecules in the olfactory process.

This work also explores the possible involvement of cysteine residues in the olfactory detection of thiol compounds. The potential importance of cysteine residues in odorant detection was discussed in Section 1.14. Given that these residues are implicated in the specific interactions between some odorants and their respective receptors as discussed previously, a hypothesis was proposed that cysteine residues could play a direct role in the detection of thiol odorants.

The involvement of cysteine residues provides a potential mechanism for sensitivity via increased receptor-odorant interactions/affinity (Figure 1.8). Interactions involving two sulphydryl groups and the subsequent generation of disulphide bonds provide an attractive mechanism for strong links between a thiol odorant and its receptor. As discussed in Section 1.14 increasing the chances that an interaction between ligand and receptor results in membrane depolarisation can improve odorant sensitivity. In this model the interaction is improved via its strength and reduced dependance on the adoption of a precise molecular conformation by the odorant ligand. The potential for the formation of disulphide linkages also permits an efficient method of receptor recycling, using reducing agents to disrupt the interaction and release the odorant.

Figure 1.8 A theoretical cycle of thiol odorant binding by an olfactory receptor

A thiol compound interacts with the olfactory receptor and forms a disulphide bond. The generation of the disulphide bond induces the internalisation of the receptor into the olfactory cilia lumen. Inside the membrane vesicle formed during internalisation, the disulphide linkage is reduced and the thiol odorant dissociates from the receptor. The olfactory receptor is then re-cycled back to the surface of the olfactory cilia.

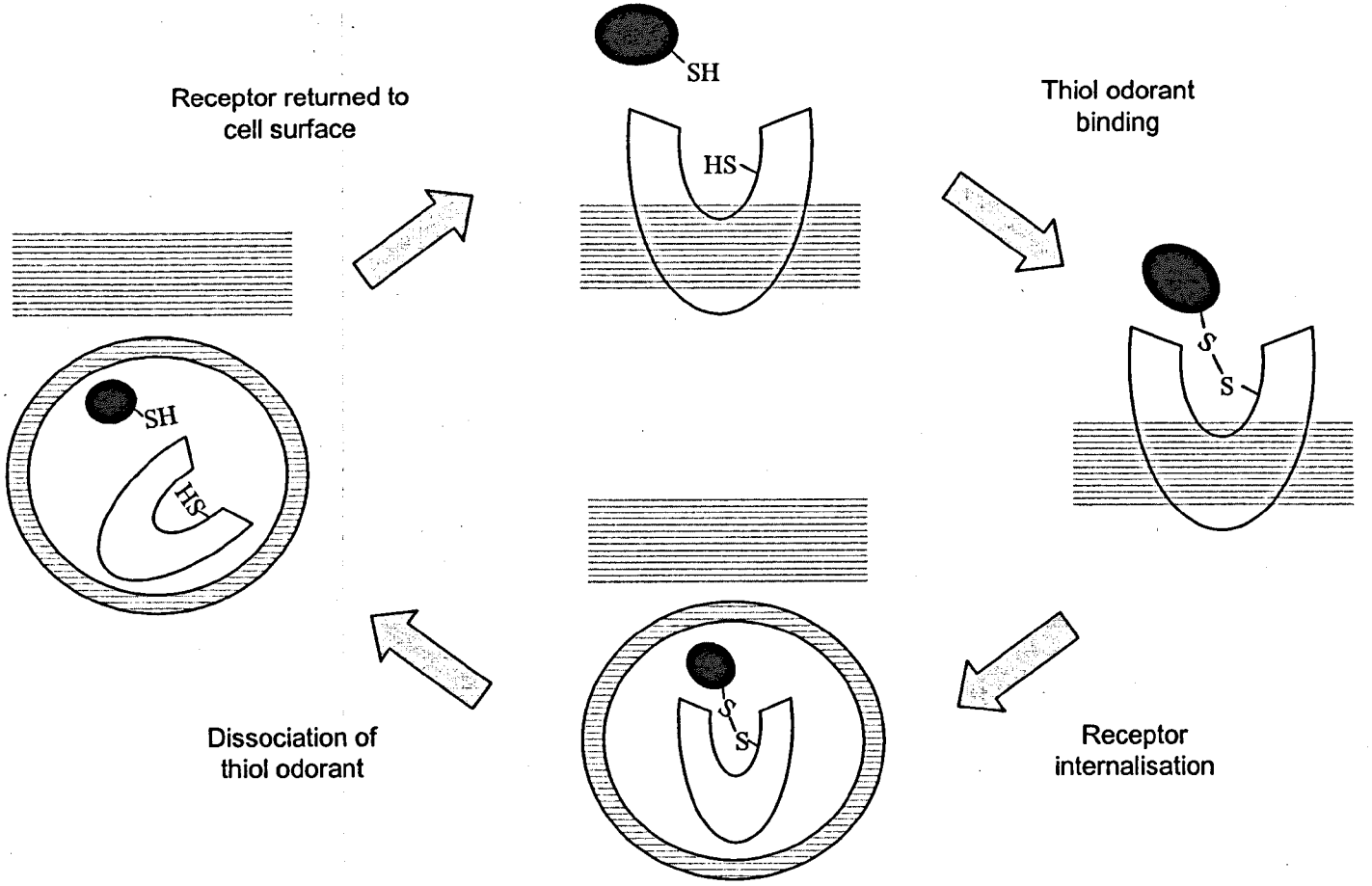
Receptor returned to cell surface
SH
HS
Thiol odorant binding
S
S
Receptor internalisation
S
S
Dissociation of thiol odorant
SH
HS

1.17 Experimental Strategy

The experimental strategy employed consists of two major approaches. The first experiments attempt to identify proteins that are unique to olfactory cilia by comparison with non-sensory nasal respiratory cilia. The same method (taken from Sklar *et al.*, 1986) was used to prepare enriched cilia fractions from nasal turbinates and the nasal septum to isolate olfactory and respiratory cilia respectively. The proteins of the enriched cilia peparations were then separated using two-dimensional polyacrylamide gel electrophoresis (2D-PAGE), which provided a 2D protein profile for olfactory and respiratory cilia to allow comparisons of proteins present in either preparation.

In addition to the requirement that a putative thiol sensor should be unique to olfactory cilia, candidate proteins should be conserved across the three model species. An identical method was used for the preparation of olfactory cilia from each species and the proteins were then separated by 2D-PAGE to allow the analysis and comparison of their 2D protein profiles.

The potential role of cysteine residues was explored using the targeted labelling of sulphydryl groups. Two labelling reagents were employed during this work, Iodoacetyl-long chain-biotin (I-LC-biotin) and Lucifer Yellow iodoacetamide (LYIA). The membrane-permeable I-LC-biotin allowed the visualisation of proteins bearing cysteine residues that could potentially interact with thiol odorants and the supplementary use of LYIA enabled the intracellular/extracellular disposition of the exposed cysteine residues to be determined.

Proteins bearing exposed cysteine residues were considered as putative candidates for thiol sensors if present in the olfactory cilia of the three model species,

present at a significantly reduced level in the cilia derived from the septum and could potentially influence membrane polarisation states.

1.18 Project aims and objectives

This work aims to elucidate possible mechanisms for the olfactory detection of thiol compounds. Proteomics techniques for protein separation and identification will be used to perform a relatively unbiased survey of the olfactory cilia proteome to discover candidate proteins with the potential to interact with thiol compounds and initiate a membrane depolarisation event. It is also hoped that this work will provide an insight into the involvement of the primary coding mechanisms of olfaction in the perception of unpleasant odours. Working towards the goal, a series of objectives were set.

The primary objective was the establishment of protocols for the preparation of enriched olfactory cilia fractions from mouse, rat and sheep nasal turbinates and respiratory cilia fractions from rat nasal septum. The next objectives were to optimise the 2D-PAGE resolution of cilia proteins to enable effective comparison of the cilia proteomes of the model species and to establish the trypsin digestion/mass spectrometry system of protein identification. The specific labelling of proteins bearing free, exposed cysteine residues was then introduced to allow the visualisation of candidate thiol sensor proteins for subsequent identification by mass spectrometry. The targeted labelling of cysteine residues was also modified in the latter stages of experimental work to investigate the metalloprotein hypothesis of receptor function.

Chapter 2

MATERIALS AND METHODS

2.1 Buffer recipes

2.1.1 Dissection Protocols

- Krebs-Ringer solution: 120mM NaCl, 5mM KCl, 1.6mM K_2PO_4, 1.2mM $MgSO_4$, 25mM $NaHCO_3$, 7.4mM glucose, pH 8.0

Animals used were obtained from the Biological Services Unit (BSU) at University of Liverpool or Leahurst Veterinary Field Station, University of Liverpool. Mice used were of in-bred strains BALB/c, CBA and CBA x wild (first generation cross) and weighed approximately 25g. Rat tissue was obtained from either Lister-Hooded or Wistar rats (180-250g). Sheep obtained were Lleyn cross-breeds aged 6-12 months.

2.1.2 Membrane/enriched cilia preparation

- Krebs-Ringer solution: 120mM NaCl, 5mM KCl, 1.6mM K_2PO_4, 1.2mM $MgSO_4$, 25mM $NaHCO_3$, 7.4mM glucose, pH 8.0
- PBS/EDTA buffer: 20mM Na_2HPO_4, 150mM NaCl, 1mM EDTA pH 8.0
- Homogenisation buffer: 10mM TrisHCl, 3mM $MgCl_2$, 1mM EDTA pH 8.0

2.1.3 One-dimensional SDS-PAGE

- 2x SDS-PAGE sample buffer: 62.5mM TrisHCl pH 6.8, 10% (v/v) glycerol, 100mM DTT, 2% (w/v) SDS, 0.001% (w/v) bromophenol blue
- SDS-PAGE running buffer: 25mM Tris, 192mM glycine, 1% (w/v) SDS

2.1.4 Two-dimensional gel electrophoresis (2D-PAGE)

- Rehydration buffer (1.25x): 8.75M urea, 2.5M thiourea, 0.35% (v/v) ampholyte, 125mM DTT, 0.001% (w/v) bromophenol blue
- Rehydration buffer: 1 volume 200mM Tris/10% (v/v) Triton X-100, 4 volumes 1.25x rehydration buffer
- Equilibration buffers: Either 2% (w/v) DTT or 2.5% (w/v) IAA added to 6M urea, 2% (w/v) SDS, 375mM TrisHCl, 20% (v/v) glycerol, 0.001 (w/v) % Bromophenol blue
- Agarose : 0.5% (w/v) agarose dissolved in SDS-PAGE running buffer
- SDS-PAGE running buffer: 25mM Tris, 192mM glycine, 1% (w/v) SDS

2.1.5 Western blotting

- Electrotransfer buffer: 15.6mM Tris, 120mM glycine, 10% (v/v) methanol
- TTBS: 0.05% (v/v) Tween-20/10mM Tris, 150mM NaCl pH 7.5
- TBS: 10mM TrisHCl, 150mM NaCl pH 7.5
- Alkaline Phosphatase buffer: 100mM TrisHCl, 100mM NaCl, 5mM $MgCl_2$ pH 9.5
- BCIP/NBT solution: Sigma Fast™ BCIP/NBT tablets or ready-to-use BCIP/NBT solution (Sigma, Dorset, UK)

2.1.6 Protein staining methods

Coomassie stain

- Coomassie brilliant blue stain: 0.25% (w/v) Coomassie brilliant blue, 50% (v/v) methanol, 12.5% (w/v) trichloroacetic acid
- Coomassie destain solution: 50% (v/v) methanol, 5% (v/v) acetic acid

Silver nitrate stain

- Fixation solution: 50% (v/v) methanol, 5% (v/v) acetic acid
- Sensitising solution: 0.2% (w/v) $Na_2S_2O_3$
- Silver nitrate solution: 0.1% (w/v) $AgNO_3$

- Development solution: 2% (w/v) Na_2CO_3, 0.05% (v/v) formaldehyde

PonceauS stain

- PonceauS stain: 0.1% (w/v) PonceauS in 5% (v/v) acetic acid
- PonceauS destain: 100mM NaOH

Amido black stain

- Amido black stain: 0.1% (w/v) Amido Black 10B/25% (v/v) isopropanol/10% (v/v) acetic acid
- Amido black destain: 25% (v/v) isopropanol/10% (v/v) acetic acid

2.1.7 Sulphydryl group labelling: Iodoacetyl-Long Chain-Biotin

- Krebs-Ringer solution: 120mM NaCl, 5mM KCl, 1.6mM K_2PO_4, 1.2mM $MgSO_4$, 25mM $NaHCO_3$, 7.4mM glucose, pH 8.0
- PBS/EDTA buffer: 20mM Na_2HPO_4, 150mM NaCl, 1mM EDTA pH 8.0
- Iodoacetyl-Long Chain-Biotin: 4mM I-LC-Biotin/100% dry DMF (Pierce - distributed by Perbio Science, Cheshire, UK)
- Deciliation buffer: 100mM TrisHCl pH 8.0
- BCIP/NBT solution: Sigma Fast™ BCIP/NBT tablets or ready-to-use BCIP/NBT solution (Sigma, Dorset, UK)

2.1.8 Sulphydryl group labelling: Lucifer Yellow Iodoacetamide

- Krebs-Ringer solution: 120mM NaCl, 5mM KCl, 1.6mM K_2PO_4, 1.2mM $MgSO_4$, 25mM $NaHCO_3$, 7.4mM glucose, pH 8.0
- PBS/EDTA buffer: 20mM Na_2HPO_4, 150mM NaCl, 1mM EDTA pH 8.0
- Lucifer Yellow Iodoacetamide: 6.5mg/ml reconstituted using milliQ water (Molecular Probes - distributed by Cambridge BioSciences, Cambridgeshire, UK)
- Deciliation buffer: 100mM TrisHCl pH 8.0

2.1.9 In-gel trypsin digestions

Manual in-gel digestions

- Destain solution: Freshly prepared 15mM $K_3Fe(CN)_6$, 50mM $Na_2S_2O_3$

Automated in-gel digestions

- Digestion buffer: 100mM NH_4HCO_3
- Destain solution: Freshly prepared 15mM $K_3Fe(CN)_6$, 50mM $Na_2S_2O_3$
- DTT: 10mM DTT prepared in 100mM NH_4HCO_3 (pH~8.2)
- IAA: 55mM IAA prepared in 100mM NH_4HCO_3 (pH~8.2)
- Extraction buffer: 1% (v/v) formic acid, 2% (v/v) acetonitrile
- Lockmass sample: Adrenocorticotrophic hormone (0.96µg/ml) prepared from stock using MALDI matrix

2.1.10 Electron Microscopy

- Dehydration series: 50%, 70%, 90%, 95%, 100% (v/v) ethanol diluted with distilled H_2O
- 100% acetone
- Resin/acetone: 30%, 70%, 100% (v/v) resin diluted into acetone where required.

2.2 Dissection Protocols

2.2.1 Rat

Adult female rats of weight 180-250g were used during these studies. The animals used were a mixture of Lister-Hooded and Wistar rats and were killed by CO_2 asphyxiation.

The animal was decapitated and the fur and skin on the top of the skull removed. A sharp knife was used to make an incision along the midline weakpoint in the skull (see Figure 2.1) and a sagittal cut extending to the tip of the nose was made to bisect the skull. Any remaining muscular connections between the two halves were severed using dissecting scissors.

To remove the nasal turbinates (see Figure 2.2), a scalpel was inserted along the rostral side of the cribiform plate. Further incisions were made along the ventral and dorsal sides of the turbinate region. The turbinates were then removed using sharp-ended tweezers with scalpel incisions being made between the turbinates and the olfactory nerve bundles as required.

The intact septum was gently removed using sharp-end tweezers. The respiratory epithelium preparations were made from the membranous tissue lining the septum. This was easily removed from the septum using a clean scalpel blade.

Dissected tissue was stored in 1ml Krebs-Ringer solution supplemented with 2mM EDTA (subsequently referred to as Krebs-Ringer/EDTA) for up to 1.5h before further processing. In the event of prolonged storage i.e. during periods where other samples were undergoing labelling procedures, the Krebs-Ringer/EDTA was replaced with fresh buffer and samples stored on ice until required.

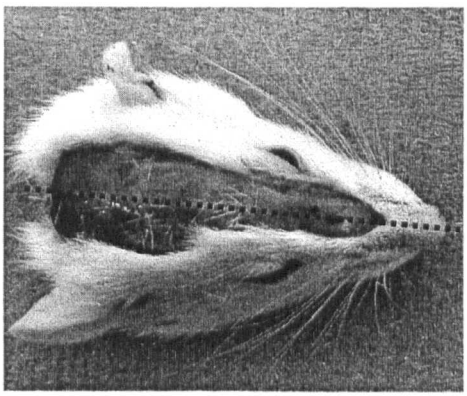

Figure 2.1 Digital photograph of the head of a female Wistar rat

The dotted line indicates the midline weakpoint.

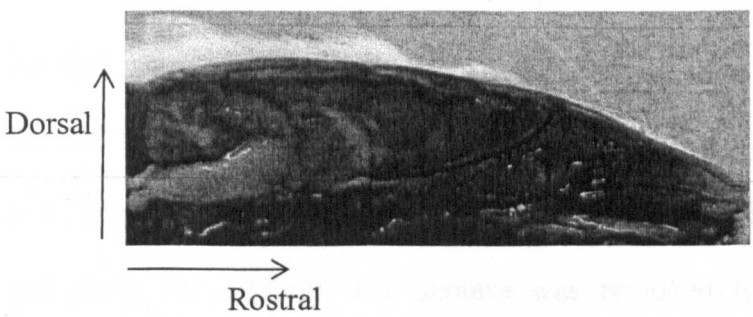

Figure 2.2 Digital photograph of the sagittal section of the head of a female Wistar rat

The boxed area encloses the nasal turbinates from which the enriched olfactory cilia preparations were derived and the solid line indicates the approximate position of the cribiform plate.

2.2.2 Sheep

Animals were purchased from local farms and were Lleyn-cross breeds. The majority of experiments (protein characterisation and labelling) were performed using the olfactory tissue of lambs aged 6-12 months. Additional samples were also taken from adult sheep. All animals were sacrificed by a lethal injection of sodium phenobarbitol, the animal was then decapitated and the skin removed from the top of the skull. The head was bisected along the midline, leaving the septum intact. The nasal turbinates were then exposed and crudely dissected using a sharp knife. Areas of respiratory epithelium were removed from the turbinates using a scalpel, before the olfactory tissue was placed in 1ml Krebs-Ringer/EDTA solution for further processing. Fresh tissue storage times averaged 30-60min.

2.2.3 Mouse

Adult animals of the in-bred strains BALB/c and CBA and CBA/wild (first generation cross) and approximately 25g in weight were used during this work and were euthanased using fluoroethane vapour.

The skin and fur from the top of the head were removed to expose the surface of the skull plates down to the tip of the nose. A scalpel was then used to make a sagittal cut along the midline. The septum was removed to expose the nasal turbinates and once exposed, the turbinates were dissected out using a scalpel and sharp-end tweezers. The tissue was stored on ice in 1ml Krebs-Ringer/EDTA as described for rat tissue samples.

2.3 Sample preparation

2.3.1 Olfactory/respiratory cilia preparations

Nasal turbinates were dissected, washed with 1ml Krebs-Ringer/EDTA and pelleted by centrifugation at 1000g, 3 min. All centrifugation steps were performed at 4°C. The wash supernatant was removed and marked as "tissue wash". Sheep turbinates tended to have increased levels of associated mucus and were therefore washed three times prior to further processing.

Enriched cilia fractions were prepared as described by Sklar et al. (1986). The tissue was resuspended in 100mM TrisHCl pH8.0 to which $CaCl_2$ was added to a final concentration of 10mM. The tissue suspension was then incubated on an end-to-end shaker for 20 min at 4°C.

The deciliated olfactory epithelium was removed by centrifugation at 6000g, 5min. The supernatant was collected and further centrifuged at 12000g, 10 min. The pellet from this high-speed centrifugation is the enriched olfactory cilia fraction and was washed once using 50µl PBS/EDTA buffer prior to storage at –20°C.

Respiratory cilia were prepared in the same way as olfactory cilia using the epithelium derived from the nasal septum as the starting material.

2.3.2 Crude membrane preparation

Crude membrane fractions were prepared as described by Chen et al. (1986). Dissected tissue was washed in 1ml Krebs-Ringer/EDTA and pelleted by centrifugation at 1000g, 3 min at 4°C. It was then homogenised in 5 volumes of 10mM TrisHCl/3mM $MgCl_2$/1mM EDTA pH 7.5 buffer using an Eppendorf pestle.

Intact tissue/cells were pelleted by centrifugation at 80g, 2 min. The supernatant was centrifuged twice further at 1500g, 10 min and the membrane

fraction isolated by a final centrifugation at 21334g, 30 min. The pellet obtained was marked as "membrane pellet" and stored at -20°C for subsequent analysis.

2.4 Protein Assay

The protein assay used in this work was a 2D-Quantification kit (Amersham Biosciences, Bucks.) based on the quantitative precipitation of proteins from 2D-gel sample buffer.

2.4.1 Protein assay method

The protein assay was performed according to the manufacturer's instructions. Briefly, samples of no greater than 50µl volume were placed in 1.5ml centrifuge tubes and mixed with 500µl "Precipitant" by a 5s vigorous vortex. Samples were left to stand at room temperature for 3 min, before 500µl "Co-precipitant" was added to each tube and the samples mixed for a further 5s. They were then centrifuged at 21334g, 10 min and the supernatant quickly removed. The protein pellets were resuspended in 100ul "Copper solution" and 400µl MilliQ water and then mixed with 1ml "Working colour reagent". Samples stood at room temperature for 20-25 min before the absorbance at 480nm was measured on a spectrophotometer using MilliQ water as a reference.

Generation of the calibration curve BSA standards, 0-50µg from a 2mg/ml stock provided, were placed in 1.5ml centrifuge tubes. An equal volume of a 2.5-fold dilution of 1x 2D-rehydration or SDS-PAGE sample buffer was added as appropriate. Protein precipitation and quantitation was performed as described above and a calibration curve prepared using Microsoft Excel. The linear equation was used to estimate protein concentration in experimental samples and the r^2 value used to

assess the accuracy of the calibration. No calibration curves with r^2 values of less then 0.95 were obtained.

Low Abundance Samples Samples with low protein levels were spiked with 20μg BSA prior to performing the quantitation assay. This pushed their absorbance values from below the 10μg protein standard into the linear region of the calibration curve. Protein concentration estimates/sample absorbances were used to achieve identical protein loading on 2D-gels.

It is accepted that the addition of a fixed amount of BSA to each sample prior to performing the protein assay introduces an additional variable and the potential for reducing the accuracy of the final results. Nevertheless it was performed to ensure that the experimental samples contained sufficient protein to fall within the linear range of the protein assay used. It was also necessary due to the inclusion of a protein precipitation step in the assay protocol (removes contaminants e.g. urea, SDS), which hinders the scaling down of the sample/reagent usage and spectrophotometry in a microcuvette.

As will be shown in Chapter 3 (section 3.2) the protein assay assisted in the equal protein loading of samples for 2D-gels but not for samples prepared for SDS-PAGE.

2.4.2 Use of "Dot Blots" for protein concentration estimation

To achieve equal protein loading on SDS-PAGE gels, the protein samples were resuspended in 10μl of 10mM Tris, 3mM $MgCl_2$, 1mM EDTA by vigorous vortex mixing. A small volume (typically 1μl) of each sample was spotted onto a piece of nitrocellulose membrane and allowed to dry. The membrane was then stained using Amido Black 10B as described in section 2.8.2.

Densitometry analysis was performed on the destained membrane using Phoretix software (get version and manufacturer). Samples were then diluted according to relative protein concentration estimates and the 1µl "dot blot" performed again. This process was repeated until all samples showed similar staining intensities as indicated by densitometry.

2.5 One-dimensional SDS-PAGE

SDS-PAGE gels were run according to the manufacturer's instructions. The gel solutions used are described in Table 2.1 and 2.2.

Samples for analysis were diluted by the addition of an equal volume of 2x SDS-PAGE sample buffer and heated at 100°C for 5 min. Samples were allowed to cool and briefly centrifuged before the appropriate quantities were loaded onto the gel. Gel loading volumes ranged from 5-20µl for mini-gels and 5-50μl for large format gels.

Two mini-gel systems were predominantly used during this work: the Protean II® and Mini-Protean® 3 systems, both produced by Bio-Rad, Herts. Gel assembly and running procedures were as described in the respective manuals.

Large format gels were also run using the Hoefer Ruby system (Amersham Biosciences, Bucks.) according to the manufacturer's guidelines.

2.6 Two-dimensional gel electrophoresis (2D-PAGE)

2.6.1 First Dimension: Isoelectric Focussing

Isoelectric focussing (IEF) was performed using immobilised pH gradient (IPG) strips purchased from BioRad, Herts. Cilia/membrane pellet samples were defrosted and resuspended in 200mM Tris/10% (v/v) Triton X-100 by vigorous vortex mixing

	7cm Mini-gels		Large format gels
	10%	*12%*	*10%*
30% (w/v) acrylamide	3.3ml	4.0ml	33ml
1.5M TrisHCl pH 8.8	2.5ml	2.5ml	25ml
MilliQ water	4.1ml	3.4ml	41.5ml
20% (w/v) SDS	25µl	25µl	500µl
10% (w/v) APS	75µl	75µl	1ml
TEMED	10µl	10µl	66µl

Table 2.1 Resolving gel solutions for 7cm and large format SDS-PAGE gels
Percentage values refer to the final concentration of acrylamide in the gel.

	7cm Mini-gels	Large format gels
30% (w/v) acrylamide	650µl	1.95ml
0.5M TrisHCl pH 6.8	1.25ml	3.75ml
MilliQ water	3.05ml	9.9ml
20% (w/v) SDS	25µl	75µl
10% (w/v) APS	50µl	150µl
TEMED	5µl	15µl

Table 2.2 Stacking gel solutions for 7cm and large format SDS-PAGE gels.

for 30s. Four volumes of 5/4 strength rehydration buffer was then added to each sample to give a final volume of 230µl for direct sample loading or 250µl for controlled protein loading. Samples were then rotated on a cylinder mixer at room temperature for at least 2h before insoluble material was removed by centrifugation at 21334g, 30 min.

Where necessary, 10µl solubilised sample was used to assess sample protein concentration using the 2D-quantitation kit (Amersham Biosciences, Bucks.)) as described in section 2.4. Samples were then diluted in rehydration buffer to acheive equal protein concentrations.

Protein samples (190µl) were gently pipetted along the length of the 11cm IEF tray. The protective film on the IPG strips was removed and the strips placed gel-side down onto the sample, ensuring that no air bubbles were trapped between the rehydration buffer and the strip. The IPG strips were then covered in a layer of mineral oil.

Isoelectric focussing was performed using the PROTEAN IEF cell (Bio-Rad, Herts.), programmed according to the focussing steps listed in Table 2.3. Once the focussing program was completed, the IEF tray was removed from the unit and the IPG strips were taken out. To remove excess mineral oil, MilliQ water was gently pipetted down the front and back of the strip three times. The strips were then placed gel side-up in an equilibration tray in preparation for the second dimension.

In cases where the second dimension was not run immediately after the IEF step, the IPG strips were removed from the focussing tray, briefly blotted on tissue paper and then stored in an equilibration tray at -20°C.

	7cm IPG Strips		11cm IPG strips	
Step	*End voltage (V)*	*Time (Vh)*	*End voltage (V)*	*Time (Vh)*
1	50	500	50	500
2	200	400	200	400
3	1000	2000	1000	2000
4	4000	25000	2000	2000
5	-	-	4000	8000
6	-	-	8000	25000
Hold	500	8 hours	500	8 hours

Table 2.3 Isoelectric focussing conditions used for 7cm and 11cm immobilised pH gradient (IPG) strips
(Vh denotes voltage hours).

	7cm IPG strip	11cm IPG strip	11cm IPG strip
	Mini-gel (12%)	*"Criterion" (12%)*	*Large format (12.5%)*
30% (w/v) acrylamide	8.0ml	12.0ml	41.7ml
1.5M TrisHCl pH 8.0	5.0ml	7.5ml	25ml
MilliQ water	6.8ml	10.2ml	32.3ml
20% (w/v) SDS	50µl	75µl	500µl
10% (w/v) APS	150µl	225µl	1ml
TEMED	20µl	30µl	66µl

Table 2.4 Solutions for the preparation of second dimension gels
Defined percentage values indicate final acrylamide concentration in the gels. Each solution is sufficient for the preparation of two gels.

Sample preparation was identical for linear and non-linear IPG strips. When 7cm IPG strips were used, the loading volume of the sample was reduced to 130µl and the solubilisation volumes were lowered accordingly.

2.6.2 IPG Strip Equilibration

IPG strips were fully immersed in freshly prepared equilibration buffer containing 2% (w/v) DTT. The strips were incubated in this buffer for 20 min at room temperature and were then transferred into a clean equilibration tray. They were then covered in a second equilibration solution containing 2.5% (w/v) IAA and were exposed to this buffer for a further 20 min, in the dark, before being placed onto the second dimension gel.

2.6.3 Second Dimension: SDS-PAGE

The solutions used to prepare the polyacrylamide gels for the second dimension are listed in Table 2.4. Equilibrated strips were placed on top of the gel, allowing the plastic backing to adhere to the back gel plate. Molecular weight markers were added by pipetting 2µl SDS-PAGE broad range marker onto the shortest edge of a small rectangle of filter paper, which was then positioned adjacent to the acidic end of the IPG strip. The strips and filter paper were sealed in place using 0.5% (w/v) agarose.

11cm large format gels The large format gels were sealed against the upper reservoir chamber according to the manufacturer's instructions and were placed in an electrophoresis tank containing SDS-PAGE running buffer. The cooling unit was switched on and 500ml SDS-PAGE running buffer poured slowly into the upper reservoir. Gels were run at 15mA per gel (constant current) for 30 min and then at

30mA per gel until the dye migration front had reached the base of the gel (typically 4-5h).

7cm mini-gels The gel was placed in a mini-Protean 3 electrophoresis tank and the inner and outer chambers were filled using approximately 1l SDS-PAGE running buffer. The gels were run at 200V (constant voltage) for 45 min or until the dye migration front had reached the base of the gel.

11cm Criterion gels The sealing tape was removed from the base of the gel casing and the gels placed in an electrophoresis tank. The gel case upper reservoir and the lower chamber of the tank were filled with SDS-PAGE running buffer and the gels run at 200V (constant voltage) for 90 min or until the dye migration front had reached the base of the gel.

2.6.4 Optimisation of rehydration buffer used for isoelectric focussing

Crude membrane preparations were performed according to the protocol described in Section 2.3 but immediately prior to the final centrifugation, the supernatants from the previous centrifugation were pooled, vortexed vigorously for 30s and distributed equally between the appropriate numbers of 500µl microfuge tubes. These microfuge tube samples were then centrifuged at 21000g, 60 min to generate a number of equivalent crude membrane protein preparations. These preparations were resuspended in 200µl of the test rehydration buffer by vigorous vortexing (30s) and subsequent incubation at room temperature 1h. Insoluble material was removed from the samples by

centrifugation at 21000g, 60 min. The supernatant was then either diluted for SDS-PAGE analysis or loaded onto IPG strips in later optimisation tests.

2.7 Western Blotting

2.7.1 Protein transfer procedure

The basic protocols for protein transfer and Western blotting were taken from Bollag and Edelstein (1991).

SDS-PAGE or 2D-gels were removed from the apparatus and equilibrated in electrotransfer buffer for 15-20 min. Two pieces of filter paper and one piece of nitrocellulose membrane were cut to match the size of the gel and pre-soaked alongside two fibre pads in electrotransfer buffer for 5 min. Western transfer apparatus including the tank, cooling unit (where used) and gel cassettes was rinsed in distilled water immediately prior to use.

The gel sandwiches were assembled and placed in a transfer tank filled with electrotransfer buffer. Where a cooling unit was utilised, it was placed in the tank immediately prior to the addition of the transfer buffer. A magnetic stirrer was also used to ensure efficient buffer circulation and cooling.

Precise transfer conditions were dependant on gel width. The BioRad mini-Protean blotting system (BioRad, Herts.) was used for protein transfer from 7cm gels at 75V (fixed voltage) for 1.5h. Large format 11cm gels were blotted using the Hoefer Transphor system (Amersham Biosciences, Bucks.) run at 100mA overnight.

Following the transfer procedure, the nitrocellulose membrane was removed from the transfer apparatus, placed in blocking solution and incubated overnight at 4°C. The SDS-PAGE gel was retained after transfer and subsequently stained to assess protein transfer efficiency.

2.7.2 Membrane development using antibodies (Western blot)

After incubation in blocking solution the membrane was rinsed in TBS (20 min, three changes of buffer). The primary antibody solution was prepared in a final volume of 15ml and incubated with the membrane for 2h at room temperature with constant agitation. The antibody solution was then removed and the membrane washed three times in TBS.

The secondary antibody was diluted appropriately in a final volume of 15ml and added to the membrane. The membrane was exposed to the secondary antibody solution for 2h before being washed twice in TBS (10 min each) and equilibrated in alkaline phosphatase buffer (5 min). Fresh BCIP/NBT solution was used to develop the membrane and the reaction was stopped by removing the solution and rinsing the membrane with TBS containing 20mM EDTA (TBS/EDTA).

2.8 Protein staining methods

2.8.1 SDS-PAGE/2D-PAGE gel compatible protein staining methods

Coomassie Blue Fast stain Gels were placed in Coomassie brilliant blue stain. Where fresh stain was used, the gel was left in the staining solution for 1h before the solution was removed and replaced with destain solution. Where recycled Coomassie stain was utilised, the incubation time for the gel was extended to an overnight period before the destaining process.

During destaining, a small piece of tissue was added into the container with the destain solution. This acted, in part to soak up part of the coomassie stain once released from the gel and improved the speed and efficiency of the destain process.

Colloidal Coomassie Stain Gels were washed in MilliQ water for 30 min with three changes of water. They were then incubated in Bio-Safe™ coomassie (Bio-Rad, Herts.) for a minimum of 60 min. The stain was then poured off and the gel destained by an overnight incubation in MilliQ water.

Silver-Stain Gels were placed in fixation solution for 25-30 min or overnight. The gel was then washed twice in MilliQ water (2 mins each) and left in fresh MilliQ water for an additional 30 min with agitation. The gel was treated with sensitising solution (3 min) and briefly rinsed with two changes of MilliQ water, before being incubated in chilled 0.1% (w/v) $AgNO_3$ at room temperature, with constant agitation for 40 min. The $AgNO_3$ solution was then removed and the gel rinsed briefly in MilliQ water.

Developing solution was added to the gel and was immediately changed upon buffer discolouration. The staining reaction was allowed to proceed as desired and stopped by washing the gel in 1% (v/v) acetic acid three times.

All gels were stored in 1% (v/v) acetic acid at 4°C, until dried or used for in-gel trypsin digestion experiments.

2.8.2 Nitrocellulose membrane compatible protein staining methods

PonceauS Stain Membranes were submerged in 0.1% (w/v) PonceauS solution for 5 min with constant agitation. Background staining was removed by repeated rinsing of the membrane in MilliQ water. Positions of the molecular weight protein bands were marked on the membrane before the stain was completely removed by a brief incubation in 100mM NaOH. Membranes were incubated in blocking solution overnight at 4°C prior to further processing.

Amido-Black Stain Membranes were stained for 1 min in 0.1% (w/v) Amido Black 10B solution and then destained in 25% (v/v) isopropanol/10% (v/v) acetic acid for 30 min. The membranes were soaked for 30 min in MilliQ water before being allowed to air dry.

2.9 Sulphydryl group labelling: Iodoacetyl-Long Chain-Biotin

Iodoacetyl-Long Chain-Biotin (I-LC-biotin) is a membrane-permeable, light sensitive labelling reagent therefore all steps were performed in the dark where possible. I-LC-Biotin adds a hydrocarbon linker and biotin group to free, surface exposed thiol groups of both intracellular and extracellular proteins.

The protein labelling strategies employed are introduced in Chapter 1. The reagent structure and mechanism can be found in Section 5.2.

2.9.1 Tissue labelling: Olfactory epithelium/respiratory epithelium

Freshly dissected nasal turbinates/septal epithelium sheets were rinsed in Krebs-Ringer/EDTA buffer and then resuspended in 1ml PBS/EDTA, to which 30µl I-LC-Biotin (or dry DMF in control experiments) was added. The biotinylation reaction proceeded over 60 min at room temperature in the dark, with gentle agitation on a rotary wheel. The tissue was then pelleted by 1000g, 3min centrifugation and resuspended in 100mM Tris pH 8.0. Enriched olfactory/respiratory cilia preparations were then obtained using the calcium shock method (Section 2.3) and either resuspended in suitable buffers for gel electrophoresis or stored at -20°C until further use.

Although tissue damage was evident during this procedure, it did not appear to adversely affect the final cilia protein yield or gel profiles (see Section 5.2).

2.9.2 Detection of I-LC-Biotin Labelled Proteins

I-LC-Biotin treated protein samples were resolved by SDS-PAGE or 2D-PAGE and blotted onto nitrocellulose as described in Section 2.7.

After an overnight incubation in blocking solution, the membrane was placed in 15ml fresh TTBS containing 0.25μg/ml streptavidin-alkaline phosphatase conjugate. The streptavidin incubation proceeded for 4h and was terminated by the removal of the conjugate-containing solution and subsequent washing of the membrane in TTBS (10 min) followed by TBS (10 min). The membrane was then equilibrated in alkaline phosphatase buffer for 10 min, before being developed using 5ml (large format gel blots) or 10ml (7cm gel blots) BCIP/NBT solution.

Large format blots were allowed to develop for 15 min before the removal of the BCIP/NBT solution and rinsing of the membrane in TBS/EDTA then stopped the reaction. Mini-gel blots (7cm) were incubated in BCIP/NBT solution for up to 1h, based on the development of satisfactory protein band/spot intensities.

The 7cm gel format membranes were incubated with the streptavidin-conjugate containing solution in containers reserved specifically for Western blots. The 11cm format membranes were placed inside pre-rinsed large plastic bottles, with the side of the membrane in contact with the gel during transfer, facing inwards. The bottles were then placed on a cylinder mixer to ensure constant rotation and even treatment of the entire membrane. The rotation of the bottle was such that the membrane did not dry out.

2.9.3 Stripping and re-probing nitrocellulose membranes

During biotin-tag detection procedures where protein loading was not consistent across all samples, it was occasionally necessary to stop the alkaline phosphatase

reaction before all lanes were optimally developed. In these cases, the nitrocellulose membranes were stripped of the streptavidin-alkaline phosphatase conjugate and reprobed.

The membrane was submerged in stripping buffer and incubated in a water bath at 70°C for 30 min with gentle agitation at the beginning and end of the incubation. The membrane was then washed twice in 0.05% (v/v) Tween-20/TBS for 10 min at room temperature. The membrane was placed in blocking solution for 1h at room temperature with constant agitation, before being stored in the same solution overnight at 4°C. The biotinylated proteins were then detected as described above.

2.10 Sulphydryl group labelling: Lucifer Yellow Iodoacetamide

Lucifer-Yellow iodoacetamide (LYIA) is a membrane-impermeable, light-sensitive thiol-targeting probe that attaches a fluorescent label to all proteins bearing free cysteine residues exposed to the extracellular environment. LYIA was stored in discreet amounts (100-600mg) at -20°C and the reagent was freshly reconstituted to a concentration of 6.5mg/ml in MilliQ water immediately prior to use. Each sample of LYIA was used for a single experiment before being discarded to avoid issues of reagent degradation.

The protein labelling strategies employed are discussed in Chapter 1. The reagent structure and mechanism can be found in Section 5.2. Although tissue damage was evident during these procedures, it did not appear to adversely affect the final cilia protein yield or gel profiles (Section 5.2).

2.10.1 Tissue labelling: Olfactory epithelium/Respiratory epithelium

The dissected nasal turbinates/septal epithelia were washed in 1ml Krebs-Ringer/EDTA buffer. The tissue was pelleted by centrifugation at 1000g, 3 min and resuspended in 1 ml PBS/EDTA buffer to which 50µl LYIA was added. The sample was then briefly vortexed and incubated in the dark for 30 min at room temperature on a rotary wheel.

The tissue was pelleted by centrifugation as before and either treated subsequently with I-LC-biotin following the protocol given in Section 2.9 or an enriched fraction of olfactory/respiratory cilia was prepared according to the method described in Section 2.3. The final cilia fractions obtained were resuspended in 1x SDS-PAGE sample buffer or stored at -20°C for subsequent SDS-PAGE analysis and Western blotting. Tissue samples treated in parallel with 50µl MilliQ water served as controls for these experiments.

2.10.2 Detection of LYIA-labelled Proteins

Protein samples treated with LYIA were resolved on one-dimensional SDS-PAGE gels run in the dark. After electrophoresis was completed, the gels were placed in 7% (v/v) acetic acid/10% (v/v) methanol for at least 30 min, in the dark, with gentle agitation. They were then scanned using a FluorS imager (BioRad, Herts) with 100s exposure time in the SyproRuby gel-scanning mode (520LP, UV wavelength, trans-illumination, high-resolution scanning).

2.11 In-gel Trypsin Digestion

2.11.1 Manual in-gel digestion

All manual in-gel digestions were performed on silver-stained gels. The protocols for in-gel digestion and peptide extraction were taken from Van Montford et al. (2002).

Gel plugs (total volume ~1mm^3) were removed from the band/spot of interest and immediately placed in 1.5ml centrifuge tubes containing 200µl MilliQ water. Once all the gel pieces had been excised, the MilliQ water was removed and replaced with 200µl freshly prepared destain solution. The gel pieces were incubated in this solution until the brown colour had completely disappeared (<1 min). The destain solution was then removed and the gel plugs rinsed twice in 500µl MilliQ water.

Each gel piece was incubated in 200µl 25mM NH_4HCO_3 at 37°C for 15 min, before the buffer was removed and replaced with fresh 25mM NH_4HCO_3 for two further 15 min washes. The gel pieces were then dehydrated by three 10 min washes in 100µl 100% acetonitrile and dried further in the Gyro-Vap for 20 min on a medium heat setting.

Trypsin (100µg/ml stock reconstituted in 50mM acetic acid) was diluted to a 12.5µg/ml working solution using 25mM NH_4HCO_3. This working solution was added to the dehydrated gel pieces, 5µl per sample. The gel pieces were allowed to rehydrate in the trypsin-containing buffer for 20-30 min before an additional 20µl 25mM NH_4HCO_3 overlay was added. Samples were then incubated overnight (at least 14h) at 30°C without agitation.

Peptide extraction for MALDI-ToF analysis Trypsin digestion gel plug samples were sonicated 5 min and the digestion overlay removed. Peptides were extracted by the addition of 30µl 1% (v/v) trifluoroacetic acid/60% (v/v) acetonitrile and

sonication for 5 min. The extraction was repeated and both extracts pooled with the digestion overlay. Samples were then lyophilised in the gyro-Vap.

The dried peptides were reconstituted in 5µl matrix buffer by 5 min sonication. Samples were then mixed with an equal volume of freshly prepared matrix solution and 1µl spotted onto the MALDI target for analysis.

Peptide extraction for tandem mass spectrometry analysis Trypsin digest samples were sonicated for 5 min and the digestion overlay removed. Peptides were extracted by the addition of 30µl 1% (v/v) formic acid/60% (v/v) acetonitrile and sonication for 5 min. The extraction was repeated and both extracts were pooled with the digestion overlay. Samples were dried in the gyroVap until the volumes were reduced to approximately 15µl and the concentration of acetonitrile substantially reduced. The samples were diluted to 17µl using 1% (v/v) formic acid and then analysed by tandem mass spectrometry.

2.11.2 Automated in-gel digestion

Automated trypsin digestions were performed using the MassPrep™ station (Micromass, Manchester). The digestion robot was set up according to the manufacturer's instructions using the buffers listed in section 2.1. The program followed was "Digestion S4.5" selecting the option to include the silver destain protocol. As part of the digestion program, the robot spotted both lockmass and trypsin digest samples directly onto a target plate for MALDI-ToF mass spectrometry analysis.

2.12 Matrix-assisted Laser Desorption Ionisation-Time of Flight (MALDI-ToF) Mass Spectrometry

2.12.1 Preparation of Matrix

Approximately 10mg α-cyano-4-hydroxycinnamic acid was placed in a 1.5ml centrifuge tube to which 1 ml matrix buffer was added. The suspension was vortexed vigorously for 30s before being centrifuged at 6934g, 2 min. The resulting supernatant was the saturated matrix solution used for peptide analysis and was used immediately for manual in-gel digestion samples and not used >8h after initial preparation during automated digestions.

2.12.2 MALDI-ToF Instrument Calibration

The MALDI-ToF mass spectrometer was calibrated and assessed for sensitivity before each use. Calibration spectra were manually acquired from a sample containing four peptides (listed masses are given to the nearest Dalton): des-Arg-Bradykinin (904Da), neurotensin (1673Da), adrenocorticotrophin hormone clip 18-39 (2465Da) and oxidised insulin β-chain (3496Da), which cover the working mass range of the instrument. The calibration sample was prepared by Dr. D. Robertson and contained a 50nM concentration of each peptide. Spectra were typically acquired at 20% laser energy but this was increased to 30% depending on instrument performance and to ensure adequate resolution of the 3495Da peptide (i.e. full isotope envelope resolved).

Ten calibration spectra were acquired and combined. The resulting spectrum was processed by background subtraction, peak smoothing and peak differentiation using MassLynx software (version 3.5 or 4). The fully processed spectrum was used to calibrate the machine by matching the mass of the monoisotopic peaks of the

calibrant peptides to those in a "MALDI mix" reference file. This calibration was then saved and applied to the instrument.

2.12.3 MALDI spectrum acquisition

Automated spectrum acquisition Mass spectra from trypsin digests performed by the digestion robot were acquired automatically. The parameters for laser firing patterns and energy ranges were set manually, depending on the latest performance levels of the machine and the estimated protein concentration of the samples. Most commonly, the laser-firing pattern was set at random and laser energies between 70-50% were used, decreasing from 70% in 5% increments. Typically 5-10 spectra were acquired per digest however this varied greatly between samples.

During automated data acquisition, mass spectra from lockmass samples of adrenocorticotrophin hormone (ACTH) were acquired as external calibrants to ensure continuing mass accuracy throughout the analysis run. The ubiquitous trypsin autolysis peak of mass 2163Da was used as an internal calibrant for individual samples.

Manual spectrum acquisition Where trypsin digests had been performed by hand or spectra had not been found during automated data acquisition, MALDI spectra were acquired manually. This permitted the thorough searching of the peptide/matrix spot on the target at varying laser energies, which were modified to appropriate levels for each sample according to the observed peptide intensities i.e. increasing laser energy to improve ionisation levels in low abundance samples. Ion counts for individual peptides were not allowed to exceed 2000 to safeguard mass accuracy.

Typically at least 15 spectra were acquired for each sample. These were then combined and processed as described for the calibration spectra.

2.12.4 MALDI plate cleaning

The MALDI target was rinsed in distilled water and then scrubbed with acetone using a cotton wool bud. The target was then sonicated in acetone for 30 min and given a final rinse in MilliQ water before being allowed to air-dry.

2.13 Protein Identification by MALDI-ToF Mass Spectrometry – Peptide Mass Fingerprint analysis

Lists of the monoisotopic masses of peptides were prepared from all the spectra acquired during a single experiment. The lists of peptides were compiled in Microsoft Excel and duplicated to give a redundant peptide list and a second list, containing peptides unique to a given sample. When a peptide occurred in more than one spectrum, the peptide was retained in the first sample in which it was found, but erased from all subsequent peptide lists. This removes known contaminant peptides e.g. those derived from trypsin autolysis from peptide search lists and also removes contaminant peaks e.g. keratins specific to that experiment. This processing improves the chances of a successful identification by allowing searches of peptides unique to a given sample.

Unique peptide lists were searched against the NCBInr database using the on-line Mascot search program (www.matrixscience.com). The peptide lists were pasted into the query section of the search form and the search parameters set according to the sample being analysed.

Tryptic peptides of sheep proteins were searched against the "mammalia" section of the database and peptide masses from rat proteins against the "rattus" sequence entries. Sheep proteins were searched against the "mammalia" database as the sheep genome has not been extensively sequenced and therefore the size of the

sheep protein database is severely restricted in comparison to the "rattus" database. Carbamidomethylation was set as a fixed modification when the trypsin digest protocol included reduction and alkylation steps e.g. samples processed by the digestion robot, or the gel pieces were derived from 2D-gels. Methionine oxidation was entered as a variable modification for all digest samples. The "miscleavage" parameter was set to allow one missed cleavage site per peptide. The accuracy window was set to 100ppm for tryptic peptides from spectra acquired automatically and to 300ppm for spectra acquired manually. The use of different accuracy limitations was due to the greater mass accuracy achieved during automated spectrum acquisition via continual calibration adjustments using lockmass samples and the 2163Da trypsin autolysis peak as external and internal spectrum calibrants respectively.

The theoretical peptide masses for the top protein hits from this search were then compared to the redundant peptide list for the sample and any matching peptides included in a second Mascot search. This allowed the reinstatement of any peptides that were removed from the unique peptides list due to a protein genuinely occurring more than once per set of in-gel digestion experiments. A protein was considered identified when its unique peptides and any additional redundant peptides gave a MOWSE score greater than the threshold value set by Mascot for the database being searched. This effectively means that listed protein identifications have a significance probability of <0.05 and thus a high probability of correct identification.

2.14 Tandem Mass Spectrometry (MS/MS)

The tandem mass spectrometry work conducted as part of this project was performed using a Quadropole Time-of-Flight mass spectrometer (Q-ToF) purchased from

Micromass, Manchester. All tandem mass spectrometry experiments were performed in collaboration with Dr. D. Robertson.

Trypsin digest samples were loaded onto a reverse phase column fitted on an UltiMate chromatography system (Dionex, Surrey) linked directly to the Q-ToF mass spectrometer. Sample loading was automated and set to "partial pick-up" to allow the maximum volume of material (10µl) to be loaded onto the column. The reverse phase column was run at a flow rate of 200nl/min with peptides eluted during a linear gradient increase of acetonitrile concentration (0-50% over 30 min). The peptides eluted from the column flowed directly into the Q-ToF instrument for analysis.

Experimental samples were analysed on the Q-ToF with a scan period of 1s and a duty cycle of 1.1s. The instrument was programmed to perform data-dependant switching to tandem mass spectrometry (MS/MS) mode upon the detection of multiply charged ions at a minimum intensity of 10 counts per second. The reverse switch to single MS mode was made after 20s or once the signal intensity of the tandem spectra ions dropped below 10 counts per second. One to three tandem acquisition functions were in operation during analysis depending on the estimated complexity of the sample.

2.15 Protein Identification by Tandem Mass Spectrometry

The chromatograms from each MS/MS acquisition function were analysed in MassLynx (version 3.5 or 4) and lists of parent ion masses and their associated charges were prepared. All the MS/MS spectra obtained from a single parent ion were combined and the background was subtracted. Sample spectra were further processed using the MaxEnt 3 algorithm to differentiate spectrum peaks into centroided peaks and combine identical mass peaks bearing different charges to give

a final spectrum of mainly singly charged ions from which the peptide sequence was determined.

Peptide sequences were predominantly called on the basis of the y ion series. Where residues/residue leaps were not conclusively identified by this series, extra data from the b ion series was then used to determine the next amino acid in the sequence. Peptides were defined as lysine- or arginine-terminating according to the presence of a y_1 ion peaks of 147Da or 175Da mass respectively. Peptide sequence data was searched against the non-redundant (nr) NCBI protein database using the BLAST algorithm (www.ncbi.nlm.nih.gov/BLAST).

The search parameters used were the default settings for searching for "short nearly exact matches". Briefly, a PAM30 scoring matrix was used with the E value threshold set at 20000, gap costs were set at 9 (existence): 1 (extension). All peptide sequences were searched against the "mammalia" section of the database.

Protein identifications were accepted when the peptide sequence search results yielded expected (E) values <0.05, where the E values represent the probability of that a given peptide match could occur at random.

2.16 Electron Microscopy

The electron microscopy work presented in this thesis was performed by Miss M. Pope using a Hitachi H-600 TEM.

2.16.1 Sample embedding

Electron microscope pictures were taken of several cilia preparations. The cilia were isolated as described in Section 2.3. The cilia pellets were then washed twice in 100mM sodium cocodylate and fixed in 100mM sodium cocodylate containing 4%

(v/v) paraformaldehyde, 2% (v/v) glutaraldehyde. They were then washed in fresh 100mM sodium cocodylate buffer and 1% (w/v) osmium tetroxide/distilled water before a final wash using distilled water.

Cilia pellets were then dehydrated by a series of five washes with increasing ethanol concentration and a final wash in 100% acetone. Once fully dehydrated, the pellets were washed sequentially in three mixtures of acetone and resin, containing 30%, 70% and 100% (v/v) resin respectively. They were then placed in 100% fresh resin and heated to 60°C.

2.16.2 Sectioning/Staining

Ultra-thin sections between 60-90nm thick were cut from resin-embedded samples and placed onto copper grids. Section staining was performed on rat cilia samples using a saturated solution of uranyl acetate in 50% (v/v) methanol, with subsequent washing in 50% (v/v) methanol. By contrast, mouse and sheep olfactory cilia preparations were stained using uranyl acetate (2% (w/v) uranyl acetate in 0.69% (v/v) maleic acid) prior to section cutting (discussed in Chapter 3).

After uranyl acetate treatment and sectioning all samples were subsequently stained with Reynolds' lead citrate solution. The sections were then given a final wash in distilled water before being examined on the electron microscope.

All biochemical protocols were performed according to the equipment/reagent manufacturer's instructions except where stated.

Chapter 3

THE ADAPTATION OF THE OLFACTORY CILIA PROTEOME

3.1 Introduction

Olfactory process begins with an interaction between an odorant molecule and an olfactory receptor. As discussed in Chapter 1, the location for this event is the surface membrane of the olfactory cilia that protrude from the dendritic terminal of olfactory receptor neurons (ORNs). The sensory role of the olfactory cilia is therefore well defined. What is less clear is how specialised these structures and their associated proteomes are and how much of their protein complement can be viewed as ORN-specific and thus likely candidates for thiol sensor proteins.

Two of the criteria for potential thiol sensor proteins set out in Section 1.16 are specificity to the olfactory system and evolutionary conservation of the receptor in mammalian species. The proteomics experiments described in this chapter were designed to address the adaptation/specialisation of olfactory cilia both cross-species and to their sensory role.

3.1.1 Conservation of olfactory cilia proteins

The identification of highly conserved cilia-localised proteins (defined as the cilia proteome) allows the relative importance of each protein to the core olfactory process to be ascertained. High levels of conservation of individual proteins within the olfactory cilia proteome imply a strict requirement of them for either basic olfactory function and/or the survival of the organism. Increased conservation of a given protein across different mammalian species may therefore predict a role of greater importance for that protein.

Olfactory sensitivity to thiol compounds in mammals is apparently well conserved across mammalian species. This implies the importance of thiol detection to mammalian survival and also the presence of significant selection pressure on the proteins responsible for thiol detection. Therefore any groups of proteins conserved between distantly related mammalian species are likely to contain proteins essential for the olfactory process in addition to candidate proteins for interactions with and detection of thiol odorants.

The model species used to assess the evolutionary conservation of cilia-associated proteins are mouse, rat and sheep. This provides two degrees of evolutionary relatedness, the closely related rat and mouse and the more distantly related sheep. These relationships lead to the prediction that the olfactory cilia proteomes of rat and mouse are likely to be very similar and very different from the sheep proteome. This hypothesis was tested by the isolation and comparison of the respective olfactory cilia proteomes, with particular interest being paid to any proteins common to all analyses.

3.1.2 Protein localisation in sensory v non-sensory epithelia

In addition to a requirement for cross-species conservation, any putative thiol sensor should be specific to the olfactory epithelium *i.e.* the sensory epithelium. Due to the adjacent anatomical location of the nasal respiratory epithelium and the presence of ciliated cells in both respiratory and olfactory epithelia (Menco and Farbman, 1987), comparative preparations of enriched respiratory cilia were used to demonstrate localisation to the olfactory epithelium.

3.1.3 Potential roles of the respiratory epithelium and cilia

Air inhaled through the mammalian nose passes along the nasal passage, first through regions lined with respiratory epithelium (nasal conchae) and then through areas lined with olfactory epithelium (nasal turbinates), before proceeding down the trachea to the lungs. The air should be at body temperature and moist before reaching the lungs and this is the primary but almost certainly not only function of the areas of respiratory epithelium (Farbman, 1992). The mucus flowing over the respiratory and olfactory epithelia traps dust particles and the motile cilia of the respiratory epithelium enable the clearance of such potentially harmful particles from the nasal airway (Weston, 1985). The respiratory epithelium also plays a protective role in the nasal passage *via* its innervation with trigeminal nerves that invoke protective reflexes such as sneezing when an irritant is inhaled (Finger *et al.*, 2003). It is also the source of a secretory protein with putative bacteriocidal properties, the production of which appears to be induced upon damage to the olfactory system (Sung *et al.*, 2002). Finally, it acts to form a physical barrier to cover a chemically destroyed olfactory epithelium whilst regeneration occurs and even covers previous sensory areas after age-related degeneration of the olfactory system (Schultz, 1960; Farbman, 1992).

Respiratory cilia will share the proteins required for the maintenance of cellular integrity and ciliary structure. Comparisons of the protein complements should also reveal the proteins present only in olfactory cilia and by implication specific to sensory cilia, such proteins fulfilling the specificity requirement of a putative thiol sensor.

3.1.4 Experimental strategy

The basic experimental strategy was to isolate the proteins of the olfactory cilia from mouse, rat and sheep, separate the proteins by gel electrophoresis and identify them using mass spectrometry (Figure 3.1.1). All protocols used are as described in Chapter 2 of this volume except where stated.

Enriched olfactory cilia fractions were prepared from the nasal turbinate tissue of the three mammalian species using the calcium shock deciliation method described in Section 2.3. The proteins of the enriched cilia fractions were separated by one-dimensional SDS polyacrylamide gel electrophoresis (SDS-PAGE) and two-dimensional polyacrylamide electrophoresis (2D-PAGE) and the protein profiles of the olfactory cilia of each species compared. In-gel trypsin digestions and MALDI-ToF mass spectrometry were then used to identify the proteins conserved across the different species.

Nasal tissue from the rat was used to investigate the specificity of proteins to the sensory (olfactory) cilia compared with non-sensory (respiratory) cilia. Rat tissue was chosen for this purpose due to the comparative ease of tissue acquisition and greater protein yields than could be achieved using mouse nasal tissue. Enriched preparations of olfactory and respiratory cilia were prepared and the proteins separated by SDS-PAGE and 2D-PAGE. A comparison of protein profiles highlighted the proteins unique to the sensory cilia, which could then identified by in-gel trypsin digestions/MALDI-ToF mass spectrometry.

Proteins unique to olfactory cilia and conserved across the model species were considered as having an important function in the sensory processes of the olfactory system and a potential role in the detection of thiol odorants.

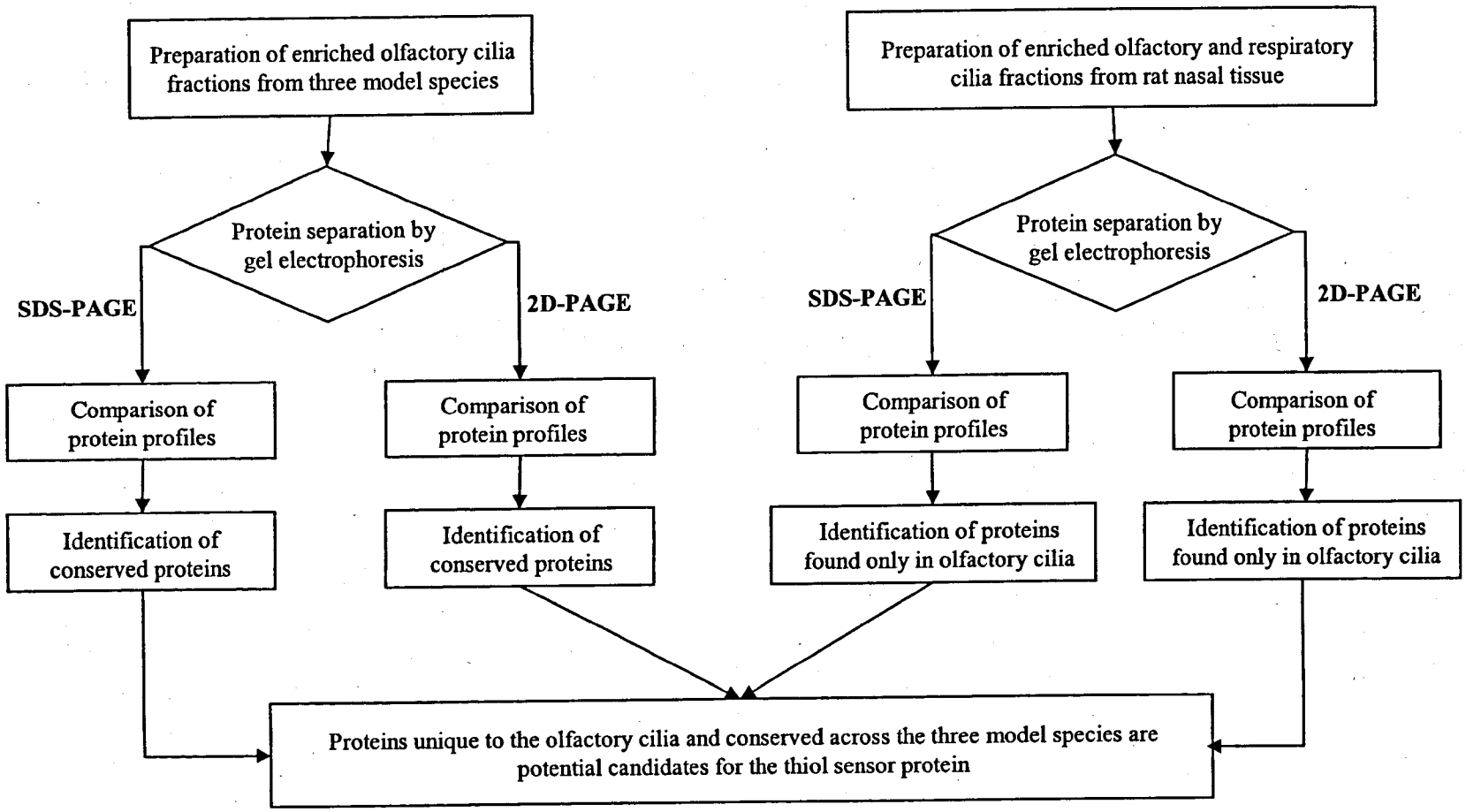

Figure 3.1.1 The basic experimental strategy to define putative candidates for thiol sensor proteins.

3.2 Method development

3.2.1 Optimisation of protein solubilisation for 2D-PAGE

The efficiency of the solubilisation of proteins in preparation for 2D-PAGE depends on both the sample buffer itself and the nature of the sample *e.g.* lipid components, mainly soluble proteins etc. The cilia preparations were expected to comprise a mixture of lipids, membrane-associated (including integral and peripheral membrane proteins) and cytosolic proteins. This provided significant challenges for solubilisation as it includes both the strongly hydrophobic membrane proteins and also cytoskeletal proteins, which are generally detergent resistant. Optimisation experiments were performed to maximise the solubility of the cilia samples and thus the representation of cilia associated proteins on a 2D-gel. Protein samples were applied to the immobilised pH gradient (IPG) strips during strip rehydration hence the sample buffer used during this 2D-PAGE work is referred to as rehydration buffer.

The most commonly used combination of denaturant and detergent in 2D-PAGE rehydration buffer is 8M urea with 4% (w/v) CHAPS (Herbert, 1999). The addition of thiourea used in combination with urea, aids the solubility and resolution of proteins during 2D-PAGE separation (Pasquali *et al.*, 1997; Molloy *et al.*, 1998; Rabilloud *et al.*, 1999). The alternative detergent Triton X-100 was also tested both alone and in combination with CHAPS. The use of Triton X-100 to solubilise olfactory epithelium membrane proteins was been reported by Fesenko *et al.* (1988) and use of rehydration buffers containing a combination of Triton X-100 and a zwitterionic detergent has also been described previously (Rabilloud *et al.*, 1999). The combinations of detergents and denaturants tested are listed in Table 3.2.1. Crude membrane preparations from deciliated nasal turbinates were used to test the

Rehydration Buffer	Denaturant	Detergent
1	8M urea	0.5% (v/v) Triton X-100
2	8M urea	4% (w/v) CHAPS
3	7M urea/2M thiourea	0.5% (v/v) Triton X-100
4	7M urea/2M thiourea	4% (w/v) CHAPS
5	8M urea	2% (w/v) CHAPS
6	7M urea/2M thiourea	2% (w/v) CHAPS
7	7M urea/2M thiourea	2% (w/v) CHAPS/0.5% (v/v) Triton X-100

Table 3.2.1 The combinations of denaturants and detergents tested to optimise the solubilisation of proteins for 2D-PAGE

Combinations of denaturants and detergents were tested to try and maximise the levels of protein representation and solubility in the rehydration buffer used during the first dimension of 2D-gel electrophoresis

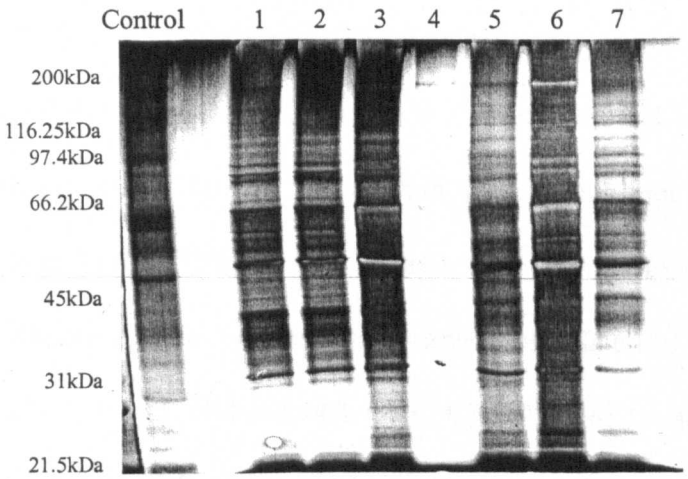

Figure 3.2.1 SDS-PAGE separation of the proteins solubilised by different combinations of denaturants and detergents

Lanes are marked according to the identity of the rehydration buffer tested as given in Table 3.2.1. The control sample is rat olfactory epithelium membrane solubilised in SDS-PAGE sample buffer

relative solubilisation efficiency of different rehydration buffers. Although these samples are not cilia preparations they most likely contain a small proportion of cilia-associated proteins from incomplete deciliation and also a similar mixture of lipids, membrane proteins and cytosolic proteins to the cilia preparations. As the yield from the crude membrane preparations was much greater than for cilia preparations it was considered that the use of the membrane preparations would provide a more efficient method of testing the solubilisation capacity of a given rehydration buffer.

Optimisation of rehydration buffer for 2D-PAGE

During the first optimisation experiment, all seven buffers given in Table 3.2.1 were tested. The solubilisation supernatant was diluted ten-fold in SDS-PAGE sample buffer. Samples were then heated at 100°C, 5 min and 20µl of each sample loaded onto an 11cm "criterion" gel for SDS-PAGE analysis. The resulting SDS-PAGE gel is shown in Figure 3.2.1. The presence of a control sample solubilised directly in SDS-PAGE buffer allows the analysis of total protein content of the crude membrane preparations; SDS-PAGE buffer contains 1% (w/v) SDS and is therefore highly efficient at protein solubilisation. The protein profiles are not easily discernable therefore solubilisation efficiency was assessed by comparisons of the relative protein concentration of each sample. The samples solubilised in buffers containing 8M urea/2% (w/v) CHAPS, 8M urea/4% (w/v) CHAPS, 2M thiourea/7M urea/0.5% (v/v) Triton X-100 and 2M thiourea/7M urea/2% (w/v) CHAPS were adjudged to contain the highest levels of protein and were therefore considered to be the most efficient at sample solubilisation.

The four most efficient rehydration buffers for the solubilisation of crude nasal turbinate membrane preparations were next tested with 7cm 2D-PAGE (Figure 3.2.2). The gels indicate good protein abundance in all samples; however the

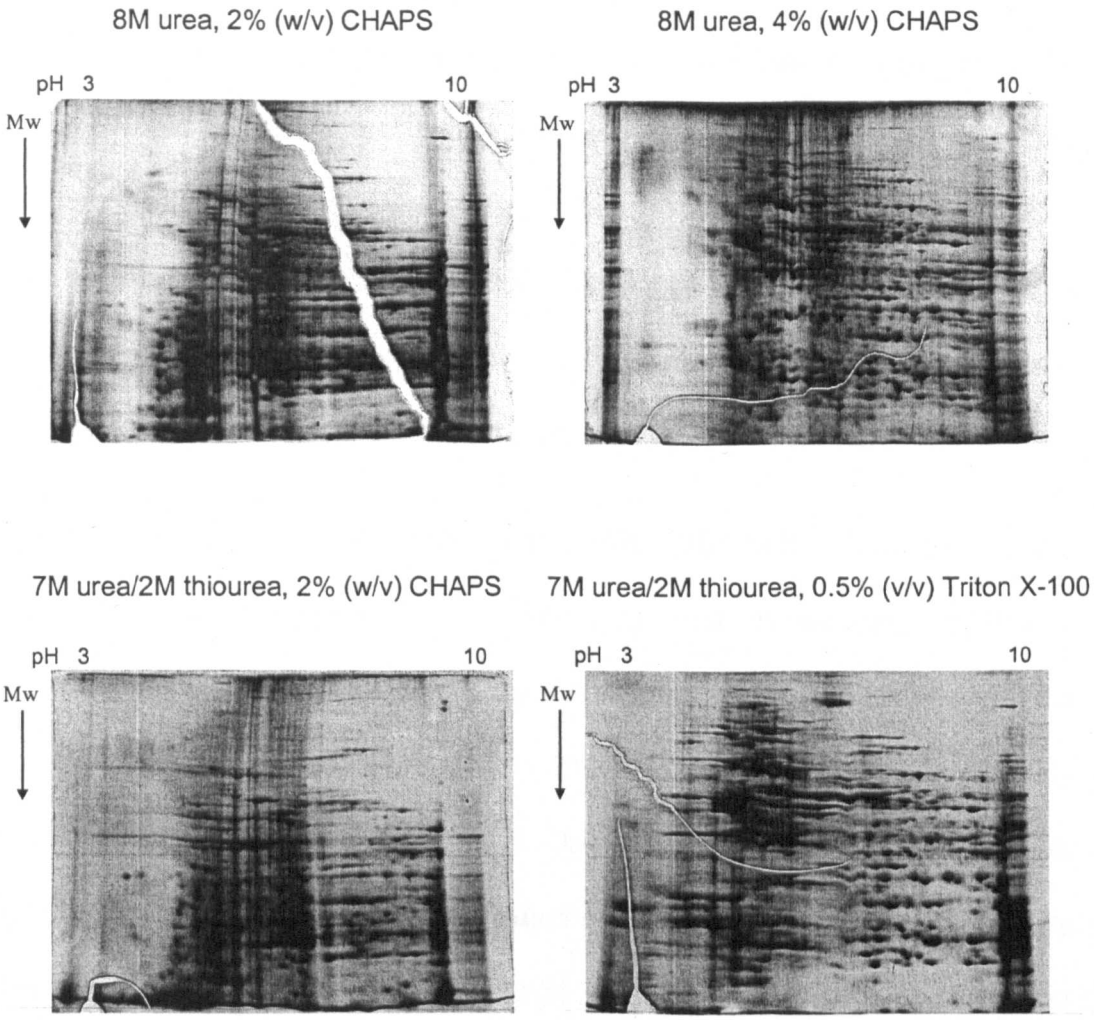

Figure 3.2.2 2D-PAGE of rat olfactory epithelium membrane preparations using the four buffers judged to give maximal protein solubilisation during previous experiments

The first dimension was performed using 7cm pH3-10 (linear gradient) IPG strips. The second dimension was run on 7cm mini-gels. pH increases from 3 to 10 left-to-right, molecular weight decreases descending vertically.

resolutions of these proteins across the full pH range was superior in 8M urea/4% (w/v) CHAPS and 2M thiourea/7M urea/0.5% (v/v) Triton X-100. These buffers were therefore compared using the separation of solubilised membrane preparations on 11cm IPG strips and the "criterion" second dimension gel system (Figure 3.2.3). The conclusion from these early rehydration buffer optimisation experiments was that the optimal buffer for the two-dimensional gel separation of olfactory and respiratory cilia protein preparations was 2M thiourea/7M urea/0.5% (v/v) Triton X-100 as this buffer provided maximal resolution of proteins across the full pH range and reduced the extent of urea deposition, which causes the clear vertical streaks in the gel run using samples prepared in 8M urea-containing rehydration buffer.

Addition of 40mM Tris and extra Triton X-100 The buffer consisting of 2M thiourea/7M urea/0.5% (v/v) Triton X-100 was used during early 2D-PAGE experiments and was later supplemented by the addition of 40mM Tris base and the increase of Triton X-100 concentration to 2% (v/v) to further improve solubility (Pasquali *et al.*, 1997; Molloy *et al.*, 1998; Olivieri *et al.*, 2001). The 7cm 2D-gels indicating the beneficial effects of the addition of Tris and extra detergent are shown in Figures 3.2.4. The 2D-gels run with 40mM Tris present in the rehydration buffer show greater protein concentration than their counterparts without. The reduced level of vertical smearing observed in 2D-gels run using samples solubilised in 2% (v/v) Triton X-100 indicates that increasing the concentration of Triton X-100 aids overall protein solubility during the 2D separation.

These experiments were performed as described above for the solubilisation tests using sheep olfactory cilia preparations instead of rat epithelial tissue. This provides an accurate view of the buffer effects on cilia preparations directly. It was possible to use sheep olfactory cilia due to the greater protein yields obtainable in

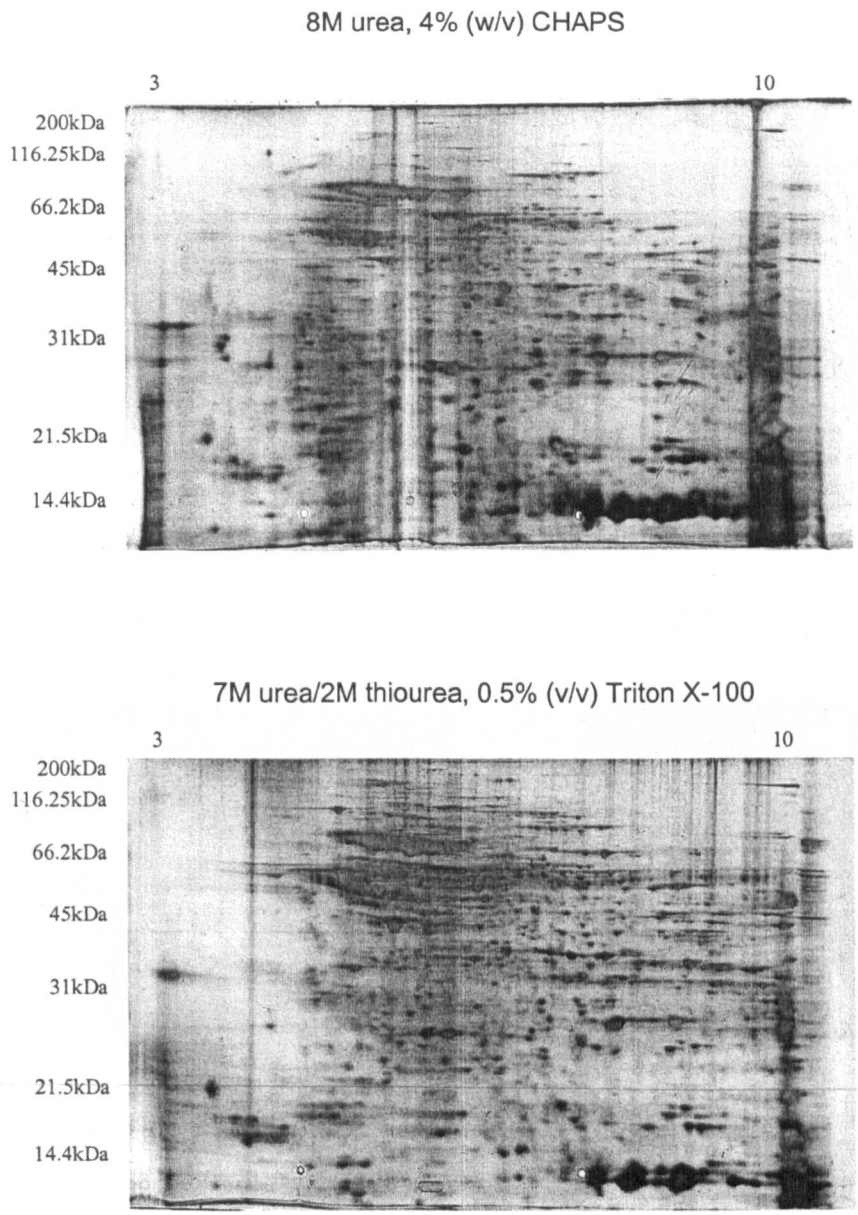

Figure 3.2.3 2D-PAGE separation of rat olfactory epithelium membrane preparations solubilised using the best two buffers from previous solubilisation experiments

Isoelectric focussing was performed using 11cm pH3-10 (linear gradient) IPG strips. The second dimension was run using the "Criterion" system.

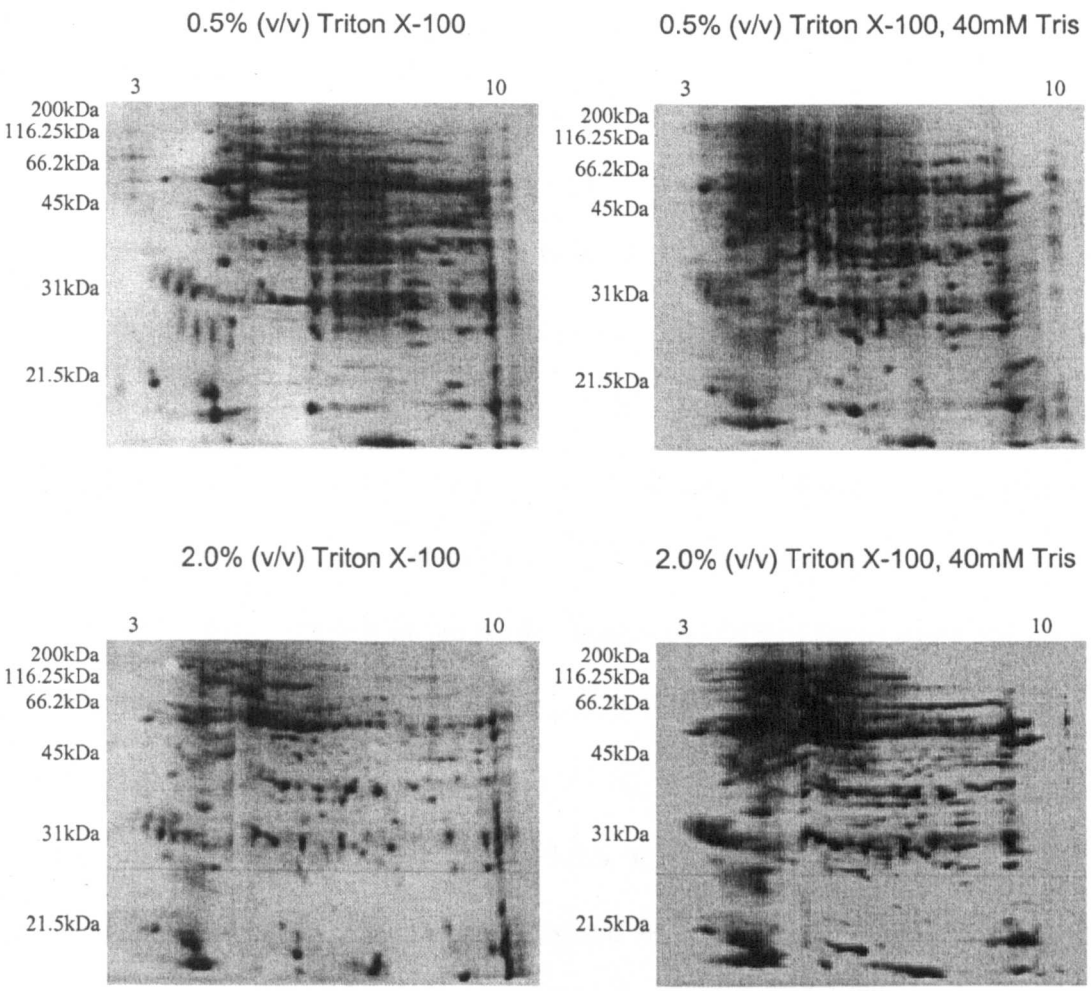

Figure 3.2.4 Protein resolution of olfactory cilia proteins is improved by the addition of 40mM Tris and increasing the concentration of Triton X-100

2D-PAGE separation of sheep olfactory cilia proteins solubilised in rehydration buffers containing 7M urea/2M thiourea to which different concentrations of Triton X-100 was added. Two rehydration buffers also contained 40mM Tris base. Solubilisation tests were performed using enriched sheep olfactory cilia preparations.

comparison to preparations derived from rat tissue. Sheep cilia preparations were not used previously due to sheep tissue being unavailable during the original tests for rehydration buffer solubilisation efficiency.

Linear versus non-linear IPG strips The final modification to the 2D-PAGE process involved a change in the IPG strip used for isoelectric focussing. In all the gels above, linear gradient strips have been used that separate proteins along a linear pH scale between pH3 and 10. The majority of proteins in the cilia preparations, as shown by these gels, are within the pH range 5-8. Non-linear gradient pH3-10 IPG strips have an identical overall pH range to linear gradient strips however the gradient of pH increase is higher at both ends of the range and lower across pH5-8. The use of these strips therefore allowed the increased resolution of the majority of cilia proteins *i.e.* those present in the pH5-8 region whilst still focussing albeit to a lesser resolution, proteins with isoelectric points outside this pH range. The gain from the use of non-linear v linear strips during 2D-PAGE separation of sheep olfactory cilia proteins is shown in Figure 3.2.5. Pairs of corresponding spots have been circled on the gels to illustrate the increased resolution within the pH5-8 range and the resultant shift in protein position. Protein pairs 1 and 2 show the decreased physical separation of proteins migrating to the pH regions <5 and >8 respectively. Pair 3 illustrates the increased physical separation and therefore protein resolution in the intermediate pH5-8 range.

3.2.2 Identification of proteins by peptide mass fingerprinting

All identifications reported in Chapter 3 were gained by in-gel tryptic digestions of protein spots followed by matrix-assisted laser desorption/ionisation time-of-flight (MALDI-ToF) mass spectrometry. The resulting peptide mass fingerprint was

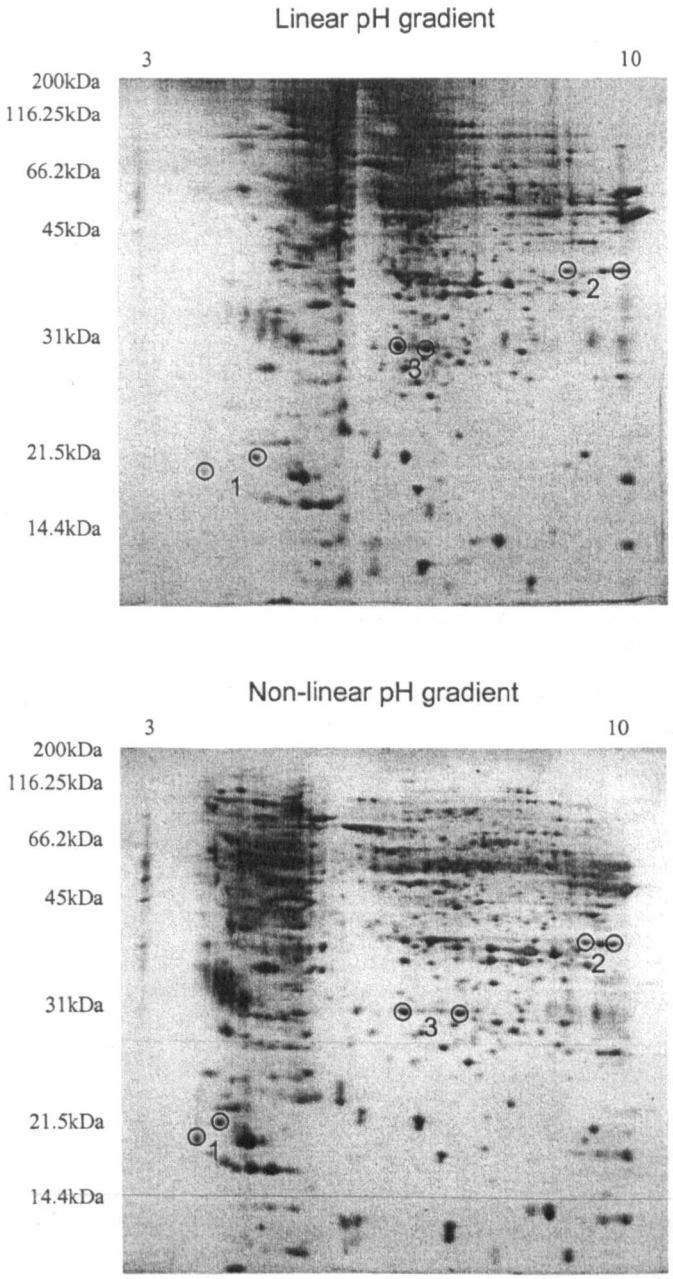

Figure 3.2.5 Protein resolution of sheep olfactory cilia proteins is improved by the use of non-linear IPG strips

Sheep olfactory cilia proteins were solubilised in 7M urea/2M thiourea, 2% (v/v) Triton X-100, 40mM Tris. Isoelectric focussing was performed using 11cm 3-10 linear pH gradient IPG strips or 11cm non-linear pH gradient 3-10 IPG strips. The blank area in the middle of the gel is likely to be the result of urea precipitation during isoelectric focussing.The second dimension was run using the Hoefer Ruby system (Amersham Biosciences, Buckinghamshire, UK).

The numbered pairs of corresponding protein spots circled in the gel demonstrate how the use of non-linear pH gradient IPG strips increases the resolution of proteins within pH5-8, at the expense of proteins outside this region.

searched against an on-line protein database as described in Section 2.13. A schematic view of the identification process is shown in Figure 3.2.6.

The peptide mass fingerprint of a protein is the combination of peptide masses that results from the enzymatic digestion of the protein by a specific endoprotease such as trypsin. The specificity of the cleavage site of the endoprotease, in the case of trypsin the peptide bond C-terminal to arginine or lysine residues (unless followed immediately by proline residues), means that the sizes of peptides generated during enzymatic digestion are directly related to the position of certain residues in the primary sequence of the protein in question. It follows therefore that the combination of peptide masses from an enzymatic digestion, collectively termed the peptide mass fingerprint, can be used to identify an individual protein.

The mass of peptides generated during manual or automated in-gel trypsin digestions (Section 2.11) was measured by MALDI-ToF mass spectrometry. The proteins in this study were a protein preparation derived from the apical membrane of a small region of nasal epithelium. This means that the protein concentration of the enriched cilia fraction is not very high, hence all cilia separation gels in this thesis were stained using the silver nitrate stain technique rather than the more mass spectrometry-friendly Coomassie stain. This low protein concentration in turn results in a low concentration of peptides generated during in-gel digestions. The MALDI-ToF mass spectrometer was therefore operated close to its limits of sensitivity.

Low concentration of peptides can have a major impact upon the resulting MALDI-ToF spectra. The ion counts are reduced as fewer ions can be detected by the mass spectrometer and the higher laser energy used to ensure maximal ionisation of the peptides present lead to increased levels of background noise picked up by the instrument. The final problem to be addressed is that the lower the levels of sample

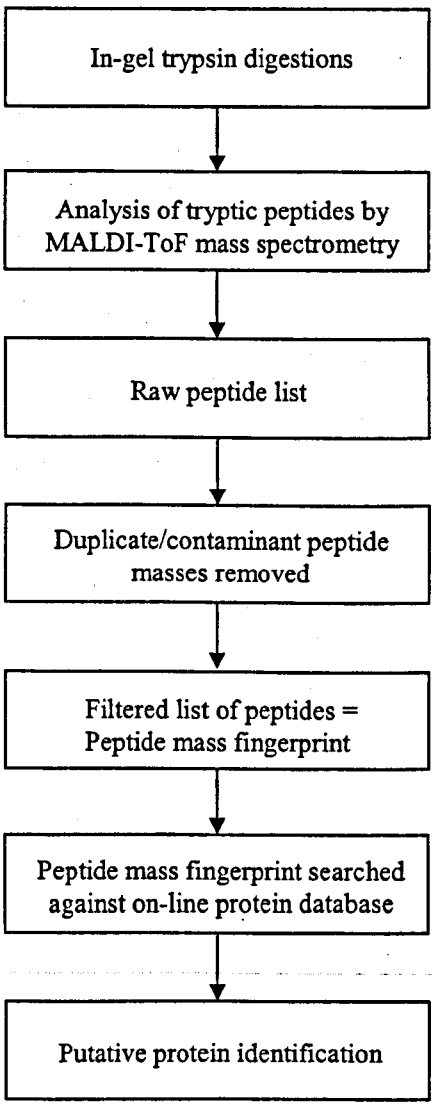

Figure 3.2.6 Strategy used in the characterisation of the cilia proteomes to identify unknown proteins by in-gel digestions and MALDI-ToF mass spectrometry

peptides, the more prominent the relative abundance of introduced contaminants such as tryptic peptides and keratins, which can mask genuine peptides from the in-gel digestion of a cilia preparation-derived protein.

Derivation of peptide mass fingerprints The potential problems of contaminant peptides in a MALDI spectrum and their increased impact in low concentration samples lead to the development of a strategy to enable only true peptides *i.e.* those derived from the in-gel digestion of a protein derived from the enriched cilia preparations, to be searched against the on-line database. All peptides were considered as potentially relevant regardless of their relative peak heights in comparison to other peptides in the same spectra.

In order for a peak mass to be noted as a potential peptide it was required to have the correct shape of isotope envelope for its given mass. This is explained diagrammatically in Figure 3.2.7. The isotope envelope is based on the relative abundance of C^{12} and C^{13} carbon isotopes in the environment therefore available for incorporation into biopolymers such as proteins. In small peptides of low mass *e.g.* ~1000Da, the amount of C^{12} incorporated is much greater than the levels of C^{13}. This dictates that the isotope envelope will be shaped such that the monoisotopic peak corresponding to the peptides containing only C^{12} atoms, is larger than the following peaks, which incorporate C^{13} atoms. Larger peptides contain greater numbers of carbon atoms increasing the likelihood of C^{13} atom incorporation. This leads to the increase of the relative numbers of peptides containing a single C^{13} atom making this second peak larger than the monoisotopic peak. This process is repeated as peptides grow larger, such that in peptides at >2500Da the third peak in the isotope envelope corresponding to the peptide incorporating two C^{13} atoms, becomes the most abundant. This pattern governs the relative abundance of the peaks in the isotope

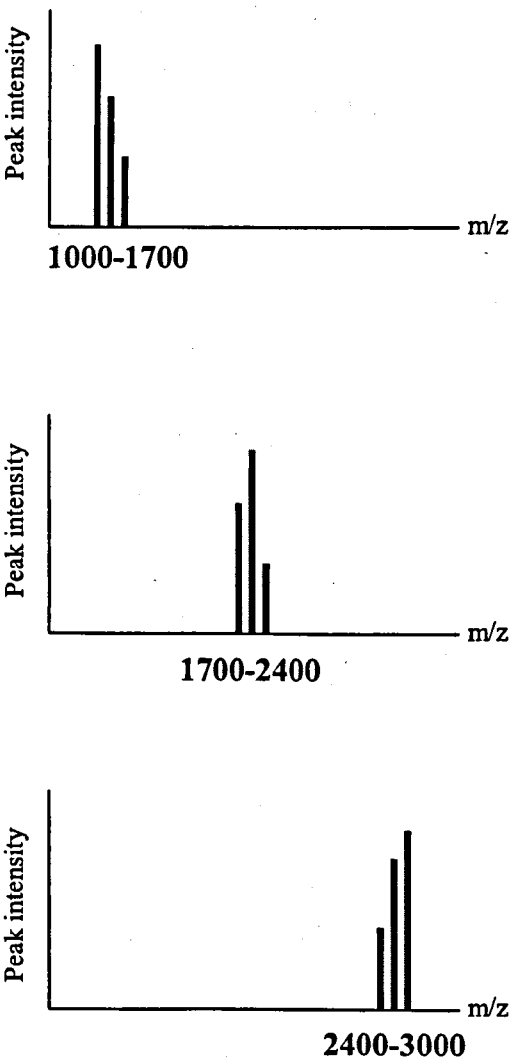

Figure 3.2.7 The relative intensities of peaks in the isotope envelope changes according to the mass of a peptide

M/z values provided for the boundaries of each isotope envelope peak distribution are approximated from personal observations. As nearly all peptides in MALDI-ToF are singly-charged, the m/z value equals the mass of the peptide.

In terms of peptide size, the three increasing mass ranges include peptides with 8-14 residues, 14-20 residues and 20-25 residues containing on average 40-70, 70-100 and 100-125 carbon atoms respectively (calculated using mean average mass of amino acid residues and mean average number of carbons in an amino acid).

envelope of simple peptides *i.e.* those not linked to sugar groups (pers. comm. D. Robertson). The requirement of a putative peptide to obey this pattern ensures that masses corresponding to glycopeptides or present as a result of instrument noise are not included in the peptide lists used to determine the protein identity.

The second requirement for peaks to be considered as genuine peptides is the maintenance of mass accuracy across the isotope envelope. This prevents the inclusion of peaks that have an apparent isotope envelope due to adjacent peaks resulting from instrument noise. It also allows the individual peptides with overlapping isotope envelopes to be differentiated.

Once all potentially relevant peptides from a mass spectrum have been listed, the masses are filtered to remove peptides that are present in spectra acquired from multiple protein spots. The unique peptide list from the in-gel digestion of an individual protein spot was used as the peptide mass fingerprint of that protein.

3.3 Results

3.3.1 Cilia preparations

The efficiency of the preparation of olfactory cilia was assessed by two methods. The first proof of cilia isolation was provided by electron microscopy analyses of olfactory cilia preparations from all the model species. Electron microscopy images of the cilia types are shown in Figure 3.3.1. All images show the presence of intact cilia vesicles either in cross-section with the characteristic 9+2 microtubule arrangement of the axoneme clearly visible, or in longitudinal section with a striated appearance.

The electron microscopy images also show apparently empty vesicle structures. The precise identity of these vesicles could not be determined. It is possible that they may be cilia membrane vesicles that have disintegrated away from the axoneme and reformed (reported by Anholt *et al.*, 1986) or they may be derived from the distal sections of the cilia, which lack the axonemal core (Chen *et al.*, 1986a). They may also represent contamination of the preparation by cellular organelles such as lysosomes. Contaminating mitochondria were also observed both during electron microscopy and later protein identification. The presence of such contaminants has been previously reported by Henderson *et al.* (1992) so biochemical analyses of the rat olfactory cilia was used to provide further evidence for cilia enrichment in the fractions prepared.

Enrichment of β-tubulin III demonstrates the enrichment of olfactory cilia The relative enrichment of olfactory cilia in the final preparation was determined by immunoblotting with a monoclonal antibody to β-tubulin subtype 3 (β-tubulin III). β-tubulin is a major component of the axoneme structure of microtubules that form the core of the cilia and maintain its shape. Immunofluorescence microscopy provided

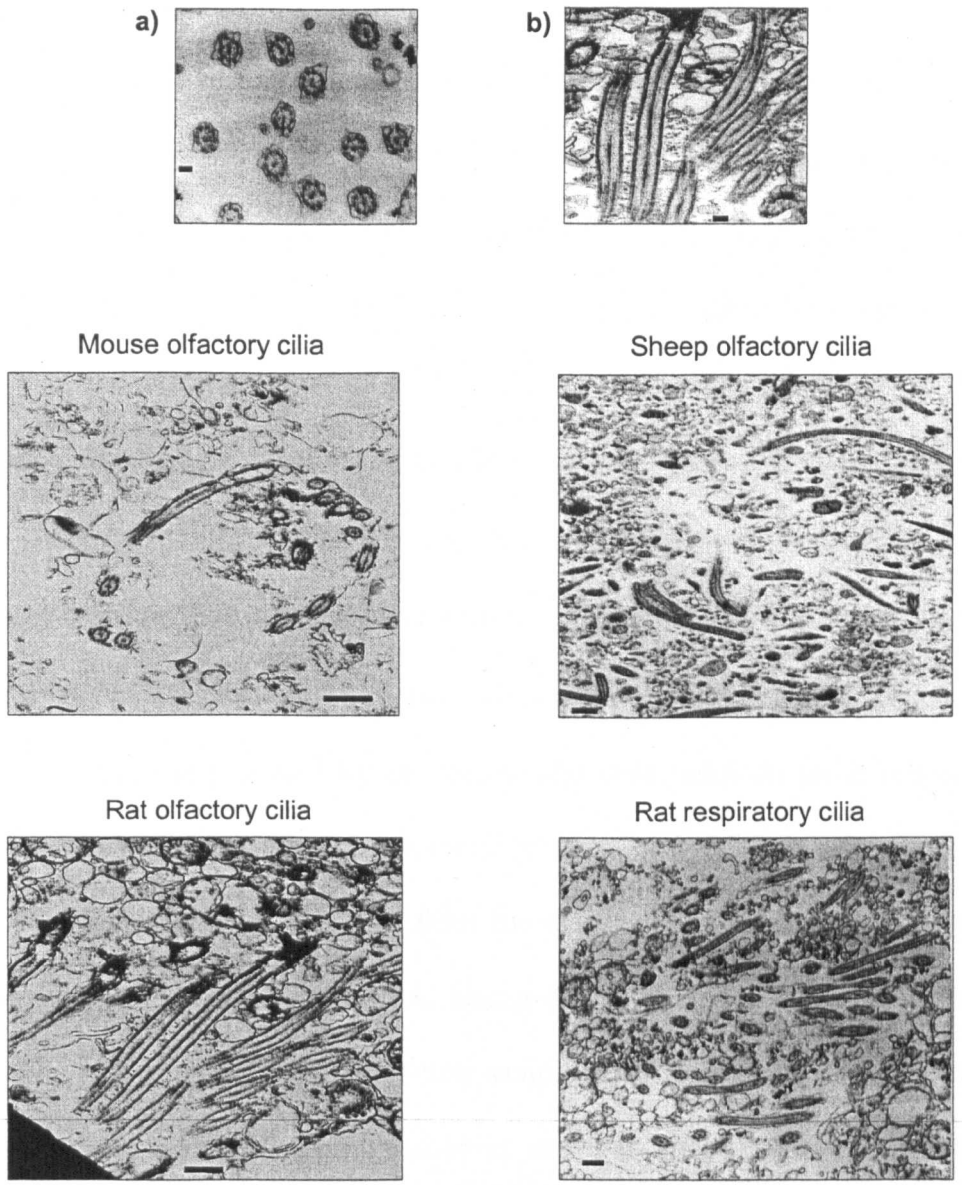

Figure 3.3.1 Electron microscopy images of mammalian olfactory and respiratory cilia

Intact cilia vesicles exhibit the characteristic 9+2 arrangement of microtubules when cut in cross-section (a) and can also appear striated when cut in a longtiduinal section as in (b). Images from olfactory cilia preparations from rat and sheep olfactory cilia respectively. Scale bars represent 0.1μm.

In the low magnification EM images of mouse olfactory cilia, sheep olfactory cilia, rat olfactory cilia and rat respiratory cilia the scale bars represent 0.5μm. Electron microscopy performed by Marion Pope.

confirmation of the enrichment of β-tubulin in the cilia layer of the olfactory epithelium (Chen *et al.*, 1986b). The use of an antibody to β-tubulin III also allowed the origin of the tubulin to be determined as this subtype is exclusive to neuronal cells. The antibody can therefore distinguish between cilia derived from ORNs, microvilli from supporting cells and any contaminating cilia from nearby respiratory epithelium and shows the enrichment of the olfactory cilia only. Although tubulin isotype synthesis is cell-type specific, there is no compartmentalisation of the subtypes within olfactory receptor neurons (Woo *et al.*, 2002). This means that a preparation enriched in olfactory cilia has a greater concentration of multiple β-tubulin subtypes including β-tubulin III, than a crude membrane preparation. The relative enrichment was calculated according to a linear relationship between the pixel intensity of the blot and the concentration of β-tubulin III present. The proof of this relationship was provided by an immunoblot performed on serial dilutions of crude membrane preparations from rat cortex (Figure 3.3.2, 3.3.3 and Table 3.3.1).

The immunoblot of samples from the olfactory epithelium and respiratory epithelium is shown in Figure 3.3.4, alongside its replica SDS-PAGE gel. The importance of the inclusion of respiratory samples is discussed later in this section. Densitometric analysis of the immunoblot and gel were used to calculate the approximate relative enrichment of the olfactory cilia preparations (Table 3.3.2). The analysis of the immunoblot indicates a poor ~2.5-fold relative enrichment of β-tubulin III in the olfactory cilia preparation by comparison to the crude membrane preparation from the olfactory epithelium. However despite using the dot blot method of protein concentration estimation (Section 2.4) it is obvious from the immunoblot replica gel that the loading of the crude membrane preparation is much greater than for the olfactory cilia samples. This difference was estimated to be

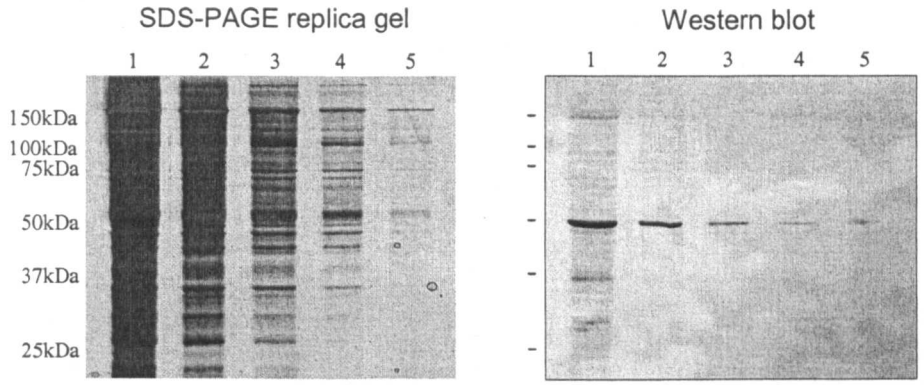

Figure 3.3.2 Detection of β-tubulin III in serial dilutions of a crude membrane fraction from rat cerebral cortex

Serial dilutions of the crude membrane preparation from rat cortex were blotted onto nitrocellulose membranes and probed with 1:1000 anti- β-tubulin III and 1:3000 goat anti-mouse IgG. Relative sample concentrations for each of the lanes are given in Table 3.3.1.

Lane	Relative concentration	Band intensity
1	1	101677
2	0.5	53113
3	0.2	13973
4	0.1	8181
5	0.05	4431
6	0	1148

Table 3.3.1 Densitometric analysis of the detection of β-tubulin III by Western blotting of serial dilutions of crude membrane preparations from rat cortex

Data obtained using the gel and blot shown in Figure 3.3.2. Band intensity values for lane 6 are taken from a blank lane adjacent to Lane 5.

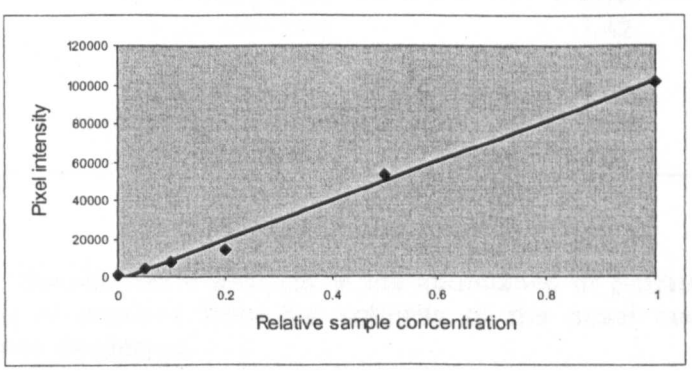

Figure 3.3.3 Relative sample concentration plotted against band intensity shows a linear relationship between the intensity of Western blot detection and β-tubulin III abundance

Equation of trendline: y= 103526x-1500.2, r^2= 0.9945.

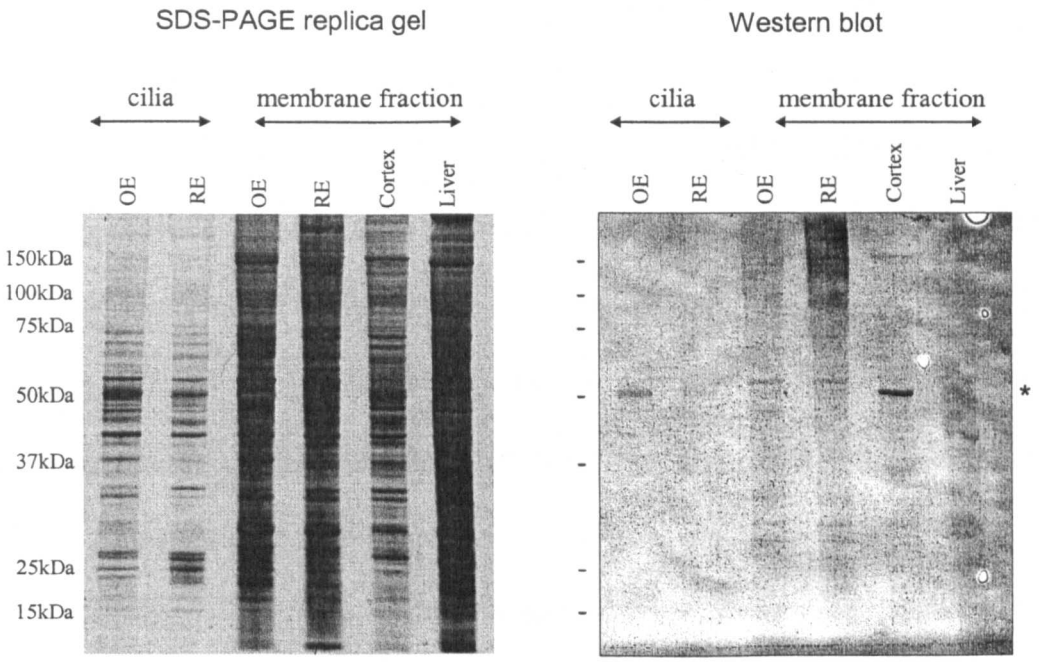

Figure 3.3.4 Detection of β-tubulin III in preparations of preparations of proteins from the epithelia of the nasal cavity and cerebral cortex membrane

Cilia preparations and crude membrane fractions were isolated as described in Section 2.3. *denotes the position of the β-tubulin III protein band. Western blot detection performed using 1:1000 anti- β-tubulin III antibody and 1:3000 goat anti-mouse IgG.

Lane	Sample	Relative enrichment
1	Olfactory cilia	3.70
2	Respiratory cilia	1.42
3	OE membrane	2.00
4	RE membrane	1.38
5	Cerebral cortex membrane	11.05
6	Liver membrane	0.92

Table 3.3.2 Densitometric analysis of the abundance of β-tubulin III in preparations of proteins from the epithelia of the nasal cavity and cerebral cortex membrane

Relative enrichment was the ratio of the relative concentrations of β-tubulin III in each sample, calculated by applying the trendline equation in Figure 3.3.3 to the band intensity values provided by densitometry analysis of the Western blot.

approximately 5-fold (from personal experience, c.f. lanes 2 and 4 in Figure 3.3.2). Taking this into consideration, the relative enrichment of β-tubulin III is likely to be greater than 10-fold in the olfactory cilia preparation compared to the crude membrane preparation. This was considered to be good biochemical evidence of the enrichment of olfactory cilia proteins in the preparation used for proteomic analyses. The strong antibody hybridisation observed with the cortical membrane fraction is likely to be the result of an increased protein concentration and potentially a higher proportion of subtype III compared to other β-tubulin subtypes in cortical neurons (25% β-tubulin in cortical neurons is subtype III, proportions in ORNs currently unknown, Banerjee *et al*, 1988).

The olfactory cilia preparations from mouse and sheep were validated by the proof of isolation of intact cilia vesicles as shown by electron microscopy (Figure 3.3.1) and the similarity of the one-dimensional SDS-PAGE protein profiles to the profile of the rat olfactory cilia sample in the crucial 45kDa/55kDa regions that contain the cytoskeletal proteins actin and tubulin (see Figure 3.3.5). The similarity in enrichment of the cytoskeletal proteins is also shown in the profiles of the 2D-PAGE protein separations of the olfactory cilia (Figure 3.3.6). The reproducibility of the protein profiles of rat and sheep olfactory cilia are demonstrated in the 2D-gels shown in Figures 3.3.7 and 3.3.8, which were run at various times over a 2 year period. As major characterisation of the mouse olfactory cilia preparations was not undertaken there are insufficient gels run of the enriched cilia fractions to show profile reproducibility.

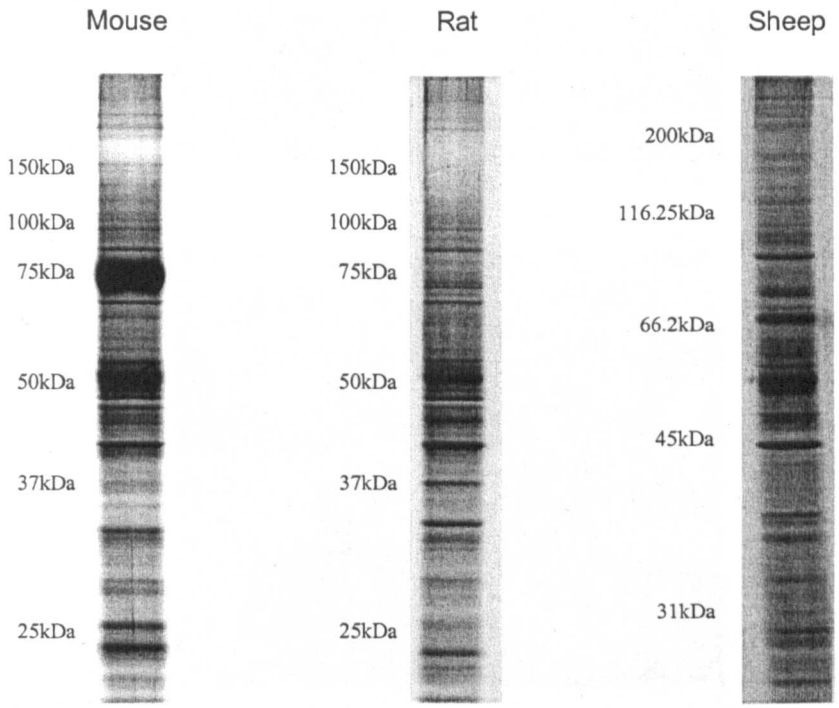

Figure 3.3.5 One-dimensional protein profiles from SDS-PAGE separation of enriched olfactory cilia preparations from mouse, rat and sheep olfactory tissue

SDS-PAGE separations performed using large format gels (final acrylamide/bisacrylamide concentration 10%).

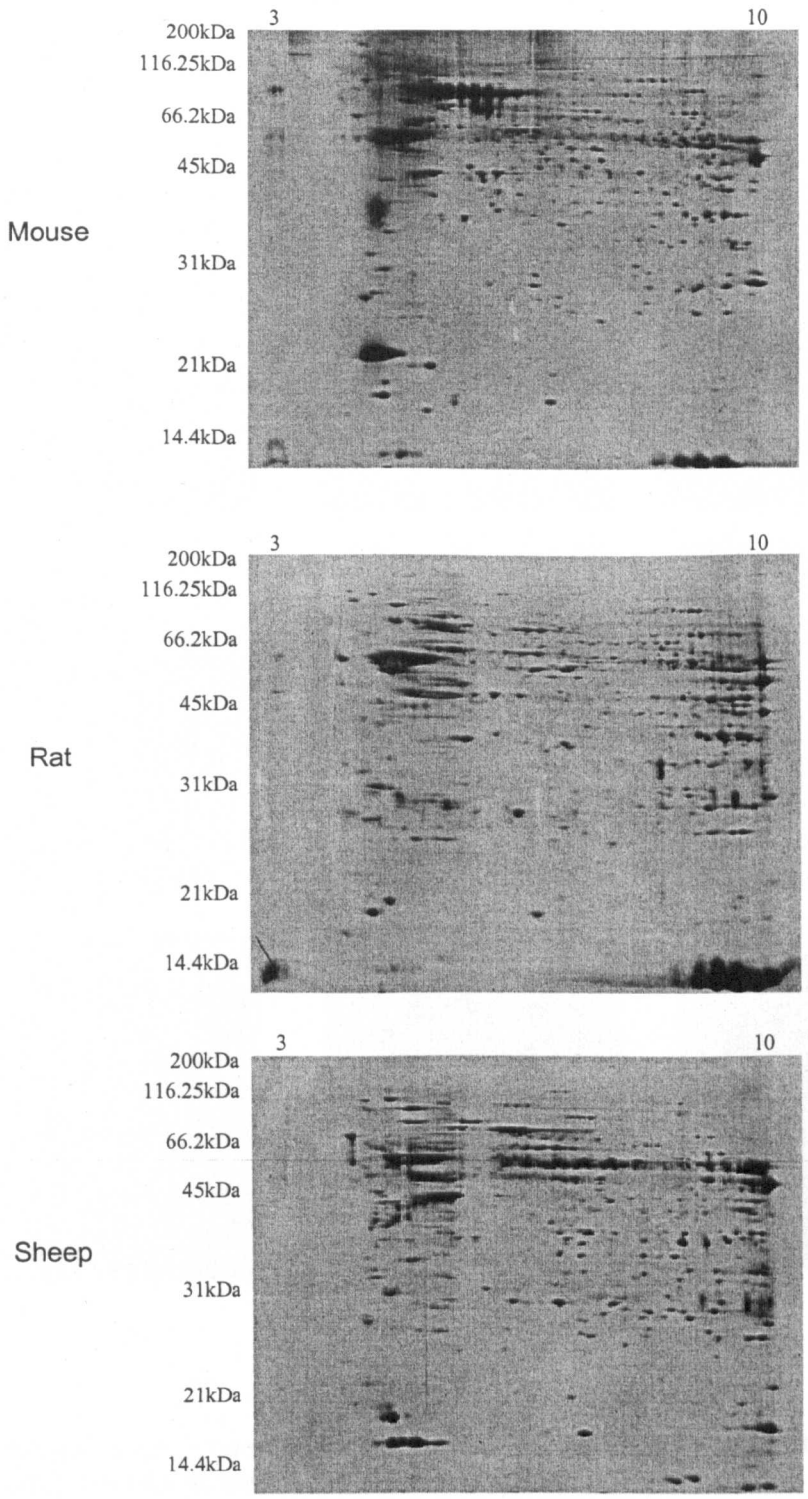

Figure 3.3.6 Two-dimensional protein profiles of olfactory cilia proteins preparaed from mouse, rat and sheep olfactory tissue

Isoelectric focussing was performed using pH3-10 (non-linear) IPG strips and the second dimension was run on large format gels (final acrylamide/bisacrylamide concentration 10%) .

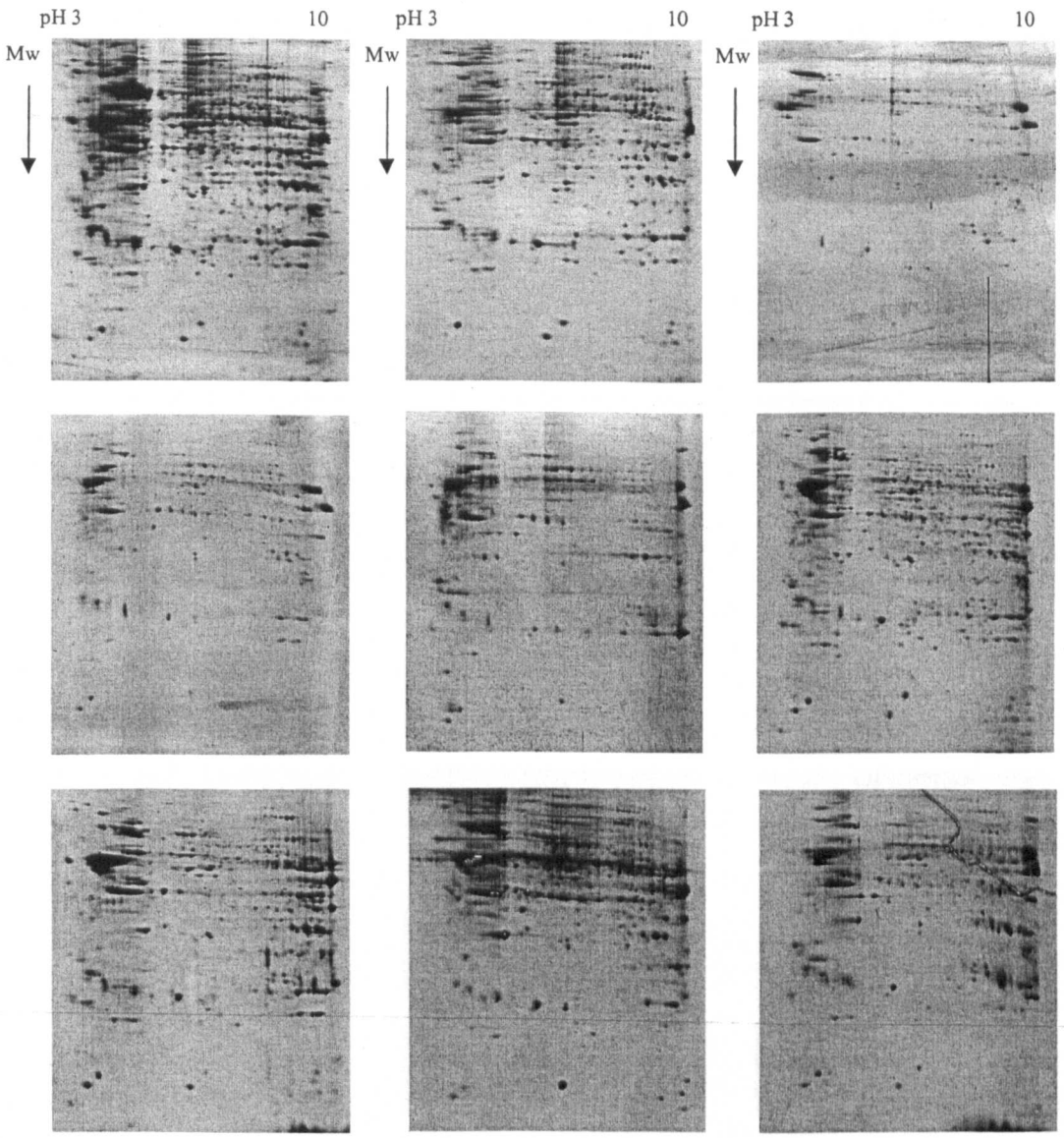

Figure 3.3.7 Two-dimensional gels of multiple preparations of rat olfactory cilia show the reproducibility of the protein profile

Isoelectric focussing of enriched rat olfactory cilia preparations was performed using 11cm 3-10 (non-linear) IPG strips. The second dimension was run on large format gels (final acrylamide/bisacrylamide concentration 10%) . All gel images oriented as shown in the top layer of gels, with the molecular mass of proteins decreasing from top-to-bottom.

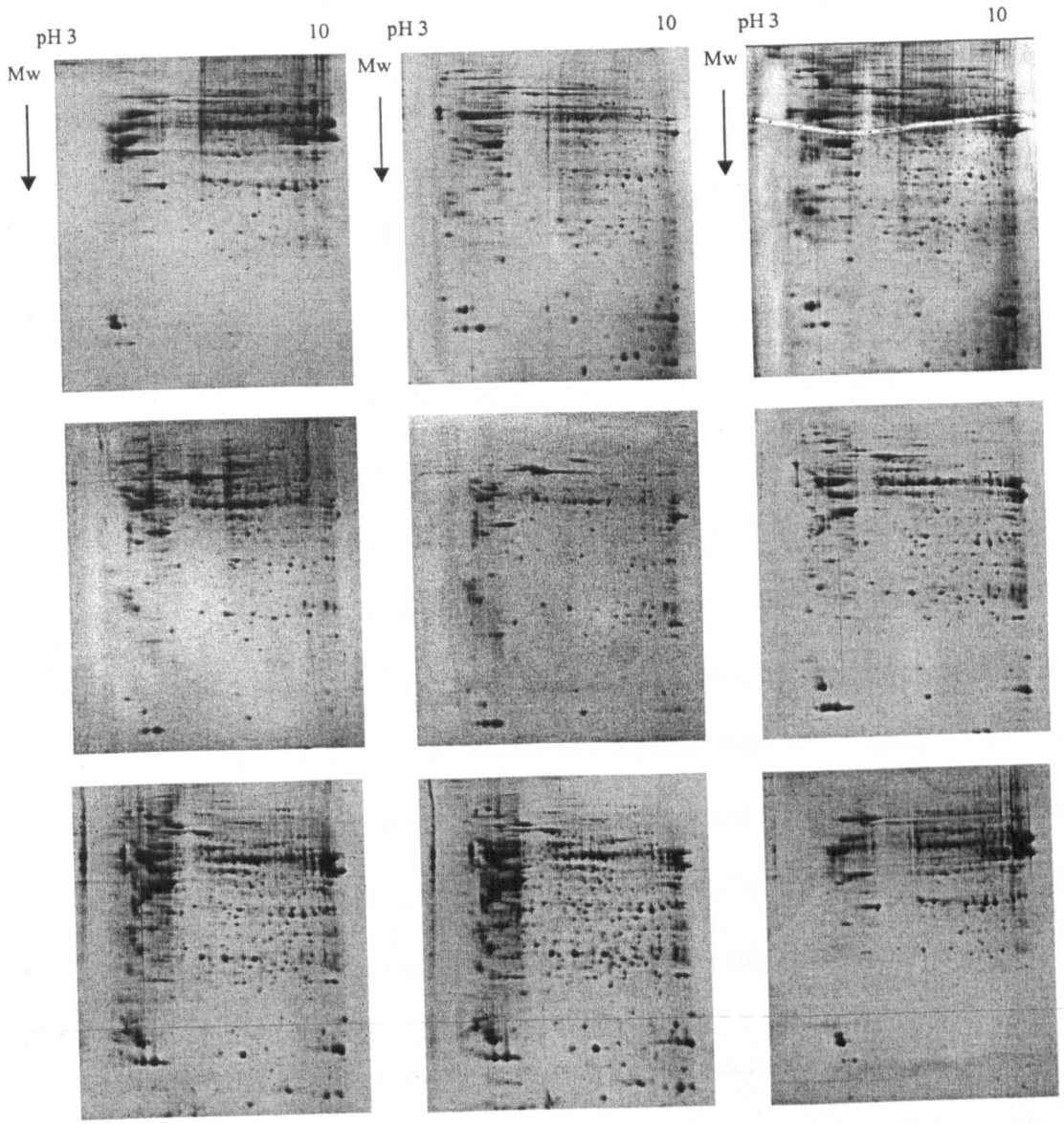

Figure 3.3.8 Two-dimensional gels of multiple preparations of sheep olfactory cilia show the reproducibility of the protein profile

Isoelectric focussing of enriched sheep cilia preparations was performed using 11cm 3-10 (non-linear) IPG strips. The second dimension was run on large format gels (final acrylamide/bisacrylamide concentration 10%) . All gel images are shown with pH increasing left-to-right and molecular mass decreasing top-to-bottom.

3.3.2 Respiratory cilia preparations

The respiratory cilia preparations are derived from the membranous lining of the nasal septum. The membrane covering the nasal septum however is not homogeneous and contains sensory regions of both the main olfactory system (including the septal organ) and vomeronasal system (Farbman, 1992; Mombaerts *et al.*, 1996). From visualisation of receptor neuron processes, it can be estimated that in the mouse at least, the non-sensory respiratory epithelium makes up just over half of the surface membrane lining the nasal septum (Mombaerts *et al.*, 1996). This means that the cilia preparation derived from the septal membrane will be composed of a mixture of cilia of olfactory and respiratory epithelial origin.

The fact that the source of the respiratory cilia sample contains a mixture of olfactory and respiratory tissue means that searching for proteins found solely in the olfactory cilia sample will not identify the proteins specific to the sensory cilia. Instead proteins with a high abundance in olfactory cilia but a lesser abundance in respiratory cilia can be investigated as potentially specific to sensory cilia. In order to be effective however, this approach requires evidence of the proportion of olfactory and respiratory cilia in the sample referred to as respiratory cilia in this thesis.

Enrichment of olfactory marker protein and β-tubulin III indicate that the respiratory cilia preparation is a mixture of olfactory and respiratory cilia An immunoblot was performed to determine how much of the lining of the nasal septum was olfactory epithelium using a polyclonal antibody to the olfactory marker protein (OMP), a protein known to be localised in the neuronal processes of olfactory receptor neurons (Margolis, 1972; Keller and Margolis, 1975).

To test the relative amounts of olfactory and respiratory epithelium in the nasal septum sample, crude membrane preparations were made from nasal turbinates

and nasal septum epithelium. The protocol followed was as described in Section 2.3 with equal protein loading achieved using the dot blot method (Section 2.4). The supernatant from the final centrifugation was collected as a cytosolic fraction of the types of epithelia and used to assess relative levels of OMP in the nasal turbinates (olfactory epithelium) and septal epithelium (olfactory/respiratory epithelium). Serial dilutions of the crude cytosolic fraction of the olfactory epithelium were used to test the relationship between pixel intensity on the immunoblot and OMP concentration (Figure 3.3.9 and Table 3.3.3). In this case, the relationship between Western blot band intensity and OMP concentration was non-linear (Figure 3.3.10). The immunoblot and densitometric analysis of the relative enrichment of OMP in olfactory epithelium *versus* septal epithelium are shown in Figure 3.3.11 and Table 3.3.4).

As the relationship between band intensity and the relative concentration of OMP is non-linear, the calculation of the relative enrichment of OMP in the three samples was calculated manually using the formula of the line of best fit (Figure 3.3.10). The results show a major difference in the level of OMP and therefore ORNs in the membrane lining the septum and the nasal turbinates. This confirms that a substantial amount of the septal lining is respiratory epithelium. However this does not automatically mean that the cilia derived from the septum show the same bias towards respiratory derivation, as the deciliation protocol was developed for olfactory cilia and may therefore be inherently biased against the isolation of respiratory cilia.

The inclusion of the respiratory cilia sample during the β-tubulin III enrichment tests provides evidence of the olfactory *versus* respiratory cilia composition of the preparation derived from the nasal septum. The results (Figure

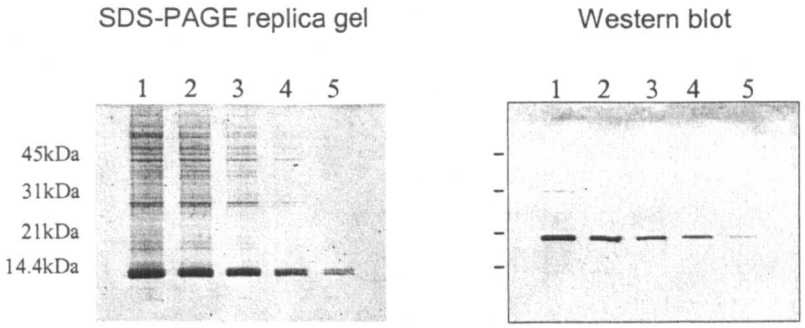

Figure 3.3.9 Specific detection of olfactory marker protein (OMP) in serial dilutions of the cytosolic fraction of rat olfactory epithelium

Serial dilutions of the cytosolic fraction of rat olfactory epithelium were blotted onto nitrocellulose and probed using 1:50000 anti-OMP and 1:5000 rabbit anti-goat IgG. The relative concentration of the protein samples are given in Table 4. The polyclonal anti-OMP antibody was a generous gift from F. Margolis.

Lane	Relative concentration	Band intensity
1	1	220351
2	0.5	170935
3	0.2	96579
4	0.1	56299
5	0.05	23411
6	0	13538

Table 3.3.3 Densitometric analysis of the abundance of OMP in serial dilutions of cytosolic fraction of rat olfactory epithelium.

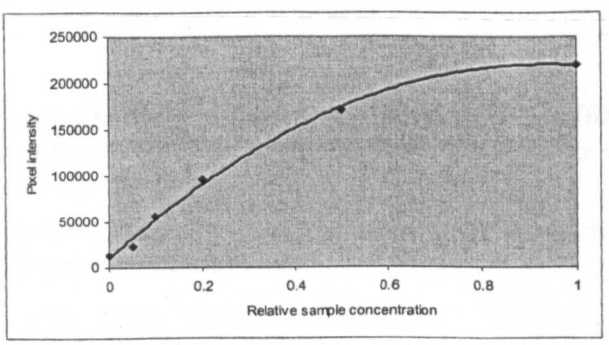

Figure 3.3.10 The relationship between relative sample concentration and Western blot detection intensity is non-linear

The band intensity values shown in Table 3.3.3 were plotted against the relative concentrations values. Equation of trendline: $y = -235688x^2 + 444491x + 10965$, $r^2 = 0.9957$.

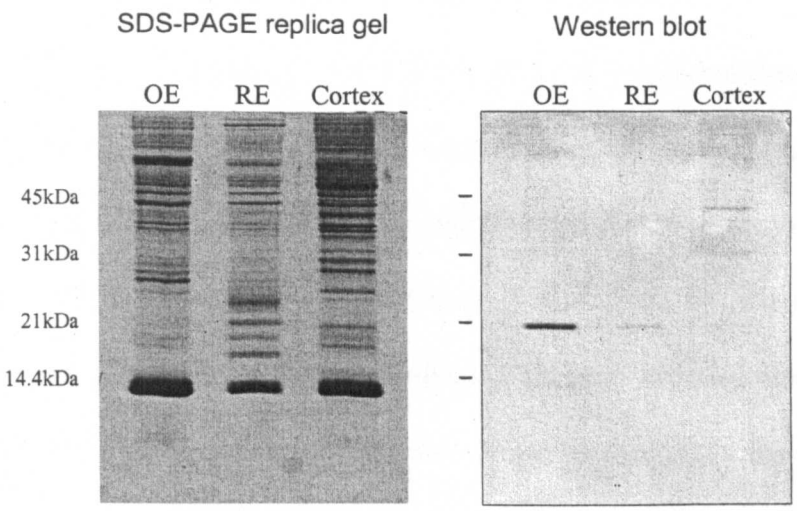

Figure 3.3.11 Detection of OMP in cytosolic fractions of olfactory epithelium (OE), respiratory epithelium (RE) and cerebral cortex

Cytosolic fractions of olfactory epithelium, respiratory epithelium and cortex were prepared from rat tissue. Samples were separated by SDS-PAGE and blotted onto nitrocellulose. They were subsequently probed using 1:50000 anti-OMP and 1:5000 rabbit anti-goat IgG.

Lane	Sample	Band intensity	Relative enrichment
1	Olfactory cilia	46433	90.00
2	Respiratory cilia	4390	1.00
3	OE membrane	2475	1.00

Table 3.3.4 Densitometric analysis of the abundance of OMP in cytosolic fractions derived from the olfactory epithelium, respiratory epithelium and cerebral cortex of the rat

Relative concentration calculated using the trendline equation from Figure 3.3.10 and converted into relative enrichment.

3.3.3 and Table 3.3.2) suggest that the ratio of respiratory cilia: olfactory cilia in this preparation (designated as respiratory cilia) is approximately 3:1.

3.3.3 Identification of proteins unique to the olfactory cilia

From the β-tubulin enrichment immunoblots it can be concluded that proteins present in the olfactory cilia protein preparation are likely to be derived from the olfactory cilia. All of the proteins present in this preparation are also likely to be found in the respiratory cilia sample, as this is known to be a mixture of cilia of olfactory and respiratory epithelial origins. Proteins with significantly reduced abundance (at least three-fold decrease from β-tubulin III enrichment evidence) in the respiratory cilia samples compared to the olfactory samples are likely to be predominantly localised to the olfactory cilia.

3.3.4 Protein profile comparisons

Figure 3.3.5 shows the one-dimensional SDS-PAGE separation of the enriched cilia fractions prepared from mouse, rat and sheep nasal turbinates. From a cursory examination of the protein profiles mouse and rat profiles appear to be similar to each other and both differ significantly from the profile observed in the sheep olfactory cilia preparation. The two areas of major similarity across the protein profiles of all three species are at ~45kDa and the cluster of satellite bands surrounding a central, strongly abundant band corresponding to proteins 50-52kDa in mass. A major difference between mouse and rat profiles is the presence of a highly abundant protein at ~75kDa in the mouse olfactory cilia sample.

The use of two-dimensional polyacrylamide gel electrophoresis (2D-PAGE) added an extra dimension of separation to gel electrophoresis, resolving proteins by

both their isoelectric point (pI) and molecular weight. Therefore to further assess both the number of proteins present in the cilia proteomes of the three species and the protein profile similarities, cilia preparations were also resolved by two-dimensional electrophoresis. Sample 2D-gels with equivalent protein loading are shown in Figure 3.3.6. The comparison of the protein resolution patterns of cilia preparations from each of the three model species again indicated that the profiles of rat and mouse bear great similarity to each other and differ substantially to the profile derived from the sheep olfactory cilia. The reproducibility of the rat and sheep protein profiles are shown in Figures 3.3.7 and 3.3.8 respectively, which show a number of gels run using identical cilia isolation procedures and 2D separation techniques. In both cases the protein separation profiles are reproducible particularly in the top half of gels (>~30kDa), although the differing protein concentration means that the intensity of some protein spots alters significantly, even to the point of absence in gels with low protein loading levels.

As with the one-dimensional protein profiles there appears to be some conserved areas across all model species. The upper half of each gel contains areas of strong similarity, principally in the top left hand corner. This region of the protein profile was also observed in a proteomic analysis of human bronchial cilia and was reported to be composed largely of the cytsoskeletal proteins actin and tubulin (Ostrowski *et al.*, 2002). These identifications were later confirmed during the cilia proteome characterisation work described in this section. Many of the protein profile differences occur in the lower portions of the gel corresponding to the low molecular weight proteins (<25kDa), again in agreement with one-dimensional separation experiments.

3.3.5 Olfactory cilia proteome characterisation

Similarity of protein profiles does not guarantee that the cilia-localised proteins in the species are identical. Conversely, this also means that despite the major differences observed in the sheep olfactory cilia proteome in comparison with mouse/rat cilia suggested by protein profile analysis, the actual proteins present may not be vastly different. Different profiles could also result from changes in individual amino acids of proteins such that their migratory movement in both dimensions can be significantly altered. Thus although the final positions of the proteins may differ between species the proteins present may not. To test this observation and identify proteins conserved across the model species, proteome characterisation work was undertaken. To assess the proteome similarity across the model species in-gel digestions and mass spectrometry were used to identify proteins from the rat and sheep olfactory cilia proteomes. Rat and sheep olfactory cilia proteomes were studied due to the observed differences in protein profiles and rat tissue preparations giving a much greater protein yield than mouse tissue.

The definition of the olfactory cilia proteome is the collection of proteins that are isolated by the cilia preparation method described in Section 2.3. The proteome will thus include integral and peripheral membrane proteins but also proteins localised to the cilia cytosol and those associated with its microtubule axoneme. It will also potentially include extracellular proteins with sufficient attachment to the cilia membrane surface despite initial tissue washes and buffer washes of the final enriched cilia fraction.

The 2D-PAGE profile differences reflect substantial differences in the olfactory cilia proteomes of rat and sheep The identifications made from 2D-PAGE separation of rat olfactory cilia and sheep olfactory cilia (Tables 3.3.5 and 3.3.6) are

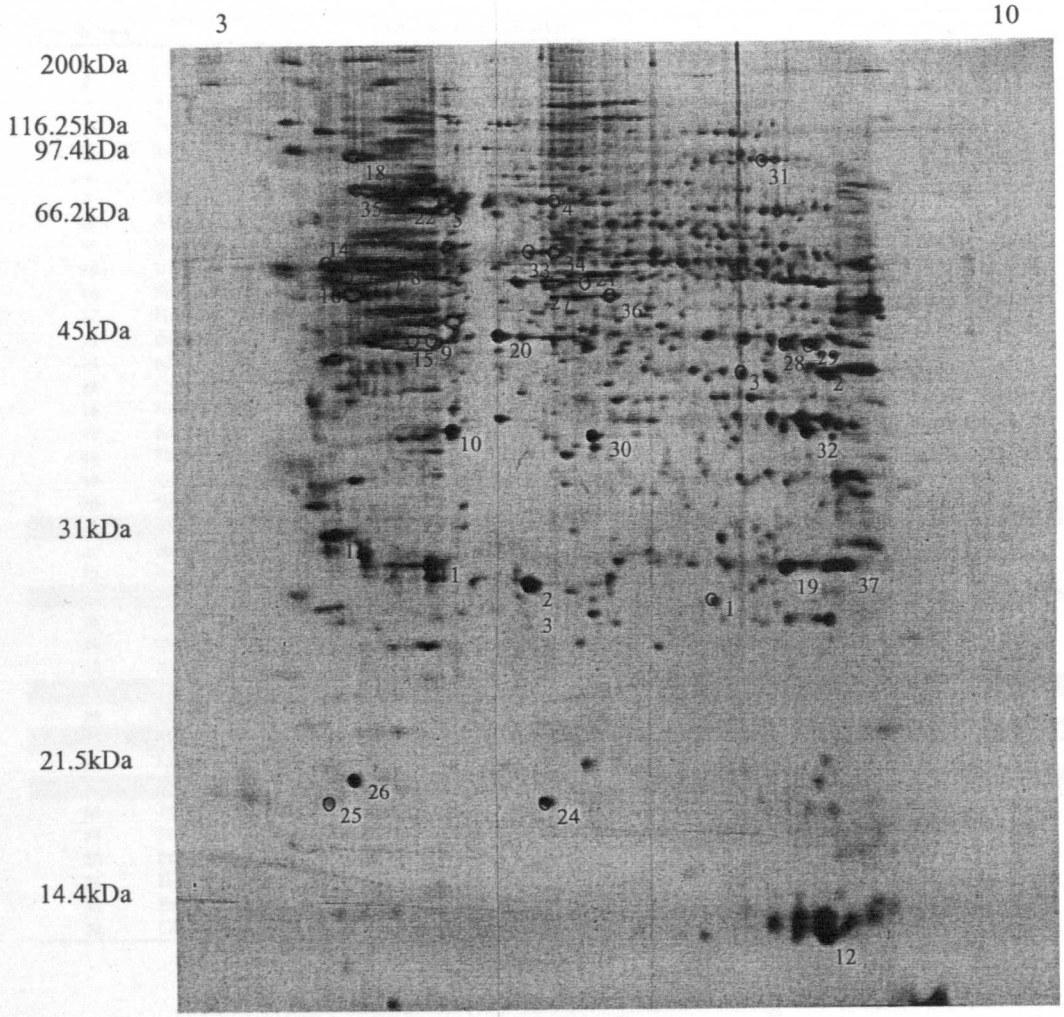

Figure 3.3.12 Protein identifications made by in-gel tryptic digestions from 2D-PAGE separation of rat olfactory cilia

Isoelectric focussing of rat olfactory cilia was performed using an 11cm pH 3-10 (non-linear) IPG strip. The second dimension was run on a large format gel (final acrylamide/bisacrylamide concentration 10%) .

Protein Spot	Putative Identification	NCBI Accession #	Mw (kDa)	Species	Mowse score
1	Glutathione-S-transferase Yb2 (chain 4)	121719	25.7	Rattus norvegicus	217/ 53
2	Thiosulfate transferase	135826	33.2	Rattus norvegicus	83/53
3	Aldehyde reductase	13591894	36.5	Rattus norvegicus	84/53
4	Serum albumin	113580	70.7	Rattus norvegicus	91/53
5	dnaK-type molecular chaperone hsp72-p1 / hsp70kDa protein 8	347019/ 13242237	71.1/ 71.1	Rattus norvegicus	161/53
6	Alpha-tubulin	223556	50.9	Rattus norvegicus	78/59
7	Alpha-tubulin	223556	50.9	Rattus norvegicus	62/53
8	Alpha-tubulin	223556	50.9	Rattus norvegicus	62/53
9	Beta-actin / gamma actin	71620/ 4501887	42.1/ 42.1	Rattus norvegicus/ Homo sapiens	103/53 (both)
10	Visinin-like 1 protein	6755983	22.3	Mus musculus	56/53
11	Similar to KIAA1662	27662706	161.9	Homo sapiens, Rattus norvegicus	81/59
12	Haemoglobin alpha 1	6981010	15.3	Rattus norvegicus	95/53
13	densin-180	16924000	16.7	Rattus norvegicus	54/53
14	p38 Mitogen activated protein kinase	13591928	41.5	Rattus norvegicus	64/53
15	Cytoskeletal gamma-actin	4501887	42.1	Homo sapiens	90/53
16	Keratin-10	21961605	59	Homo sapiens	73/67
17	Keratin-10	21961605	59	Homo sapiens	73/67
18	Heat shock protein HSP 90-beta	1346320	83.6	Rattus norvegicus	124/54
19	Glutathione-S-transferase Yb2	28933457	25.7	Rattus norvegicus	79/57
20	Secretory protein, 45kD	34878986	100.2	Rattus norveigus	63/57
21	Aldehyde dehydrogenase, mitochondrial	3121992	48.2	Rattus norvegicus	141/57
22	Heat shock protein 8	13242237	70.8	Rattus norvegicus	87/57
23	Peroxiredoxin 6	16758348	24.8	Rattus norvegicus	58/57
24	Similar to mitochondrial ribosomal protein L15	34866074	38.9	Rattus norvegicus	60/57
25	Cytochrome b5	224985	10.4	Rattus norvegicus	75/57
26	Olfactory marker protein	92567	18.7	Rattus norvegicus	58/57
27	Aldehyde dehydrogenase	16073616	48.2	Rattus norvegicus	138/57
28	Citrate synthase	18543177	51.8	Rattus norvegicus	88/57
29	Creatine kinase	34856772	42.7	Rattus norvegicus	59/57
30	Citrate synthase	18543177	51.8	Rattus norvegicus	66/57
31	Malate dehydrogensase 1	37590235	36.5	Rattus norvegicus	57/57
32	Mitochondrial aconitase	13242312	85.4	Rattus norvegicus	145/57
33	Thiosulphate sulphurtransferase	135826	33.2	Rattus norvegicus	93/57
34	Protein diulphide isomerase A3 precursor	1352384	56.9	Rattus norvegicus	51/57
35	Protein diulphide isomerase A3 precursor	1352384	56.9	Rattus norvegicus	176/57
36	Heat shock 70kD protein 5	25742763	72.3	Rattus norvegicus	133/57
37	Enolase 1, alpha	6978809	47.4	Rattus norvegicus	118/57
38	Glutathione S-transferase	204501	25.8	Rattus norvegicus	148/57

Table 3.3.5 Protein identifications made during the characterisation of the rat olfactory cilia proteome

Grey shaded rows are proteins predominantly localised to nuclei/mitochondria (source: NCBI protein database annotation and Matews and van Holde, 1996). A MOWSE score greater than 1 has a probability of occuring by chance of $p<0.05$.

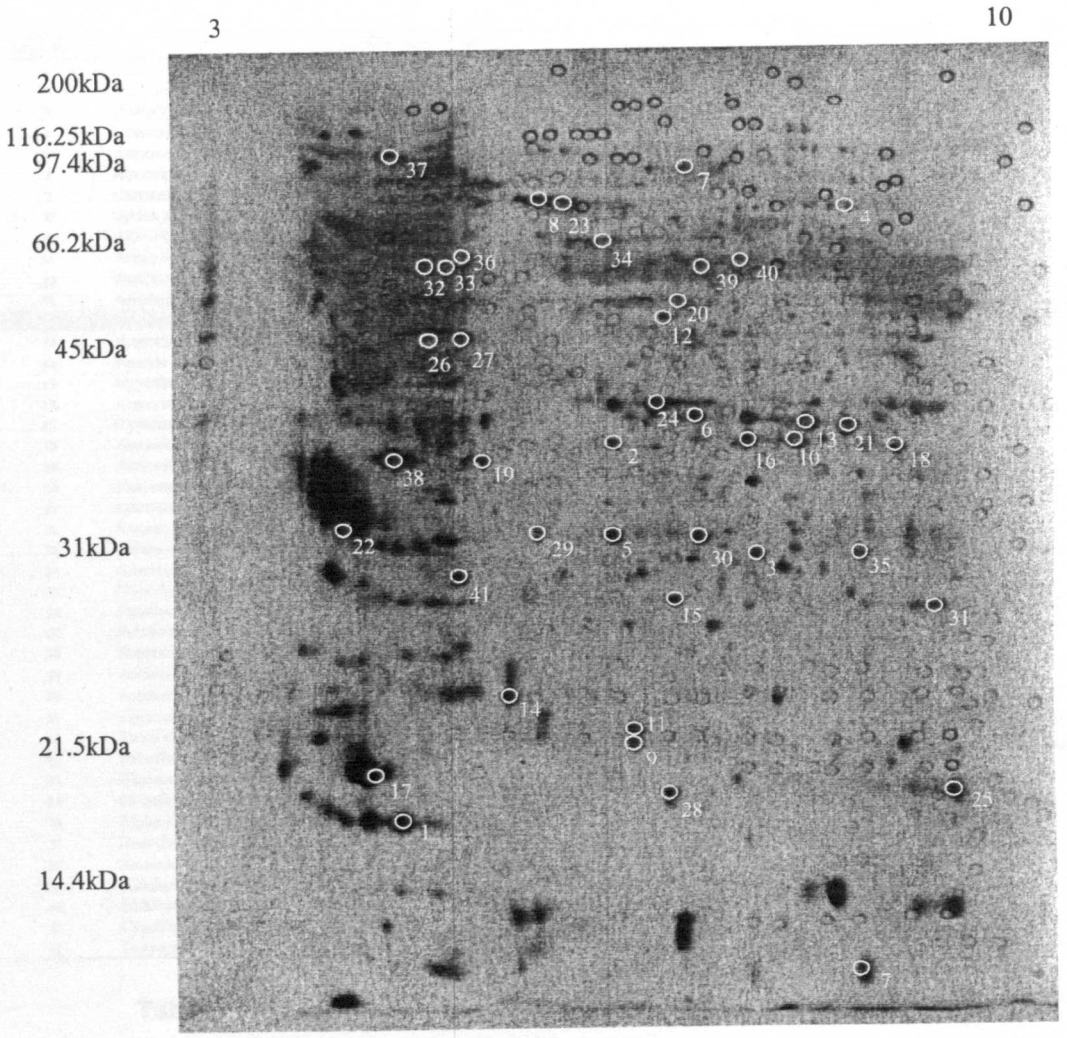

Figure 3.3.13 Protein identifications made by in-gel tryptic digestions from 2D-PAGE separation of sheep olfactory cilia

The small circles visible on the right-hand side of the gel are artefacts from the scanning process.

Isoelectric focussing of sheep olfactory cilia was performed using an 11cm pH 3-10 (non-linear) IPG strip. The second dimension was run on a large format gel (final acrylamide/bisacrylamide concentration 10%) .

Protein Spot	Putative Identification	NCBI Accession #	Mw (kDa)	Species	Mowse score
1	CTCL tumour antigen se20-7 (fragment)	11385652	73.9	Homo sapiens	69/65
2	Unamed protein product	14042893	74.3	Homo sapiens	75/65
3	Phosphoinositide 3-kinase T96	7434348	15.3	Homo sapiens	96/66
4	Coatomer protein complex subunit gamma 2	8567340	98.8	Mus musculus	73/65
5	Antioxidant protein 2/1-cys peroxiredoxin	5902790	25.1	Bos taurus	79/66
6	Annexin I	1168463	39.2	Bos taurus	84/66
7	Carbonic anydrase VII	10304383	29	Mus musculus	74/66
8	Serum albumin precursor	113582	71.1	Ovis aries	250/66
9	ADP-ribosylation factor 3	4502203	20.6	Homo sapiens	77/66
10	Annexin II	113948	38.9	Bos taurus	179/66
10	Annexin I	1168463	39.2	Bos taurus	113/66
11	Annexin I	1168463	39.2	Bos taurus	134/66
12	Similar to Zinc-finger protein 93	12643428	72.7	Homo sapiens	69/66
13	Annexin II	113948	38.9	Bos taurus	166/66
14	Ferritin heavy chain	2119694	16.6	Cricetulus griseus	67/66
15	Hypothetical protein XP_118960	20558048	10.6	Homo sapiens	77/66
16	Annexin I	1168463	39.2	Bos taurus	113/66
17	Cytochrome b5	10120990	10.6	Bos taurus	111/65
18	Annexin II	113948	38.9	Bos taurus	150/66
19	Annexin V	284588	36	Bos taurus	139/66
20	Non-neural enolase (alpha isozyme)	13637776	47.4	Mus musculus	70/66
21	cytochrome b5 reductase	999817	31	Sus scrofa	72/66
22	Katanin p80 subunit B1	14775184	73.3	Homo sapiens	77/65
23	Serum albumin precursor	113582	71.1	Ovis aries	180/66
24	Annexin I	1168463	39.2	Bos taurus	124/66
25	Hypothetical protein	21739306	71.9	Homo sapiens	82/67
26	Putative beta-actin	49868	39.4	Mus musculus	82/66
27	Putative beta-actin	49868	39.4	Mus musculus	94/65
28	Superoxide dismutase (Cu-Zn)	134627	15.7	Ovis aries	80/67
29	Antioxidant protein 2	27807167	25.1	Bos taurus	68/67
30	Antioxidant protein 2	27807167	25.1	Bos taurus	111/67
31	Thioredoxin peroxidase II	6942233	22.5	Cricetulus griseus	76/67
32	Tubulin, beta 2/ class Ivb beta tubulin	5174735/ 27368062	50.3/ 50.2	Homo sapiens	83/67
33	Tubulin, beta 2/ class Ivb beta tubulin	5174735/ 27368062	50.3/ 50.2	Homo sapiens	83/67
34	Glucose regulated protein 58kDa	27805905	57.3	Bos taurus	151/67
35	Glutathione S-tranferase M1	28461273	25.8	Bos taurus	71/67
36	Alpha-tubulin	10881132	49.7	Macaca mulatta	124/67
37	Heat shock protein 90-alpha (HSP 86)	17865490	83.4	Equus caballus	87/67
38	Annexin V	284588	36	Bos taurus	141/67
39	Aldehyde dehydrogenase 1A1	1706388	55.4	Ovis aries	122/67
40	Aldehyde dehydrogenase 1A1	1706388	55.4	Ovis aries	72/67
41	Cytochrome P450-11beta	303794	57.4	Rattus norvegicus	69/67
41	Tropomyosin-3	24119203	29	Homo sapiens	70/67

Table 3.3.6 Protein identifications made during the characterisation of the sheep olfactory cilia proteome

Grey shaded rows are proteins thought to be predominantly localised to the nucleus. Source: protein annotation at NCBI database (www.ncbi.nlm.nih.gov). A MOWSE score greater than 1 has a probability of occuring by chance of $p<0.05$.

provided with the accompanying reference 2D-gels (Figures 3.3.12 and 3.3.13 respectively). During the characterisation of the rat olfactory cilia proteome a total of 38 identifications were made, corresponding to 31 different proteins. Analysis of the sheep olfactory cilia proteome provided 43 protein identifications comprising 31 individual proteins. A brief comparison between the proteins found in rat and sheep olfactory cilia indicated that overall less than half of the proteins identified are present in both. This figure includes 7 proteins that were present in different subtypes in the olfactory cilia of the two species *e.g.* HSP90-beta identified in rat tissue and HSP90-alpha in sheep cilia.

The grey shaded rows in the tables of identifications contain proteins predominantly found in mitochondria or nuclei. These proteins are therefore likely to be present in the preparations as a result of contamination rather than true localisation to the olfactory cilia and are not discussed further in this section. Proteins with a distribution split between mitochondrial and cytosolic pools are classified on available information concerning isoform distribution or are designated cytosolic by default.

Three major classes of proteins are found in both rat and sheep olfactory cilia proteomes There are however important areas of similarity that provide evidence for the proteins crucial to the function of olfactory cilia. The first region and set of identifications common to both the species is located in the top left quarter of the gels. This area corresponded to the cytoskeletal proteins, including actin, tubulin and in rat olfactory cilia keratin. The shared 2D-gel migration characteristics were the result of highly conserved protein sequences as indicated by the similarity of the peptide mass fingerprints (Figures 3.3.14 and 3.3.15).

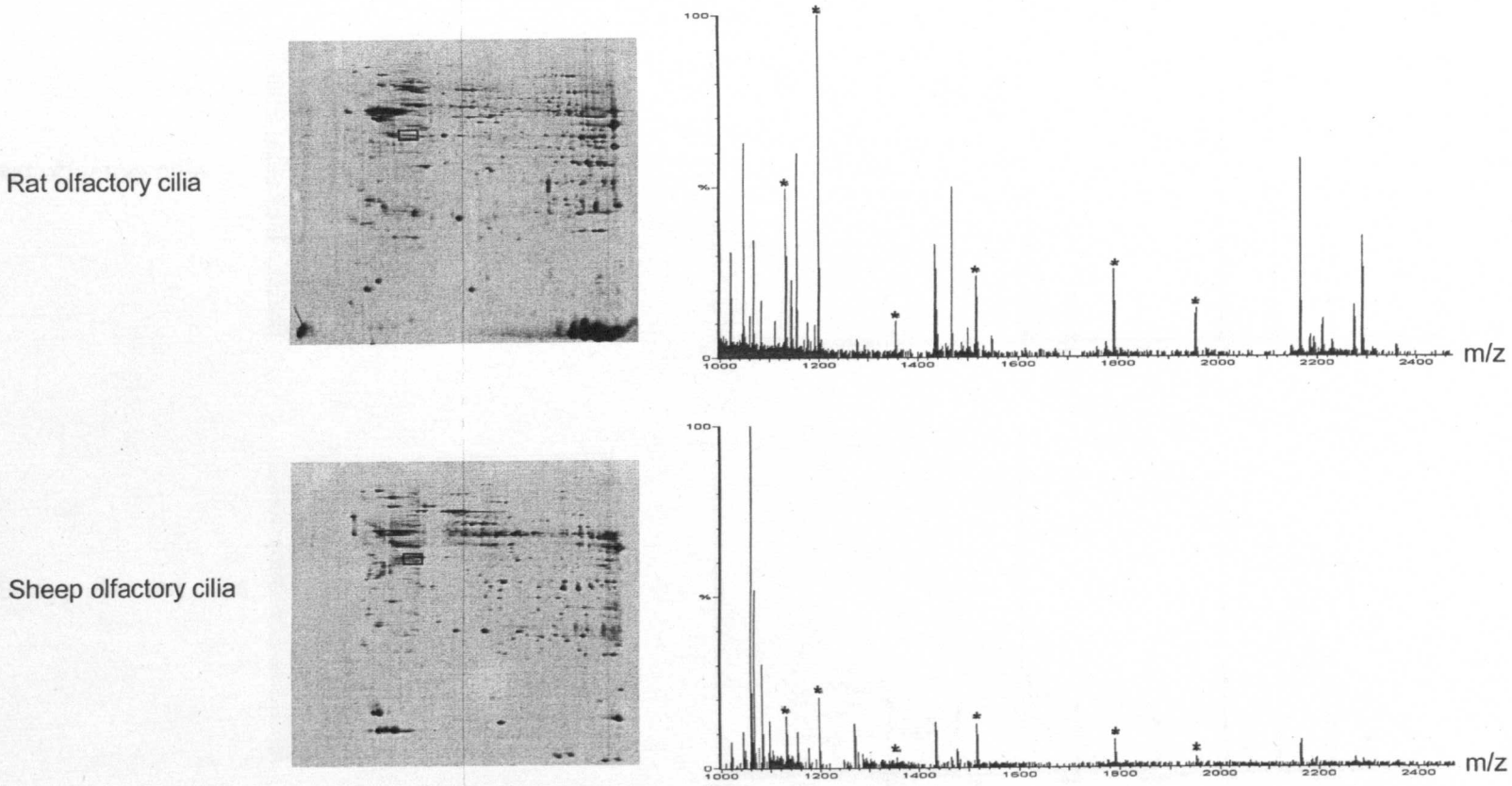

Figure 3.3.14 The common position of β-actin in the 2D-gel profile and the similarities of the peptide mass fingerprint indicate that the sequence of this protein is highly conserved between rat and sheep

The boxed areas of the 2D-gel represent the location of the β-actin protein in the protein profiles of rat and sheep olfactory cilia. The spectra shown alongside the gels are the MALDI spectra obtained from the in-gel digestions of proteins in the boxed regions on the respective cilia preparations. *denotes peptides from β-actin.

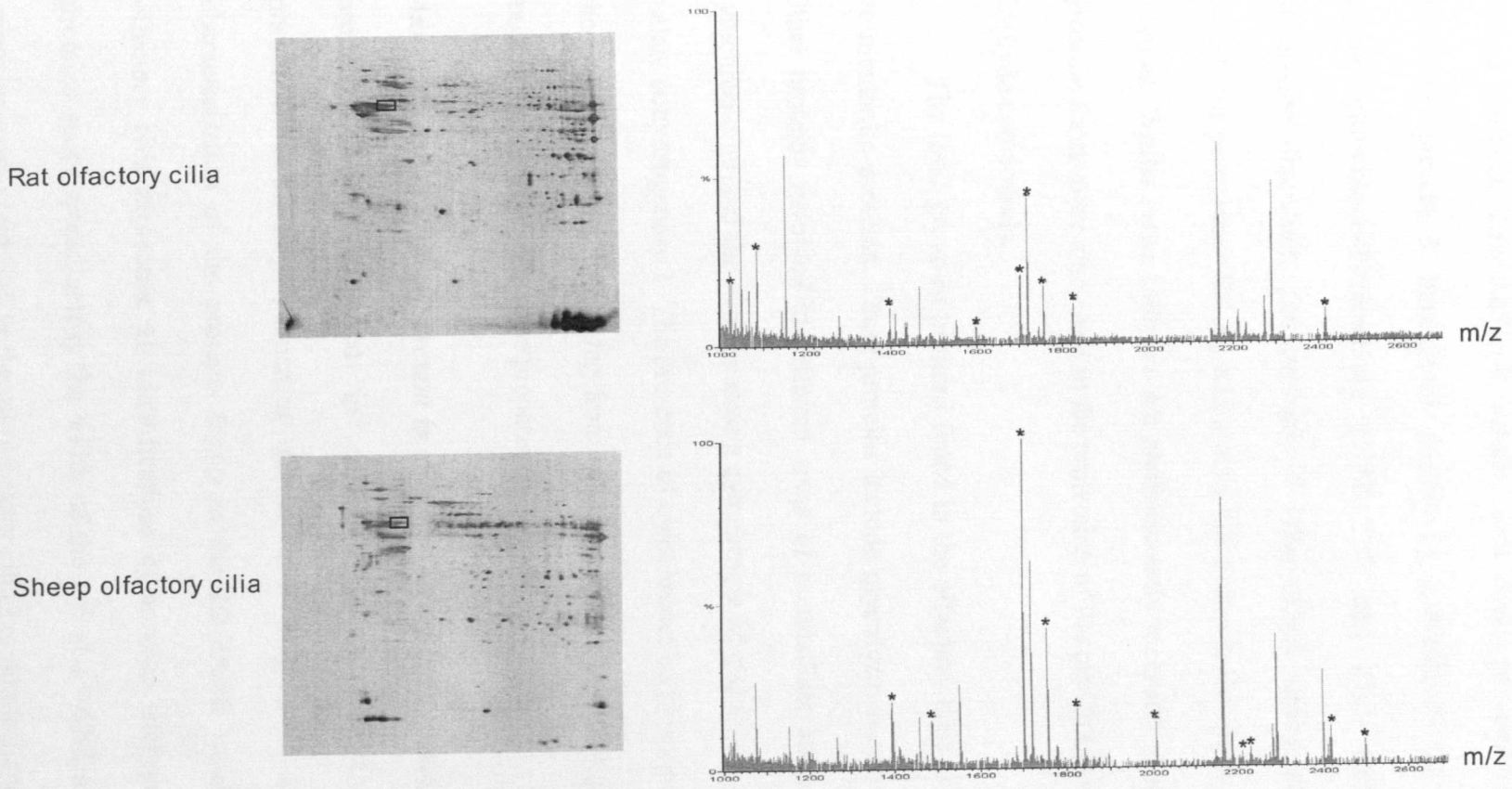

Figure 3.3.15 The common position of α-tubulin in the 2D-gel profile and the similarities of the peptide mass fingerprint indicate that the sequence of this protein is highly conserved between rat and sheep

The boxed areas of the 2D-gel represent the location of the α-tubulin protein in the protein profiles of rat and sheep olfactory cilia. The spectra shown alongside the gels are the MALDI spectra obtained from the in-gel digestions of proteins in the boxed regions on the respective cilia preparations. *denotes peptides from α-tubulin.

A second area of similarity was another category of proteins that dominate the putative olfactory cilia proteome identifications: cellular detoxification and defence proteins. This category includes heat shock proteins (HSP 90 subtypes, HSP70kDa protein 5, heat shock protein 8), subunits of the biotransformation enzyme glutathione-S-transferase (GST Yb2 and M1), antioxidant enzymes (superoxide dismutase, peroxiredoxin 6 (also called antioxidant protein 2) and thioredoxin peroxidase II). An addition to this group is the aldehyde dehydrogenase enzymes. Whilst some subtypes are predominantly localised to mitochondria, other cytosolic forms play a key role in the protection of the cell from potentially cytotoxic aldehyde compounds.

The third group of proteins found in the olfactory cilia of both rat and sheep are metabolic proteins. These proteins include glycolysis enzymes such as enolase. Other proteins involved in different areas of metabolism are aldehyde reductase, cytochrome b5 and the accompanying cytochrome b5 reductase, creatine kinase and malate dehydrogenase 1. The presence of cytochrome b5 is particularly prominent in sheep olfactory cilia, appearing from visual analysis of the 2D-gels to be one of the most abundant proteins in the preparation.

Annexins are exclusively present in sheep olfactory cilia Annexins are a family of proteins widely expressed in eukaryotes that exhibit calcium-dependant phospholipids-binding properties (Benz and Hofmann, 1997). During the characterisation of the proteins found in the 2D-PAGE separation of the sheep olfactory cilia proteome, 10 identifications of annexin subtypes were made from proteins spots spread across the width of the gel at 35-40kDa. In comparison, no annexins were identified in the rat olfactory cilia preparation and with the exception of annexin V, there were no unidentified protein spots in an equivalent position on

the rat olfactory cilia 2D-gel. The absence of annexin subtypes I and II in rat olfactory cilia is considered to be significant as they are present at a relatively high abundance in the sheep olfactory cilia preparation and form a prominent part of the overall protein profile. The presence of annexins may therefore represent an adaptive difference between the olfactory systems of the two species.

3.3.6 Mouse olfactory cilia characterisation

Detailed proteome characterisation of enriched mouse olfactory cilia preparations was not undertaken due to the striking similarity of the protein profile with that of the rat olfactory cilia. However there is one substantial difference between the olfactory cilia preparations of the mouse, rat and sheep: a cluster of highly abundant proteins present exclusively in mouse olfactory cilia preparations. This difference is easily discernable in both the 1D and 2D protein profiles shown in Figure 3.3.5 and Figure 3.3.6 respectively although the apparent mass suggested by the gels differs from ~75kDa in SDS-PAGE separation (hence designation of these proteins as the 75kDa cluster) to ~90kDa in 2D-PAGE. This 75kDa cluster and was repeatedly found in the analysis of the mouse olfactory cilia proteomes of four different inbred strains (Figure 3.3.16). This demonstrates that the cluster is not specific to an individual strain.

The 75kDa cluster is magnified in Figure 3.3.17. The cluster appears as a row of proteins with identical mass but differing pIs. Suggesting that these proteins may be closely related in sequence and potentially isoforms of a single protein. In-gel tryptic digestions were performed on three spots of the cluster indicated in Figure 3.3.17, alongside the resulting MALDI spectra. Despite the differences in the peak heights, the spectra of digests d5 and d7 are very similar and both share little similarity with the d3 spectrum. d5 and d7 are therefore likely to be the isoforms of a

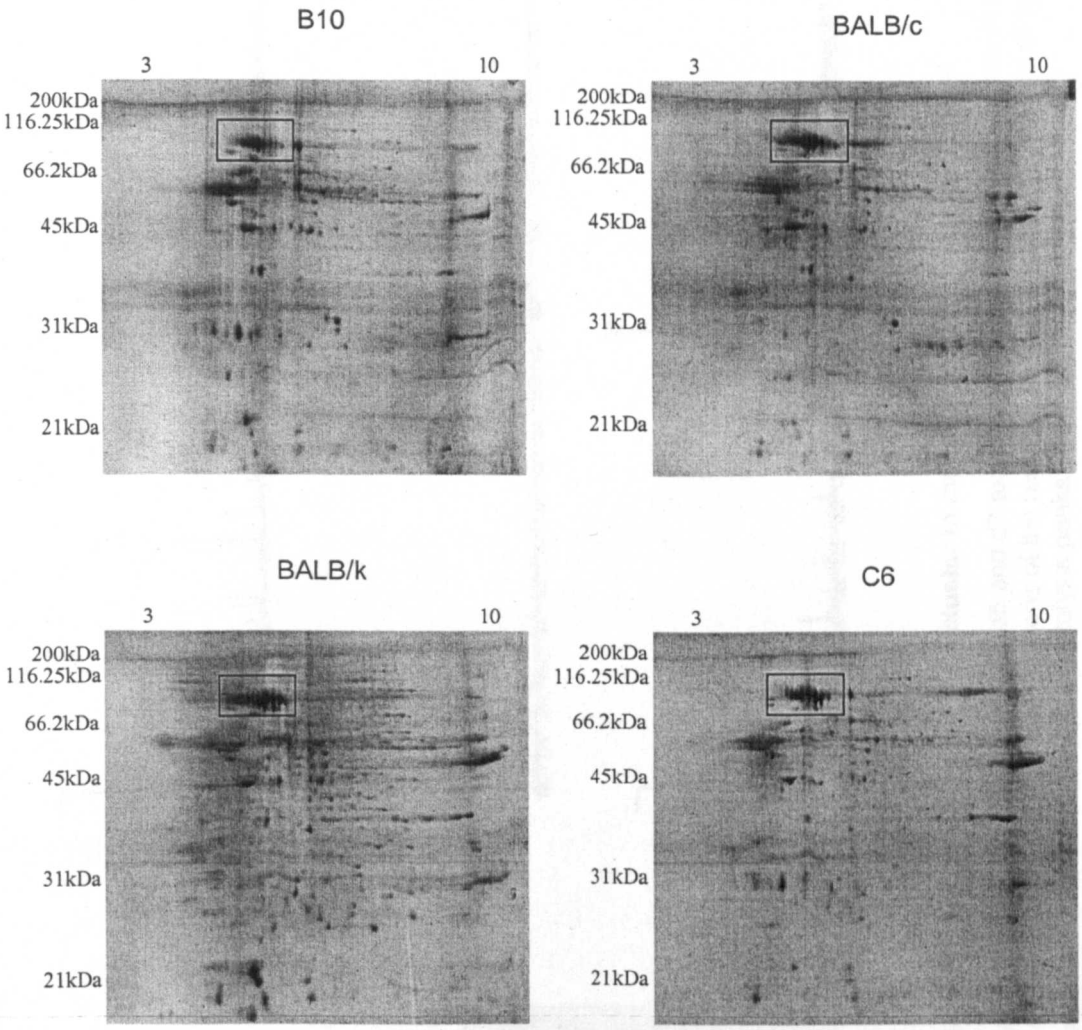

Figure 3.3.16 Two-dimensional gels of olfactory cilia preparations from different strains of in-bred mice demonstrate that the 75kDa cluster appears reproducibly and is not strain-specific

Enriched olfactory cilia fractions were prepared from nasal turbinates dissected from two mice of each strain. Isoelectric focussing was performed using 7cm pH 3-10 (linear) IPG strips. The second dimension was run using 7cm mini-gels. The boxed regions in each gel surround the 75kDa cluster.

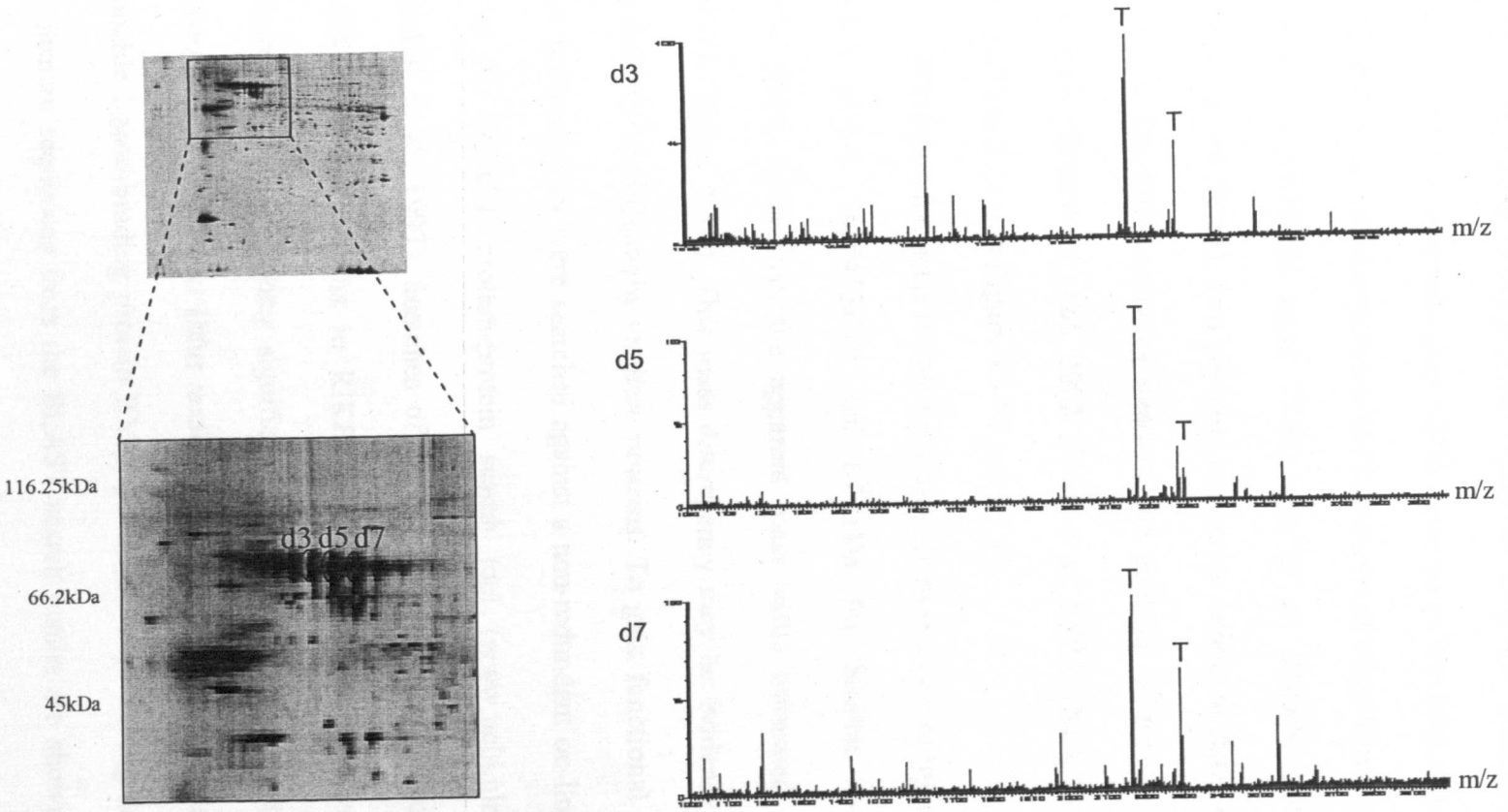

Figure 3.3.17 Analysis of selected proteins from the 75kDa cluster in mouse olfactory cilia preparations

The magniified 2D-gel image shows the three protein spots d3, d5 and d7 excised from the 75kDa protein cluster in mouse olfactory cilia preparations for in-gel trypsin digestion. Comparisons of the resulting MALDI spectra indicate that d5 and d7 have related protein sequences. T denotes the major trypsin autolysis peaks observed in all samples.

single protein whilst d3, with a very different peptide mass fingerprint is more distantly related if similar at all.

75kDa cluster contains two proteins related to rat RYF3 Searching the peptide lists against the on-line non-redundant NCBI database (www.ncbi.nlm.nih.gov) failed to identify d3 but provided conclusive identifications of d5 as Similar to RIKEN cDNA 5430413K10 (MOWSE score 73/61) and d7 as RIKEN cDNA 5430413K10 (MOWSE score 78/61); two proteins sequences predicted from the computational analysis of the Mus musculus genome and analysis of mouse cDNA sequences respectively (Strausberg *et al.*, 2002; Kawai *et al*, 2001). The spectra used to identify d5 and d7 are shown in Figure 3.3.18 and 3.3.19.

The predicted mass of these proteins (from primary sequence) is 62.8kDa for RIKEN cDNA 5430413K10 and 67.3kDa for Similar to RIKEN cDNA 5430413K10, lower than the apparent mass value estimated from SDS-PAGE analysis (Figure 3.3.5). This mass discrepancy may be evidence of covalent post-translational modifications to these proteins. To gain functional information about these proteins, they were searched against a non-redundant on-line protein database using the BLAST protein-protein search tool (www.ncbi.nlm.nih.gov/BLAST, Altschul *et al.*, 1997). Searches of the protein sequences of both RIKEN cDNA 5430413K10 and Similar to RIKEN cDNA 5430413K10 gave identical results (Figure 3.3.20) identifying significant similarity between these proteins and an unnamed protein product (*Mus musculus*), vomeromodulin (*Rattus norvegicus*) and probable ligand-binding protein RYF3 (RYF3) (*Rattus norvegicus*). Alignments of the protein sequences from the BLAST search results are shown in Figure 3.3.21. The alignments show that there is extensive sequence similarity between the RIKEN cDNA 5430413K10, Similar to RIKEN cDNA 5430413K10, unnamed protein

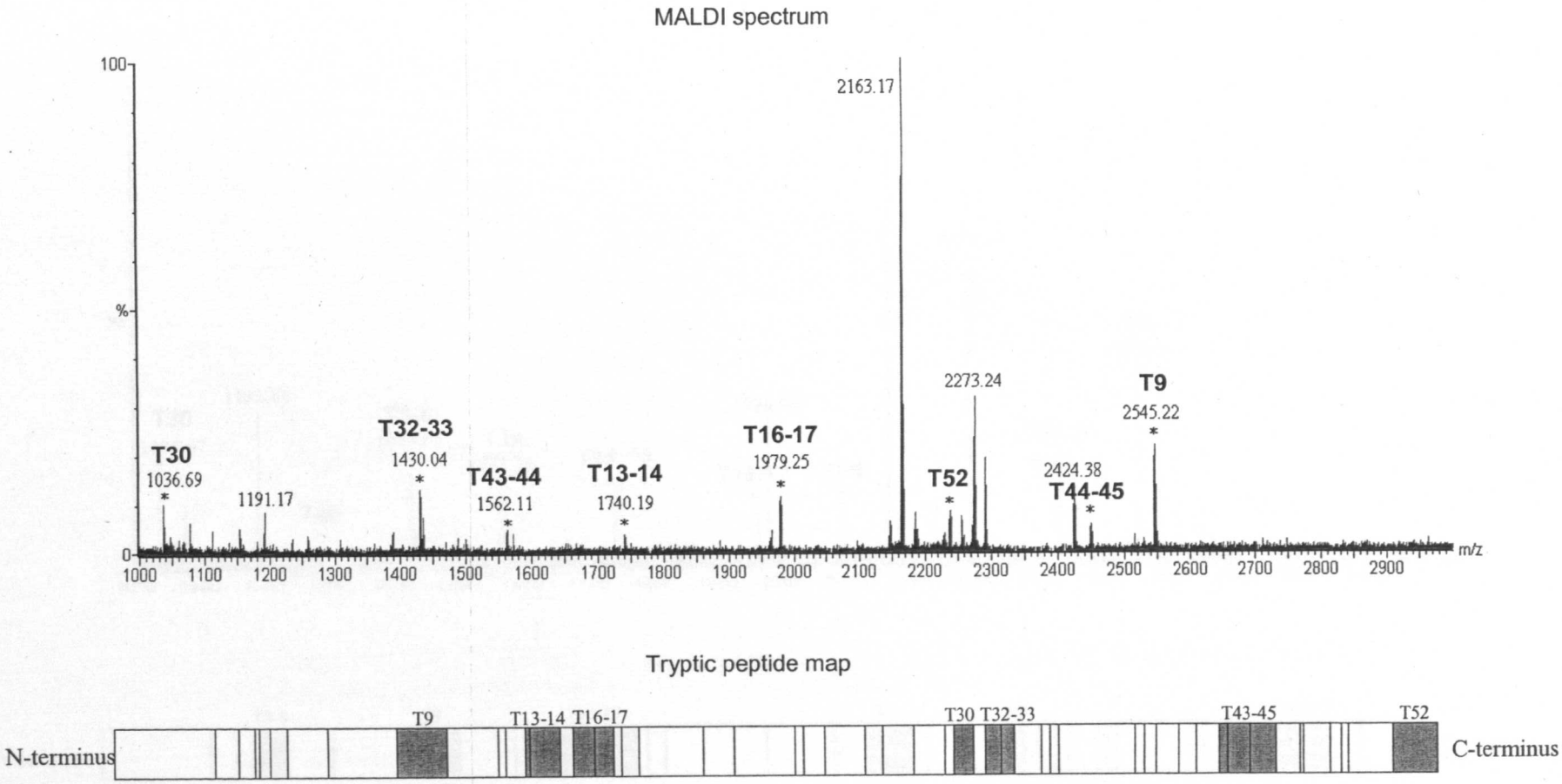

Figure 3.3.18 Analysis of the tryptic peptides from protein spot d5

The MALDI-ToF spectrum from in-gel tryptic digestion of spot d5 provided 8 peptides (marked with their tryptic peptide numbers) used to identify the protein as Similar to RIKEN cDNA 5430413K10. The tryptic peptide map indicates the positions of the observed peptides along the protein sequence of Similar to RIKEN cDNA 5430413K10, where the grey boxes indicate the tryptic peptides seen in the MALDI spectrum.

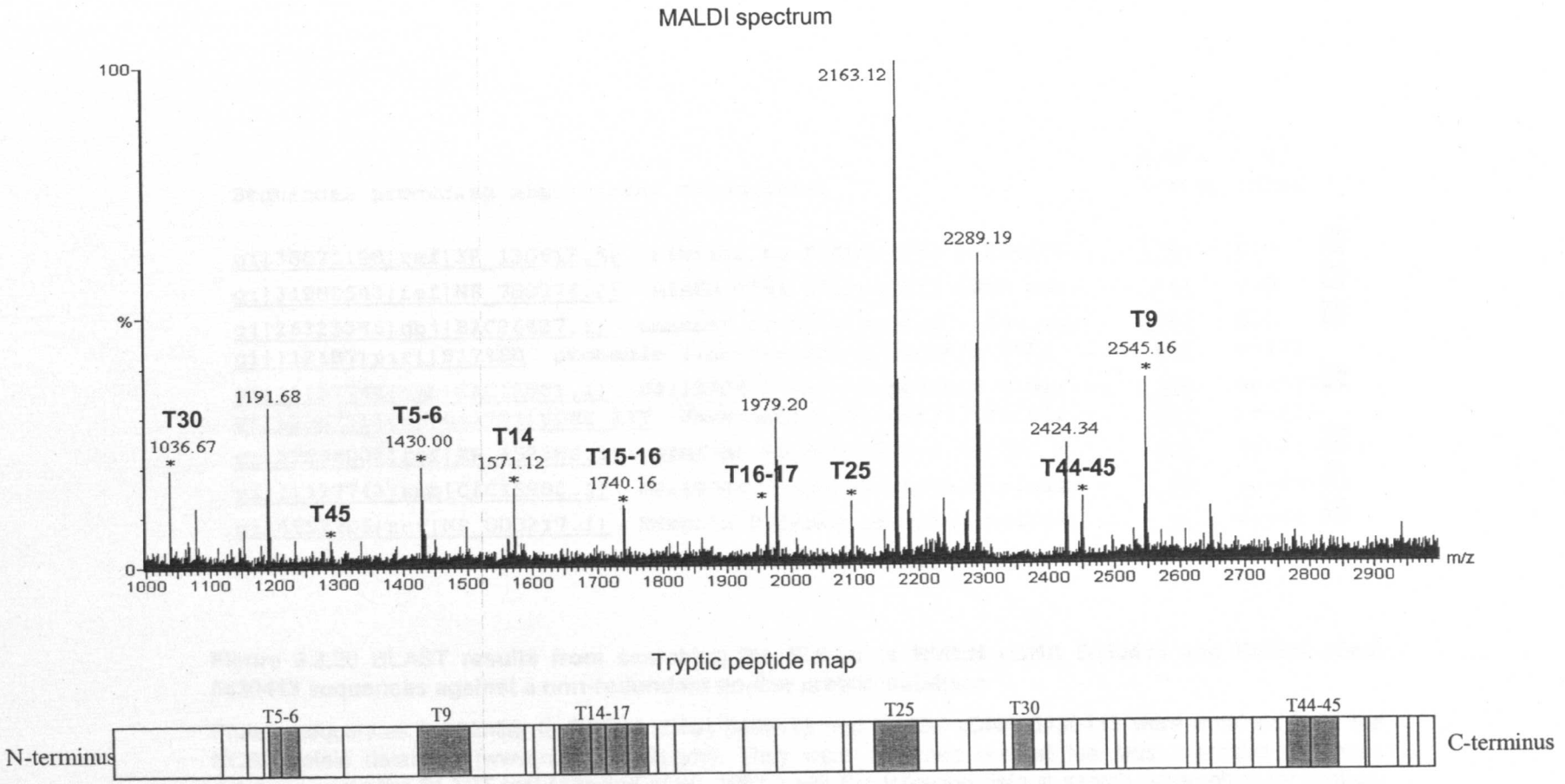

Figure 3.3.19 Analysis of the tryptic peptides from protein spot d7

The MALDI-ToF spectrum from in-gel tryptic digestion of spot d5 provided 8 peptides (marked with their tryptic peptide numbers) used to identify the protein as RIKEN cDNA 5430413K10. The tryptic peptide map indicates the positions of the observed peptides along the protein sequence of RIKEN cDNA 5430413K10, where the grey boxes indicate the tryptic peptides seen in the MALDI spectrum.

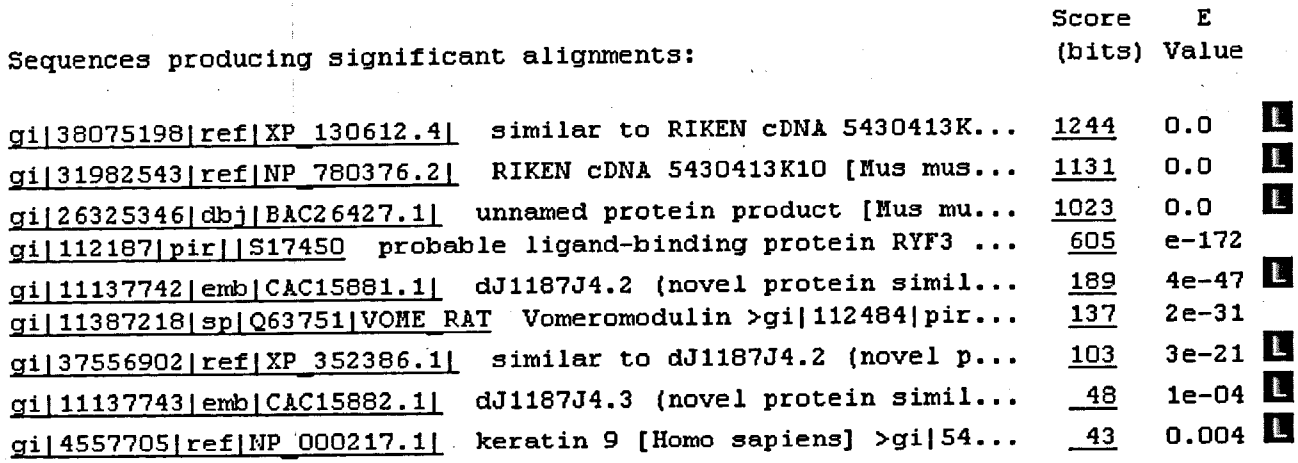

Sequences producing significant alignments:	Score (bits)	E Value	
gi|38075198|ref|XP_130612.4| similar to RIKEN cDNA 5430413K...	1244	0.0	L
gi|31982543|ref|NP_780376.2| RIKEN cDNA 5430413K10 [Mus mus...	1131	0.0	L
gi|26325346|dbj|BAC26427.1| unnamed protein product [Mus mu...	1023	0.0	L
gi|112187|pir||S17450 probable ligand-binding protein RYF3 ...	605	e-172	
gi|11137742|emb|CAC15881.1| dJ1187J4.2 (novel protein simil...	189	4e-47	L
gi|11387218|sp|Q63751|VOME_RAT Vomeromodulin >gi|112484|pir...	137	2e-31	
gi|37556902|ref|XP_352386.1| similar to dJ1187J4.2 (novel p...	103	3e-21	L
gi|11137743|emb|CAC15882.1| dJ1187J4.3 (novel protein simil...	48	1e-04	L
gi|4557705|ref|NP_000217.1| keratin 9 [Homo sapiens] >gi|54...	43	0.004	L

Figure 3.3.20 BLAST results from searching the Similar to RIKEN cDNA 5430413 and RIKEN cDNA 5430413 sequences against a non-redundant on-line protein database

Protein sequences for Similar to RIKEN cDNA 5430413 and RIKEN cDNA 5430413 were obtained from the NCBI protein database (www.ncbi.nlm.nih.gov). They were searched against the *Mus musculus* sequence database using the BLAST tool (Altschul *et al.*, 1997) with the following default search parameters for protein-protein BLAST: E value threshold 10, wordsize 3, BLOSUM62 matrix, gap costs existence 11, extension 1. dJ1187J4.2/ dJ1187J4.3 are annotated as novel proteins similar to rat RYF3.

Figure 3.3.21 Alignments of the protein sequences from proteins with significant homology to RIKEN cDNA 5430413K10

The protein sequences of the proteins proposed to have significant sequence homology according to the BLAST search results were acquired from the NCBI protein database (www.ncbi.nlm.nih.gov) in FASTA format. The sequences were then pasted into the web-based BCM searchlauncher protein alignment tool (searchlauncher.bcm.tmc.edu/multi-align.html, Smith *et al.*, 1996).Sequences were then aligned using the CLUSTAL W1.8 alignment method. RIKEN cDNA refers to RIKEN cDNA 5430413K10. Proteins with the prefix "sim" are designated as similar to the given protein.

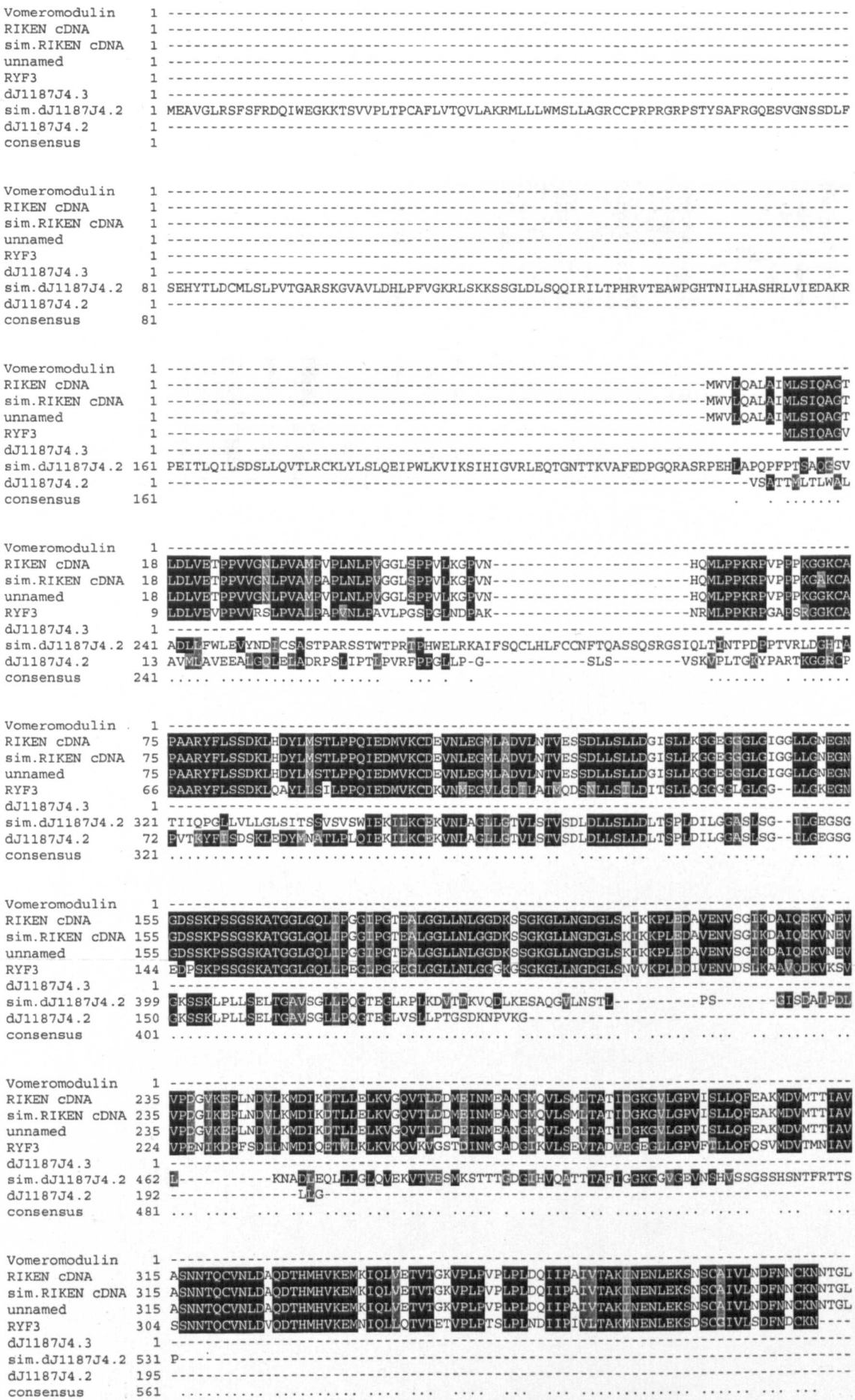
Vomeromodulin
RIKEN cDNA
sim.RIKEN cDNA
unnamed
RYF3
dJ1187J4.3
sim.dJ1187J4.2
dJ1187J4.2
consensus

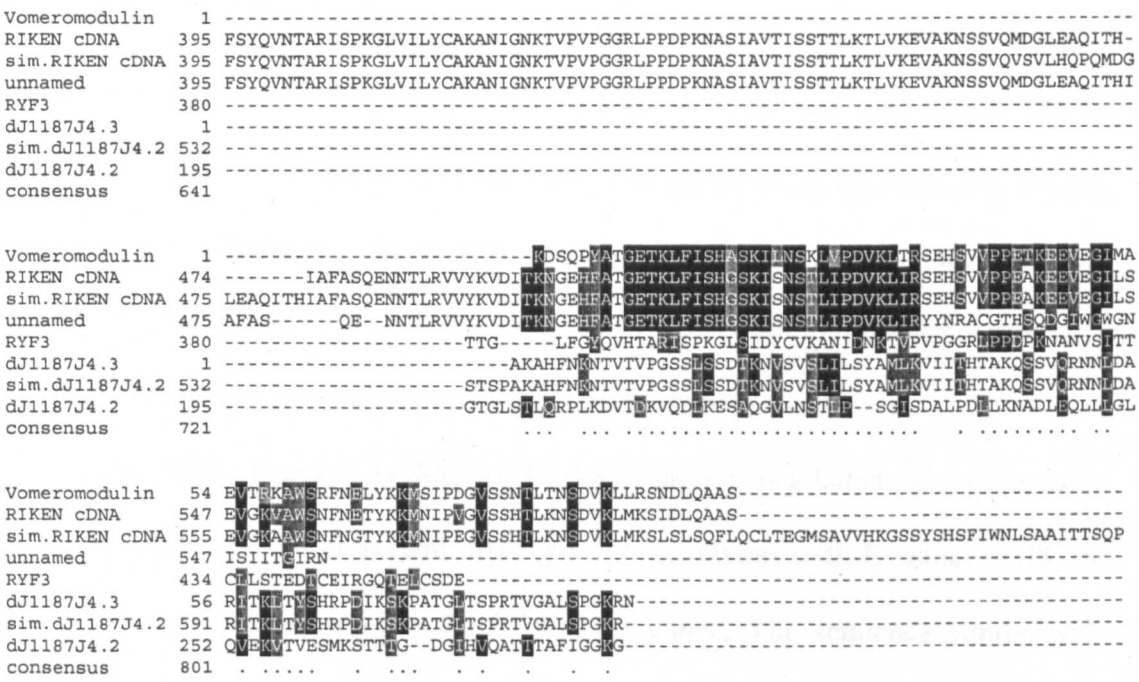
Vomeromodulin 1
RIKEN cDNA 395 FSYQVNTARISPKGLVILYCAKANIGNKTVPVPGGRLPPDPKNASIAVTISSTTLKTLVKEVAKNSSVQMDGLEAQITH-
sim.RIKEN cDNA 395 FSYQVNTARISPKGLVILYCAKANIGNKTVPVPGGRLPPDPKNASIAVTISSTTLKTLVKEVAKNSSVQVSVLHQPQMDG
unnamed 395 FSYQVNTARISPKGLVILYCAKANIGNKTVPVPGGRLPPDPKNASIAVTISSTTLKTLVKEVAKNSSVQMDGLEAQITHI
RYF3 380
dJ1187J4.3 1
sim.dJ1187J4.2 532
dJ1187J4.2 195
consensus 641
Vomeromodulin 1
RIKEN cDNA 474 -------IAFASQENNTLRVVYKVDITKNGEHFATGETKLFISHGSKISNSTLIPDVKLIRSEHSVVPPEAKEEVEGILS
sim.RIKEN cDNA 475 LEAQITHIAFASQENNTLRVVYKVDITKNGEHFATGETKLFISHGSKISNSTLIPDVKLIRSEHSVVPPEAKEEVEGILS
unnamed 475 AFAS------QE--NNTLRVVYKVDITKNGEHFATGETKLFISHGSKISNSTLIPDVKLIRYYNRACGTHSQDGIWGWGN
RYF3 380 ----------TTG-----LFGMQVHTARISPKGLSIDYCVKANIENKTVPVPGGRLPPDPKNANVSITT
dJ1187J4.3 1 -----------AKAHFNKNTVTVPGSSLSSDTKNVSVSLILSYAMLKVIITHTAKQSSVQRNNLDA
sim.dJ1187J4.2 532 ----------STSPAKAHFNKNTVTVPGSSLSSDTKNVSVSLILSYAMLKVIITHTAKQSSVQRNNLDA
dJ1187J4.2 195 ----------GTGLSTLQRPLKDVTDKVQDLKESAQGVLNSTLP--SGHSDALPDLLKNADLEQLLLGL
consensus 721
Vomeromodulin 54 EVTRKAWSRFNELYKKVSIPDGVSSNTLTNSDVKLLRSNDLQAAS
RIKEN cDNA 547 EVGKVAWSNFNETYKKVNIPVGVSSHTLKNSDVKLMKSIDLQAAS
sim.RIKEN cDNA 555 EVGKAAWSNFNGTYKKVNIPEGVSSHTLKNSDVKLMKSLSLSQFLQCLTEGMSAVVHKGSSYSHSFIWNLSAAITTSQP
unnamed 547 ISIITSIRN
RYF3 434 GLLSTEDTCEIRGQTELCSDE
dJ1187J4.3 56 RITKLTVSHRPDIKSKPATGLTSPRTVGALSPGKRN
sim.dJ1187J4.2 591 RITKLTVSHRPDIKSKPATGLTSPRTVGALSPGKR
dJ1187J4.2 252 QVEKVTVESMKSTTTG--DGIHVQATTTAFIGGKG
consensus 801

product and probable ligand-binding protein RYF3. The high level of sequence conservation between these proteins shows that these are all very closely related proteins likely to share a common function. The presence of a C-terminal domain with extensive homology to vomeromodulin, a putative pheromone-transporter (Khew-Goodall *et al.*, 1991; Krishna *et al.*, 1995), suggests that these proteins may be involved in olfactory and/or vomeronasal perireceptor processes.

The result ranked seventh in the BLAST search was a human keratin protein, keratin 9. This was one of several hits for keratin subtypes with E values<0.05, the commonly used probability threshold for significance. The sequence similarity is confined to residues 130-200 and this glycine-rich region of the Similar to RIKEN cDNA 5430413K10 proteins aligns to the N-terminal and C-terminal globular domains of keratin (Figure 3.3.22). This localised abundance of glycine residues could play an important role in protein structure as these amino acids allow the polypeptide chain to adopt unusual conformations (Branden and Tooze, 1999).

Localisation of Similar to RIKEN 5430413K10 gene To determine chromosomal localisation and whether multiple genes for the RIKEN cDNA 5430413K10 proteins exist, the cDNA sequence for Similar to RIKEN cDNA 5430413K10 was searched against an on-line *Mus musculus* genome database (Figure 3.3.23). This search resulted in 30 putative sequence alignments ranging in length from 40-505bp, all of which were located on chromosome 2. Seven overlapping contigs with an average sequence identity of 95.9% cover the sequence of almost the entire protein. The coding sequences are expected to be fragmented as the DNA search sequence is derived from a translation of mRNA and as such does not contain introns.

The contigs with homology to Similar to RIKEN cDNA appear to exist in pairs of sequences in separate regions of the genome sequence and with slightly

```
>gi|4557705|ref|NP_000217.1|  keratin 9 [Homo sapiens]
gi|547748|sp|P35527|K1CI_HUMAN  Keratin, type I cytoskeletal 9 (Cytokeratin 9)
gi|2119236|pir||I37984  keratin 9, type I, cytoskeletal - human
gi|453155|emb|CAA52924.1|  keratin 9 [Homo sapiens]
gi|545257|gb|AAC60619.1|  cytokeratin 9; CK 9 [Homo sapiens]
          Length = 622

 Score = 42.7 bits (99), Expect = 0.004
 Identities = 43/170 (25%), Positives = 66/170 (38%), Gaps = 33/170 (19%)

Query: 137 GGEGGGLG---IGGLLGNEGNGDSSKPSSGSKATGGLGQLIPGGIPGTEALGGLLNLGGD 193
           GG GGG     +GG  G    G       G  ++GG G    GG  G    G     GG
Sbjct: 74  GGSGGGFSASSLGGGFGGGSRGFGGASGGGYSSSGGFGGGFGGGSGGGFGGGYGSGFGGL 133

Query: 194 KSSGKGLLNGDG----------LSKIKKPLEDAVENVSGIKDA-------IQEKVNEVVP 236
              G G   GDG          + ++   L   ++ V  +++A       IQ+  ++  P
Sbjct: 134 GGFGGGAGGGDGGILTANEKSTMQELNSRLASYLDKVQALEEANNDLENKIQDWYDKKGP 193

Query: 237 DGIKEPLNDVLKM--DIKDTLLELKVG----------QVTLDDMEINME 273
            I++  +       D+KD +++L VG           ++TLDD  I  E
Sbjct: 194 AAIQKNYSPYYNTIDDLKDQIVDLTVGNNKTLLDIDNTRMTLDDFRIKFE 243


 Score = 39.7 bits (91), Expect = 0.035
 Identities = 29/70 (41%), Positives = 31/70 (44%), Gaps = 1/70 (1%)

Query: 137 GGEGGGLGI-GGLLGNEGNGDSSKPSSGSKATGGLGQLIPGGIPGTEALGGLLNLGGDKS 195
           GG GGG G  GG  G+ G G  S   SG    GG G    GG  G  + G   N GG
Sbjct: 503 GGYGGGSGSRGGSGGSYGGGSGSGGGSGGGYGGGSGGGHSGGSGGGHSGGSGGNYGGGSG 562

Query: 196 SGKGLLNGDG 205
           SG G   G G
Sbjct: 563 SGGGSGGGYG 572
```

Figure 3.3.22 The amino acid region bearing sequence homology to keratin proteins is rich in glycine resiudes

The alignment shown was produced during a sequence homology search using the BLAST tool and shows the region of homology between Similar to RIKEN cDNA 5430413K10 (*Mus musculus*) and keratin 9 (*Homo sapiens*).

differing % identities. These are likely to represent sequences aligning to "Similar to..." and RIKEN cDNA itself, which shares 97% amino acid identity with Similar to RIKEN cDNA in its translated form. The homologous sequences are confined to a single chromosome, chromosome 2 and are found in the 156.1-156.2Mb region. Interestingly this is almost immediately downstream of a group of putative ORF sequences that include the protein Plunc, a secretory protein expressed in the nasal cavity of rats (Sung *et al.*, 2002).

3.3.7 2D-protein profiles of rat olfactory and respiratory cilia are almost identical

Equal protein concentrations of enriched cilia preparations from respiratory and olfactory cilia were resolved by 2D-PAGE (Figure 3.3.24). The resulting protein profiles are incredibly similar, to the extent that almost all proteins appear to have corresponding spots in both gels. Additional 2D-PAGE separations of rat respiratory cilia preparations are shown in Figure 3.3.25 and as observed with rat olfactory gels the majority of profile variation is a product of the differing protein loadings. The protein identifications and corresponding reference 2D-gel are shown in Table 3.3.7 and Figure 3.3.26. Characterisation studies on the rat respiratory cilia proteome lead to the identification of 39 discreet 2D-PAGE spots corresponding to 37 individual proteins. These identifications are not identical to those listed for olfactory cilia due to differences in the protein spots identified in the two analyses. Although every attempt was made to analyse the corresponding spots in both preparations the identification of proteins from both was not always possible *i.e.* significant identification scores were not always obtained for both samples. Where identifications were made from equivalent protein spots in respiratory and olfactory gels, 11 out of 15 identifications were identical. Therefore it can be reasonably

Karyotype diagram

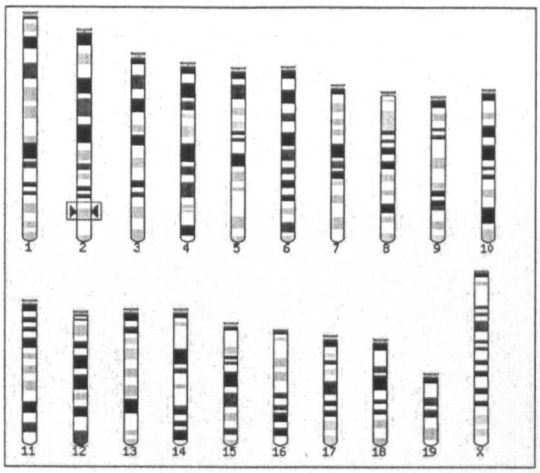

Sequence alignment results

Links	Query			Genome				Stats			
	Start	*End*	*Ori*	*Name*	*Start*	*End*	*Ori*	*Score*	*E-val*	*%ID*	*Length*
[A] [S] [C]	342	846	+	Chr:2	156156717	156157221	+	2525	2.4e-292	100.00	505
[A] [S] [C]	342	846	+	Chr:2	156107340	156107844	+	2507	1.6e-289	99.60	505
[A] [S] [C]	60	341	+	Chr:2	156154780	156155061	+	1410	2.4e-292	100.00	282
[A] [S] [C]	60	341	+	Chr:2	156105404	156105685	+	1374	1.6e-289	98.58	282
[A] [S] [C]	1285	1507	+	Chr:2	156161600	156161830	+	884	1.2e-289	89.66	232
[A] [S] [C]	1285	1507	+	Chr:2	156112221	156112451	+	875	2.0e-286	89.22	232
[A] [S] [C]	906	1117	+	Chr:2	156158132	156158337	+	799	2.4e-292	88.21	212
[A] [S] [C]	906	1117	+	Chr:2	156108753	156108958	+	799	1.6e-289	88.21	212
[A] [S] [C]	1469	1612	+	Chr:2	156162370	156162512	+	660	2.4e-292	95.83	144
[A] [S] [C]	1469	1612	+	Chr:2	156112991	156113133	+	651	3.9e-289	95.14	144
[A] [S] [C]	1853	1978	+	Chr:2	156165303	156165428	+	630	2.4e-292	100.00	126
[A] [S] [C]	1853	1978	+	Chr:2	156115904	156116029	+	612	8.2e-285	98.41	126
[A] [S] [C]	674	952	+	Chr:2	156157353	156157635	+	552	1.5e-201	70.10	291
[A] [S] [C]	674	952	+	Chr:2	156107974	156108256	+	543	1.5e-199	69.76	291
[A] [S] [C]	1050	1191	+	Chr:2	156158992	156159133	+	435	2.3e-273	79.86	144
[A] [S] [C]	1050	1191	+	Chr:2	156109613	156109754	+	426	1.5e-270	79.17	144
[A] [S] [C]	1772	1857	+	Chr:2	156165057	156165142	+	412	2.4e-292	97.67	86
[A] [S] [C]	1772	1857	+	Chr:2	156115653	156115738	+	394	1.3e-285	95.35	86
[A] [S] [C]	1248	1385	+	Chr:2	156160274	156160409	+	369	2.4e-292	77.30	141
[A] [S] [C]	1248	1385	+	Chr:2	156110895	156111030	+	369	1.6e-289	77.30	141
[A] [S] [C]	1612	1697	+	Chr:2	156162669	156162758	+	363	2.4e-292	92.22	90
[A] [S] [C]	1612	1697	+	Chr:2	156113290	156113379	+	363	3.9e-289	92.22	90
[A] [S] [C]	1452	1787	+	Chr:2	156164000	156164333	+	336	2.1e-265	62.15	354
[A] [S] [C]	1	133	+	Chr:2	156152663	156152796	+	322	5.0e-241	71.64	134
[A] [S] [C]	1712	1788	+	Chr:2	156114875	156114952	+	321	2.4e-282	91.03	78
[A] [S] [C]	1	133	+	Chr:2	156103290	156103423	+	313	1.3e-240	70.90	134
[A] [S] [C]	1186	1249	+	Chr:2	156159475	156159538	+	293	2.4e-292	95.31	64
[A] [S] [C]	1186	1249	+	Chr:2	156110096	156110159	+	284	1.6e-289	93.75	64
[A] [S] [C]	1672	1711	+	Chr:2	156162975	156163013	+	167	7.1e-281	92.50	40
[A] [S] [C]	1672	1711	+	Chr:2	156113596	156113634	+	158	3.0e-277	90.00	40

Figure 3.3.23 30 genomic sequences share significant homology to the Similar to RIKEN cDNA 5430413K10 cDNA sequence

The cDNA sequence for Similar to RIKEN cDNA 5430413K10 was searched against the Ensembl mouse genome sequence database at www.ensembl.org. The highlighted area of the karyotype diagram indicates the region of chromosome 2 which contains the homologous sequences. %ID values report the levels of sequence identity between aligned sequences. E value provides a probability value for the significance of the sequence alignment.

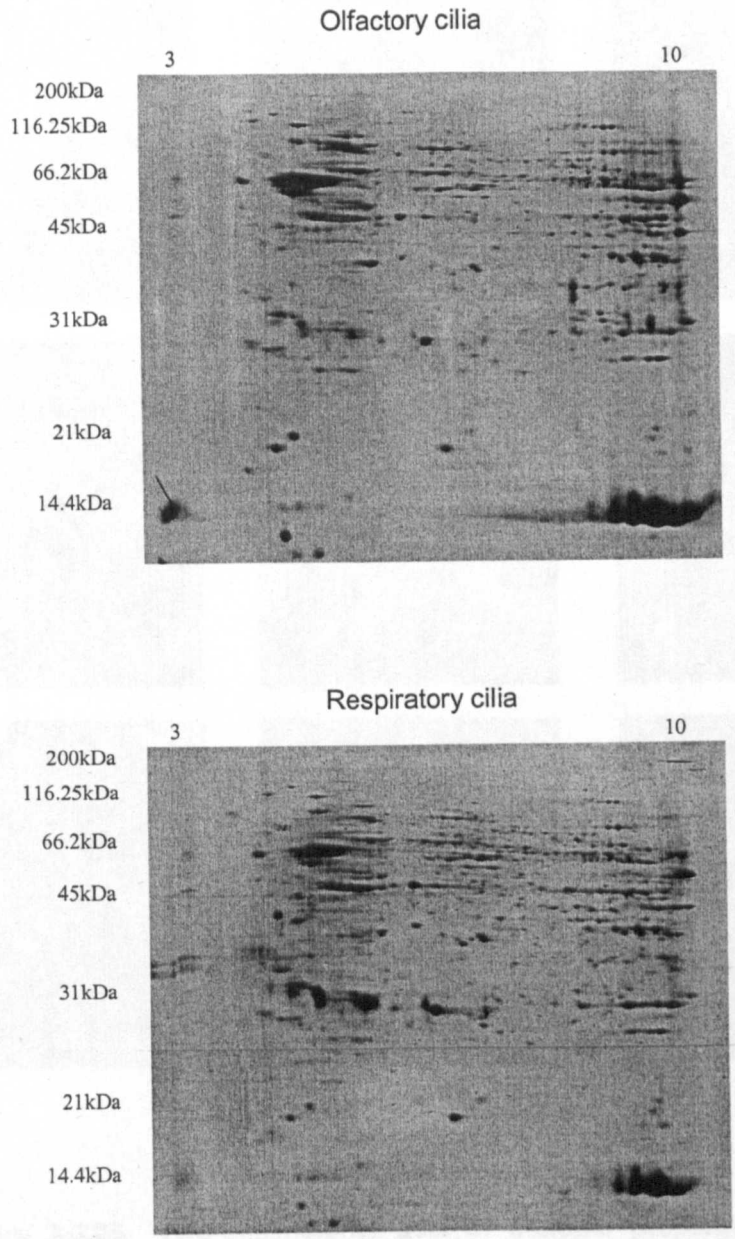

Figure 3.3.24 Two-dimensional protein profiles of rat olfactory cilia and rat respiratory cilia

2D-gels performed using 11cm pH3-10 (non-linear) IPG strips and the large format second dimension gel system .

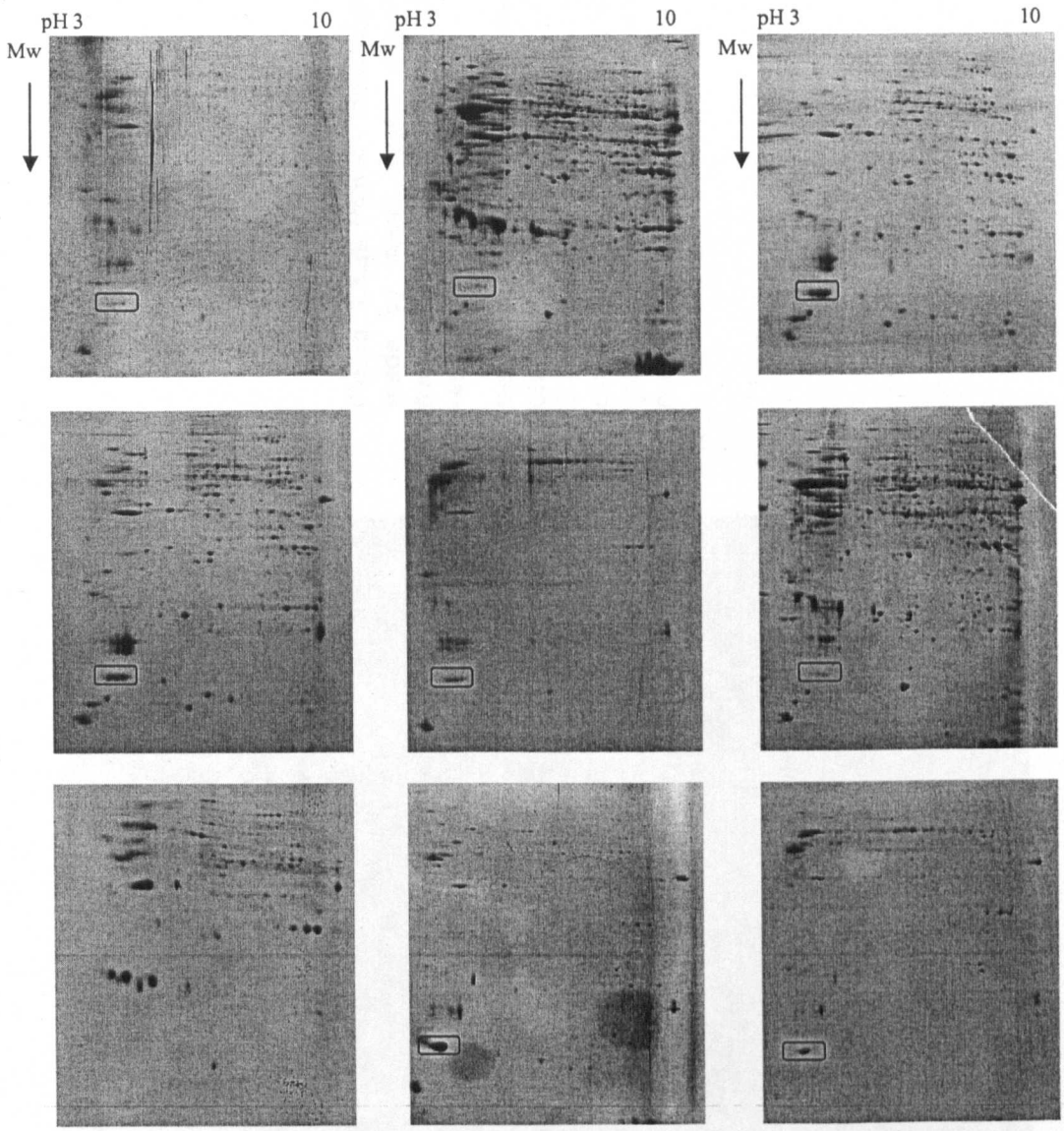

Figure 3.3.25 Two-dimensional gels of multiple preparations of rat respiratory cilia show the reproducibility of the protein profile

Isoelectric focussing of enriched rat respiratory cilia preparations was performed using 11cm 3-10 (non-linear) IPG strips. The second dimension was run on large format gels (final acrylamide/bisacrylamide concentration 10%) . The boxed region indicates the position of the protein identified as OBP during cilia proteome characterisation. All gels images are oriented as shown for the top layer of gels, with pH increasing left-to-right and molecular mass decreasing top-to-bottom.

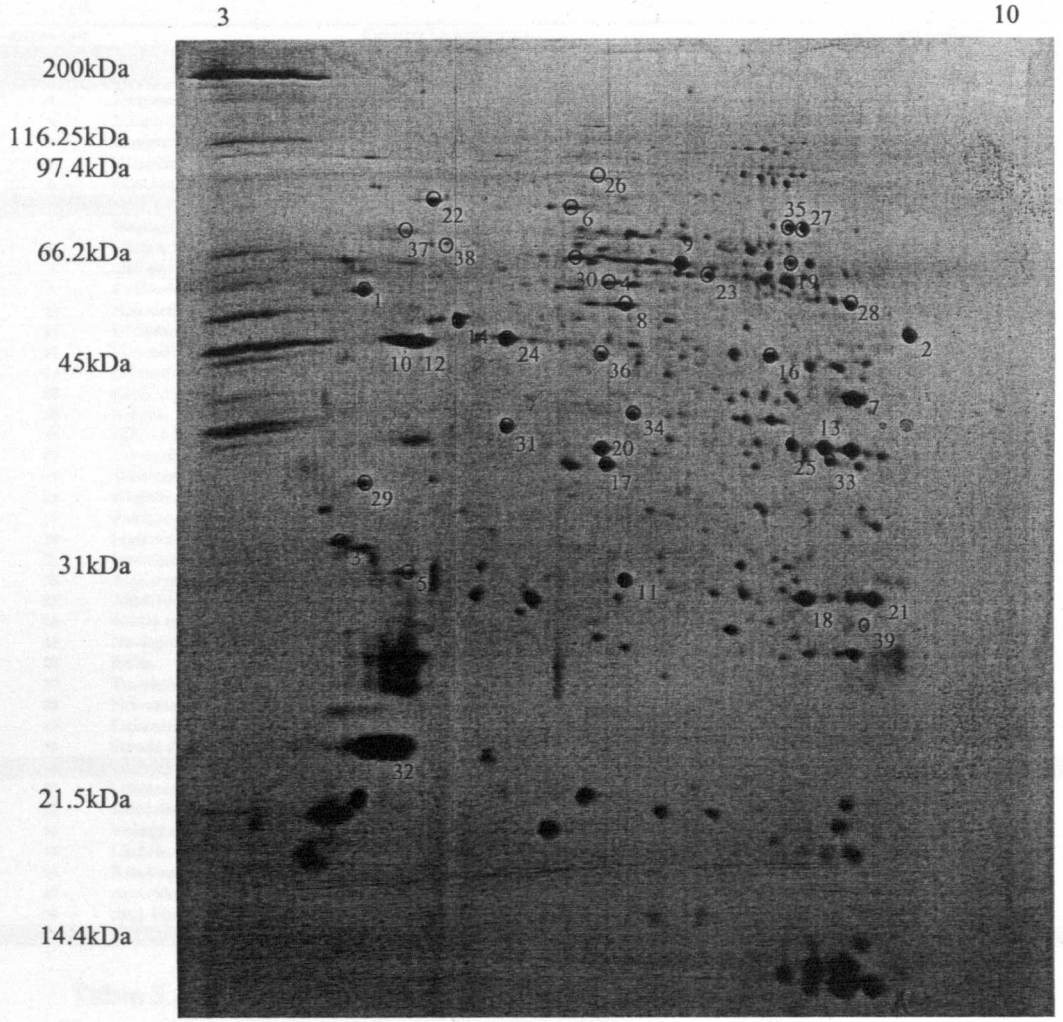

Figure 3.3.26 Protein identifications made by in-gel tryptic digestions from 2D-PAGE separation of rat respiratory cilia

Isoelectric focussing of rat olfactory cilia was performed using an 11cm pH 3-10 (non-linear) IPG strip. The second dimension was run on a large format gel (final acrylamide/bisacrylamide concentration 10%) .

Protein Spot	Putative Identification	NCBI Accession #	Mw (kDa)	Species	Mowse score
1	H+-transporting ATP synthase F1-beta chain (mitochondrial)	92350	50.7	Rattus norvegicus	74/54
2	Eukaryotic translation elongation factor 1 alpha 2/ Elongation factor 1 alpha 1	15805031/ 119146	50.5/ 50.4	Rattus norvegicus	68/53
3	Tyrosine 3-monooxygenase	6756041	27.9	Mus musculus	104/54
4	2-3-cyclic nucleotide phosphodiesterase	116560	46	Rattus norvegicus	54/53
4	Interleukin-18	3063923	18.7	Rattus norvegicus	66/54
5	Vimentin (fragment)	14389299	53.8	Rattus norvegicus	65/54
6	Albumin	19705431	70.7	Rattus norvegicus	67/66
7	Synaptonemal complex protein-1 (fragment)	3041729	117	Rattus norvegicus	61/54
7	Huntingtin-interacting protein 1 related	12718814	121.2	Rattus norvegicus	70/53
8	Enolase I, alpha	6978809	47.4	Rattus norvegicus	74/53
9	Carboxylesterase ES-10 precursor/ cholesterol esterase	92053/ 1162964	62.4/ 62.4	Rattus norvegicus	99/53 (both)
9	Unknown protein	807677	77.1	Rattus norvegicus	68/53
10	Beta-actin/ cytoskeletal gamma actin	71620/ 4501887	42.1/ 42.1	Rattus norvegicus, Homo sapiens	78/54 (both)
11	Glutathione-S-transferase M5	4099365	27.1	Rattus norvegicus	130/53
12	Beta-actin / gamma actin	71620/ 4501887	42.1/ 42.1	Rattus norvegicus, Homo sapiens	98/53 (both)
13	Glyceraldehyde-3-phosphate dehydrogenase	8393418	36.1	Rattus norvegicus	71/53
14	Creatine kinase, brain isoform	6978659	43	Rattus norvegicus	69/53
15	Selectin	8393450	137.3	Rattus norvegicus	65/53
16	SEC-14 like 2	16758646	46.6	Rattus norvegicus	68/53
17	2-3-cyclic nucleotide phosphodiesterase	116560	46	Rattus norvegicus	60/53
18	Sulfotransferase, phenol-preferring 2	13929030	35.9	Rattus norvegicus	138/53
18	Glutathione-S-transferase Yb2 subunit (chain 4)	121719	25.9	Rattus norvegicus	285/53
19	Phosphoglycerate kinase 1	16757986	44.9	Rattus norvegicus	80/53
20	Malate dehydrogenase-like enzyme	15100179	36.6	Rattus norvegicus	81/53
21	Glutathione transferase 3 / Glutathione-S-transferase Yb1 / Glutathione-S-transferase Yb2	111704/ 204503/ 8393502	25.9/ 26.1/ 26.1	Rattus norvegicus	185/53
22	dnaK-type molecular chaperone hsp72-p1 / hsp70kDa protein 8	347019/ 13242237	71.1/ 71.1	Rattus norvegicus	153/ 53
23	Aldehyde dehydrogenase-3	14010869	50.7	Rattus norvegicus	76/53
24	45kDa secretory protein	4164418	46.5	Rattus norvegicus	130/53
25	Na-dependant neurotransmitter transporter NTT73	730198	82.5	Rattus norvegicus	64/53
26	Ezrin	17902245	54.3	Rattus norvegicus	122/53
27	Transketolase	1729977	68.3	Rattus norvegicus	55/53
28	Nck-associated protein 1	1708980	130.1	Rattus norvegicus	89/53
29	Lipocortin V	2981437	33.9	Rattus norvegicus	107/53
30	Protein disulphide isomerase A3 / ER-60 protease	1352384	57	Rattus norvegicus	147/53
31	Lactate dehydrogenase B	6981146	36.9	Rattus norvegicus	76/53
32	Odorant binding protein 1F	6468756	20	Rattus norvegicus	68/53
33	Thiosulfate sulfurtransferase	135826	33.4	Rattus norvegicus	115/53
34	Voltage-dependant N-type calcium channel alpha-1-beta subunit	1705855	264.4	Rattus norvegicus	55/53
35	Clathrin, heavy polypeptide	9506497	193.2	Rattus norvegicus	56/53
36	Beta-catenin	9972860	86	Rattus norvegicus	53/53
37	rhoA-binding serine/threonine kinase alpha	6981478	160.5	Rattus norvegicus	73/53
38	rhoA-binding serine/threonine kinase alpha	6981478	160.5	Rattus norvegicus	74/53
39	Probable RNA-directed DNA polymerase	112262	60.8	Rattus norvegicus	71/53

Table 3.3.7 Protein identifications made during the characterisation of the rat respiratory cilia proteome

Grey shaded rows are proteins predominantly localised to mitochondria/nuclei (source: NCBI protein database annotation). MOWSE scores provide a measurement of significance for each identification. A MOWSE score greater than 1 has a probability of occuring by chance of $p<0.05$.

predicted that even in the absence of definitive identifications for all proteins, corresponding protein spots represent the same protein in the respiratory and olfactory cilia preparations.

Proteins identified in rat respiratory cilia preparations fall into the same broad categories as proteins identified in olfactory cilia of sheep and rat The proteins identified in the different cilia types analysed here can be grouped into six broad categories: cytoskeletal and associated proteins, signal transduction proteins, cellular detoxification proteins, extracellular proteins, vesicle/protein trafficking proteins and metabolic proteins (Table 3.3.8). In all cilia types the dominating groups of proteins are functionally associated with the cytoskeleton and cellular protection systems, required to maintain the structure and viability of the cilia throughout constant exposure to the external environment. It is notable that the bias towards cytoskeletal-associated and cellular detoxification proteins is much greater in the partially characterised olfactory cilia proteomes than in the respiratory cilia.

The other major group of proteins identified was the metabolic enzymes. These constitute approximately 2% in sheep olfactory cilia and 11% in rat olfactory and 12% respiratory cilia (percentage values given to nearest integer). This may indicate increased levels of mitochondrial contamination in rat cilia preparations as some of these proteins *e.g.* malate dehydrogenase have both cytosolic and mitochondrial pools, potentially associated with the tissue damage sustained during the dissection/deciliation procedures utilised.

Odorant-binding protein identified in respiratory cilia Odorant binding protein 1F was among the identifications made from rat respiratory cilia preparations. As shown in Figure 3.3.26 (identifications reference gel) this protein is resolved by 2D-PAGE

Protein preparation	Cytoskeletal and associated proteins	Signal transduction proteins	Cellular detoxification proteins
Sheep olfactory cilia	Putative beta-actin Alpha-tubulin Tubulin, beta 2/ class Ivb beta tubulin Tropomyosin-3	Phosphoinositide 3-kinase T96 ADP-ribosylation factor 3	Antioxidant protein 2/1-cys peroxiredoxin Superoxide dismutase (Cu-Zn) Antioxidant protein 2 Thioredoxin peroxidase II Heat shock protein 90-alpha (HSP 86) Glutathione S-tranferase M1 Glucose regulated protein 58kDa Cytochrome P450 11B
Rat olfactory cilia	Alpha-tubulin Beta-actin / gamma actin Cytoskeletal gamma-actin Keratin-10	p38 Mitogen activated protein kinase	Glutathione-S-transferase Yb2 (chain 4) Thiosulfate transferase dnaK-type molecular chaperone hsp72-p1 / hsp70kDa protein 8 Heat shock protein HSP 90-beta Glutathione-S-transferase Yb2 Heat shock protein 8 Peroxiredoxin 6 Thiosulphate sulphurtransferase Heat shock 70kD protein 5 Glutathione S-transferase
Rat respiratory cilia	Vimentin (fragment) Beta-actin/ cytoskeletal gamma actin Huntingtin-interacting protein 1 related Ezrin rhoA-binding serine/threonine kinase alpha	2-3-cyclic nucleotide phosphodiesterase Nck-associated protein 1 Beta-catenin	Glutathione-S-transferase M5 Glutathione-S-transferase Yb2 subunit (chain 4) Glutathione transferase 3 / Glutathione-S-transferase Yb1/Yb2 dnaK-type molecular chaperone hsp72-p1 / hsp70kDa protein 8 Thiosulfate sulfurtransferase

Table 3.3.8 Summary of the major groups of proteins identified in the olfactory cilia proteomes of rat and sheep and the rat nasal respiratory cilia proteome.

Proteins that are considered to be predominantly localised to the mitochondria are considered to be contaminant proteins and are therefore not included in this table.

Assignment of functional groups is based on known functions of proteins. Source: protein entry annotations in the NCBI Protein database (www.ncbi.nlm.nih.gov) except in the following cases: Ezrin (Berryman *et al.*, 1993), rhoA-binding kinase alpha (Leung *et al.*, 1996), p38 MAPK (Bustamante *et al.*, 2003), ADP-ribosylation factor 3 (Li *et al.*, 2002), GRP58 (Nover *et al.*, 1991), cytochrome b5 (Sasame *et al.*, 1975), cytochrome P450 (Ding *et al.*, 1991). The placement of cytochrome P450 is determined by any available information on the putative role of the protein in the olfactory system. Many other proteins potentially fall into multiple categories and these were sorted according to the most basic function of the protein.

Protein preparation	Metabolic proteins (non-mitochondrial)	Extracellular proteins	Vesicle/protein trafficking
Sheep olfactory cilia	Non-neural enolase Aldehyde dehydrogenase 1A1 Cytochrome b5 Cytochrome b5 reductase	Serum albumin precursor	Phosphoinositide 3-kinase T96 Coatomer protein complex subunit gamma 2 ADP-ribosylation factor 3 Annexin II
Rat olfactory cilia	Malate dehydrogenase 1 Enolase 1, alpha Aldehyde reductase Creatine kniase Aldehyde dehydrogenase Cytochrome b5	Serum albumin Haemoglobin alpha 1 Secretory protein, 45kD	
Rat respiratory cilia	Enolase I, alpha Glyceraldehyde-3-phosphate dehydrogenase Phosphoglycerate kinase 1 Transketolase Aldehyde dehydrogenase-3 Malate dehydrogenase-like enzyme	Interleukin-18 Albumin 45kDa secretory protein Odorant binding protein 1F	Clathrin, heavy polypeptide

into a narrow band with pI values ~5 and an approximate molecular weight of 23kDa (slightly greater than the predicted mass). The protein band identified as OBP has a putative counterpart in only one of the rat olfactory cilia gels (top-left corner gel in Figure 3.3.6). This is in stark contrast to the OBP occurrence patterns in respiratory cilia which whilst not absolutely constant is present on 7 of the 9 2D-PAGE gels shown in Figure 3.3.19 (circled).

The precise function(s) of these proteins have not yet been determined however the occurrence of OBPs in association with respiratory but not olfactory cilia may be indicative of a non-sensory role for these proteins in the main olfactory system of the rat. A chemosensory role in the accessory olfactory system however cannot be discounted.

3.4 Discussion

3.4.1 Preparation of enriched cilia fractions

The most important requirement for studying the adaptation/specialisation of the olfactory cilia proteome was the ability to prepare an enriched fraction of cilia of proven relevance. In the present study, enriched cilia fractions were prepared from nasal turbinate tissue or the nasal septum using the calcium shock method of deciliation. This basic method, with various adjustments, was developed during the 1980s and has been used to isolate cilia from a variety of species including rainbow trout (Rhein and Cagan, 1980), catfish (Boyle *et al.*, 1987), frog (Anholt *et al.*, 1986; Chen *et al.*, 1986a) and rat (Sklar *et al.*, 1986). These methods all advocated the use of 10mM $CaCl_2$ (final concentration) for deciliation as was used here, the actual protocol utilised was from Sklar *et al.* (1986). This method was used for the isolation of olfactory cilia from the nasal turbinate tissue of rat, mouse and sheep and also for the preparation of enriched respiratory cilia fractions from rat septal membrane. The application of the same deciliation protocol for the preparation of olfactory and respiratory cilia has been reported in the literature (Chen *et al.*, 1986a) and cilia isolation appeared to be effective in both cases. The precise levels of olfactory and respiratory cilia enrichment were demonstrated by electron microscopy, the resulting images indicating the presence of intact cilia in a highly vesicular preparation and by biochemical characterisation of the relative distribution of β-tubulin III in both cilia preps and the respective levels of OMP found in the tissue sources for each cilia type.

Respiratory cilia from the neighbouring anterior region of the olfactory epithelium were used as a non-sensory control in the investigation of the sensory adaptation of olfactory cilia. It is recognised that the nasal septum contains regions of

sensory olfactory epithelium (the septal organ and vomeronasal organ). The deliberate use of respiratory cilia from the nasal septum rather than the trachea (which contains no olfactory tissue) stems from the consideration that the two types of epithelia may be adapted to different roles as they are exposed to different environments. In contrast, olfactory and nasal respiratory epithelia have a common developmental origin – the olfactory placodal epithelium - and are likely to share proteins required for optimal performance in the nasal environment and control for processes unique to the nasal cavity *e.g.* the chemical detoxification systems required. The proteins involved specifically in sensory processes will be present at a much lower abundance in the cilia preparations derived from the septum compared to the olfactory turbinates.

As it is difficult to precisely define and dissect sensory and non-sensory regions in the rat nasal mucosa (Nef *et al.*, 1989) the characterisation studies were performed using cilia isolated from the entire septum including sensory regions to ensure the greatest reproducibility possible. This reproducibility would have been necessary to prove sensory *versus* non-sensory protein distribution and any protein profile differences. Dissection of purely respiratory epithelium from the nasal cavity is more straightforward in larger mammals (Nef *et al.*, 1989) and therefore any future characterisation work on non-sensory cilia should be undertaken using tissue from sheep or cattle, which could provide a yield of purely respiratory cilia rather than a mixture of cilia types.

The relevance of the enriched preparations to studies of the olfactory and respiratory cilia proteomes is also reinforced by the identification of proteins that are known to be associated with cilia or apical membranes of epithelia *e.g.* HSP90 and HSP70 (Nover *et al.*, 1991; Williams and Nelson, 1997), ezrin (Berryman *et al.*,

1993) and the high relative abundance of the cytoskeletal proteins. The low levels of purely mitochondrial, ribosomal or nuclear proteins identified during the proteome characterisation also reinforce the relevance and enrichment of the cilia preparation, although it is conceded that selected metabolic proteins have not been classified as mitochondrial on the basis that there are also cytosolic pools of the enzymes and thus the localisation of such proteins cannot be assigned with great confidence. The majority of proteins identified here are associated with the cytoskeleton and/or the protection of cell viability during exposure to environmental stress.

One important consideration that has not been addressed here is the assessment of contamination from the microvilli of sustentacular cells in the olfactory mucosa and non-ciliated cells of the respiratory mucosa. Many xenobiotic-metabolising proteins are localised to the apical regions of these cell types (Thornton-Manning and Dahl, 1997) and their presence in both olfactory and respiratory cilia preparations is potentially indicative of microvillar contamination. The contribution, if any of proteins derived from microvilli is very difficult to assess, as there are to the author's knowledge, no commercially available antibodies able to distinguish proteins from microvilli and cilia. Pixley *et al.* (1997) reported the generation of a monoclonal antibody capable of specifically binding to the membranes of microvilli on sustentacular cells, however this antibody also bound to both the ciliated and non-ciliated cells in the respiratory mucosa. It was therefore concluded that at present there is not an effective way of biochemically determining the extent of contamination from microvilli in the cilia preparations used in this work. As the olfactory cilia preparations were enriched in the neuron-specific marker β-tubulin III, they are likely to be dominated by proteins from cilia and thus any contamination from microvillar proteins is regarded as low level.

3.4.2 The olfactory cilia proteome: cross-species adaptation and conservation

The comparison of the 2D protein profiles of the olfactory cilia preparations from rat and sheep nasal turbinates indicated little similarity, the one area of exception being the dominance of the cytoskeletal proteins in the protein profiles. This lack of similarity is also observed in the protein identifications made from the rat and sheep preparations. Despite the profile differences and the identification of few common proteins (*e.g.* enolase, cytochrome b5, GST) the proteomes of both sheep and rat olfactory cilia do share certain major features - they are both dominated by three major classes of proteins: cytsoskeletal proteins, cellular detoxification proteins and metabolic enzymes.

Cytoskeletal proteins Actin forms the cytoskeletal basis for cell movement and shape and in epithelial cells β-actin tends to be localised to the apical surface, hence the abundance in ORN cilia preparations (Becker *et al.*, 2000; Bustamante *et al.*, 2003). Tubulin proteins are an absolute requirement for the maintenance of the three-dimensional structure of both cilia and flagella (Luck, 1984) and as previously cited, both actin and tubulin were also identified in a recent proteomic analysis of human bronchial cilia (Ostrowski *et al.*, 2002). Keratin proteins are intermediate filament proteins commonly found in epithelial cells to provide mechanical strength (Rhodin, 1974) and are known to be present in the olfactory epithelium (Chen *et al.*, 1986b).

The identification of keratin proteins by enzymatic digestion procedures is problematic in that keratin is an abundant protein that has many isoforms (two classes containing at least 15 keratins each – Becker *et al.*, 2000) and can be found in many sources, not least of which is human skin. Contamination of digest samples is therefore a major problem and determining the origin of any keratin proteins identified by mass spectrometry is strictly required. In this work, the peptide lists

obtained from a set of simultaneously performed in-gel digestions are filtered to remove repeatedly occurring peptides. This processing removes any keratin contamination found in multiple samples including keratin contamination from the gel itself, preparation and digestion buffers and the trypsin stock. It also will exclude any general contamination introduced by sample handling and equipment *i.e.* from gloves and Gyro-Vap. It does not however guard against one-off contamination incidents such as an individual micropipette tip containing amounts of keratin that enable the generation of sufficient peptides for a significant Mowse score to be obtained during the on-line searching of a peptide mass list. Whilst it is acknowledged that this is a particular concern in work on low abundance proteins (as many in-gel digestions performed during this work were) if the filtering process was not efficiently excluding contaminant keratin peptides it is unlikely that only two keratin identifications would have been made throughout the proteome characterisation work. In the keratin identifications made, the gel plug was taken from a region of perhaps the highest protein concentration on the gel. It is also likely from the identifications made from the immediately surrounding areas, that a sample protein potentially masked by the presence of contaminating keratin peptides would be a tubulin isoform; a protein that is not only abundant enough to not be masked by low level keratin contamination but is also shown by multiple in-gel digest experiments to generate sufficient tryptic peptides to allow its significant identification.

Whilst the identification of keratin in this case is considered to be genuine, immunohistochemistry indicates these proteins are unlikely to be present at high levels in the olfactory cilia (Chen *et al.*, 1986b). Therefore the most likely derivation of the keratin found in rat olfactory cilia preparations is from cellular damage

sustained during the initial dissection procedures and/or the deciliation process, where keratin has subsequently adhered to the cilia vesicle preparation/been encapsulated during cilia dissociation.

Cellular detoxification proteins These proteins all have a protective function in the cell whether by the chemical transformation of odorant molecules to compounds that can be metabolised and removed from the cell by GST (Ben-Arie *et al.*, 1993), protection against oxidative stress by peroxiredoxins (Arnér and Holmgren, 2000; Fatma *et al.*, 2001; Wang *et al.*, 2003b) or heat shock proteins induced by multiple stress factors *e.g.* high levels of ethanol, amino acid homologues, certain heavy metals (Burden *et al.*, 1990).

Heat shock proteins The presence of heat shock proteins in olfactory cilia may not be the result of induction but of constitutive expression in eukaryotic/higher organism cells *e.g.* HSP70 and HSP90 (Kabakov and Gabai, 1997). The naming of these families belies the variety of functions that these proteins perform in the cell. By virtue of different binding partners, the HSP90 and HSP70 family members are involved in the regulation of cytoskeleton dynamics, cell shape, protein transport and protein sorting (Lindquist and Craig, 1988). The role of these proteins in nasal cilia is likely to be protective, ensuring that the effects of constant contact with the external environment do not adversely affect the cellular functions of the epithelial cells.

Heat shock proteins may also be present in cilia due to putative roles in the formation and maintenance of microtubular structures (Williams and Nelson, 1997). Heat shock proteins are known to be associated with microtubules and the intermediate filament cytoskeleton, binding to tubulin and actin respectively (Nover *et al.*, 1991; Williams and Nelson, 1997). Specific association of heat shock proteins with the ciliary axonemes has also been observed in the cilia of *Tetrahymena*

thermophila and human bronchial epithelium (Williams and Nelson, 1997; Ostrowski *et al.*, 2002). In the bronchial cilia characterisation, four types of heat shock protein were identified from 2D-PAGE gels (Ostrowski *et al.*, 2002), a result consistent with the multiple proteins observed in both olfactory cilia in rat and sheep and also in the nasal respiratory cilia.

Biotransformation/antioxidant enzymes The major biotransformation enzyme observed in the olfactory cilia of rat and sheep was glutathione-S-tranferase (GST). GST is a phase II biotransformation enzyme that conjugates glutathione to its substrates as part of a process that increases the solubility of hydrophobic substrates and aids in their inactivation and clearance (Ben-Arie *et al.*, 1993). Its active form is a homo- or heterodimer a of 25kDa subunits. The GST subunits Yb1 and Yb2 identified in rat olfactory and respiratory cilia are the most abundant subunits observed in the olfactory epithelium (Ben-Arie *et al.*, 1993). Whilst it was shown that GST is present in the sustentacular cells surrounding the ORNs (Reed *et al.*, 2003), the resolution of the microscopy images shown was not sufficient to distinguish the dendritic processes of ORNs or their terminal knobs and cilia. Therefore expression in ORNs cannot be ruled out. Expression in ORNs in addition to sustentacular cells would also explain the broad apical and narrower basal localisation reported by Ben-Arie *et al.* (1993). This latter report argues the case for GST expression in sustentacular cells alone citing the presence of GST in glial cells of the brain but not neurons. It must however be remembered that ORNs are sensory neurons exposed to the external environment and are therefore more likely to be directly exposed to potentially harmful molecules than the neurons of the central nervous system. This consideration explains why ORNs are likely to contain GST within their dendritic cilia – the region exposed to the external environment, and also

explains the requirement for multiple transformation enzymes and stress-response proteins.Antioxidant proteins are recruited by cells to prevent irreparable damage caused by reactive oxygen species originating from both the external environment and generated cellular signalling processes and metabolism (Arnér and Holmgren, 2000, Reed *et al.*, 2003). Superoxide dismutases are a family of antioxidant proteins that protect the cells from the effects of superoxide anions. The superoxide dismutase form identified in both the rat and sheep olfactory cilia is the Cu/Zn-binding cytosolic form of the enzyme which has been demonstrated to be present in the nasal mucosa of rats, mice and humans (Reed *et al.*, 2003). The other major group of antioxidant proteins observed in the olfactory cilia preparations is the peroxiredoxins, which aid in the clearance of reactive oxygen species by catalysing the reduction of hydrogen peroxide. Subtypes of peroxiredoxin 6 (also known as antioxidant protein 2) a thiol-specific antioxidant, are commonly found in areas that exhibit high cell turnover rates including the olfactory and respiratory epithelia. Furthermore the localisation of these proteins to olfactory cilia has been previously reported proteins (Peshenko *et al.*, 1998; Novoselev *et al.*, 1999).

The olfactory cilia of both rat and sheep therefore contain a large number of proteins designed to provide protection from potentially cytotoxic chemicals and other stresses that may result from their exposure to the external environment. These proteins include both the classical stress-induced heat shock proteins and an array of powerful antioxidant and biotransformation enzymes including some more commonly associated with hepatocytes than neurons (Ben-Arie *et al.*, 1993). This high proportion of proteins devoted to cellular protection may also be supplemented from the unlikely source of metabolic proteins.

Metabolic proteins Aldehyde dehydrogenase, enolase and cytochrome b5 are present in both rat and sheep olfactory cilia preparations and they are all present at levels comparable with the majority of proteins in the protein profiles. The number of metabolic proteins present in almost equal abundance to the proteins reviewed above raises questions as to the possible source and functions of these proteins. Certainly if these metabolic enzymes are a form of contamination it calls into sharp question the purity of the preparations. Yet the olfactory cilia preparations show a ten-fold enrichment of the cilia-associated protein β-tubulin III over a crude membrane preparation, itself an insoluble cellular fraction. Therefore the number of contaminating cytosolic proteins not genuinely associated with the cilia should be minimal.

Selected enzymes including carboxylesterases and aldehyde dehydrogenase subtypes are present in the olfactory and nasal respiratory mucosa as xenobiotic-metabolising enzymes (Thorton-Manning and Dahl, 1997). The increased levels of these and other metabolic proteins may also govern the rate-limiting steps in a particular set of reactions, enhancing certain metabolic pathways in ORN dendrites according to their requirements. These enzymes could therefore provide additional options for metabolic pathways *e.g.* the enrichment of transketolase, an enzyme linking the pentose phosphate and glycolysis pathways in the mouse cornea, allows the adaptation of cellular metabolism to changing requirements (Sax *et al.*, 1996). However metabolic enzymes could also play an additional role in the cell and it may be this secondary function that results in the observed abundance and localisation.

There are precedents for the dual roles of selected metabolic enzymes in the visual system and specifically the lens and corneal epithelia. In the corneal epithelium, 30-40% soluble protein is class III aldehyde dehydrogenase, one of the

abundant metabolic enzymes identified in all cilia types. This is perhaps a much greater abundance level than would be expected for a solely metabolic role and indeed it has been hypothesised that in the cornea soluble proteins are recruited to fulfil an additional structural function in the establishment of a refractive index (Cuthbertson *et al.*, 1992; Sax *et al.*, 1996). Aldehyde dehydrogenase is not the only enzyme recruited as a so-called enzyme-crystallin. Others include enolase and GST (Cuthbertson *et al.*, 1992), again observed in both rat and sheep olfactory cilia preparations. These three proteins are also found in respiratory cilia and therefore appear to be over-expressed (according to expected metabolic requirements) in both sensory and non-sensory epithelia. Although it is deeply unlikely that these proteins are being recruited to the cilia of ciliated cells because of their refractive properties, there are other potential roles they could play. One function could involve the maintenance of cellular conditions *e.g.* pH, free ion concentration, *via* the structural/chemical properties of the upregulated proteins. An alternative hypothesis is that the catalytic properties of the enzymes may be employed to assist in the response to and recovery from cellular stress. Aldehyde dehydrogenase III, highly expressed in the corneal epithelium, is proposed to be part of the cell machinery dealing with oxidative stress damage by detoxifying the aldehydes created during lipid peroxidation (Bilgihan *et al.*, 1998). In animals lacking the class III subtype, aldehyde dehydrogenase 1A1 (the subtype observed in sheep olfactory cilia) is thought to play a similar role (Pappa *et al.*, 2003).

The potential for secondary roles of metabolic proteins is under continuing investigation in the cornea and lens epithelia. The levels of these proteins in the cilia of both the olfactory and respiratory epithelia indicate that the nasal cavity is another

region in which metabolic proteins could be performing multiple tasks and assisting in the maintenance of cilia structure and viability.

3.4.3 Evidence for cross-species adaptation in the mouse and sheep

Annexin isoforms in sheep olfactory cilia The major groups of proteins discussed in Section 3.4.2 are common to both rat and sheep olfactory cilia proteomes. There is however one group of proteins that forms a significant part of the sheep cilia protein profile and yet has failed to be identified in rat olfactory cilia preparations: the annexins.

Annexins are nearly ubiquitous in tissues of both higher and lower eukaryotes including fish, birds, *C.elegans* and mammals (Benz and Hofmann, 1997). Annexins can form up to 2% of the total protein content of a cell, are expressed in both neurons and glial cells and are thought to play an important role in vesicle trafficking and endocytosis courtesy of their ability to bind phospholipids in a Ca^{2+}-dependant manner (Burgoyne and Clague, 1994; Schnitzer *et al.*, 1995). In addition to phospholipid binding, annexins are also capable of Ca^{2+}-mediated interactions with actin (Hamre *et al.*, 1995) and annexin I is known to be localised to the cilia of ciliated cells in rabbit tracheal epithelium (Mayran *et al.*, 1996). Both annexin subtypes I and II are known to be present in the olfactory epithelium (Hamre *et al.*, 1995) and in addition annexins I, II and V were identified during the characterisation of the human respiratory cilia proteome (Ostrowski *et al.*, 2002). The only surprising thing about the occurrence of annexins I and II in olfactory cilia preparations was their prominence in the 2D-protein profile of sheep preparations but apparent absence in both rat cilia types investigated.

One suggested role for annexins is in endocytosis. During the proteome characterisation work, clathrin heavy chain and heat shock protein 8 (aka Hsc70 and a member of the HSP70 protein family) were both found in rat cilia preparations. This constitutes evidence of a clathrin-dependant endocytosis pathway, the main method for receptor internalisation in eukaryotic cells (Kabakov and Gabai, 1997; Becker *et al.*, 2000) and the major route for olfactory receptor internalisation in channel catfish (Rankin *et al.*, 1999). Studies of the localisation of annexin II found the protein to be associated with the inner surface of plasma membrane of selected cell types, endosomes and clathrin-coated pits (reviewed by Burgoyne and Clague, 1994). Annexin II also co-localises with caveolae, a common alternative method of protein-mediated endocytosis (Schnitzer *et al.*, 1995). This indicates that annexin II is not specific to one endocytic pathway and therefore the upregulation of annexins in sheep olfactory cilia is unlikely to be a result of different endocytic mechanisms in rat *versus* sheep ORNs.

Although annexin II abundance cannot be linked to a specific pathway, the upregulation of defined annexins may reflect a greater importance for calcium in endocytosis and/or vesicle trafficking in sheep olfactory cilia. Alternatively as ion channel activity has also been reported for multiple annexin subtypes including I, II and V (Benz and Hofmann, 1997), the increased abundance of annexins in sheep olfactory cilia preparations may indicate an additional Ca^{2+}-dependant mechanism for ion homeostasis in the olfactory system of this species. A final note is that Ca^{2+} initiates many odour adaptation mechanisms (Zufall and Leinders-Zufall, 2000). This could potentially link the increased expression of annexins I and II in sheep olfactory cilia to a different mechanism of odorant adaptation in this species compared to rat. Alternatively the increased expression of Ca^{2+}-binding proteins, which potentially

reduce the levels of free Ca^{2+} inside cilia, may have an adverse effect on odorant adaptation.

75kDa cluster of proteins associated with mouse olfactory cilia preparations The protein profiles of rat and mouse olfactory cilia were very similar, the only major difference being a cluster of highly abundant proteins of approximate mass 75kDa present in mouse olfactory cilia preparations. These proteins were identified by in-gel tryptic digestion and MALDI-ToF mass spectrometry as the previously unobserved protein products of RIKEN 5430413K10 (NCBI accession 31982543) and "Similar to" RIKEN 5430413K10 (NCBI accession 38075198) sequences derived from mouse cDNA studies. From protein sequence homology analysis these proteins shared 97% sequence identity. They also shared 97% homology with an unnamed protein product (*Mus musculus*) and 68% homology with the previously uncharacterised probable ligand-binding protein RYF3 (RYF3, *Rattus rattus*). The levels of sequence homology observed enable the characterisation of these proteins as member of the same subfamily and suggest that these proteins share a similar structure and function.

From SDS-PAGE analysis the RIKEN cDNA proteins have an approximate mass of 75kDa, greater than that predicted by the protein sequence analysis and thus highly suggestive of post-translational modifications. This modification is likely to be glycosylation as the region homologous to RYF3 includes three putative sites for N-linked glycosylation (Dear *et al.*, 1991). The RYF3 protein sequence is derived from a nasal epithelium-specific mRNA transcript, expressed exclusively in the lateral nasal glands (Dear *et al.*, 1991). The expression of the RIKEN cDNA 5430413K10 proteins in the lateral nasal glands of nasal cavity may also be supported by the localisation of their genomic sequences to an area almost

immediately downstream of Plunc, a known nasal cavity secretory protein (Sung *et al*, 2002). This proximity potentially resulting in similar expression patterns for both proteins. Another protein shown to share significant protein sequence homology with the RIKEN cDNA 5430413K10 proteins is vomeromodulin, an N-glycosylated protein produced in multiple glands in the nasal cavity including the lateral nasal glands (Khew-Goodall *et al.*, 1991). The region of significant (71%) homology between vomeromodulin and the C-terminal regions of the RIKEN cDNA proteins studied, suggests a pheromone-binding function for these proteins.

From the protein identifications made and sequence homology to RYF3 and vomeromodulin it can be deduced that the 75kDa cluster in mouse olfactory cilia contains members of a pheromone/odorant binding family of proteins. The major differences in the peptide mass fingerprints between the adjacent proteins d3 and d5 suggesting the existence of a diverse range of proteins within the 75kDa cluster. The observation of these proteins in the olfactory cilia of mice suggests their high levels of abundance in the mucus covering the olfactory epithelium and/or that they have specific binding partners within olfactory cilia. These proteins may therefore represent a class of pheromone-binding proteins present and acting in the main olfactory system of the mouse. This would represent a major adaptation of olfaction in mice to allow the enhanced detection of pheromones by the main olfactory system.

Further investigation using immunohistochemistry and *in situ* hybridisation techniques would allow the localisation and regions of origin for these proteins to be determined. In addition, the other proteins present in the 75kDa cluster should be identified and characterised using MALDI-ToF and/or tandem mass spectrometry methodologies to determine whether the 75kDa cluster does indeed contain multiple members of a novel pheromone-binding family of proteins.

3.4.4 Sensory adaptation of cilia in the nasal epithelium

The 2D protein profiles of olfactory and respiratory cilia preparations are almost identical indicating a high level of common proteins in sensory and non-sensory cilia. This similarity is also reflected in the number of protein identified in both gels and the shared categories into which the majority of protein identifications made can be placed. It should be noted that where in-gel digestions were performed on corresponding protein spots from olfactory and respiratory cilia preparations, the identifications matched in 71% of cases. This means that even though the number of shared proteins identified is perhaps not as great as anticipated, corresponding spots in the olfactory and respiratory cilia 2D-gels are highly likely to contain the same proteins and that the almost identical protein profiles is likely to reflect almost identical cilia proteomes. This observation is not due to high levels of contamination from olfactory cilia as the respiratory cilia preparation was shown to have a three-fold lower β-tubulin III concentration than olfactory whilst retaining an identical SDS-PAGE protein profile. In addition there is no evidence of a second, low abundance population of proteins, which would be apparent by a lowering of protein intensity of spots corresponding to those present in olfactory cilia preparations and the emergence of novel protein spots in the respiratory gels.

Previous studies, using lectins and monoclonal antibodies to compare the protein complements of olfactory and respiratory cilia, have shown a great deal of difference between sensory and non-sensory cilia. However these were predominantly performed on amphibians and the cilia types were dissected from different anatomical regions: the olfactory epithelium being dissected from the nasal chambers and the respiratory cilia prepared from palate tissue (Anholt *et al.*, 1986; Chen *et al.*, 1986a). The protein differences observed are therefore as likely to be the

result of the differing environments as differing cilia types. The common anatomical location is perhaps the reason why so many proteins appear to be present in both the respiratory and olfactory preparations in the rat as both cilia types are adapted for survival in the nasal cavity.

When reviewing the similarity of the protein profiles it is necessary to take note of the limitations of the separation procedures employed. Differences may also lie in the low abundance proteins, which despite the use of sensitive silver-nitrate protein staining methods may remain undetected. In addition, observations based on 2D-PAGE analysis may well indicate major conservation of proteins between sensory and non-sensory tissue due to the reduced solubility of the proteins that may be qualitatively or quantitatively different *e.g.* integral membrane proteins such as adenylyl cyclase (Lazard *et al.*, 1989) and olfactory receptors (Menco *et al.*, 1997). Additional experiments are required to specifically test whether the membrane proteins differ between the cilia types. It is possible that due to the shared environment, metabolic and structural requirements of cilia in the nasal cavity, the proteins enriched in the cilia membranes may be the only differences in the cilia proteomes.

Odorant binding proteins were observed in respiratory but not olfactory cilia preparations The one consistent difference observed between sensory and non-sensory cilia types was the presence of odorant binding proteins (OBPs) in the non-sensory respiratory cilia preparation. Odorant-binding proteins (OBPs) are low molecular weight, extracellular proteins of the lipocalin superfamily (Pes and Pelosi, 1995) and they and their homologues are associated with the olfactory apparatus of a variety of species from Drosophila to porcupines (reviewed Eisthen, 2002).

OBPs were originally investigated as potential olfactory receptors because of their strong binding to radioactive odorants (Pelosi *et al.*, 1982; Pevsner *et al.*, 1985). Although the specific function(s) of OBPs have not yet been determined, several roles have been proposed including the translocation of hydrophobic odorants across the mucus layer, co-stimulation (with odorants) of olfactory receptors and the removal of odorants both from olfactory receptor binding sites and the olfactory mucosa entirely (Breer *et al.*, 1994; Pes and Pelosi, 1995; Boudjelal *et al.*, 1996). The putative function is changed dramatically however, if it is considered that during the analysis of the three cilia proteomes described in this chapter, OBPs were only identifed in rat respiratory cilia preparations.

In the case of sheep olfactory cilia preparations it is entirely possible that the presence of OBP remains undetected in these studies. The presence of OBP in a wide variety of species suggests that OBPs are likely to be found in sheep nasal mucus. It is obvious from Figure 3.3.13 that not all of the proteins in the mass range ~20kDa (mass predicted for OBPs – Pevsner *et al.*, 1985; Pes and Pelosi, 1995) have been identified and there is no reference 2D-gel to allow educated guesswork as to the presence of OBPs from shared protein profiles. It is therefore impossible to conclude whether or not OBP is present in the olfactory cilia preparations of sheep.

The protein band identified as OBP occured in 7/9 2D-PAGE separations of rat respiratory cilia in contrast to only 1/9 2D-gels of rat olfactory cilia. The absence of total consistency is likely to reflect the extracellular nature of this protein *i.e.* its localisation to the overlying mucus. This automatically suggests that the difference in OBP occurrence is a result of differing efficiencies of mucus removal during the preparation of the enriched cilia fractions. To test this hypothesis, a comparison was made of the levels of haemoglobin in the olfactory and respiratory cilia preparations.

If efficiency of mucus removal through tissue washing was causing the artefactual occurrence of OBP in respiratory preparations, the levels of haemoglobin should also be increased in comparison to olfactory cilia preparations as this protein would also be present in the extracellular environment of the tissue post-dissection and fail to be removed by inefficient washing. By analysis of the multiple 2D-gels shown in Figures 3.3.6 and 3.3.19 it can be observed that the levels of haemoglobin (cluster of spots at the very bottom right edge of the gel images) in respiratory cilia preparations does not correspond to the presence/concentration of the OBP band. In addition, in rat olfactory preparations where haemoglobin is in higher abundance, potentially indicative of less efficient tissue washing, there is still no band corresponding to OBP (the pair of spots in the lower left corner of the rat olfactory cilia gels were identified as olfactory marker protein and cytochrome b5). This suggests that OBP presence in respiratory cilia preparations is the result of specific interactions with the cilia surface as opposed to inefficient mucus removal.

Immunohistochemical analysis has demonstrated that OBPs are present in both the Bowman's glands of the lamina propria (over which the olfactory epithelium lies) and the lateral nasal glands (Pevsner *et al.*, 1986). The secretions from these glands cover the surface of the olfactory epithelium, respiratory epithelium and vomeronasal organ (Schultz, 1960; Khew-Goodall *et al.*, 1991). This means that OBPs are certainly exposed to both olfactory and respiratory epithelia and therefore the lack of a band corresponding to OBP (as identified in respiratory cilia) in the nearly all of the rat olfactory cilia 2D-PAGE protein profiles is considered to be significant.

The first explanation for the differential presence/absence of OBPs in olfactory and respiratory cilia preparations is that there are multiple isoforms of

OBPs in the rat nasal cavity with specific localisations. Multiple subtypes of OBP within one species are certainly not uncommon (Pes and Pelosi, 1995; reviewed by Eisthen, 2000) and it has been suggested that OBPs may interact with particular classes or ORNs in insects (insert). It is also true that OBP subtypes may not share high sequence identity. Mouse OBPIa and OBPIb only share 58% identity (Pes and Pelosi, 1995) and this level of primary structure difference would easily account for the lack of corresponding band in olfactory cilia preparations. It is therefore possible that the OBP associated with olfactory mucus has not been identified due to only partial characterisation of the cilia proteome. This explanation does have one failing point however, in that a band corresponding to the OBP identified in rat respiratory cilia was observed in one of the rat olfactory cilia 2D-PAGE separations, indicating the presence of OBP 1F in the olfactory mucus under some circumstances.

An alternative explanation for the localisation patterns of OBP in the nasal mucosa could have implications for the functions currently ascribed to these proteins. OBP is an extracellular protein present in the mucus overlying both the olfactory and respiratory regions of the nasal cavity. If as discussed above, the presence/absence of OBP cilia preparations depends on specific interactions with the cilia surface, the differential occurrence in the olfactory *versus* respiratory preparations could be due to greater affinity of OBP for the respiratory cilia surface. A glycosylated receptor for OBP in bovine nasal mucosa has been reported (Boudjelal *et al.*, 1996) and these authors also reported evidence of specific binding of OBPs to the respiratory but not olfactory epithelium. The existence of a receptor/class of receptors for OBP in the respiratory cilia would explain the more common association of OBP with the respiratory cilia as there would be a much higher affinity interaction between the protein and cilia surface. Non-specific binding to respiratory cilia is discounted by

the similar occurrence levels of BSA and haemoglobin in both types of cilia preparation.

The potential existence of an OBP-binding receptor exclusively found in respiratory cilia would impact upon the potential functions of these proteins. It becomes more likely that the role of OBP in the olfactory system involves the clearance of odorants from the overlying mucus rather than co-stimulation of receptors. Although they may still act as facilitators for hydrophobic odorants crossing the mucus layer, it is likely from this study's findings that their main function is in the removal of odorants from the olfactory cilia environment.

3.4.5 Identification of proteins by 2D-PAGE and MALDI-ToF mass spectrometry

Identification of proteins by peptide mass fingerprinting There are two key areas of importance in identifying proteins by peptide mass fingerprinting. The first is the filtering out of contaminant peptides (described extensively in Section 3.2) and the second is the searching of the peptide lists against on-line protein databases.

The peptide mass fingerprinting score system is based on the likelihood that all of the peptide masses being searched can be derived from any single protein within the database. The inclusion of peptides from different proteins *e.g.* trypsin autolysis peaks, keratin contamination, multiple co-localising proteins, makes this matching more difficult as the probability of all peptides being derived from a single protein is reduced. The filtering process allows the exclusion of non-peptide peak masses (*i.e.* matrix-derived peaks) from the search list and also removes peptides derived from protein contaminants introduced during either the gel separation or in-gel digestion procedures. The filtering-out of peptides occurring in multiple samples

also aids in the identification of co-localised proteins in cases where an additional isoform of one of the proteins is present in another region of the gel.

Evaluation of protein identifications and database searching The protein identifications listed in Tables 3.3.5, 3.3.6 and 3.3.7 were all made according to their MOWSE scores. This score represents the probability of the observed peptides being derived from the suggested protein. Only identifications in which the MOWSE score was equal to or greater than 1 were considered to be significant. This represents protein identifications made with a 0.05 or less probability that they occurred by chance.

The denominator of the MOWSE score is a variable property of the database a peptide list was searched against. The relative number of entries that could be expected from an individual species in a particular database and also the levels of characterisation of the appropriate genome determined the choice of database. The *Rattus* database contains a concentrated set of proteins characterised during the volumes of work that have been performed using rat tissue. The large numbers of *Rattus* sequences available mean that searching this database provides a good chance to find a genuine protein match, whilst confining the search to a single species adds an extra piece of information about the protein *i.e.* animal origin.

When confining the search to protein sequences from a given species however, the search process is biased towards proteins of only that species. Whilst this is unlikely to cause significant problems in a database of a well-characterised animal such as the rat or mouse, it could potentially cause problems in other species such as the sheep. This animal is much less studied by the biochemistry community so there are markedly less protein entries in the sheep database compared with rat or mouse databases. A search confined to an *Ovis aries* database would decrease the

chances of the identification of proteins as the number of entries is significantly reduced. In this work, tryptic peptides from sheep proteins were searched against the Mammalia protein database. This enabled the identification of proteins from amongst included sheep entries but also allowed cross-species matching to identify proteins by the similarity of their peptide mass fingerprint to a protein from a different but potentially related organism such as *Bos taurus*.

Underrepresentation of plasma membrane proteins It is clear from only a brief survey of the proteins identified during this work that proteins involved in signal transduction are massively under-represented. The main reasons for this could lie in their frequent membrane-associated localisation, which while it almost guarantees the protein's presence in a cilia vesicle preparation often imposes solubility restrictions. This also explains why so many major membrane-bound proteins are demonstrably absent from the identification tables listed, including olfactory receptors. Santoni *et al.* (2000) describe three major reasons for the underrepresentation of membrane proteins: low abundance levels, pI values greater than 8 and lack of solubility. With levels of adenylyl cyclase estimated to account for 1% of cilia membrane surface protein (Lazard *et al.*, 1989) and the use of immobilised pH gradient (IPG) strips covering pH range 3-10, this leaves only two major problems for insoluble/poorly soluble proteins: getting into a 2D-gel and being subsequently identified by peptide mass fingerprinting.

In order to perform the first dimensional separation according to pI the buffer must not contain an effective level of anionic or cationic detergents. This prohibits the use of SDS in sample preparation unless samples are sufficiently concentrated that they can withstand two orders of magnitude worth of dilution and ultracentifugation (Fountoulakis and Takács, 2001). Instead uncharged or

zwitterionic detergents such as Triton X-100 and 3-[3-cholamidopropyl)-dimethylammonio]-1-propane sulfonate (CHAPS) are commonly used. The rehydration buffer in which samples are prepared for the first dimension of 2D-PAGE also contains a high concentration of chaotropic agents. This combination of relatively weak (by comparison with SDS) detergents and chemicals designed to denature proteins create significant solubility problems for any samples containing a significant proportion of membrane proteins (reviewed by Herbert, 1999).

Solubility may also be a problem for the efficient analysis of peptides derived from hydrophobic proteins such as membrane proteins (van Montford *et al.*, 2002a). The impact of this potential problem was briefly investigated by analysing the mass and hydrophobicity properties of the peptides observed in 20 tryptic digestions of BSA. The properties of the peptides observed in these digestions were used to set parameters for the peptides likely to be observed by MALDI-ToF mass spectrometry. These parameters chiefly describe the mass and hydrophobicity of potential peptides. The hydrophobicity measure used here was the HPLC value, which represents the theoretical elution time for a peptide passing through a hydrophobic chromatography column and is therefore directly proportional to peptide hydrophobicity. The mass and HPLC parameters were applied to the theoretical tryptic digests of six proteins likely to be expressed in the olfactory epithelium: two cytosolic proteins (β-actin, OMP), two integral membrane proteins (adenylyl cyclase III, voltage-gated K^+-channel) and two olfactory receptors (human OR1A1, rat OR51E2). The graphical results from this analysis are shown in Figure 3.4.1. They indicate that the hydrophobicity of peptides generated from insoluble proteins is similar to that generated from soluble proteins and point to the peptide mass being a greater problem in the identification of membrane proteins by peptide mass fingerprinting.

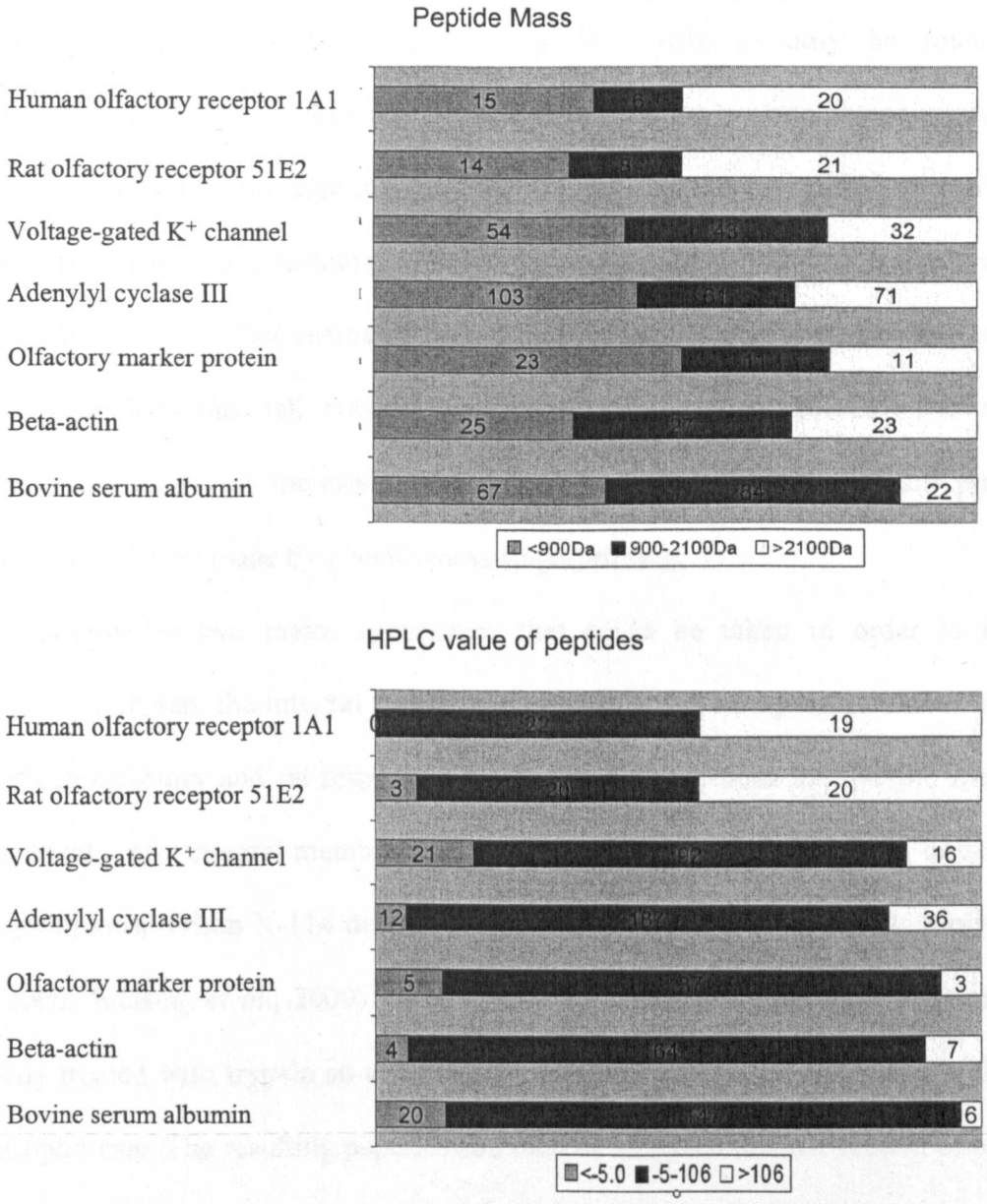

Figure 3.4.1 The underrepresentaion of membrane proteins in the cilia proteome characterisation may be partly due to a bias in the mass of peptides produced during in-gel tryptic digestion of these proteins

Protein sequences for BSA (*bos taurus*), adenylyl cyclase III (*homo sapiens*), voltage-gated potassium channel (*rattus norvegicus*), olfactory marker protein (*rattus norvegicus*) and the olfactory receptors were obtained from SwissProt protein database using the SRS tool available at www.expasy.ch. Theoretical tryptic digestions were performed on the sequences and the resulting peptides were grouped according to their mass and HPLC scores. The data labels indicate the number of peptides falling within each mass/HPLC range. The HPLC value is proportional to the hydrophobicity of the peptide.

This is a result of the limitations placed on the positions that can be adopted by bulky, charged residues such as the lysine and arginine amino acid targets for trypsin, in membrane proteins. As these residues are likely to only be found in extramembranous regions, they are likely to have either a transmembrane section(s) between serial lysine or arginine residues or very few amino acids between two lysine/arginine residues, resulting in a bias in the mass of peptides to both extremes of peptide size. This bias increases the number of peptides generated during in-gel tryptic digestions that fall outside the working range of the MALDI-ToF mass spectrometer used and therefore reduces the probability of a significant protein identification being made by peptide mass fingerprinting.

There are two major approaches that could be taken in order to more effectively compare the integral membrane proteins of the cilia preparations from rat and sheep olfactory and rat respiratory epithelia. Both methods involve the specific enrichment of integral/membrane-associated proteins by sodium carbonate precipitation or Triton X-114 detergent partitioning (Bordier *et al.*, 1981; Molloy *et al.*, 2000; Wissing *et al.*, 2000). Once membrane proteins are enriched they can be directly treated with trypsin so avoiding any solubility problems associated with gel electrophoresis. The resulting peptides can then be analysed and the protein of origin identified by multi-dimensional chromatography and tandem mass spectrometry (Blonder *et al.*, 2002). Alternatively the enriched membrane preparations could be resolved by SDS-PAGE and analysed by in-gel digestion and MALDI-ToF mass spectrometry. Modifications to the basic in-gel trypsin digestion method could then be introduced to avoid the potential problems of peptide mass and hydrophobicity. Such modifications involve the use of alternative protein cleavage reagents *e.g.* cyanogen bromide (Kraft *et al.*, 2001; van Montford *et al.*, 2002a) and the

introduction of the detergent octyl-β-glucoside either during enzymatic digestion (Katayama *et al.*, 2001) or subsequent peptide extraction (van Montford *et al.*, 2002b).

3.4.6 Protein conservation and the consequences for the role of thiols in the olfactory system

The characterisation studies of the cilia proteomes described here have not indicated the existence of a set of proteins both conserved in the olfactory cilia and unique to these structures. On the basis of this conclusion and according to the criterion set out in the Introduction, these experiments have failed to highlight potential candidates for olfactory-specific thiol sensor proteins.

Studies into the cilia proteomes have however, reinforced the importance of thiols in the olfactory system. The commonly used laboratory thiol β-mercaptoethanol is known to enhance the survival of multiple types of neuron in culture including olfactory receptor neurons (Grill Jr and Pixley, 1993). The low molecular weight thiol glutathione is known to be present as part of the cellular detoxification system (Peshenko *et al.*, 1998). Dithiothreitol, another thiol compound commonly used in the laboratory is one of the most potent non-physiological activators for peroxiredoxin 6 (Novoslev *et al.*, 1999), a thiol-specific peroxiredoxin of which multiple isoforms have been identified in olfactory cilia. In addition thiol transferase enzymes were observed in cilia preparations. In summary, despite the importance of thiols in the olfactory system, no thiol sensor proteins meeting the required criteria have been identified during the characterisation of the olfactory and respiratory cilia proteomes.

Chapter 4

THE ROLE OF EXPOSED CYSTEINE RESIDUES IN OLFACTORY CILIA

4.1 Introduction

As remarked at the end of Chapter 3, thiol groups (also referred to as SH or sulphydryl groups) play an important role in the olfactory epithelium. Thiol groups are found in low molecular weight metabolites such as glutathione, which accounts for over 90% nonprotein sulphur in a cell (Meister, 1995) and are also incorporated into proteins in cysteine residues. Sulphydryl groups participate in a number of different reactions including alkylation, oxidation and thiol-disulphide exchange (Figure 4.1.1), the chemical versatility due to the ability of the sulphur atom to act as both soft electrophile and soft nucleophile (Torchinsky, 1981; Clayden, 2001). The only reaction specific to SH groups is the thiol-disulphide exchange, which can proceed under physiological temperature and pH conditions (Torchinsky, 1981) and could provide the basis for a high strength, reversible interaction between a thiol odorant and its sensor protein.

The role of protein-bound thiol groups in olfaction has been studied in many species (Villet, 1974; Singer *et al.*, 1975; Menevse *et al.*, 1978; Shirley *et al.*, 1983; Seebingkert and Lynch, 2001; Broillet, 2002). Derivatisation of sulphydryl groups by thiol-directed reagents such as N-ethyl maleimide (NEM – for structure see Figure 4.1.2) irreversibly decreases the electrical potentials generated in response to odorant stimulation in both vertebrate and invertebrate species (Levisohn Getchell and Gesteland, 1972; Villet, 1974; Menevse *et al.*, 1978; Shirley *et al.*, 1983), demonstrating the importance of cysteine residues in olfaction. However the use of membrane-permeable reagents such as NEM makes it difficult to define the

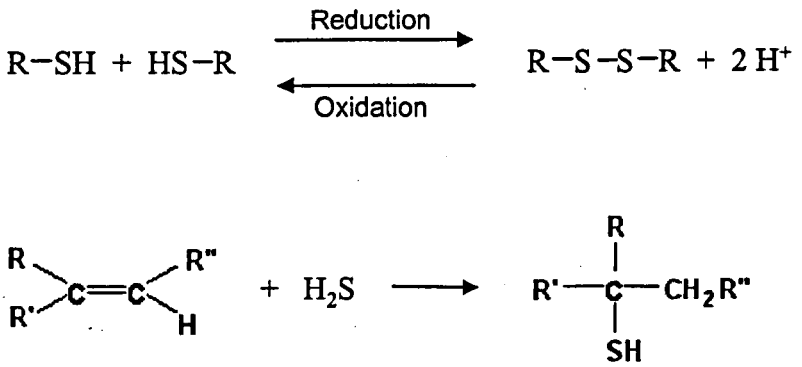

Figure 4.1.1 Examples of the reactions participated in by sulphydryl groups

a) Reduction and oxidation of sulphydryl groups enables the reversible formation of covalent disulphide bonds **b)** Addition of sulphydryl groups across unsaturated carbon bonds.

Source: Ohno and Oae, 1977.

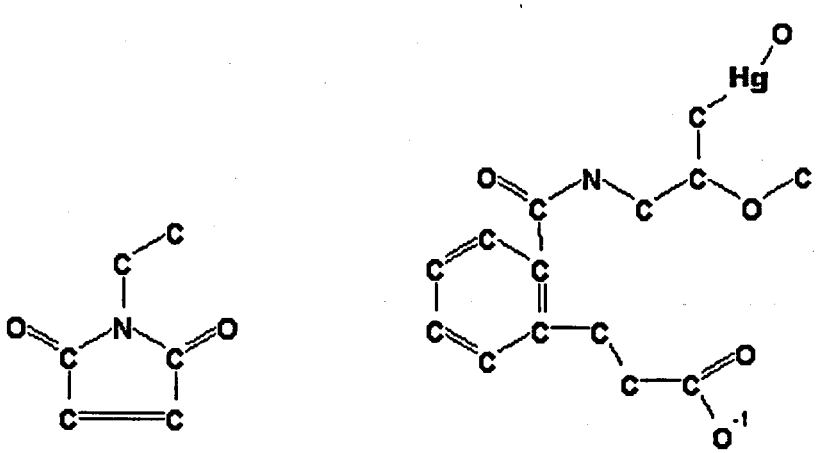

N-ethylmaleimide Mersalyl

Figure 4.1.2 The chemical structures of two compounds used to derivatise sulphydryl groups

N-ethylmaleimide forms a thioether bond with sulphydryl groups by nucleophilic addition across the unsaturated carbon-carbon bond. Mersalyl interacts with sulphydryl group via its Hg atom.

nature/identity of the target molecule. Experiments using mersalyl (Figure 4.1.2), a membrane-impermeable reagent, demonstrated that the derivatisation of extracellular cysteine residues reduced the amplitude of the electrical response to odorant stimuli in groups of neurons. Furthermore this effect could be avoided by prior exposure of the olfactory tissue to selected odorants (Menevse *et al.*, 1978; Shirley *et al.*, 1983). These findings firmly implicate extracellular cysteine residues in odorant detection.

The individual proteins derivatised by sulphydryl-directed reagents have yet to be characterised. Any proteins bearing exposed cysteine residues have the capacity for strong interactions with thiol compounds *via* disulphide linkages. The greater strength of disulphide linkages in comparison to non-covalent interactions would theoretically permit a greater period of interaction between a ligand and its receptor, leading to a greater probability that ligand-receptor interactions are sufficient to induce receptor activity, even at low concentrations of freely diffusing ligand. If olfactory receptors are targets for sulphydryl-directed reagents, thiol odorant detection *via* disulphide interactions provides a potential mechanism for thiol odorant sensitivity in a receptor-mediated odorant detection pathway. Subsequent reduction of the thiol odorant-receptor mixed disulphide bond *e.g.* by receptor internalisation, would reverse receptor derivatisation allowing the olfactory receptor to be occupied by a thiol odorant and recycled with minimal long-term consequences (see Figure 4.1.9, Chazot and Strange, 1992).

NEM reactivity has also suggested additional candidates for the protein sites of key cysteine residues for olfaction. In addition to targeting olfactory receptors, thiol odorants could also interact with downstream targets in the receptor-mediated pathway such as $G_{\alpha OLF}$ (Giusti *et al.*, 2003), voltage-gated K^+ channels (Seebungkert and Lynch, 2001) and cyclic nucleotide-gated channels (Lane Brown *et al.*, 1998);

interactions with such proteins allowing thiol odorants to cause membrane depolarisation, whilst circumventing the traditional olfactory receptor protein. This non-receptor-mediated hypothesis for the olfactory detection of thiols permits the inclusion of any proteins (intra- or extracellular) bearing exposed cysteine residues and capable of influencing membrane depolarisation as potential thiol sensor candidates.

As defined in the Introduction, any thiol sensor candidate protein must be suspected to be conserved across the three model mammalian species used in the present study, the rat, mouse and sheep. The role of any putative thiol receptor in olfaction also implies that the protein may have sensory-specific functions and/or localisation to the olfactory cilia preparations. A combination of membrane-impermeable and membrane permeable reagents was used to specifically label proteins associated with olfactory cilia (mouse, rat and sheep) and respiratory cilia (rat), which bear exposed cysteine residues. Labelled cilia preparations were then separated by gel electrophoresis and the identity of the derivatised proteins determined by peptide mass fingerprinting or *de novo* sequencing.

To investigate the number and identities of all potential thiol sensor proteins, intact olfactory tissue from the three species was treated with the membrane-permeable, sulphydryl-targeting reagent iodoacetyl-long chain-biotin (I-LC-biotin). I-LC-biotin derivatises accessible thiol groups within the tissue, covalently attaching a biotin tag to any proteins bearing exposed cysteine residues (see Figure 4.2.1 and 4.2.2 for reagent structure and reaction scheme). As the olfactory cilia are the only sensory regions of the epithelium to have direct interactions with odorants, they remain the likely location of any putative thiol sensor proteins, whether or not detection is receptor-mediated. Therefore the survey of proteins bearing exposed

cysteine residues is limited to cilia-associated proteins, which were isolated post-I-LC-biotin treatment by deciliation (as described in Section 2.3). Blotting SDS-PAGE/2D-PAGE separations of olfactory cilia proteins onto a nitrocellulose membrane and detection of the biotin tag using a streptavidin-alkaline phosphatase conjugate revealed the individual proteins derivatised.

To address the issue of potential thiol sensors with external cysteine residues within the olfactory mucus or olfactory cilia an additional, membrane-impermeable reagent Lucifer Yellow iodoacetamide (LYIA) was utilised. This permitted the direct visualisation of any proteins bearing external cysteine residues *via* the in-gel detection of the fluorescent group attached to accessible thiol groups.

4.2 Method development

To investigate the potential for thiol odorant detection *via* disulphide interactions with a target protein, olfactory and respiratory tissue was treated with two sulphydryl-targeting reagents: I-LC-biotin and LYIA. Bovine serum albumin (BSA) and erythrocytes were used to monitor reagent activity in aqueous and membrane-containing protein preparations respectively.

I-LC-biotin is a membrane-permeable sulphydryl-reactive reagent and was used to derivatise all proteins in the olfactory/respiratory epithelia with exposed cysteine residues *i.e.* cysteine residues on the surface of proteins and not involved in disulphide bonds (Figure 4.2.1). I-LC-biotin consists of a biotin moiety attached to an iodoacetamidyl group *via* a long hydrocarbon tail and attaches the biotin moiety to any proteins containing exposed cysteine residues (Figure 4.2.2). The covalent attachment of the tag allows labelled proteins to be resolved by SDS-PAGE/2D-PAGE and blotted onto nitrocellulose for detection of biotin *via* a streptavidin-alkaline phosphatase conjugate (described in Section 2.9).

The reaction time courses for I-LC-biotin labelling of BSA and erythrocyte proteins are shown in Figure 4.2.3 and 4.2.4 respectively. The time course of the BSA-labelling reaction showed that the extent of biotinylation increased with time, although similar biotin levels were detected at 1.5h and 3h (Figure 4.2.3). Analysis of I-LC-biotin activity in the erythrocyte preparation also demonstrated increased biotin labelling in the extended timepoints. However, whilst the 3h sample in the erythrocyte time course clearly exhibited the greatest labelling intensity, the profile of biotinylated proteins remains consistent across all timepoints. Therefore during longer reaction times, although increased labelling undoubtedly occurs, there is no evidence of increasing reagent accessibility to protein substrates *i.e.* no evidence of a

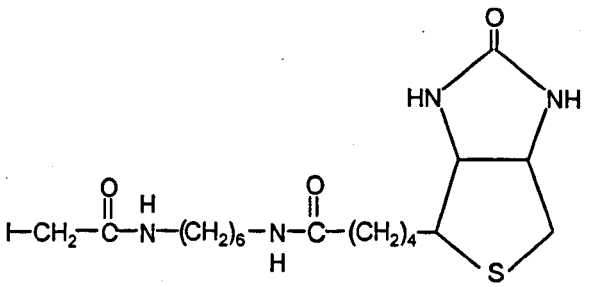

Figure 4.2.1 Chemical structure of the sulphydryl-targeting reagent Iodoacetyl-Long Chain-biotin

Source: EZ-Link™ Iodoacetyl-LC-Biotin Product information sheet 21333. Perbio Science, Cheshire, UK.

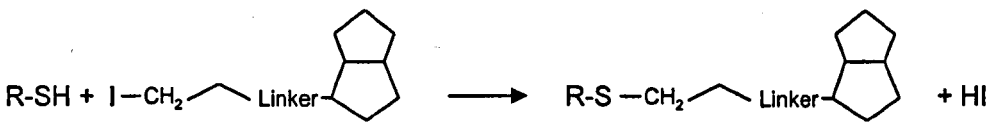

Figure 4.2.2 Mechanism for Iodoacetyl-Long Chain-Biotin reaction with exposed thiol groups

The Iodoacetyl-Long Chain Biotin reaction covalently attaches a biotin moiety to proteins bearing exposed cysteine residues. The biotin tag can later be detected using enzyme-linked streptavidin conjugates.

Source: EZ-Link™ Iodoacetyl-LC-Biotin Product information sheet 21333. Perbio Science, Cheshire, UK.

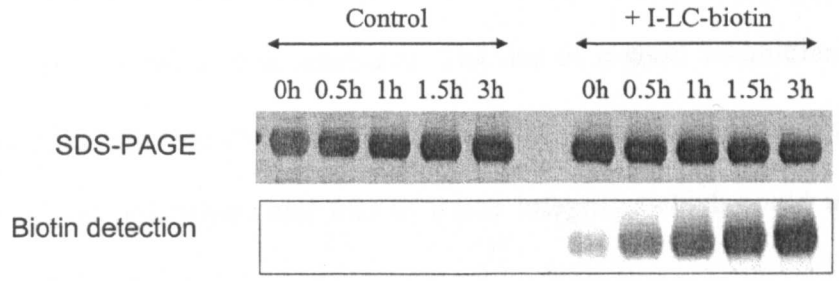

Figure 4.2.3 Reaction time course for the labelling of BSA using I-LC-biotin

I-LC-biotin (15µl of 4mM I-LC-biotin) or an equal volume of dry DMF was added to 500µl PBS/EDTA containing 50µg BSA. Reactions were allowed to proceed for 0h, 0.5h, 1h, 1.5h and 3h before being quenched by the addition of 500µl 200mM DTT. Samples were desalted to remove unbound I-LC-biotin and analysed by SDS-PAGE. Proteins were subsequently blotted onto a nitrocellulose membrane, which was probed using 2.5µg/ml streptavidin-alkaline phosphatase conjugate to detect biotinylated proteins (Section 2.8).

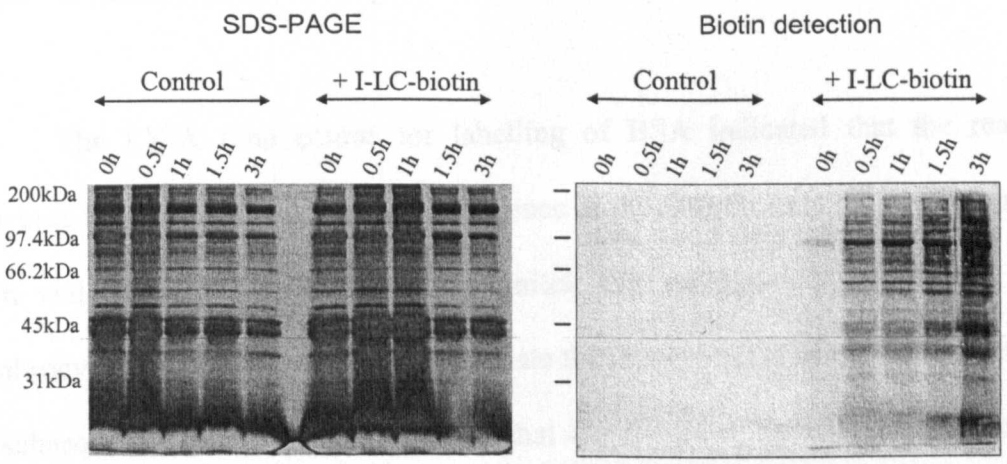

Figure 4.2.4 Reaction time course for the labelling of erythrocytes using I-LC-biotin

I-LC-biotin (3µl of 4mM I-LC-biotin) or an equal volume of dry DMF was added to 100µl PBS/EDTA containing resuspended horse erythrocytes. Reactions were allowed to proceed for 0h, 0.5h, 1h, 1.5h and 3h before being quenched by the addition of 100µl 200mM DTT. Samples were desalted by repeated washing of the erythrocytes to remove unbound I-LC-biotin. The erythrocyte proteins were separated by SDS-PAGE and blotted onto a nitrocellulose membrane for biotin detection (Section 2.8).

difference in biotinylation rates between proteins putatively inside and outside the erythrocyte membrane. During this study I-LC-biotin was allowed to react for 1h, as in both BSA and erythrocyte labelling experiments a substantial degree of protein labelling was detected at this timepoint. The use of a short incubation period also limited the time between tissue harvesting, labelling and deciliation. This minimised the potential for proteolysis and loss of tissue integrity, which could interfere with subsequent deciliation.

LYIA is a membrane-impermeant reagent that attaches the fluorescent Lucifer yellow group to proteins bearing extracellular exposed cysteine residues (Figure 4.2.5 and 4.2.6, Tang *et al.*, 1998). Therefore it was used to determine the number of proteins within olfactory cilia preparations that have extracellular cysteine residues accessible to thiol odorants in the mucus layer. Direct UV scanning of protein preparations resolved by SDS-PAGE was used to detect the Lucifer yellow tag.

The LYIA time course for labelling of BSA indicated that the reaction proceeds rapidly with little obvious difference in the fluorescence detection from the 0.5h and 3h samples (Figure 4.2.7). Initial experiments using LYIA to label erythrocyte surface proteins failed to indicate the incorporation of the fluorescent tag. A subsequent experiment demonstrated that the failure of protein labelling in this case was likely to be due to the concentration of derivatised proteins being below the detection threshold or the absence of target sites, rather than reagent inactivity (Figure 4.2.8). The BSA labelling using the same freshly prepared LYIA stock was significant, indicating that the reagent was functional during the erythrocyte experiments performed alongside. In the control BSA sample there remained an easily distinguishable BSA band in the UV scan. This is likely to be due to the high

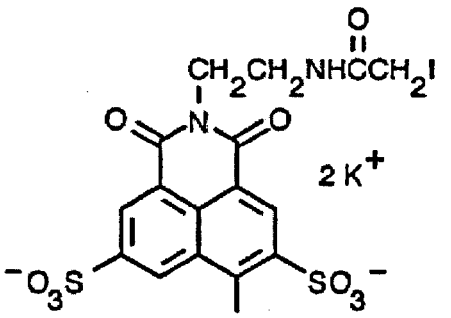

Figure 4.2.5 Chemical structure of the membrane-impermeable, sulphydryl targeting reagent Lucifer Yellow iodoacetamide (LYIA)

Source: Data on product L-1338 at www.molecularprobes.com.

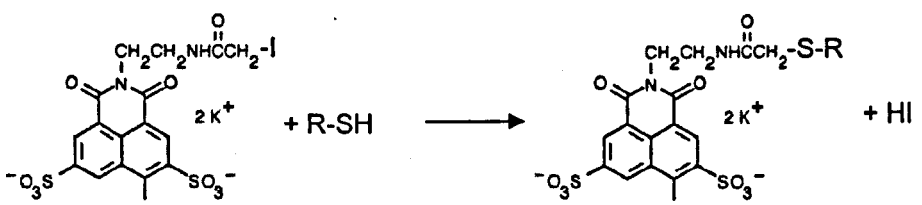

Figure 4.2.6 Reaction mechanism for Lucifer Yellow iodoacetamide

Lucifer Yellow iodoacetamide reaction involves nucleophilic substitution of the iodine atom by the thiol group. The unsaturated rings of the Lucifer Yellow group give it its fluorescent properties and enable the detection of proteins modified by this reagent by in-gel UV scanning.

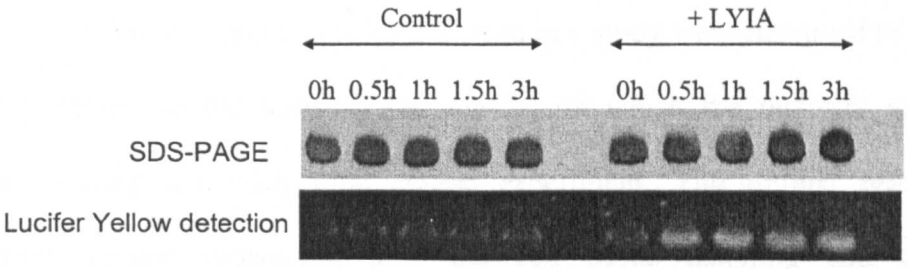

Figure 4.2.7 Reaction time course for the labelling of BSA using LYIA

LYIA (25µl 6.5mg/ml stock) was added to 500µl PBS/EDTA containing 50µg BSA. Reactions were allowed to proceed for 0h, 0.5h, 1h, 1.5h and 3h before being quenched by the addition of 500µl 200mM DTT. Samples were desalted to remove unreacted LYIA and analysed by SDS-PAGE. Lucifer Yellow tags were detected by scanning the gel under UV light (see Section 2.9).

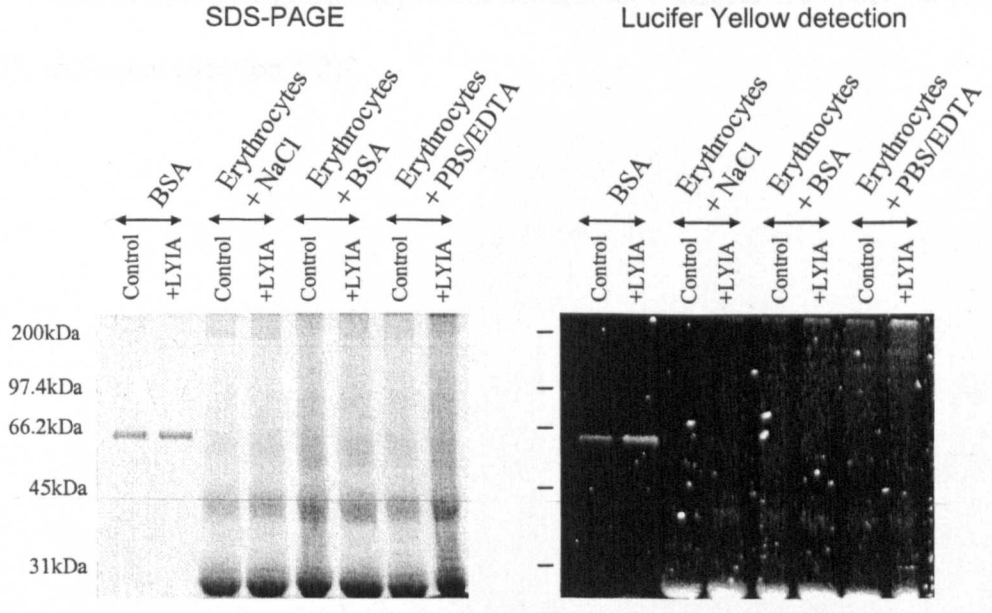

Figure 4.2.8 LYIA failed to label any proteins in the horse erythrocyte preparations

Erythrocytes were isolated from fresh horse blood by centrifugation at 5000rpm, 10 min. Erythrocytes were resuspended in PBS/EDTA and distributed between six 0.5ml microfuge tubes. Samples volumes were made up to 100µl by adding 10µl 2mg/ml BSA, 0.9%(w/v) NaCl (BSA buffer) or 10µl PBS/EDTA. As an additional control for LYIA activity, two samples containing 90µl PBS/EDTA and 10µl 2mg/ml BSA were prepared. LYIA (25µl 6.5mg/ml stock) or MilliQ water was added to all tubes and the reaction allowed to proceed for 30 min before excess reagent was removed by three 100µl PBS washes of the erythrocytes. The erythrocyte proteins were separated by SDS-PAGE and the Lucifer Yellow tag detected by direct UV scanning of the gel (see Section 2.9). SDS-PAGE gel stained by coomassie blue.

BSA protein concentration present, which also explains the detection of highly abundant protein bands in the erythrocyte preparations on the same gel.

The labelling reactions using LYIA in this study were restricted to 0.5h. This was determined on the basis of the speed with which the majority of labelling occurred during the BSA time course experiment. The limited reaction time minimises sample processing time between tissue labelling and subsequent deciliation. Limiting the LYIA reaction period also reduces the potential cytotoxicity of the reagent (Archer *et al.*, 1995). The maintenance of consistent cilia protein profiles in control and labelled samples suggested no significant tissue damage occurred during LYIA-treatment. Dual-labelling experiments performed in Chapter 5 also indicated that no significant protein denaturation effects are observed following LYIA treatment (Section 5.2).

4.3 Results

4.3.1 I-LC-biotin labelling of olfactory cilia proteins: 2D-PAGE analysis

The profiles of I-LC-biotin derivatised proteins of the olfactory cilia preparations from mouse, rat and sheep were species-specific to a large extent, although as with the 2D-protein profiles reviewed in Chapter 3, the highly conserved cytoskeletal proteins (boxed regions) maintained their migration and labelling characteristics in all species (Figure 4.3.1). These conclusions were based on spot number rather than intensity, as the protein concentration in the different preparations was clearly different. This divergence did not correspond directly to relative protein loading as the staining of 2D-PAGE replica gels strongly suggested the greatest protein concentration was in the rat olfactory cilia preparations, which also contained the lowest number of detected biotin-tagged proteins. The biotin detection blots from mouse, rat and sheep cilia preparations are provided in more detail in Figures 4.3.2 and 4.3.3 alongside their corresponding replica gels. Rat olfactory cilia preparations contained fewer labelled proteins following I-LC-biotin treatment and by implication, fewer proteins with exposed cysteine residues than the mouse and sheep cilia preparations. Whilst little similarity between the rat and sheep labelling could be predicted by their differing overall 2D protein profiles, the apparent increase in numbers of biotinylated proteins in the mouse olfactory cilia preparations compared to the rat was unexpected. This result suggested that despite very similar 2D profiles (see equivalent loading gels in Figure 3.3.6), the protein complements of mouse and rat olfactory cilia certainly differ in levels of exposed cysteine residues and therefore may also be more functionally distinct than initial protein profile comparisons suggested. Alternatively this distinction may be highlighting differences in the mucosal lining of the olfactory cilia and/or differential reagent diffusion during

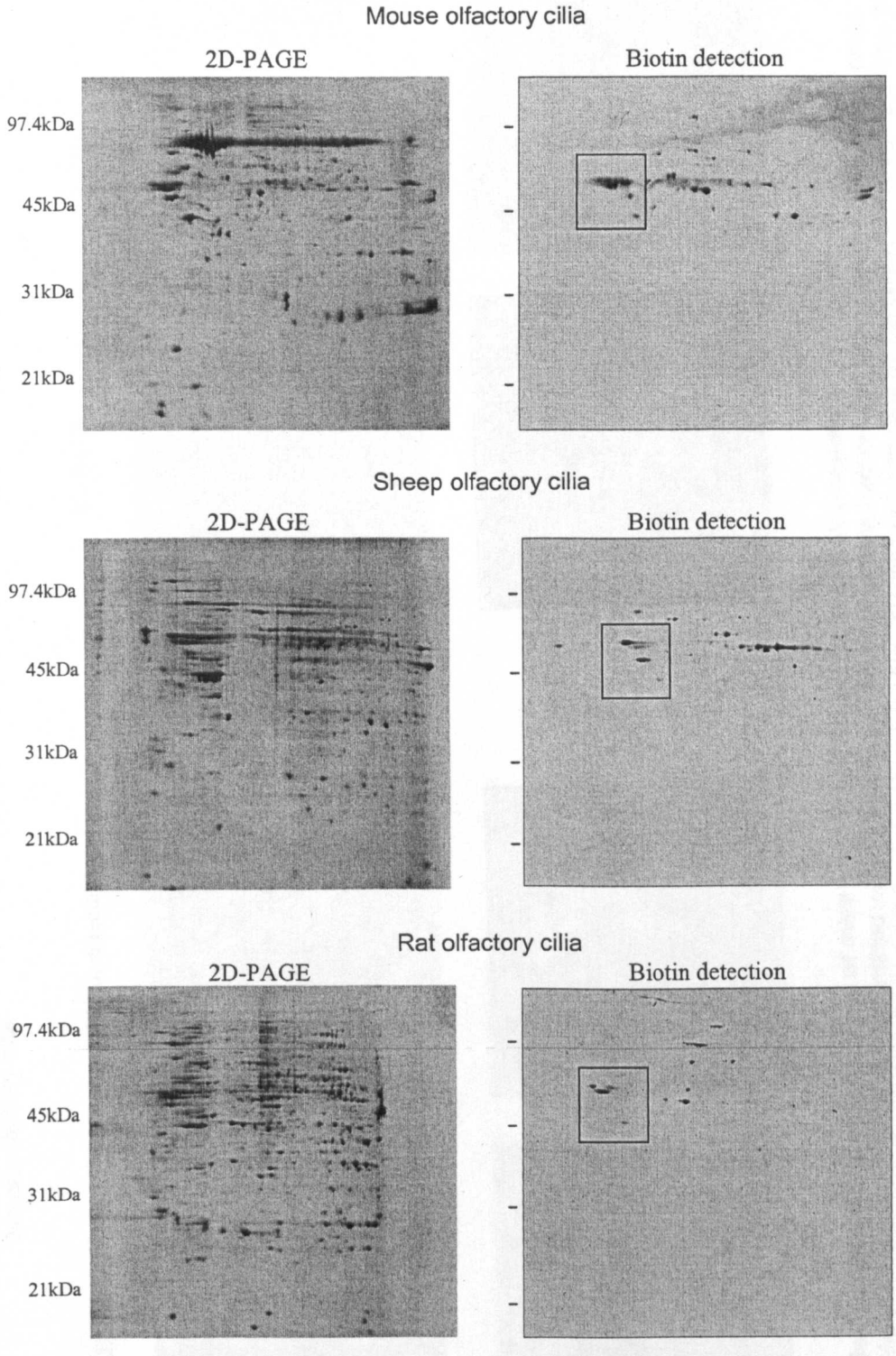

Figure 4.3.1 A subset of proteins in the olfactory cilia of the mouse, rat and sheep have exposed cysteine residues

I-LC-biotin treated olfactory cilia proteins were resolved by 2D-PAGE and blotted onto nitrocellulose for the detection of biotin tags. Boxed regions indicate the detection of biotin tags on the cytoskeletal proteins of all three species.

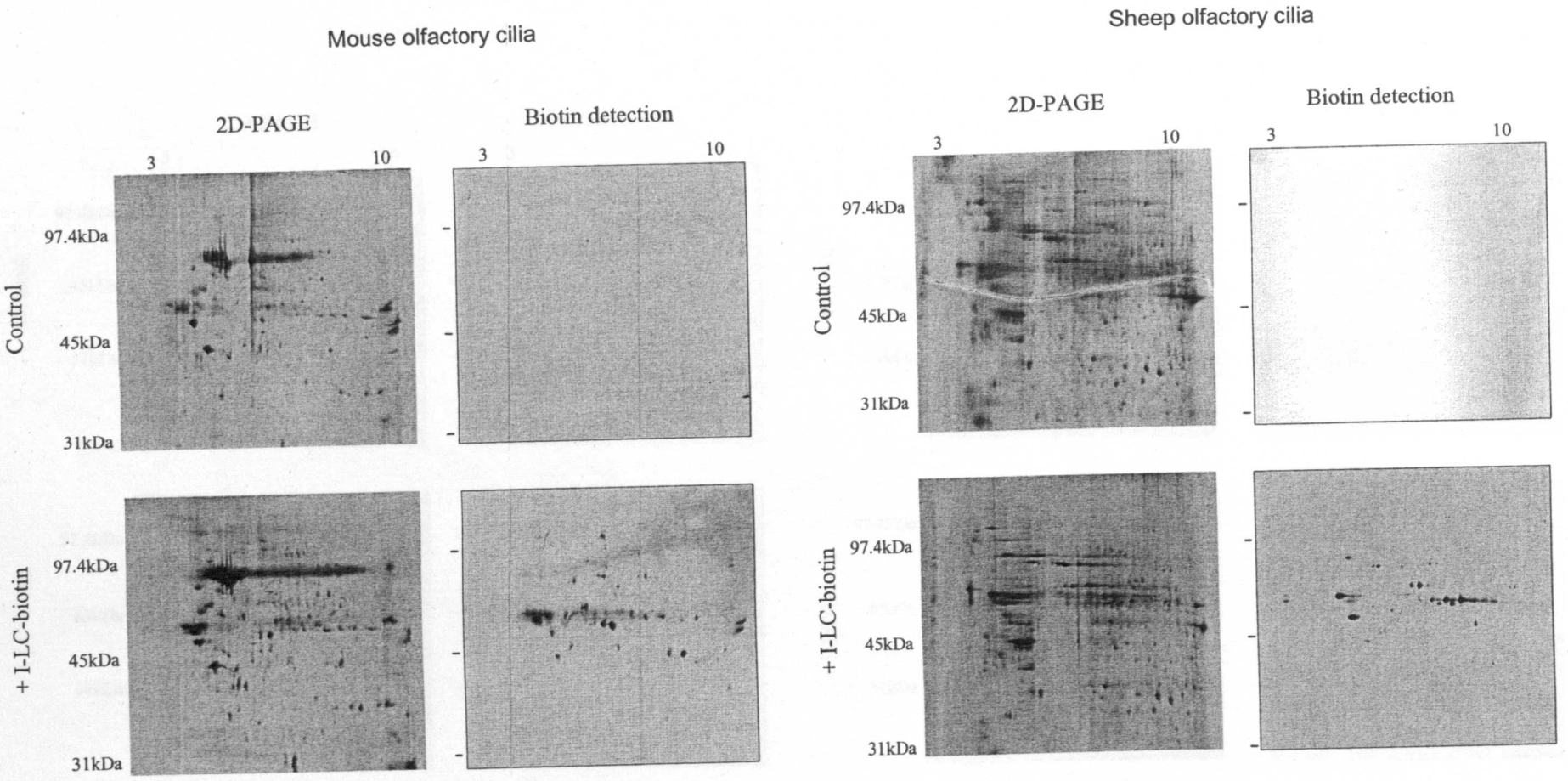

Figure 4.3.2 Selected proteins in the olfactory cilia of mice and sheep bear exposed cysteine residues
The olfactory epithelia of the mouse and sheep were treated with I-LC-biotin and an enriched cilia fraction was then prepared. This protein preparation was then separated by 2D-PAGE and blotted onto a nitrocellulose membrane for the detection of biotin tags as described in Section 2.8. The 2D-gel separation of mouse olfactory cilia proteins was performed using a 7cm pH 3-10 Linear IPG strip hence the slightly distorted appearance of the profile in comparison with that shown in Chapter 3.

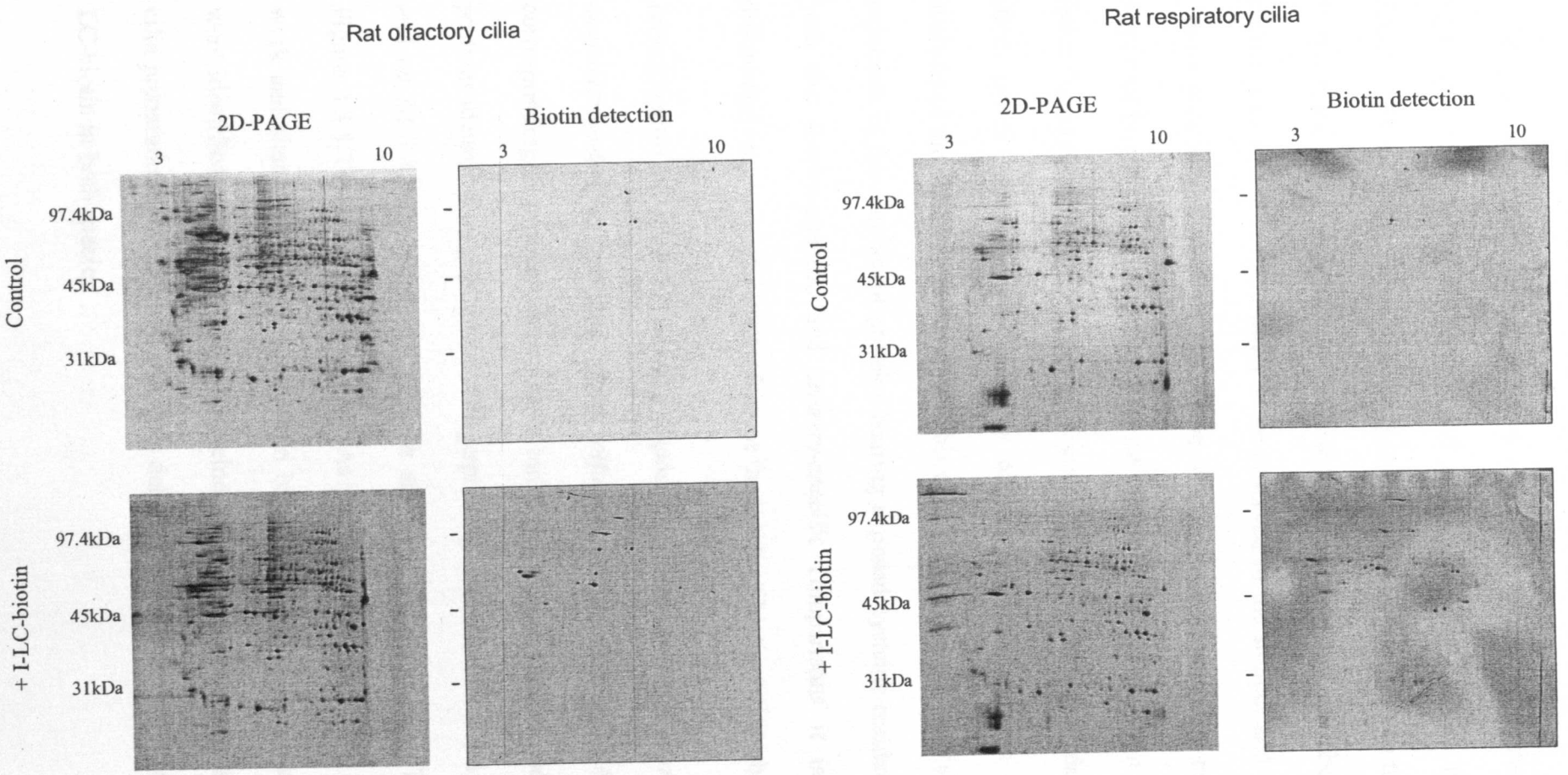

Figure 4.3.3 Detection of the proteins in rat olfactory and respiratory cilia bearing exposed cysteine residues
Olfactory and respiratory epithelia of the rat were treated with I-LC-biotin. The cilia were then isolated and the proteins resolved by 2D-PAGE. They were then blotted onto a nitrocellulose membrane and the biotin tags were detected by probing the blot with a streptavidin-alkaline phosphatase conjugate as described in Section 2.8.

exposure to the turbinates rather than the cilia protein complement itself. It is unlikely to be an artefact of the surface area of the turbinates, as the structures are physically very similar in the rat and mouse differing only in scale and thus theoretically maintain a consistent surface area: cilia protein ratio in the two species. Furthermore, physical differences leading to the restriction of the labelling reagent's surface area access is more likely to be observed in the smaller and therefore more closely packed turbinates of the mouse olfactory system contrary to the increased degree of biotinylation observed. The rat olfactory cilia preparation also contained fewer biotinylated proteins than its respiratory cilia counterpart despite evidence (from protein staining) of marginally higher protein loading in the 2D-PAGE analysis of the olfactory preparation. This could potentially reflect a sensory-specific reduction in the number of proteins bearing exposed cysteine residues. However in both the species-specific and sensory-specific comparisons it is possible that differential reagent access may influence the levels of biotinylation observed.

Identification of proteins bearing exposed cysteine residues during 2D-PAGE characterisation of rat and sheep olfactory cilia The 2D-PAGE gel spots corresponding to proteins shown to be biotinylated were excised and the individual proteins identified by peptide mass fingerprinting. The identifications made for sheep and rat I-LC-biotin derivatised proteins are given in Figure 4.3.4/Table 4.3.1 and Figure 4.3.5/Table 4.3.2 respectively. As predicted from previous characterisation work and shared regions of the protein biotinylation profile, cytoskeletal proteins were identified as having exposed cysteine residues in both sheep and rat olfactory cilia preparations. In addition, aldehyde dehydrogenase subtypes were labelled by I-LC-biotin in both species.

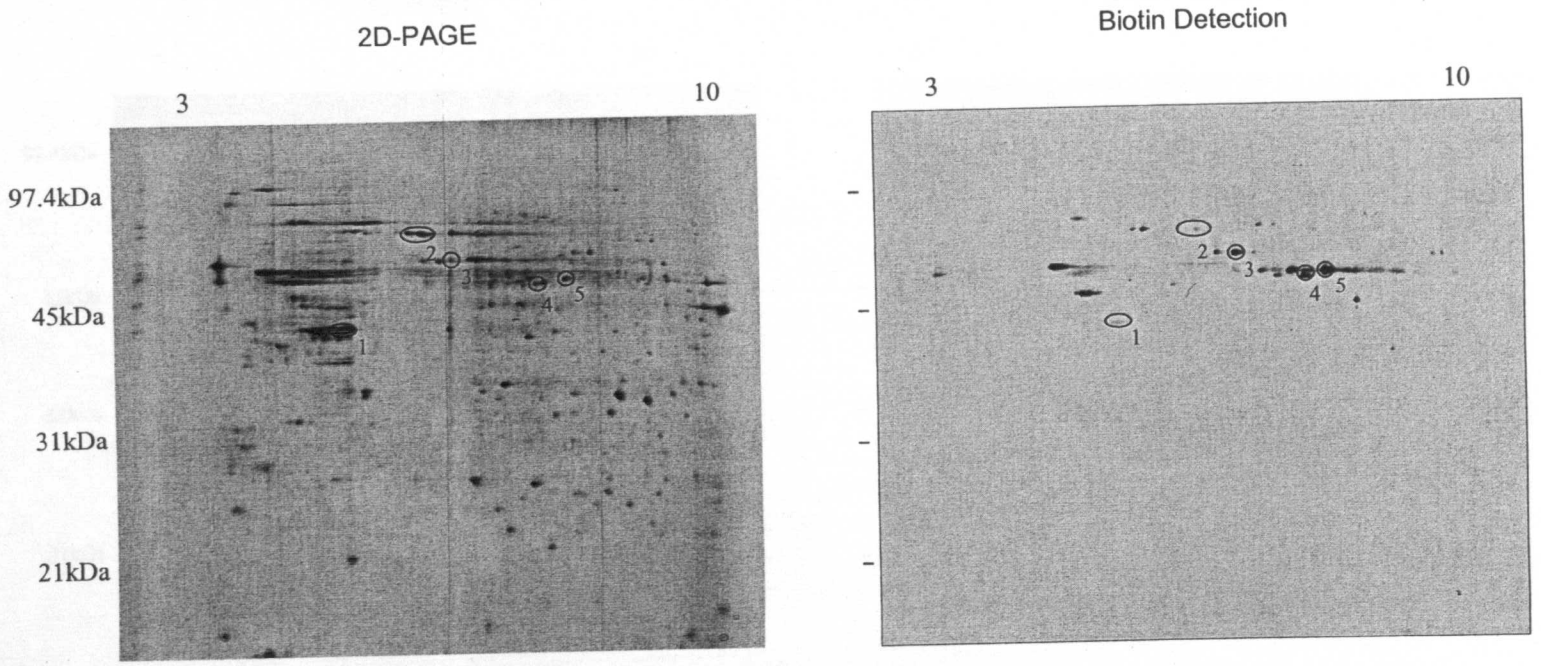

Protein Spot	Putative Identification	NCBI Accession #	Mw (kDa)	Species	Mowse score
1	Putative beta-actin	49868	39.4	Mus musculus	94/65
2	Serum albumin precursor	113582	71.1	Ovis aries	250/66
3	Glucose regulated protein 58kDa	27805905	57.3	Bos taurus	151/67
4	Aldehyde dehydrogenase 1A1	1706388	55.4	Ovis aries	122/67
5	Aldehyde dehydrogenase 1A1	1706388	55.4	Ovis aries	72/67

Figure 4.3.4/Table 4.3.1 Identification of proteins in the sheep olfactory cilia with exposed cysteine residues
Proteins labelled using I-LC-biotin were identified by comparing the biotin detection blot shown to the gel used to illustrate the protein identifications made during the characterisation of the sheep olfactory cilia proteome in Chapter 3.

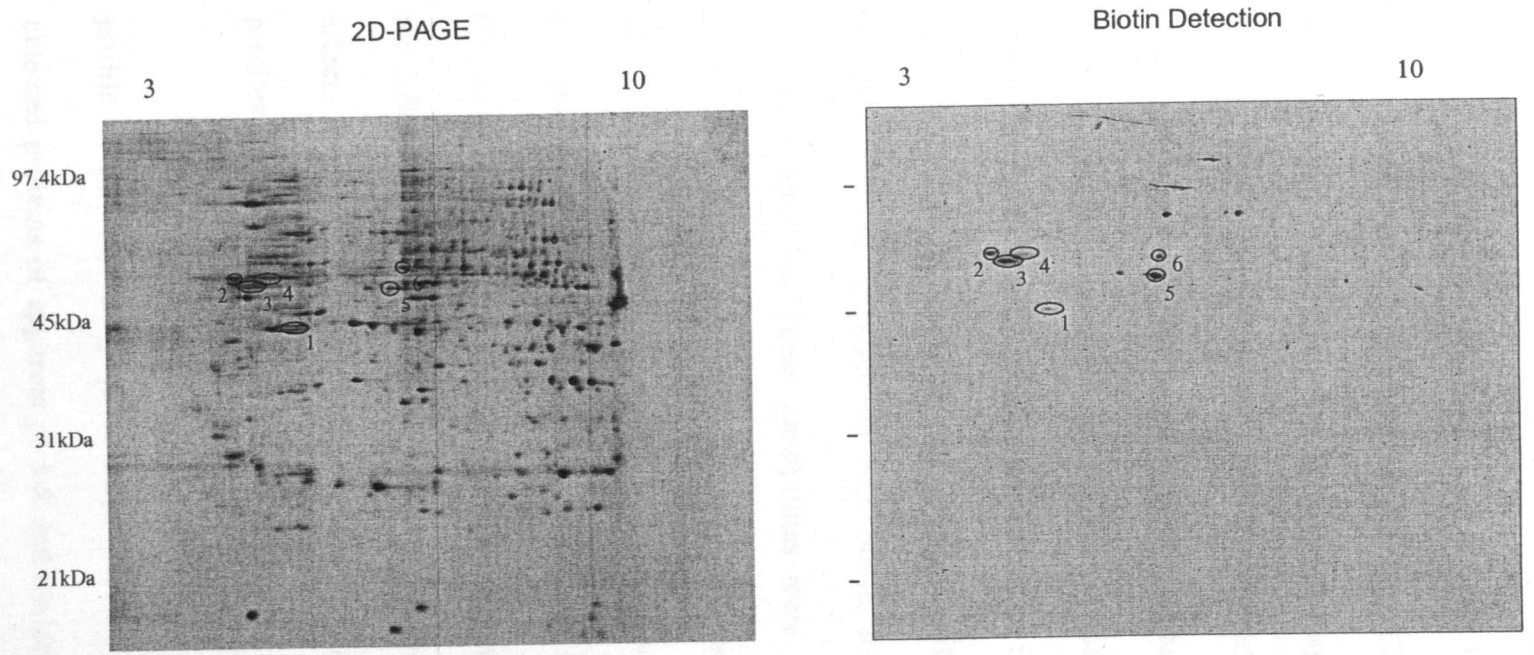

Protein Spot	Putative Identification	NCBI Accession #	Mw (kDa)	Species	Mowse score
1	Beta-actin / gamma actin	71620/ 4501887	42.1/ 42.1	Rattus norvegicus/ Homo sapiens	103/53 (both)
2	p38 Mitogen activated protein kinase	13591928	41.5	Rattus norvegicus	64/53
3	Keratin-10	21961605	59	Homo sapiens	73/67
4	Alpha-tubulin	223556	50.9	Rattus norvegicus	78/59
5	Aldehyde dehydrogenase	16073616	48.2	Rattus norvegicus	138/57
6	Enolase 1, alpha	6978809	47.4	Rattus norvegicus	118/57

Figure 4.3.5/Table 4.3.2 Identification of proteins in the rat olfactory cilia bearing exposed cysteine residues
Proteins labelled with I-LC-biotin were identified by comparing the above biotin detection blot with the data obtained during the characterisation of the rat olfactory cilia proteome in Chapter 3.

4.3.2 Differential labelling of rat olfactory and respiratory cilia proteins by I-LC-biotin: 2D-PAGE analysis

The results of two separate I-LC-biotin labelling experiments on rat olfactory and respiratory cilia are given in Figures 4.3.3 and 4.3.6. The biotinylation profiles differ between these studies both as a result of very different protein concentrations and a variation in procedure that led to the increased agitation of samples in Figure 4.3.6. However, both experiments indicated that olfactory cilia preparations contain fewer proteins with exposed cysteine residues by comparison to respiratory cilia. This may represent a significant adaptation of olfactory cilia to limit the numbers of proteins bearing exposed cysteine residues and therefore free thiol groups available for I-LC-biotin labelling. Alternatively the observed differences may have resulted from greater restrictions imposed on I-LC-biotin accessibility in the olfactory versus respiratory epithelia. These possibilities were examined further during a set of experiments using 12nmol and 24nmol I-LC-biotin per mg tissue (equivalent to the addition of 30µl and 60µl of stock I-LC-biotin solution to half nasal turbinate tissue dissected from a single animal) to label proteins of rat olfactory and respiratory cilia (Figures 4.3.6 and 4.3.7). Theoretically, if reagent diffusion is the sole determinant of the differing labelling profiles increasing the levels of reagent should alleviate this effect. Alternatively if accessibility differences are not significant, the labelling profiles should not alter according to reagent concentrations.

Increased levels of I-LC-biotin had little effect upon the overall biotinylation profile of rat respiratory cilia, other than the appearance of additional, weakly-detected proteins of apparent pI 5-8 and molecular mass ~70kDa. By contrast, the labelling profile of olfactory cilia proteins altered significantly between the experiments using different I-LC-biotin concentrations. The proteins derivatised

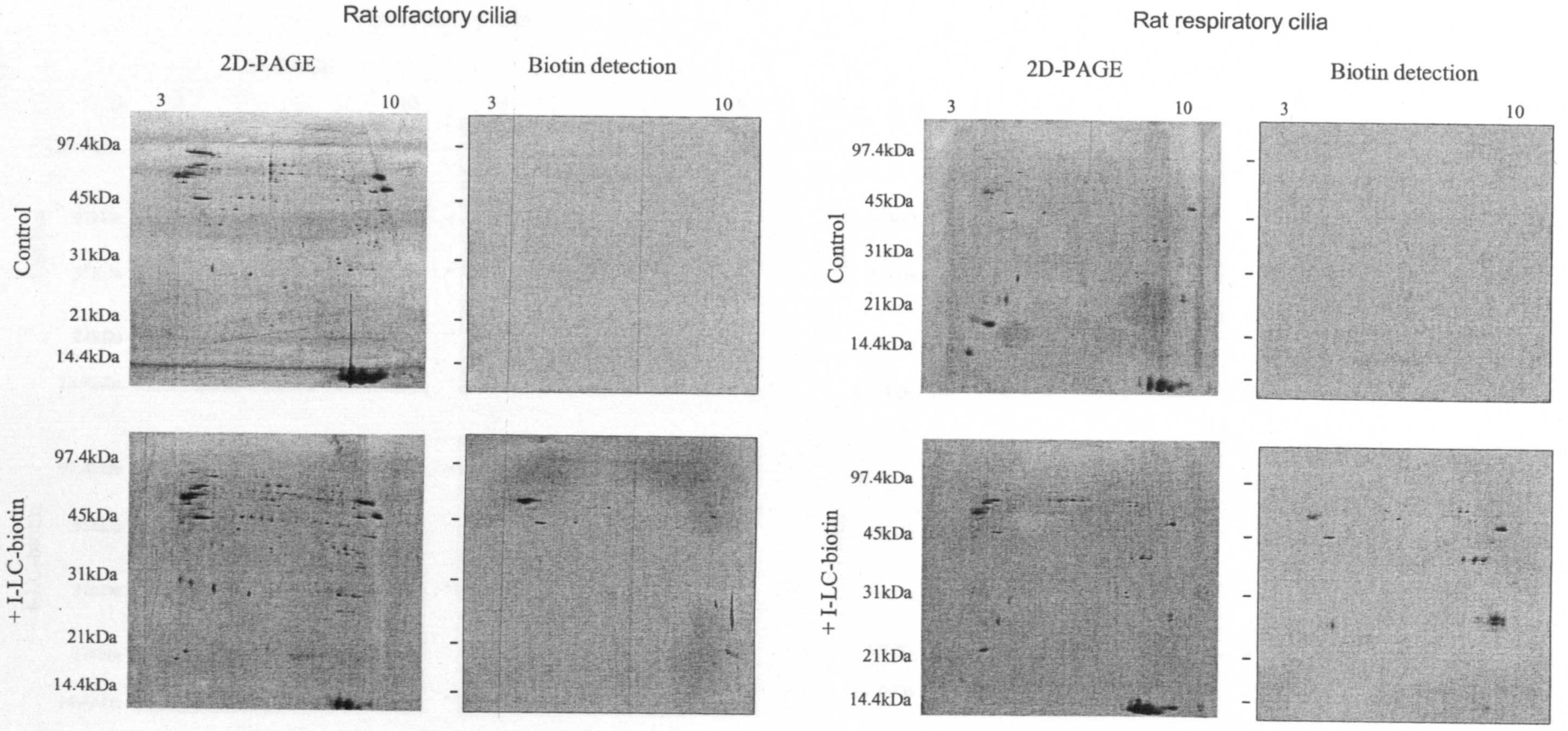

Figure 4.3.6 Selected proteins of the rat olfactory and respiratory cilia are labelled during tissue treatment with 12nmoles/mg tissue I-LC-biotin.

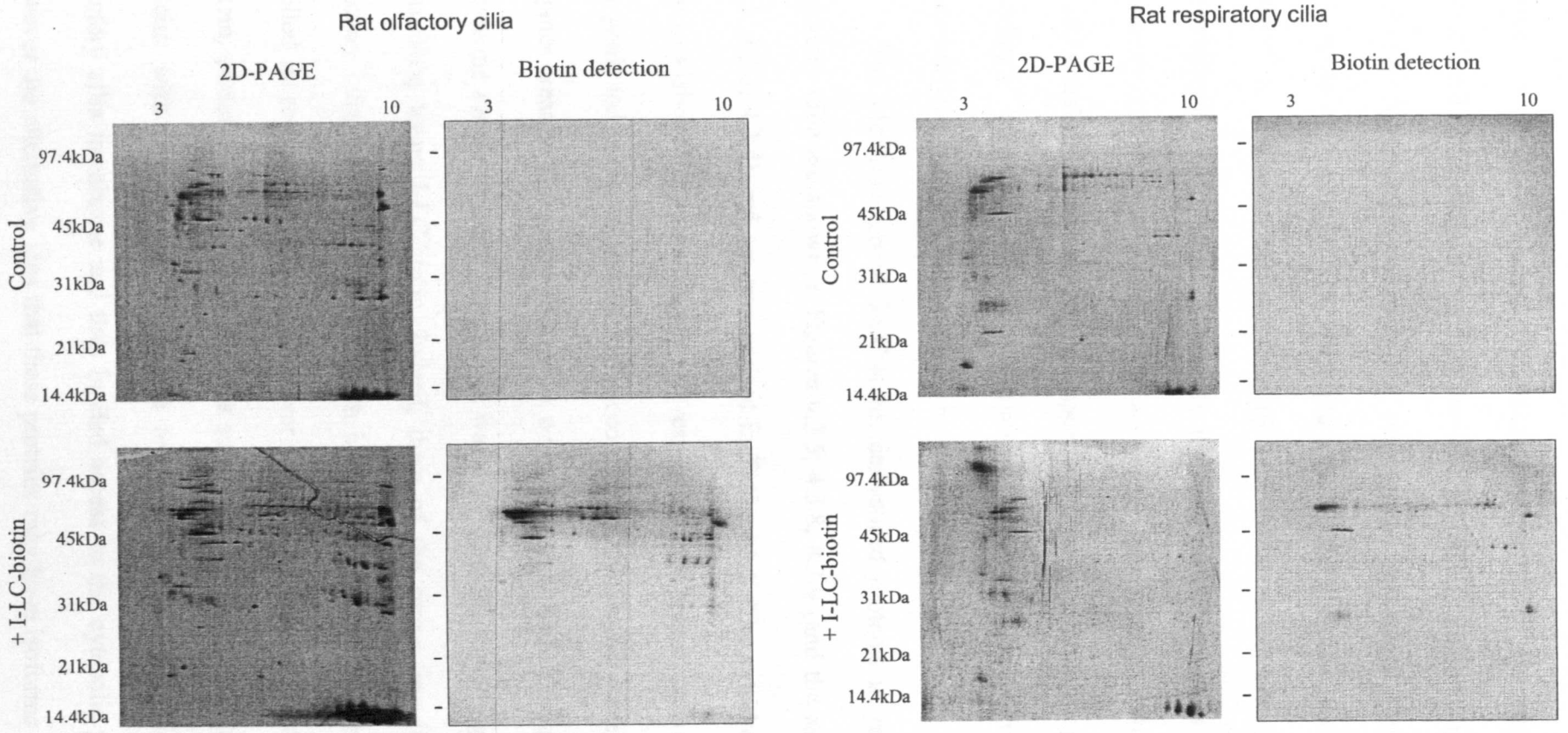

Figure 4.3.7 The use of increased levels of I-LC-biotin during labelling reactions leads to increased numbers of biotinylated proteins in the olfactory cilia

Olfactory turbinates and respiratory epithelia samples were treated with 60µl 4mM I-LC-biotin for 1h (24nmoles/mg tissue). The preparation and analysis of the cilia proteins was then performed as described in Section 2.8.

during exposure to the lower reagent level were again biotinylated during treatment of tissue with the increased I-LC-biotin concentration; however they became outnumbered by additional, strongly detected proteins (number of proteins difficult to estimate due to combination of faint staining and inadequate protein resolution in some areas of the gel). The increased number of proteins observed following exposure to a greater concentration of I-LC-biotin demonstrated that substrate accessibility is a definite influence in the differing labelling profiles of olfactory and respiratory cilia and also potentially in the species-specific effects observed. Some of the additional proteins labelled were specific to the rat olfactory cilia preparations providing evidence for sensory/neuron-specific adaptations in the accessibility/reactivity of exposed cysteine residues.

The identification of I-LC-biotin derivatised proteins in rat olfactory and respiratory cilia are shown in Figures 4.3.5, 4.3.8, 4.3.9 (and the associated Tables 4.3.2, 4.3.3, 4.3.4) and are summarised in Table 4.3.5. The cytoskeletal protein β-actin was labelled in both olfactory and respiratory cilia preparations and α-tubulin is also predicted to be present in both according to the shared protein profiles. The enzymes creatine kinase and enolase Iα were labelled in both, although the labelling of creatine kinase in rat olfactory cilia was only detected following treatment with 24nmol/mg tissue I-LC-biotin. Indeed, three of the seven proteins identified in olfactory cilia following treatment with increased levels of I-LC-biotin were also labelled in respiratory cilia at the lower level of reagent used (45kDa secretory protein, creatine kinase and GST). This suggested the differential labelling of cilia proteins with I-LC-biotin may be the result of restricted diffusion through the olfactory cilia membrane and thus limited access to the cytosolic proteins within. However the alternative idea that these proteins may have isoforms in the olfactory

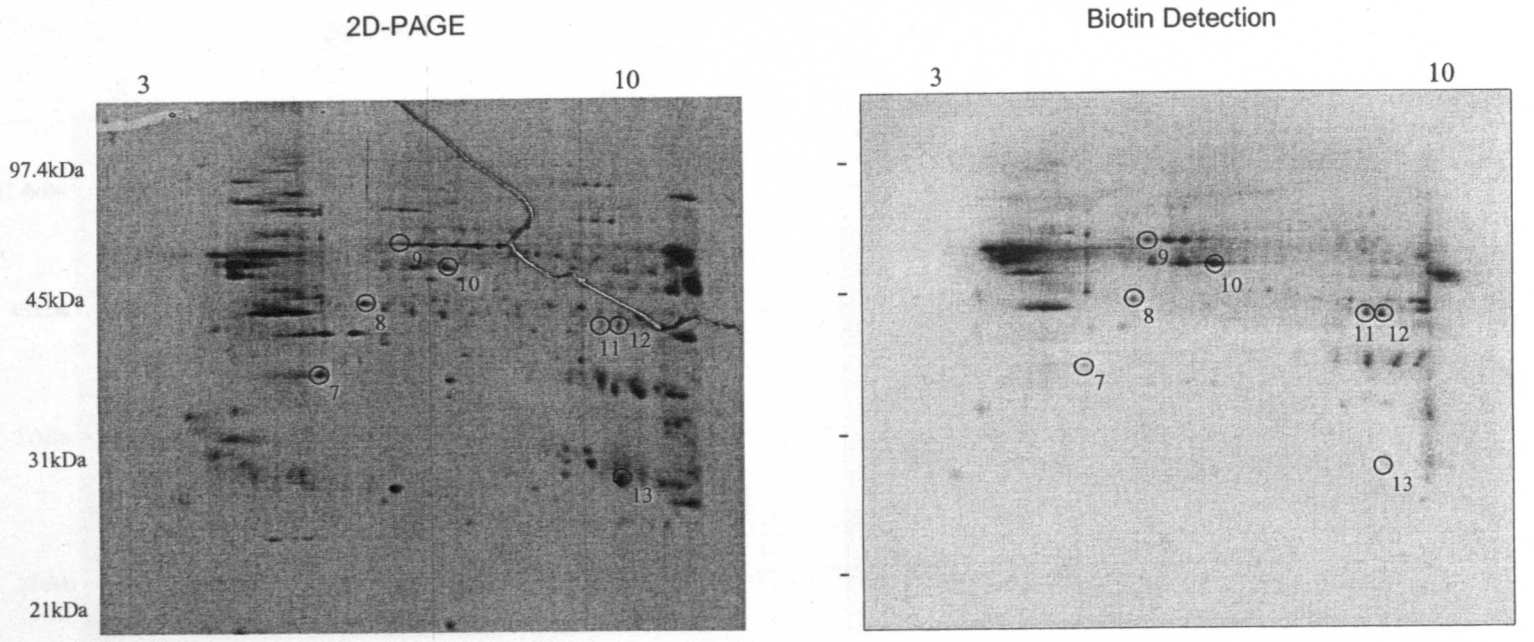

Protein Spot	Putative Identification	NCBI Accession #	Mw (kDa)	Species	Mowse score
7	Visinin-like 1 protein	6755983	22.3	Mus musculus	56/53
8	Secretory protein, 45kD	34878986	100.2	Rattus norveigus	63/57
9	Thiosulphate sulphurtransferase	135826	33.2	Rattus norvegicus	93/57
10	Aldehyde dehydrogenase, mitochondrial	3121992	48.2	Rattus norvegicus	141/57
11	Citrate synthase	18543177	51.8	Rattus norvegicus	88/57
12	Creatine kinase	34856772	42.7	Rattus norvegicus	59/57
13	Glutathione-S-transferase Yb2	28933457	25.7	Rattus norvegicus	79/57

Figure 4.3.8/Table 4.3.3 Additional proteins in the rat olfactory cilia demonstrated to have exposed cysteine residues upon treatment with 24nmol I-LC-biotin/mg tissue

Proteins labelled with I-LC-biotin were identified using data obtained during the characterisation of the rat olfactory cilia proteome in Chapter 3. Shaded protein identifications are likely to be of mitochondrial origin and are therefore regarded as contaminants.

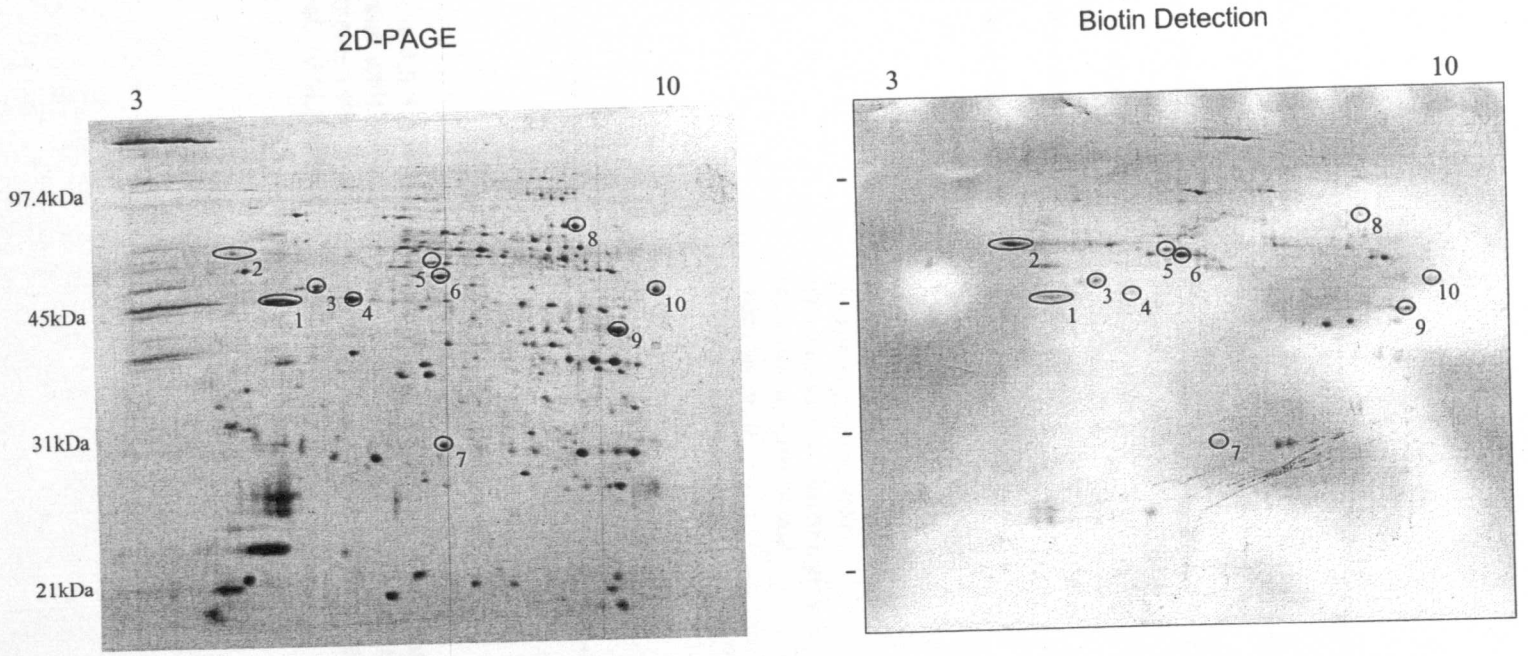

Protein Spot	Putative Identification	NCBI Accession #	Mw (kDa)	Species	Mowse score
1	Beta-actin/ cytoskeletal gamma actin	71620/ 4501887	42.1/ 42.1	Rattus norvegicus, Homo sapiens	78/54 (both)
2	H+-transporting ATP synthase F1-beta chain (mitochondrial)	92350	50.7	Rattus norvegicus	74/54
3	Creatine kinase, brain isoform	6978659	43	Rattus norvegicus	69/53
4	45kDa secretory protein	4164418	46.5	Rattus norvegicus	130/53
5	2-3-cyclic nucleotide phosphodiesterase	116560	46	Rattus norvegicus	54/53
5	Interleukin-18	3063923	18.7	Rattus norvegicus	66/54
6	Enolase I, alpha	6978809	47.4	Rattus norvegicus	74/53
7	Glutathione-S-transferase M5	4099365	27.1	Rattus norvegicus	130/53
8	Clathrin, heavy polypeptide	9506497	193.2	Rattus norvegicus	56/53
9	Synaptonemal complex protein-1 (fragment)	3041729	117	Rattus norvegicus	61/54
10	Eukaryotic translation elongation factor 1 alpha 2/ Elongation factor 1 alpha 1	15805031/ 119146	50.5/ 50.4	Rattus norvegicus	68/53

Figure 4.3.9/Table 4.3.4 Rat respiratory cilia proteins identified as bearing exposed cysteine residues
Proteins labelled with I-LC-biotin were identified by comparing the biotin detection blot shown above, to data obtained during the characterisation of the rat respiratory cilia proteome in Chapter 3. Shaded protein identifications are likely to be of mitochondrial origin and are therefore regarded as contaminants.

Sheep olfactory cilia	Rat olfactory cilia	Rat respiratory cilia
Putative beta-actin	Beta-actin/gamma actin	Beta-actin/cytoskeletal gamma actin
Serum albumin precursor	P38 Mitogen activated protein kinase	H^+ transporting ATP synthase F1-beta chain
Glucose regulated protein 58kDa	Keratin-10	Creatine kinase, brain isoform
Aldehyde dehydrogenase 1A1	Alpha-tubulin	45kDa secretory protein
Aldehyde dehydrogenase 1A1	Aldehyde dehydrogenase	2,3-cyclic nucleotide phosphodiesterase
	Enolase I, alpha	Interleukin-18
		Enolase I, alpha
	Visinin-like 1 protein	
	Secretory protein, 45kD	Glutathione-S-transferase M5
	Thiosulphate sulphurtransferase	Clathrin, heavy polypeptide
	Aldehyde dehydrogenase, mitochondrial	Synaptonemal complex protein-1
	Citrate synthase	Eukaryotic translation elongation factor 1 alpha 2/Elongation factor 1 alpha 1
	Creatine kinase	
	Glutathione-S-transferase Yb2	

Table 4.3.5 Summary of olfactory/respiratory cilia proteins derivatised during treatment of tissue with the sulphydryl-targeting reagent I-LC-biotin
Proteins listed in italics were the olfactory cilia proteins labelled following exposure to increased levels of I-LC-biotin.

cilia with lesser reactivity cannot be discounted. One final note is that whereas the subtypes of aldehyde dehydrogenase present in olfactory cilia of both rat and sheep were labelled by I-LC-biotin, aldehyde dehydrogenase-3 in rat respiratory cilia was not clearly identified as being biotinylated. This suggested the presence of distinct isoforms in olfactory *versus* respiratory cilia bearing differentially exposed/reactive cysteine residues and potentially serving alternative functions.

4.3.3 I-LC-biotin derivatisation of cilia proteins: SDS-PAGE analysis

One crucial problem with the 2D-PAGE analysis of the cilia proteomes is that proteins with poor solubility, including integral cilia membrane proteins, are underrepresented. Therefore analysis of the I-LC-biotin derivatisation of cilia proteins was also performed using the stronger solubilising conditions of SDS-PAGE.

Three major bands of exposed cysteine-containing proteins dominate the 1D labelling profile of mouse, rat and sheep olfactory cilia preparations Bands of approximate mass 40, 55 and 70kDa were labelled strongly in all three model species (Figure 4.3.10). Of these, the 70kDa band is likely to correspond to endogeneous biotin-containing proteins such as pyruvate carboxylase. This is clearly indicated by the SDS-PAGE gels/blots shown in Figure 4.3.11, which demonstrate that this band is amongst a group of high molecular weight proteins visualised during the biotin detection of untreated tissue preparations. The band at 40kDa in rat olfactory cilia preparations was identified as β-actin/gamma actin by peptide mass fingerprinting (Figure 4.3.12).

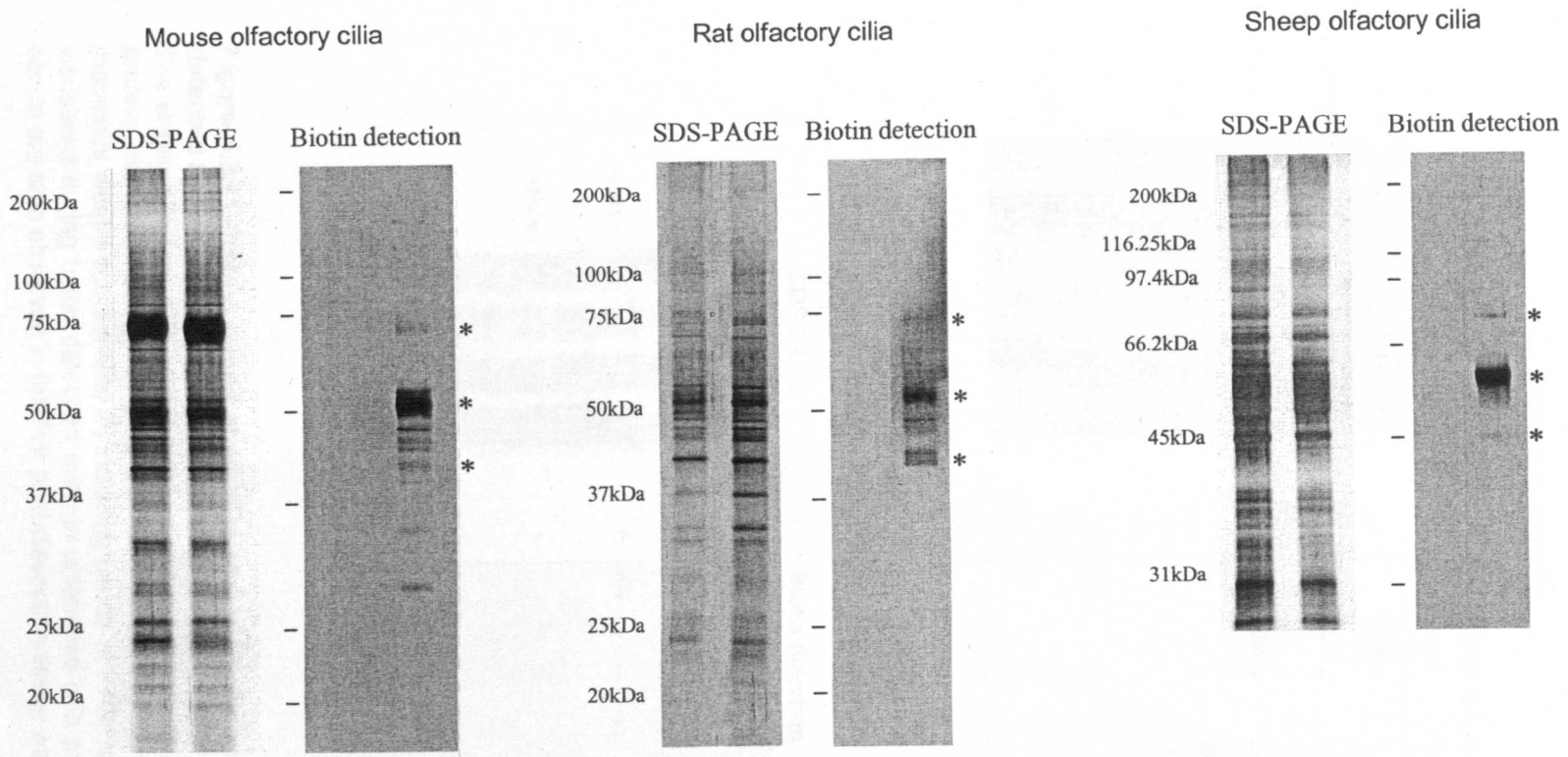

Figure 4.3.10 SDS-PAGE analysis of the I-LC-biotin labelling profiles of mouse, rat and sheep olfactory cilia reveals three major bands conserved across all species

Cilia preparations were resolved by SDS-PAGE and blotted onto nitrocellulose to allow the detection of biotinylated proteins using a streptavidin-alkaline phosphatase conjugate. SDS-PAGE separation of mouse and rat cilia preparations was performed using large format gels, where as the sheep cilia preparation was resolved using mini-gels hence the differing sizes of the gels/blots shown. *denotes the position of the three bands which appear to be biotinylated in all the model species.

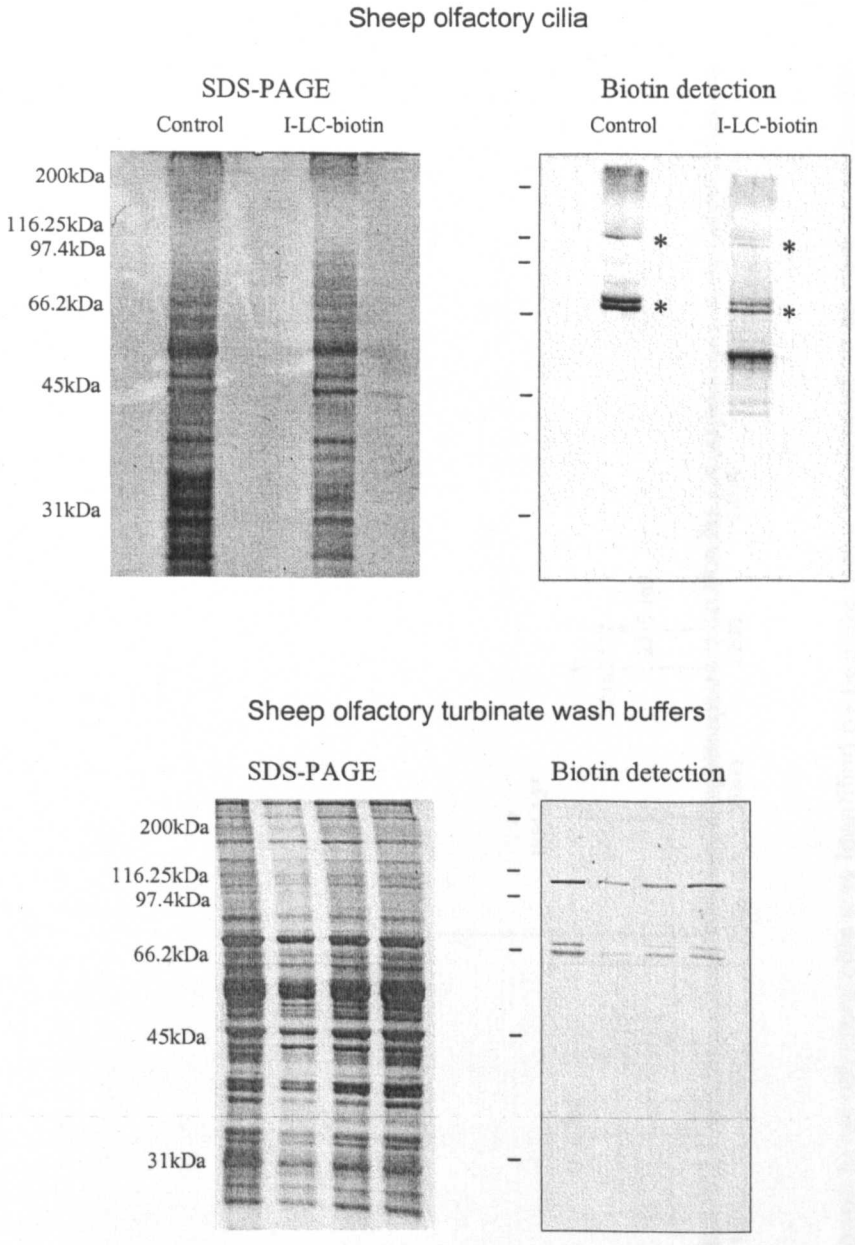

Figure 4.3.11 Protein bands at ~70kDa and ~100kDa are non-specifically detected by the streptavidin-alkaline conjugate

The sheep olfactory cilia preparations shown are insoluble fractions from cilia protein treatment using 1% (v/v) Triton X-100. They contain multiple high molecular weight components (*) including bands at ~70kDa and ~100kDa are visualised during biotin detection even in unlabelled cilia preparations. These bands are also observed in the four post-dissection tissue wash buffers shown.

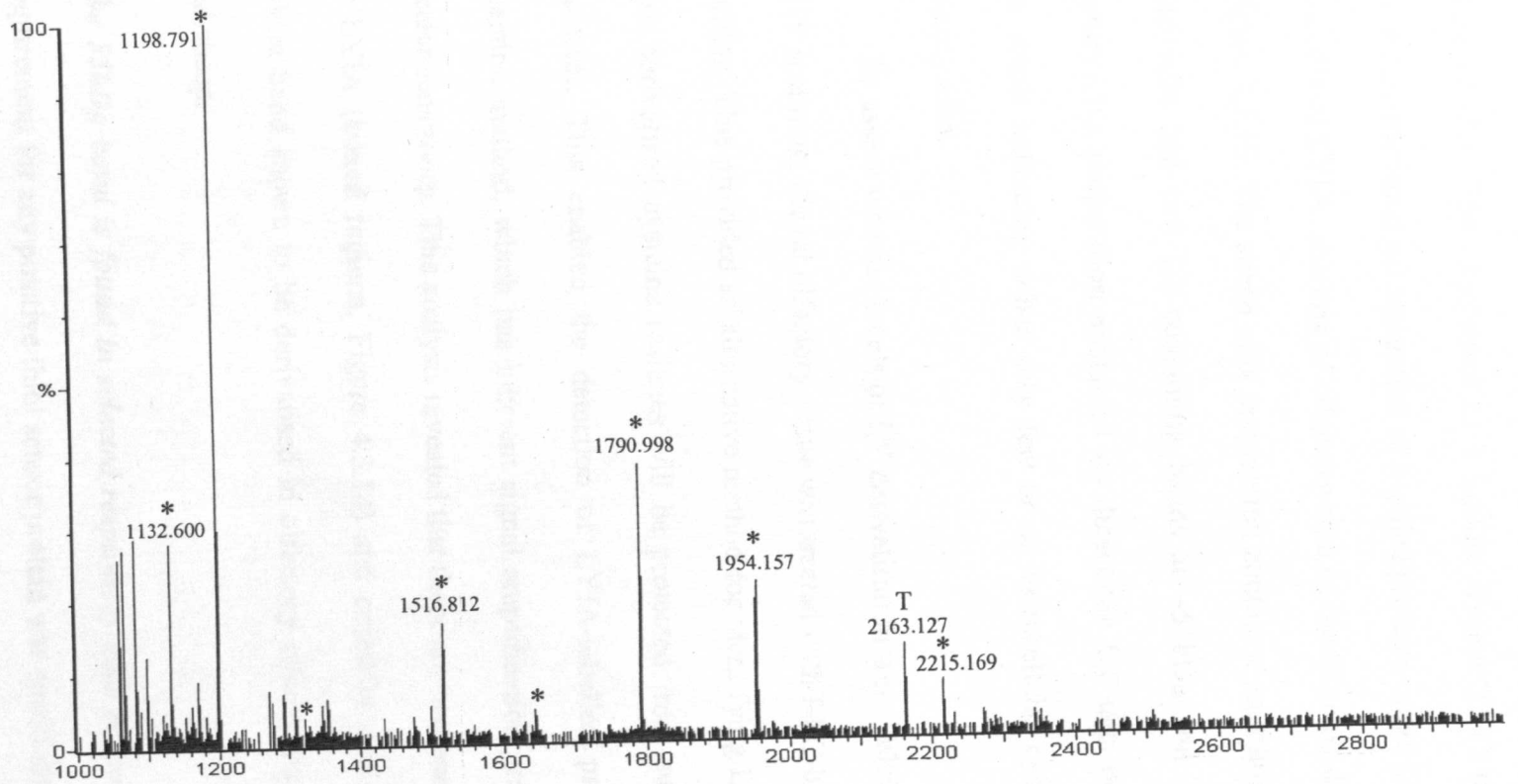

Figure 4.3.12 The abundant 40kDa band in rat olfactory cilia was identified by peptide mass fingerprinting as beta/gamma actin

The peaks from the above MALDI-ToF mass spectrum were used to derive a peptide mass fingerprint for the 40kDa protein band in rat olfactory cilia. The peptide masses were then searched against an on-line database (see Section 2.12) and the protein identified as beta/gamma actin with a MOWSE significance score of 104/57. The peptides marked by * are derived from beta/gamma actin. "T" denotes Ions corresponding to trypsin autolysis products.

The 55kDa band contains protein(s) with an exposed, extracellular cysteine residue The membrane-impermeable sulphydryl-targetting reagent Lucifer Yellow Iodoacetamide (LYIA) was used to label proteins bearing an exposed extracellular cysteine residue. The attachment of a Lucifer Yellow (LY) tag was detected by scanning an unstained gel separation of labelled proteins under UV light.

The results of LYIA labelling of olfactory cilia of the three model species are shown in Figure 4.3.13. The sheep cilia preparation contained multiple labelled bands, the mouse cilia had two LY-containing bands at ~55kDa and ~40kDa and the rat olfactory cilia preparation contained no detectable LY tags on any proteins. This latter result indicating either very few or no extracellular cysteine residues in rat olfactory cilia.

To assess whether levels of LY derivatisation were below the detection levels of UV scanning, the rat olfactory tissue was treated with I-LC-biotin following LYIA labelling. This provided an alternative method for identifying LY-tagged proteins, as these derivatised cysteine residues will be protected from subsequent I-LC-biotin treatment. This enabled the detection of LYIA-labelled proteins by the biotin detection method, which has inherent signal amplification properties and therefore greater sensitivity. This analysis revealed that there are two bands that are derivatised by LYIA (boxed regions, Figure 4.3.14) and crucially one of these bands is the 55kDa band shown to be derivatised in olfactory cilia preparations of both mouse and sheep.

The 55kDa band is found in selected respiratory cilia preparations An additional requirement for any putative thiol sensor protein was specificity to the olfactory cilia. To test the localisation of the biotinylated 55kDa protein band two types of respiratory cilia preparations were made. The first contained the cilia derived from

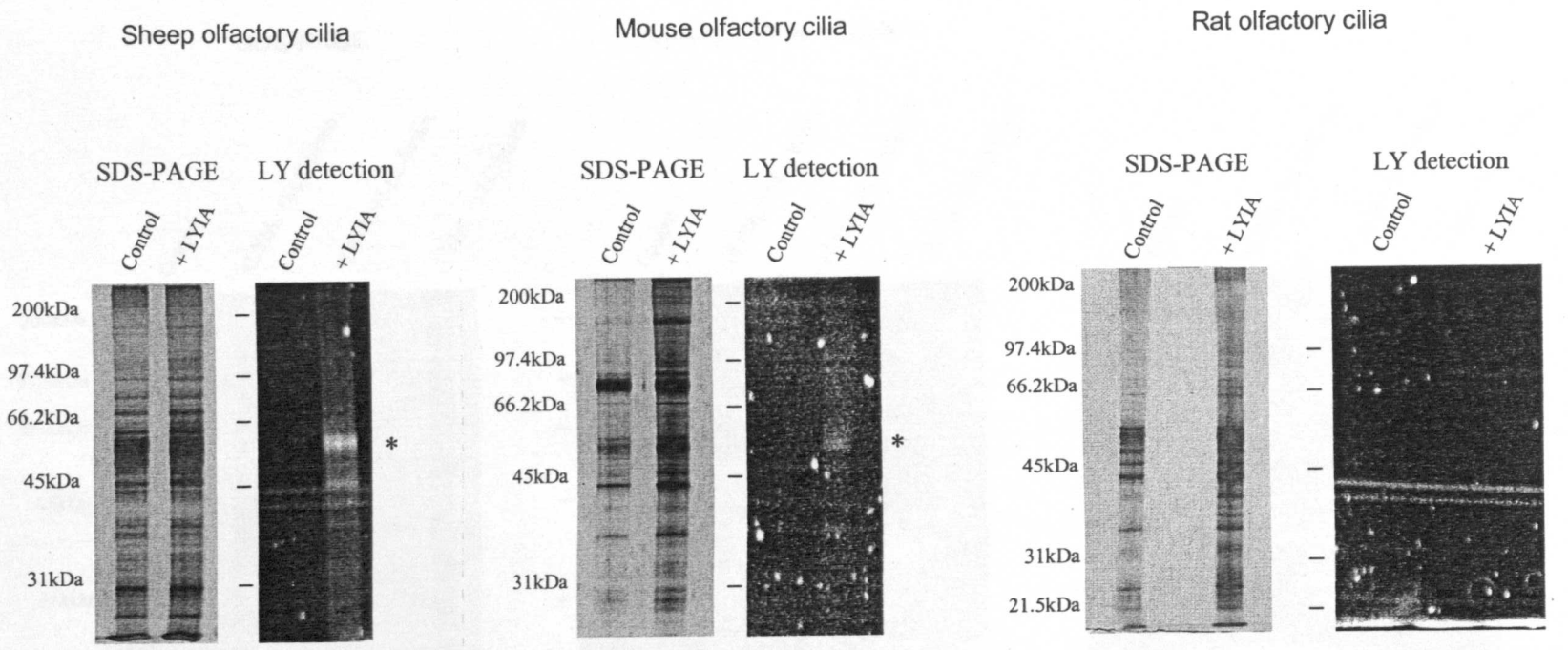

Figure 4.3.13 LYIA labelling of olfactory cilia preparations from the sheep, mouse and rat
Lucifer Yellow (LY) groups attached to proteins were detected by scanning the SDS-PAGE gel in UV light. * denotes the position of the 55kDa band, derivatised by LYIA in both the sheep and mouse olfactory cilia preparations.

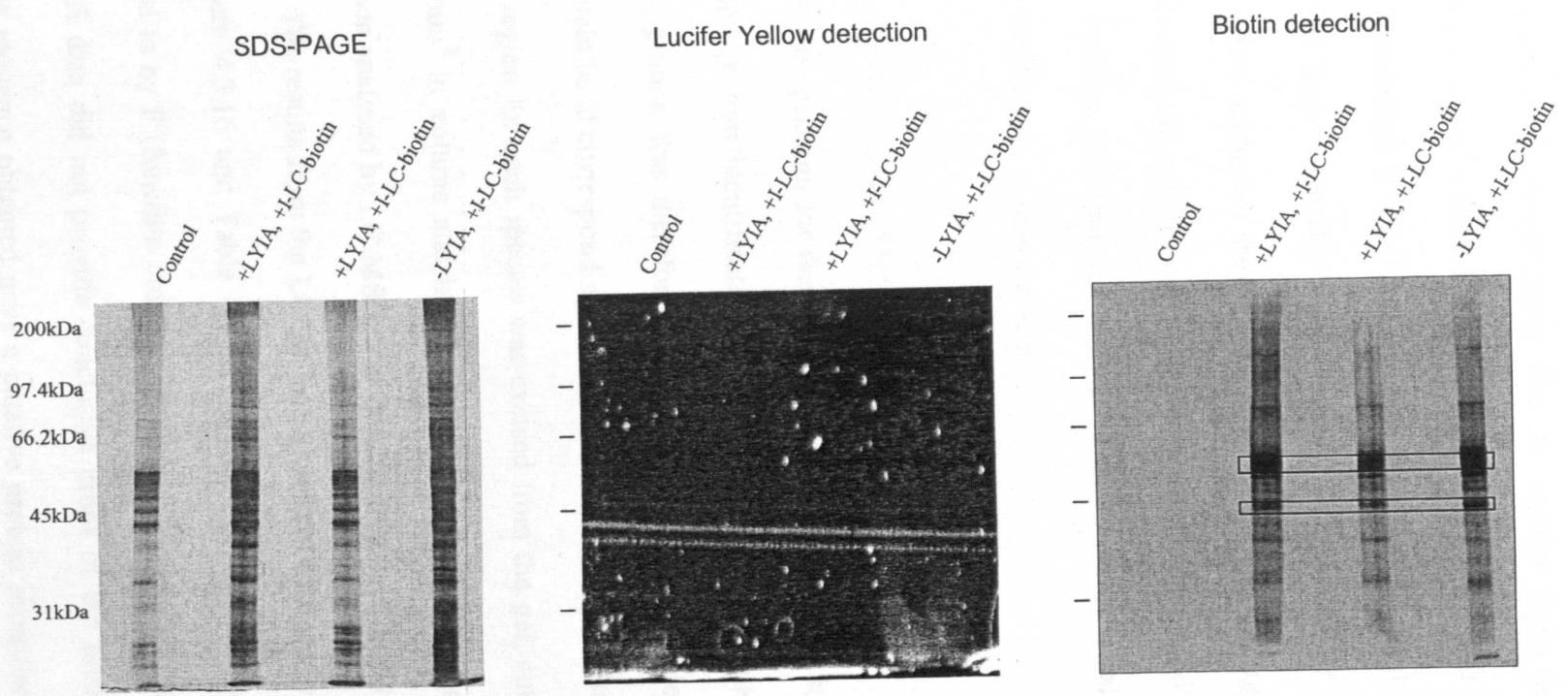

Figure 4.3.14 Detection of LYIA derivatisation by protection from subsequent I-LC-biotin treatment
The replica gel was scanned in UV light prior to protein visualisation by silver nitrate staining. The biotin detection blot onto which the cilia proteins were transferred are consistent with the protection of proteins in the 55kDa and 45kDa regions from I-LC-biotin derivatisation by previous treatment with LYIA.

the entire epithelial lining of the septum. The second respiratory cilia fraction was prepared from only the rostral half of the septal lining, a region containing a much lower proportion of sensory tissue than the septum lining as a whole (Farbman, 1992). This analysis indicated that the heavily-labelled band within the 50-55kDa region is biotinylated in olfactory cilia prepared from the nasal turbinates, respiratory cilia derived from the whole septum but not in the enriched cilia fraction isolated from the rostral section of the septum (Figure 4.3.15). This suggests that the proteins within this band not only have the conservation across the model species and external cysteine residues required for a putative thiol sensor candidate, but also show apparent localisation to sensory cilia.

4.3.4 Identification of the 55kDa band

The MALDI spectrum for the 55kDa band did not provide sufficient peptides for a significant protein identification to be made by peptide mass fingerprinting. The tryptic digestion was therefore analysed further using tandem mass spectrometry. The protein band corresponding to the most strongly biotinylated band within the 50-55kDa region for each species was excised from the gel, cut into pieces no greater than $1mm^3$ in volume and in-gel tryptic digestions performed. Tryptic digestions were then analysed by LC-MS/MS as described in Section 2.14/2.15.

The results from the LC-MS/MS analysis of the sheep 55kDa band are shown in Figure 4.3.16 and Table 4.3.6. Individual peptide sequences are subsequently referred to by F (function number)_(precursor ion mass to the nearest integer). The MS/MS data did not provide conclusive proof of the identity of this band as no peptide sequence obtained gave a putative protein identification where $E<0.05$, the threshold of significance used in this study. However, out of the 23 sequences

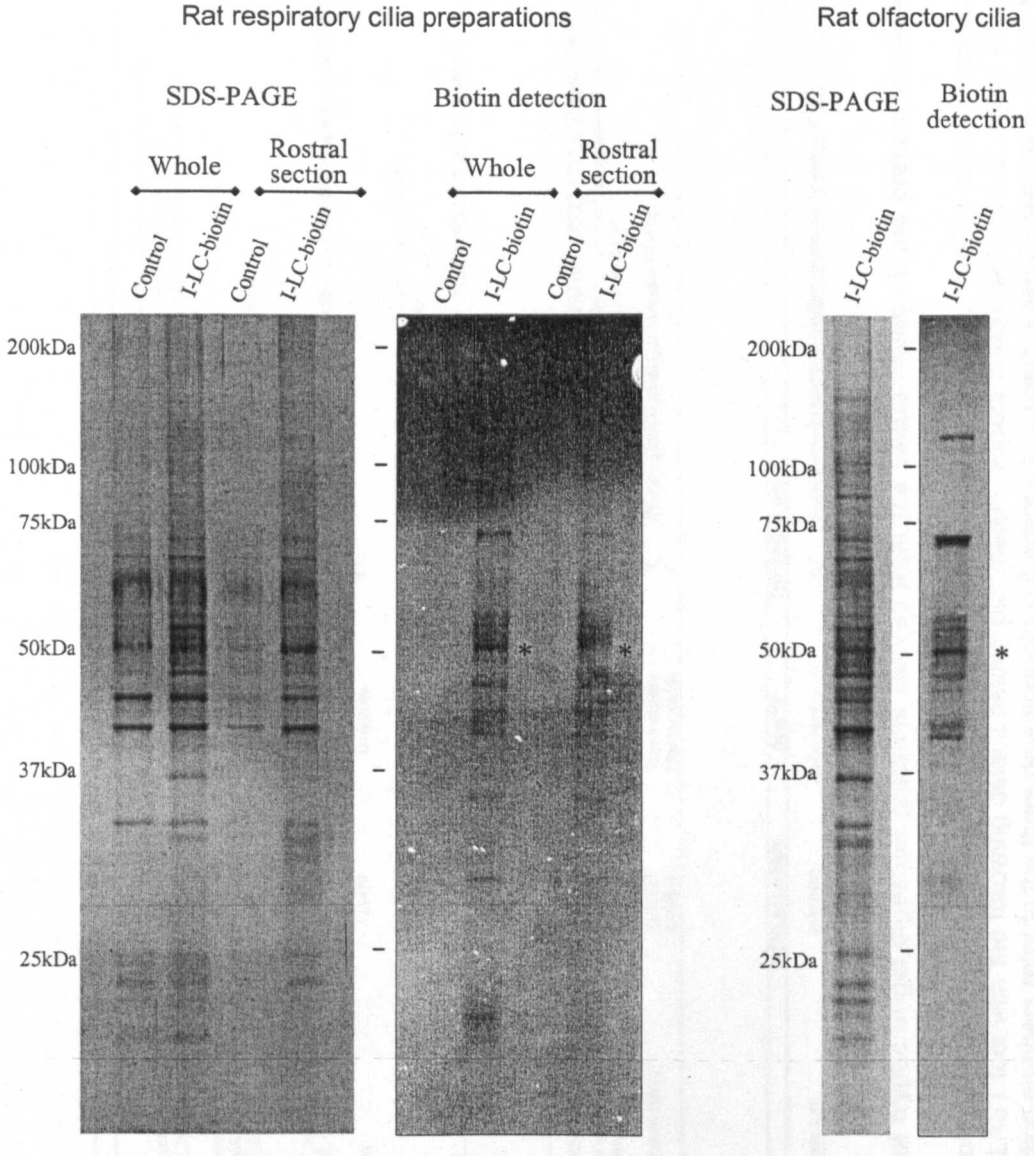

Figure 4.3.15 Substantial I-LC-biotin labelling of specific bands within the 55kDa region occurs only in cilia derived from a tissue containing a significant proportion of olfactory epithelium

The dissected regions of the septal epithelium were treated identically with 30µl I-LC-biotin. Enriched cilia fractions were then prepared and separated by large format SDS-PAGE. The proteins were then blotted onto a nitrocellulose membrane to allow the detection of the biotin tag. "Whole" cilia preparations were derived from the epithelium lining the entire septum. "Rostral section" cilia were prepared from the epithelial lining of the most rostral half of the septum. *denotes the 55kDa band apparently specific to olfactory regions of the nasal cavity.

Function 2

BLAST Identifications

Precursor ion	Sequence	Top hit	NCBI accession #	Species	Top score	Notes
1494.3964	SGK					
811.5299	HVYTK	Alpha-2-macroglobulin	2144118	Mus musculus	701	Multiple hits to alpha macroglobulin and hit to vomernasal 1 receptor 110 (E=5492)
1263.5294	VLEWGSSLDR	Similar to hypothetical protein	27481518	Mus musculus/Homo sapiens	15	Two hits for similar to olfactory receptor proteins (E=388)
1034.54	ASGMSTAW	Hypothetical protein XP_161747	20826322	Mus musculus	247	Multiple hits for homocysteine-inducible stress proteins (E=1448)
1021.5382	LLSDSSCK	Trypsin				
1133.4871	MPTTTTVR	Similar to hypothetical protein	27697304	Rattus norvegicus	37	Hit for GPCR 50 (E=216)
1382.4678	(NN)SQSNYELWK	Similar to KIAA0876 protein	20875654	Homo sapiens	15	
1343.5822	(V)QVDEVQQ(SF)	Hypothetical protein XP_243402	27717781	Rattus norvegicus	11	Multiple hits for alpha mannosidase
1154.5504	CETSYPDVLK	Trypsin				
1036.5461	YQC					
1530.5138	EYCVLVNVSVPK	Hypothetical protein XP_239883	27692574	Rattus norvegicus	136	
954.6752	NLMQALHK	RIKEN cDNA 6030465J18	20901702	Mus musculus	67	Multiple hits for taste receptors (E=522) and A kinase anchor protein (E=522)
2164.2832		Trypsin				
1280.5931	ANVSTVLTSK	Haemoglobin alpha chain	122410	Ovis aries	0.19	
1434.5646	-	Trypsin				
1072.5782	MFLSFQGNK	Artemis protein	13872809	Homo sapiens	67	Multiple hits for similar to olfactory receptor (E=389)
1275.5706	(QV)VVYPDVL	Solute carrier family 7	6912670		67	Multiple hits for trypsin (E=701)
1577.51	GLLSGAT	EDG1	12829916	Homo sapiens	941	Hits for EDG1 in 50 different species
1266.8248	NLGNVLVWLVK	Haemoglobin beta chain	122585	White rhinoceros	0.18	Hit for odorant receptor (E=6.3) and olfactory receptor-like protein (E=6.3)

Function 3

BLAST Identifications

Precursor ion	Sequence	Top hit	NCBI accession #	Species	Top score	Notes
1185.5934	TLQLHNNFAK	Nuclear matrix protein SNEV	19527358	Mus musculus	37	Multiple hits for cytochrome P450 2E1 (E=216) and various GPCRs (E=699)
914.5533	LYEVVK	Alpha 3 type VI collagen isoform precursor	17149807	Homo sapiens	701	Hit for G-protein coupled receptor 113 (E=941) and cytochrome P450 (E=941)
1435.542	AQYQEALER	Testicular acid phosphatase isoform	14861860	Homo sapiens	11	Three hits for A kinase anchor protein 9 (E=161)
2164.2612	NEQFLSASK	Trypsin	2507249	Bos taurus	4.7	
1544.4188	NFFEVWEAV	Ubiquitin conjugating enzyme E2G 2	7717436	Homo sapiens	28	Hit for a putative pheromone receptor (E=120)
1176.5109	FCSWMENK	Olfactory receptor 49	6754932	Mus musculus	50	

Function 4

BLAST Identifications

Precursor ion	Sequence	Top hit	NCBI accession #	Species	Top score	Notes
1136.5317	NSNSYPDVLK	Trypsin				
1303.6874	DSNLEWLTVVK	Similar to ribosomal protein L31	20848480	Rattus norvegicus	6.3	Multiple hits for similar to putative pheromone receptors (ES20)

Table 4.3.6 LC-MS/MS analysis of tryptic in-gel digestion products derived from the 55kDa protein band present in sheep olfactory cilia preparations

The peptide sequences gained from LC-MS/MS data analysis were searched against the non-redundant NCBI protein database using the "short, nearly exact sequences" BLAST tool with the following default search parameters: expect 20000, wordsize 2, matrix PAM30 and gap costs existence9 extension1. Function numbers refer to the three data acquisition functions that operate simultaneously to collect MS/MS data on co-eluting peptides.

Figure 4.3.16 Selected MS/MS spectra provide evidence that the 55kDa band present in sheep cilia preparations may contain proteins similar to olfactory receptors

LC-MS/MS spectra are shown with sequence annotation derived from the y ion series. The alignment between the predicted peptide sequence and olfactory receptor-like protein is also provided. "|" between sequence alignments indicates shared residues and "+" denotes substitutions of amino acids with equivalent structural/chemical characteristics. The quoted molecular mass of each ion corresponds to the mass of the precursor ion in its 1+ charge state.

MS/MS spectrum for precursor ion 1263.5294

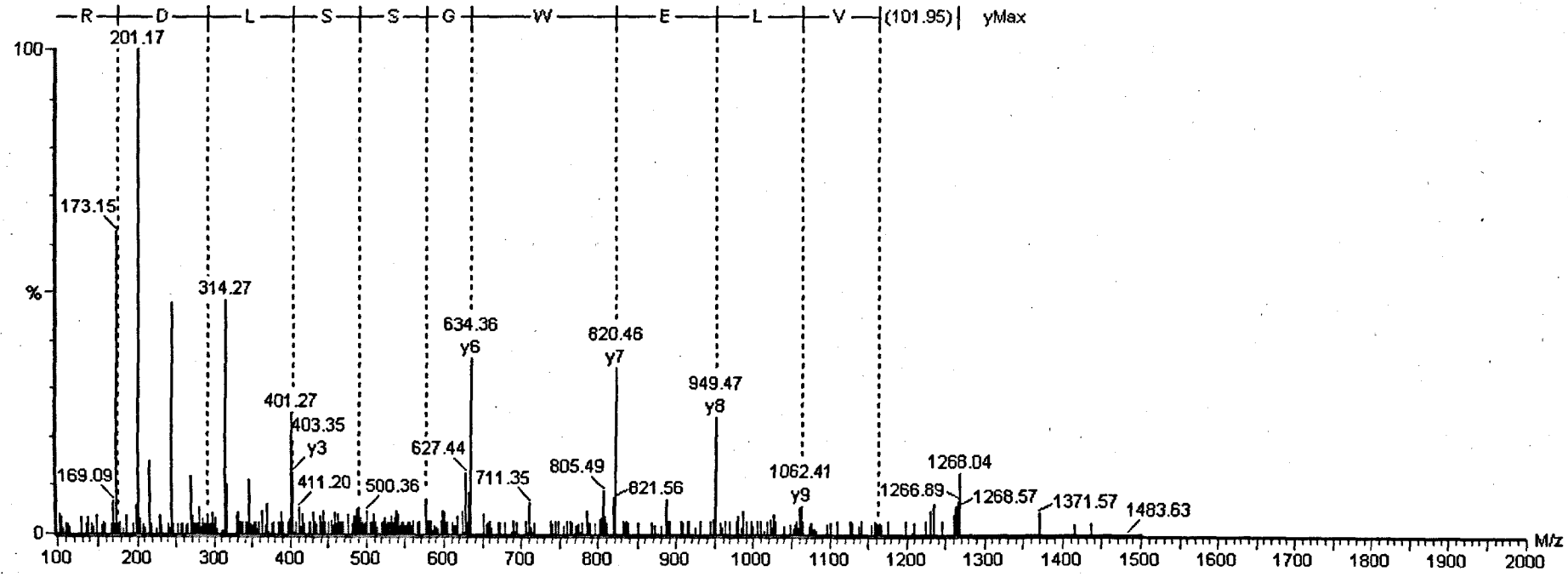

Sequence alignments

```
                                Query:      2   LEWGSSL   8
                                            |||||||
Similar to hypothetical protein MGC37938:  17   LEWGSSL   23

                                Query:      1   VLEWGSSL   8
                                            || ||| |
  Similar to olfactory receptor MOR256-4:  146   VLAWGSGL   153
```

MS/MS spectrum for precursor ion 811.5299

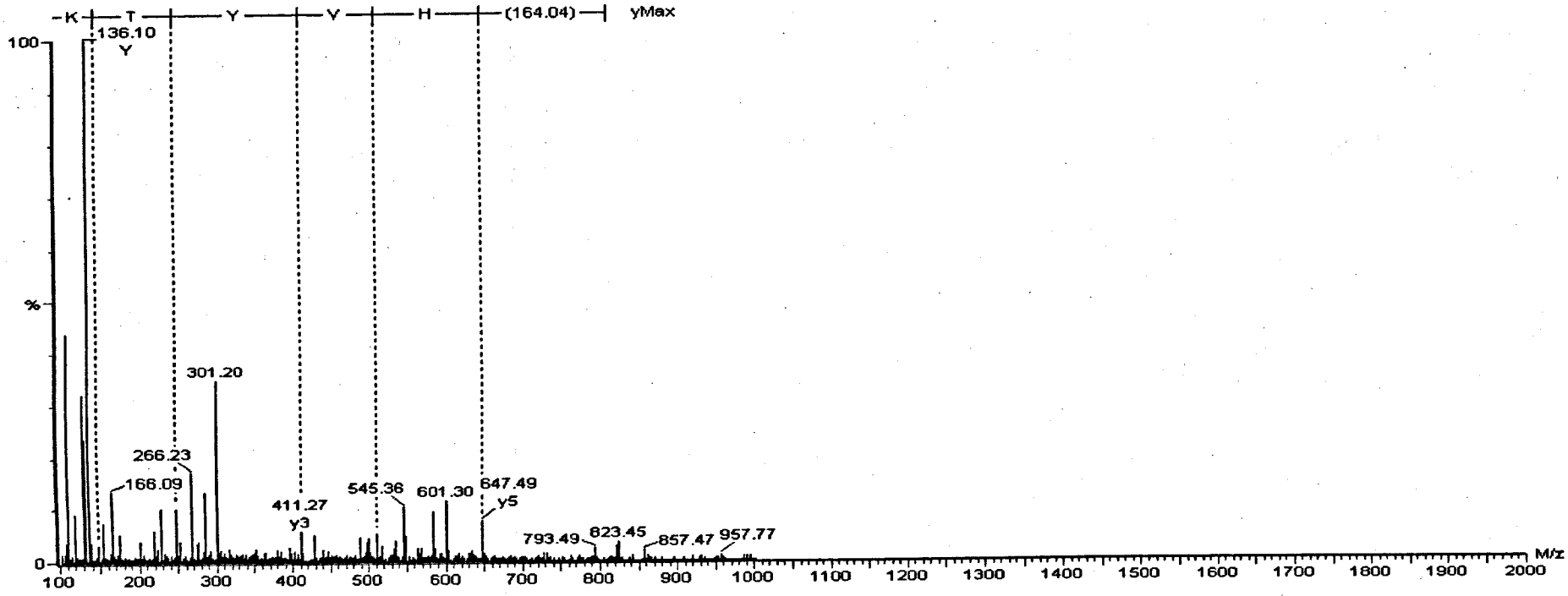

Sequence alignments

```
                                Query:    1  HVYTK  5
                                          |||||
Alpha-macroglobulin precursor: 1145  HVYTK  1149

                                Query:    1  HVYTK  5
                                          |||||
  Vomeronasal 1 receptor, I10:  146  HVYTK  150
```

MS/MS spectrum for precursor ion 1133.487

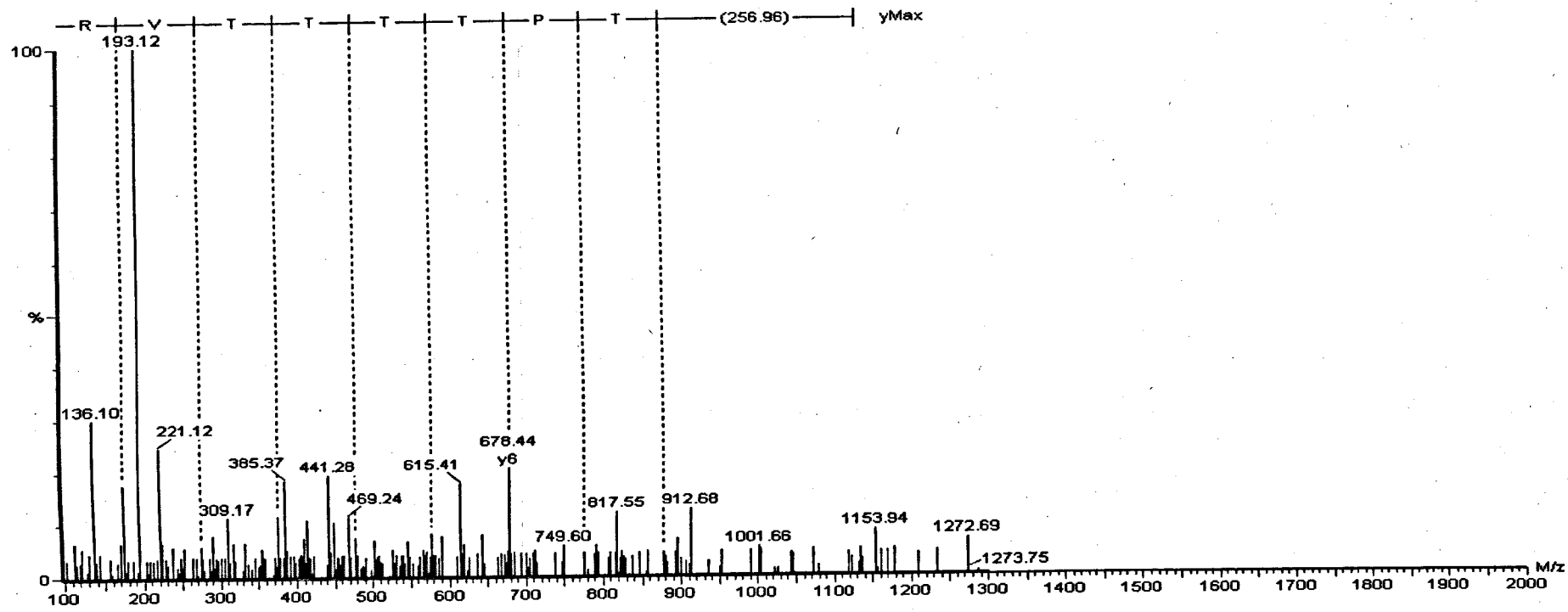

Sequence alignments

```
                Query:      1   HPTTTTVR   6
                                ||||||  |
Similar to hypothetical protein:  190   HPTTTTTR   197

                Query:      1   HPTTTTV   6
                                ||  ||||
  G-protein coupled receptor 50:  496   HPATTTV   502
```

MS/MS spectrum for precursor ion 954.6752.

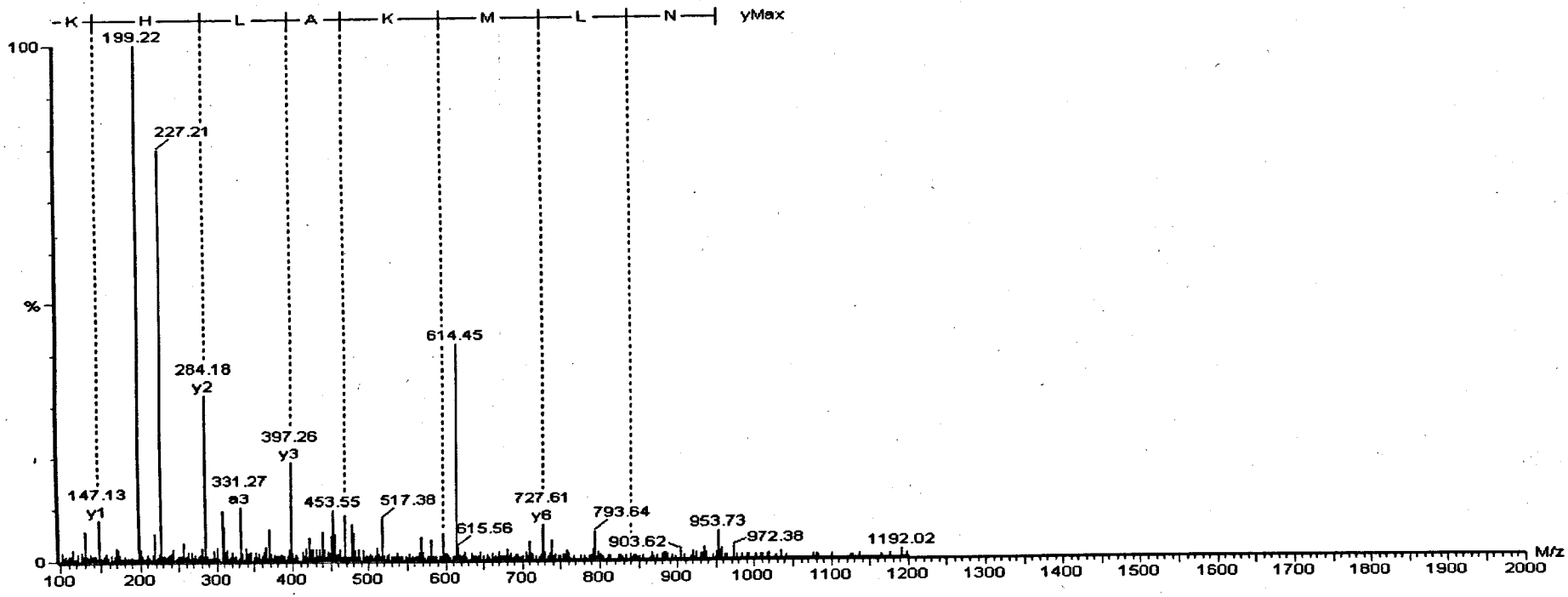

Sequence alignments

```
                    Query:      1   NLMQALHK   8
                                    ||||||  |
Similar to RIKEN cDNA 6030465J18:  196   NLMQALKK   203

                    Query:      1   NLMQALHK   8
                                    |||||
          Taste receptor, type 1:   73   NLMQAMRF   80
```

MS/MS spectrum for precursor ion 1072.5782

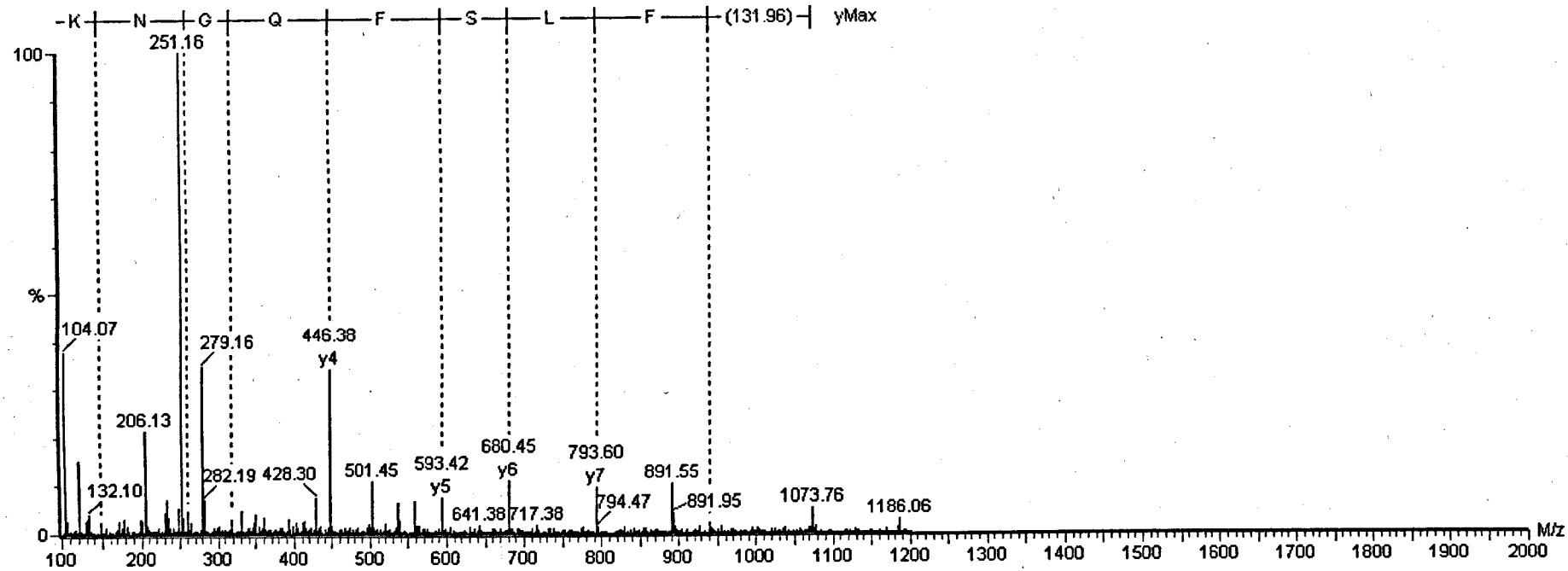

Sequence alignments

```
                    Query:    1   MFLSFQGN   8
                              |||  ||||
Artemis protein:  121   MFL-FQGN   127

                    Query:    1   MFLSF   5
                              |||||
Similar to olfactory receptor MOR212-3:  29   MFLSF   33
```

MS/MS spectrum for precursor ion 1576.5027

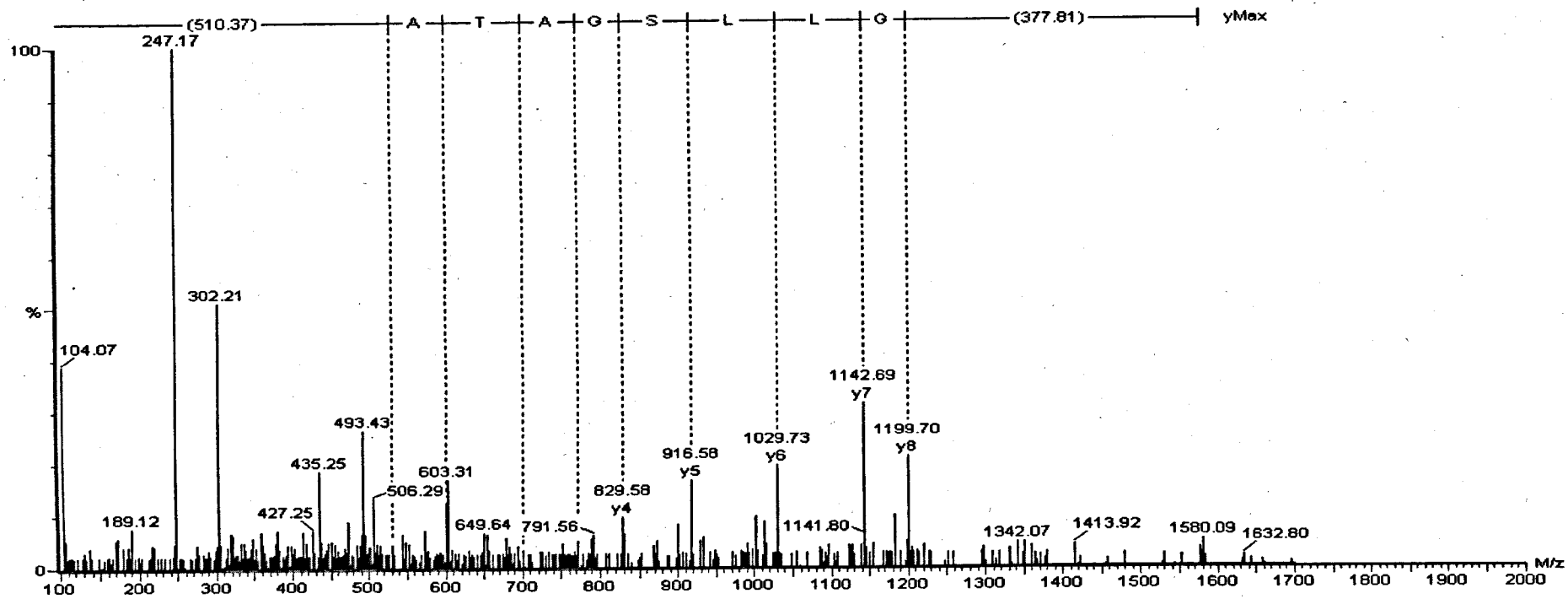

Sequence alignments

```
Query:     2   LLSGAT   7
               ||||||
 EDG1:    63   LLSGAT   68
```

MS/MS spectrum for precursor ion 1266.8248

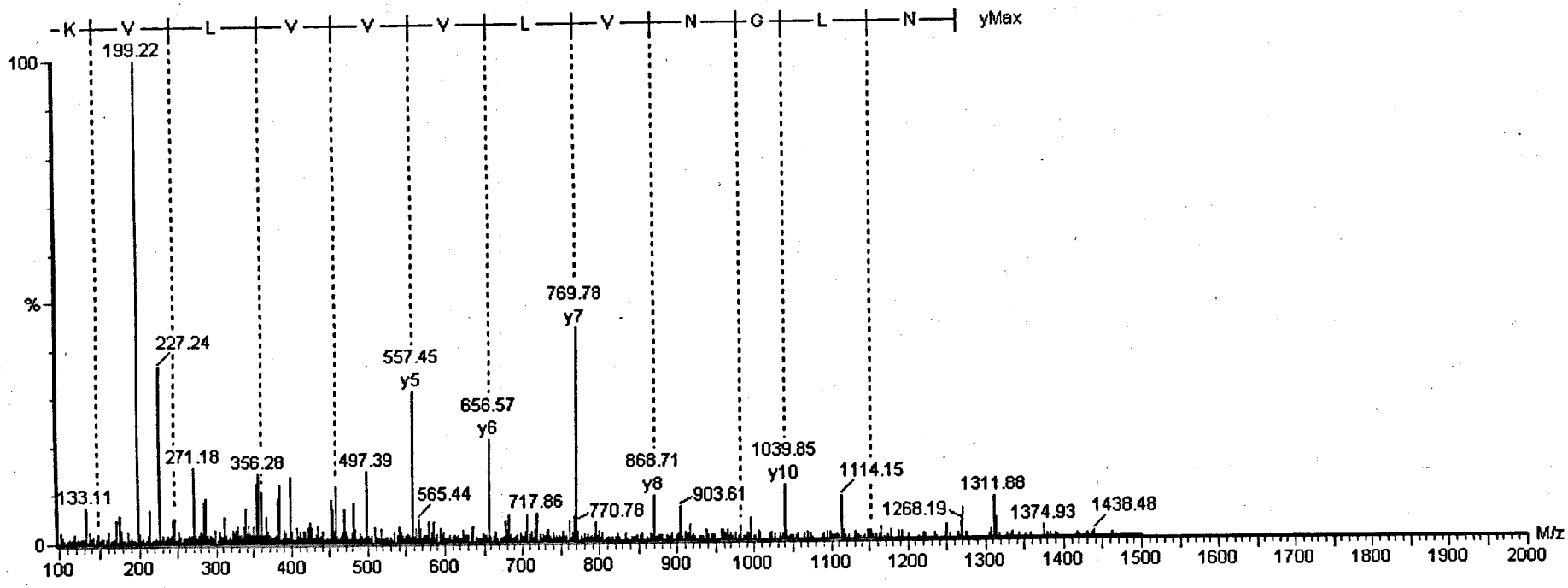

Sequence alignments

```
                                Query:   2   LGNVLVVVLVK   12
                                             |||||||||  |
Haemoglobin beta chain:  106   LGNVLVVVLAK   116

                                Query:   2   LGNVLVVLLVK   12
                                             |||+|+||||
Similar to olfactory receptor MOR212-3:  14   LGNLLIVVLVD   24
```

MS/MS spectrum for precursor ion 1185.5934

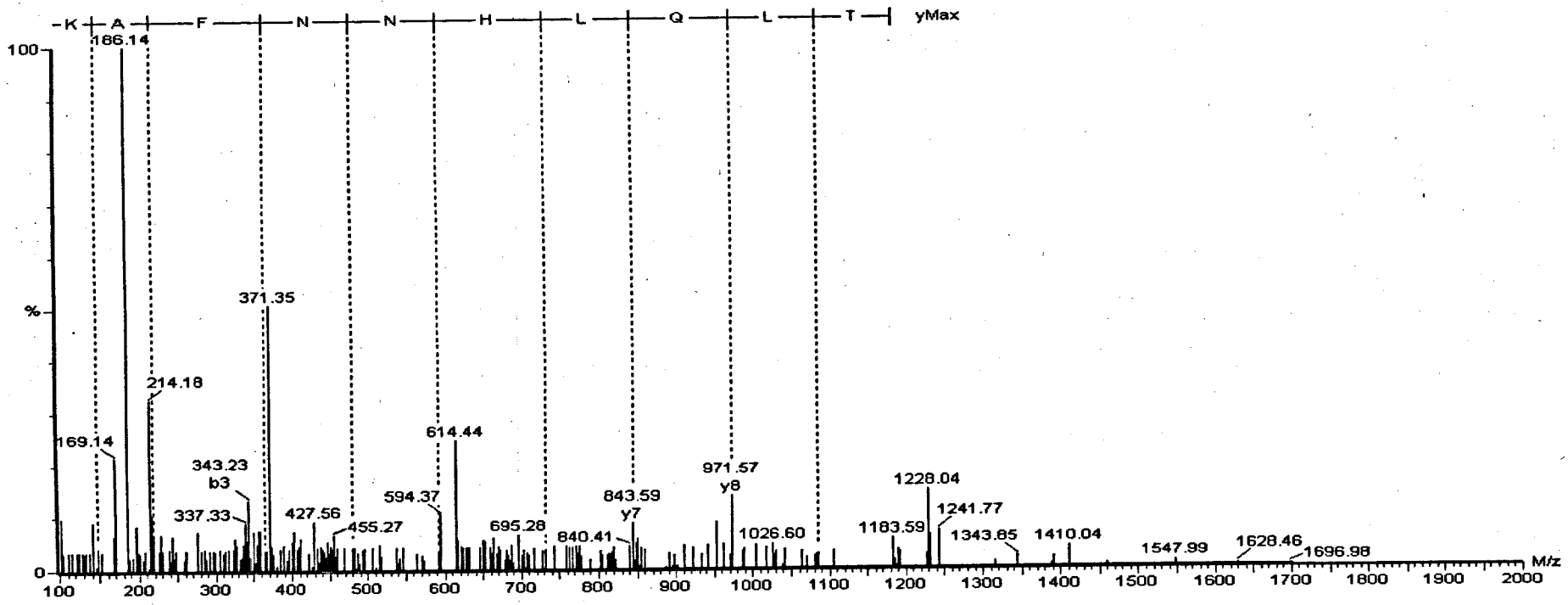

Sequence alignments

```
Query:                          1  TLQLHNNF  8
                                   ||||  |||
Nuclear matrix protein SNEV:  429  TLQLDNNF  436

Query:                          1  TLQLHNNF  8
                                   |  ||||
G protein-coupled receptor 49:  214  VLHLHNNR  221
```

MS/MS spectrum for precursor ion 914.5533

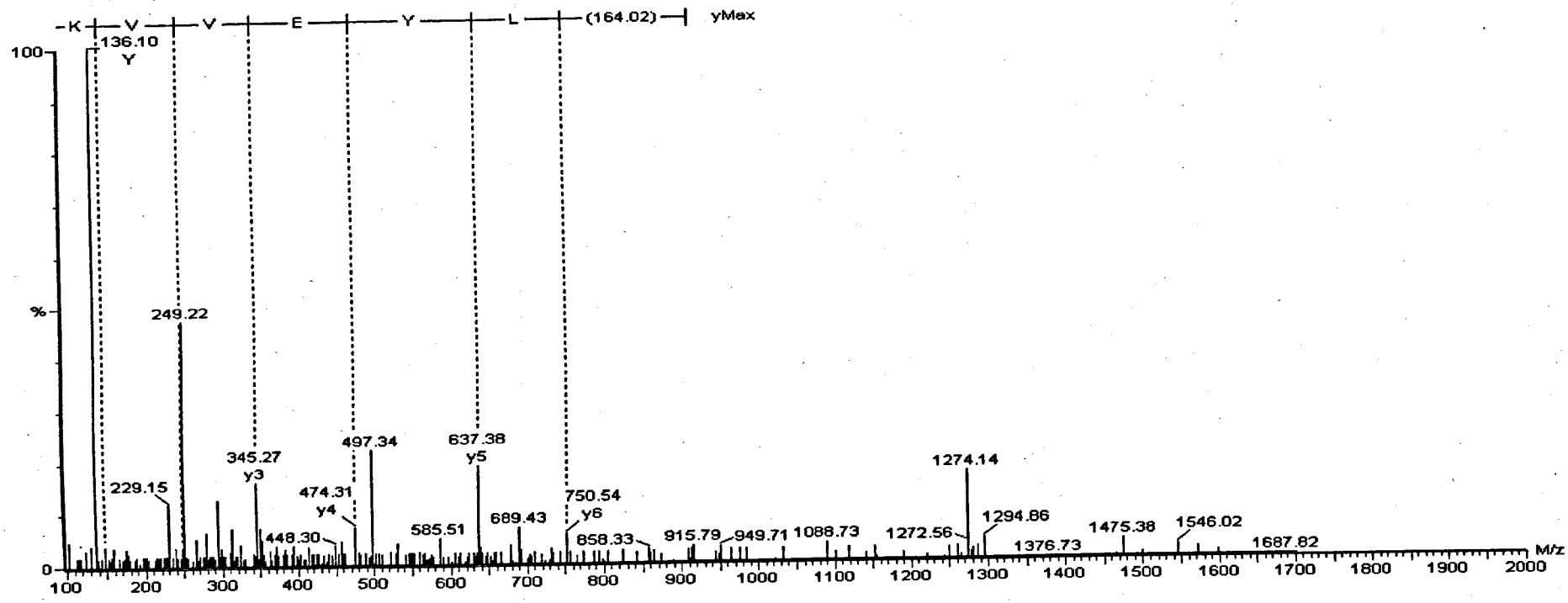

Sequence alignments

```
                    Query:      1  LYEVVK   6
                               ||+|||
Alpha 3 type VI collagen isoform 3 precursor:  62  LYDVVK  67

                    Query:      1  LYEVV    5
                               |||||
G protein-coupled receptor 113: 323  LYEVV   327
```

MS/MS spectrum for precursor ion 1544.4188

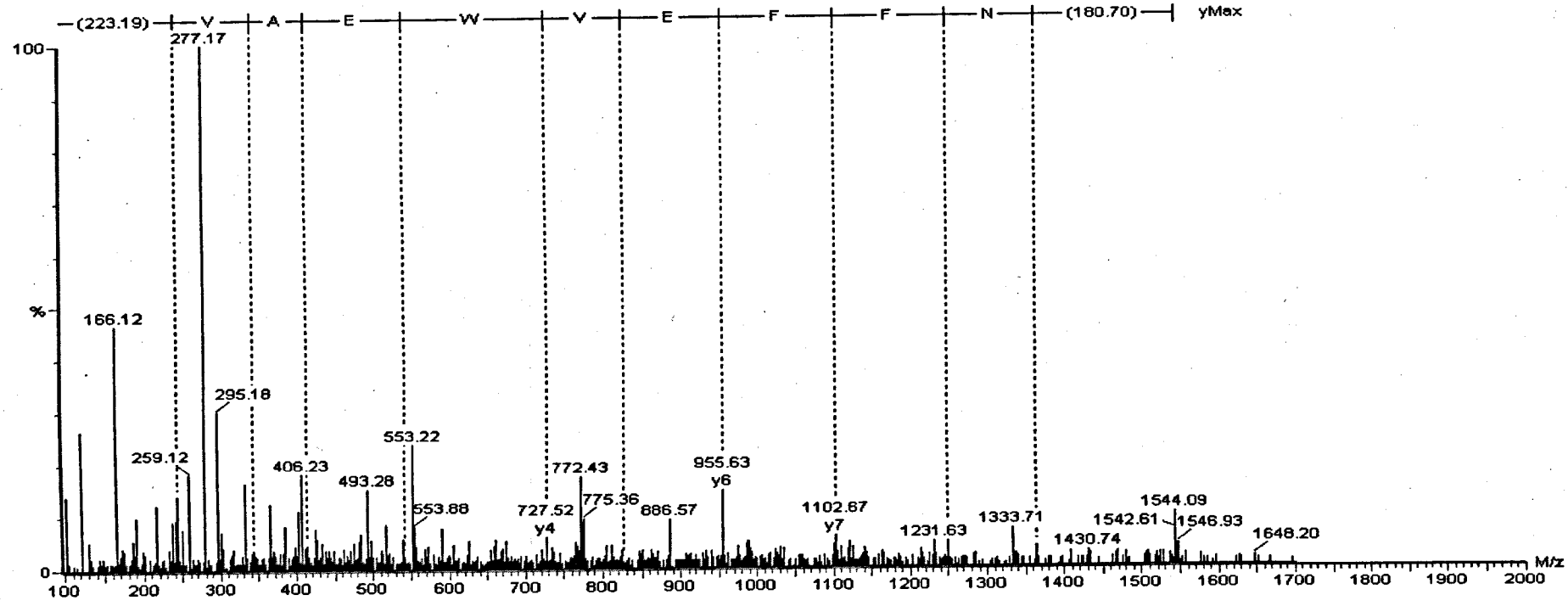

Sequence alignments

```
                                Query:      1   NFFEVWEA   8
                                            ||||  |||
Ubiquitin-conjugating enzyme E2G2:     33   NFFE-WEA   39

                                Query:      1   NFFEVWE
                                            ||||  |+
                Putative pheromone receptor:  251   NFFETWD 323
```

MS/MS spectrum for precursor ion 1176.5109

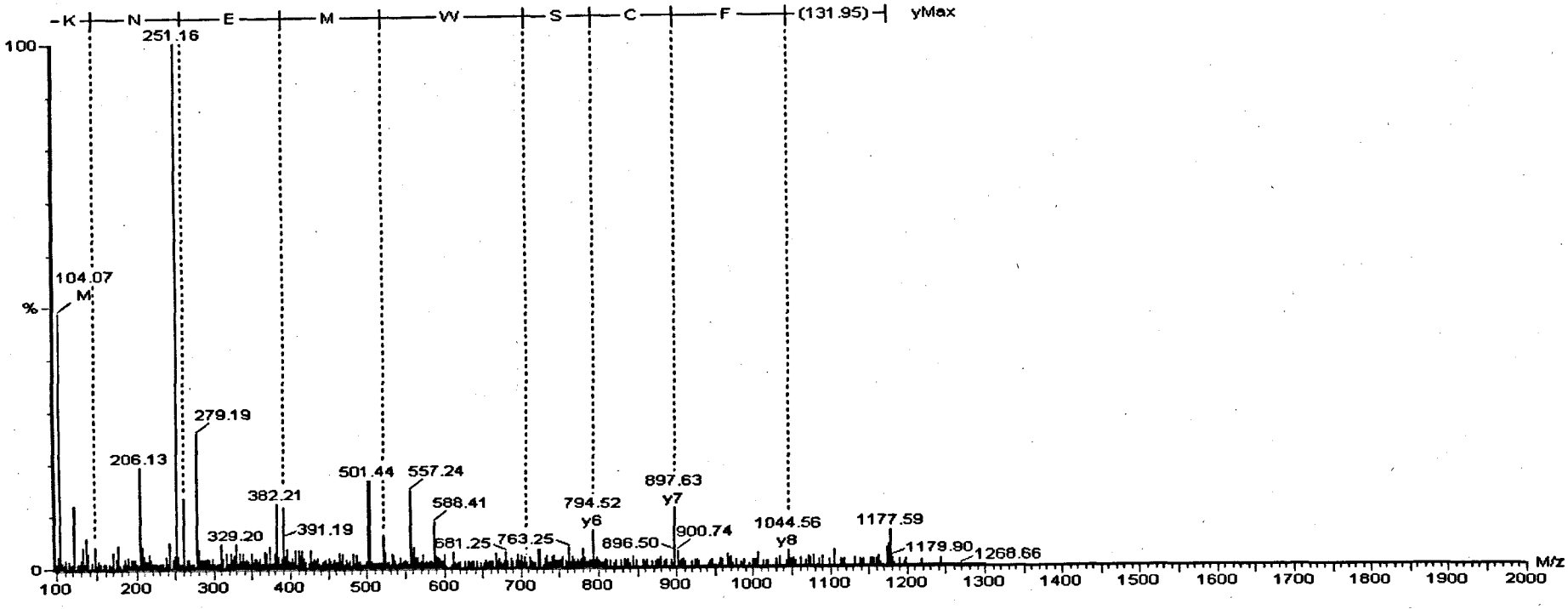

Sequence alignments

```
Query:                      1   FCSWM   5
                                |||||
Olfactory receptor 49:    144   FCSWM   148
```

MS/MS spectrum for precursor ion 1303.6784

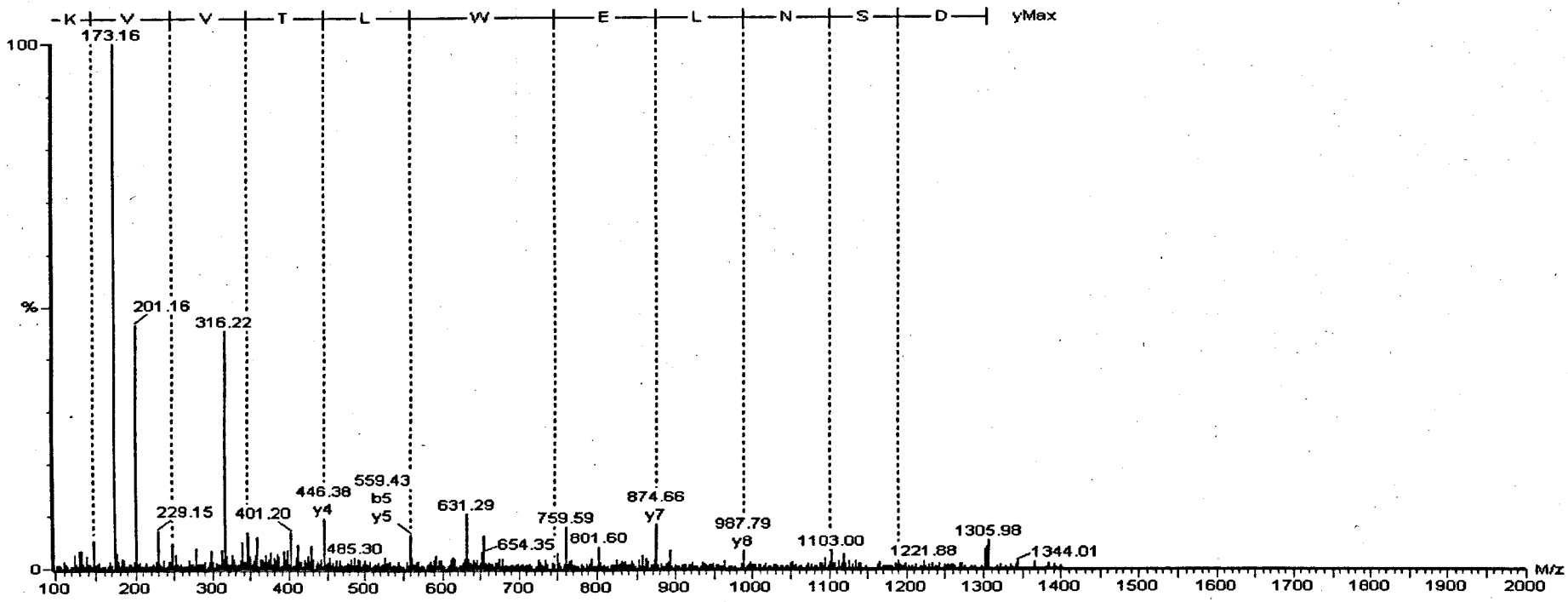

Sequence alignments

```
                    Query:      2   SNLEWLT   8
                                    |||||||
Similar to ribosomal protein L31:      59   SNLEWLT   65

                    Query:      2   SN--LEWLTV   9
                                    ||  ||||||
Similar to putative pheromone receptor:    128   SNHSLEWLTV   137
```

searched against the non-redundant NCBI protein database (www.ncbi.nlm.nih.gov) using the BLAST search tool (Altshul *et al.*, 1997), searches of 12 peptides indicated homology between peptides of the 55kDa protein band in sheep olfactory cilia and seven transmembrane-spanning receptors (F2_811, F2_1263, F2_1133, F2_954, F2_1072, F2_1577, F2_1266, F3_1185, F3_914, F3_1544, F3_1176 and F4_1303). Furthermore 8 of these sequences aligned to various types of chemoreceptor including putative pheromone receptors and taste receptors (F2_811, F2_1263, F2_954, F2_1072, F2_1266, F3_1544, F3_1176 and F4_1303) and 4 aligned directly to olfactory receptors or proteins annotated as "Similar to olfactory receptors" (F2_1263, F2_1072, F2_1266, F3_1176). Sequences derived from LC-MS/MS analysis of the tryptic peptides from the 55kDa band of mouse and rat olfactory cilia preparations detailed in Figure 4.3.17/Table 4.3.7 and Figure 4.3.18/Table 4.3.8, also suggested that this band may contain seven-transmembrane spanning receptors and potentially olfactory receptors (mouse: F2_1649, F2_1524, F2_1825; rat: F2_1144, F2_2009, F2_1329). Whilst none of the E values for the alignments for olfactory receptor-like sequences observed in the LC-MS/MS analysis of the 55kDa band from sheep, mouse and rat were below the threshold level of significance, the fact that peptide sequences from all three species showed homology to these types of membrane proteins is considered to be significant.

Only one putative protein identification from a peptide sequence gave a score of $E<0.05$; peptide sequences derived from rat (F2_2009.5671) conclusively identified α-tubulin ($E=9e^{-5}$) and an α-tubulin-aligning peptide was also observed in the mouse 55kDa tryptic digest (F2_1701), albeit with a non-significant E value ($E=1.4$). Other sequences in the rat and mouse tryptic digests also match to β-tubulin

Function 2

		BLAST Identifications				
Precursor Ion	**Sequence**	**Top hit**	**NCBI accession #**	**Species**	**Top score**	**Notes**
1649.8035	NCYCLGSNL	Hypothetical protein XP_242668	27660713	Rattus norvegicus	121	Hit for seven-transmembrane helix receptor (E=219)
1065.4764	STMQELN	Keratin		Homo sapiens		
1033.5197	TLLEGF	Keratin		Homo sapiens		
807.4411	LAWDFR	Keratin		Homo sapiens		
1020.5051	LLSDSSCK	Trypsin		Bos taurus		
1381.7393	ALEESNYELWK	Keratin		Homo sapiens		
1155.5934	GTSYPDVLK	Trypsin		Bos taurus		
1524.7314	LCQAPLL	Similar to PYRIN-containing APAF1-like protein	27675274	Homo sapiens/Rattus norvegicus	16	Two hits for mucin 5, a hit for seven-transmembrane helix receptor (E=951)
1825.2113	QYPPSLVL	Hypothetical protein XP_243178	27663096	Rattus norvegicus	90	Multiple hits for seven transmembrane helix receptor (E=293) and olfactory receptor (E=293)
2166.1243	LDVVEGNEQFLSASK	Trypsin				
1601.9113	NVDLEPG	D-3 phosphoglycerate dehydrogenase	3122875	Mus musculus	121	Multiple hits for beta tubulin (E=219) and G protein-coupled receptor kinase (E=1276)
1701.962	GLFVDLEPGELEEVR	Tubulin alpha 6	27711678	Mus musculus/Rattus norvegicus	1.4	Additional lower score hits to beta tubulin isotypes (E=3.5)

Table 4.3.7 LC-MS/MS analysis of tryptic in-gel digestion products derived from the 55kDa band in mouse olfactory cilia preparations

The peptide sequences gained from LC-MS/MS data analysis were searched against the non-redundant NCBI protein database using the "short, nearly exact sequences" BLAST tool with the following default search parameters: expect 20000, wordsize 2, matrix PAM30 and gap costs existence9 extension1.

Figure 4.3.17 MS/MS spectra provide evidence that the 55kDa band present in mouse cilia preparations contains tubulin proteins and additional proteins potentially similar to olfactory receptors
LC-MS/MS spectra are shown with sequence annotation derived from the y ion series. The alignment between the predicted peptide sequence and the putative identifications are also provided. "|" between sequence alignments indicates shared residues and "+" denotes substitutions of amino acids with equivalent structural/chemical characteristics. The quoted molecular mass of each ion corresponds to the mass of the precursor ion in its 1+ charge state.

MS/MS spectrum for precursor ion 1524.7314

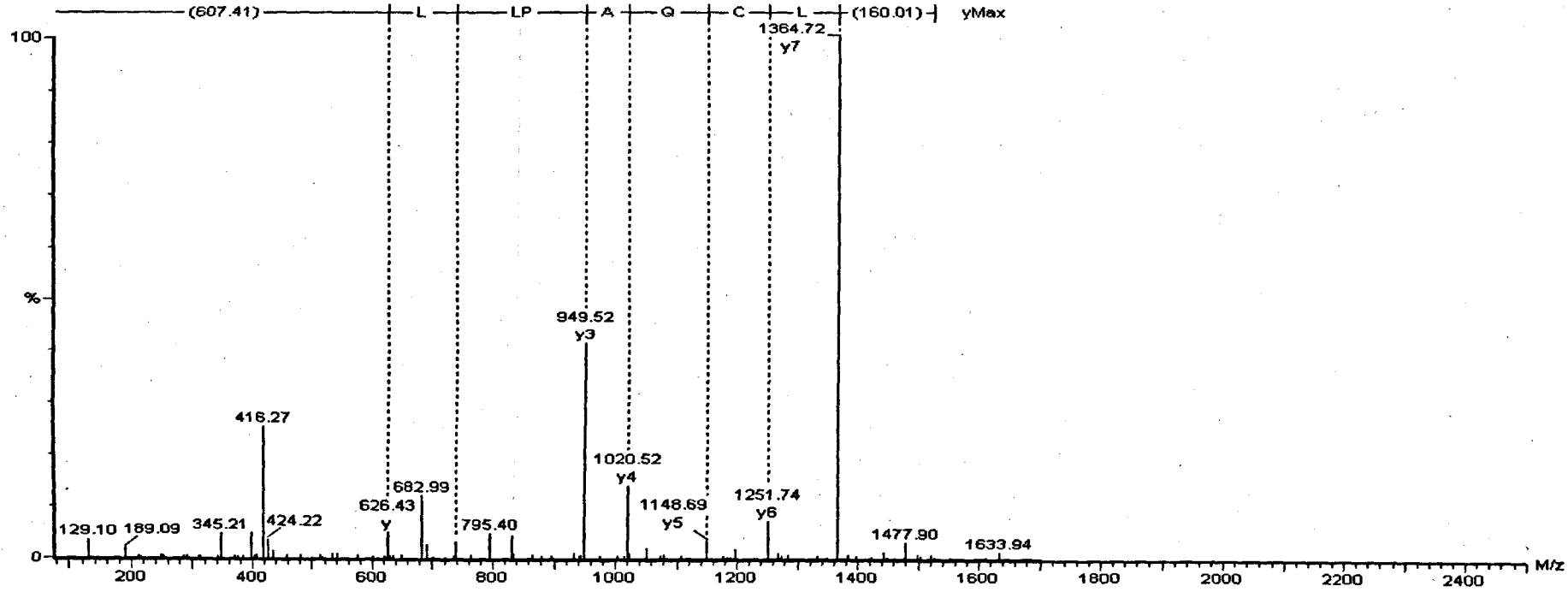

Sequence alignments

```
                                    Query:      1   LCQAPLL   7
                                                    |||||||
Similar to PYRIN-containing APAF1-like protein 4:   399   LCQAPLL   405

                                    Query:      1   LCQAPLL   7
                                                    |||||
          Seven transmembrane helix receptor:   254   LCQAPGP   260
```

MS/MS spectrum for precursor ion 1825.3113

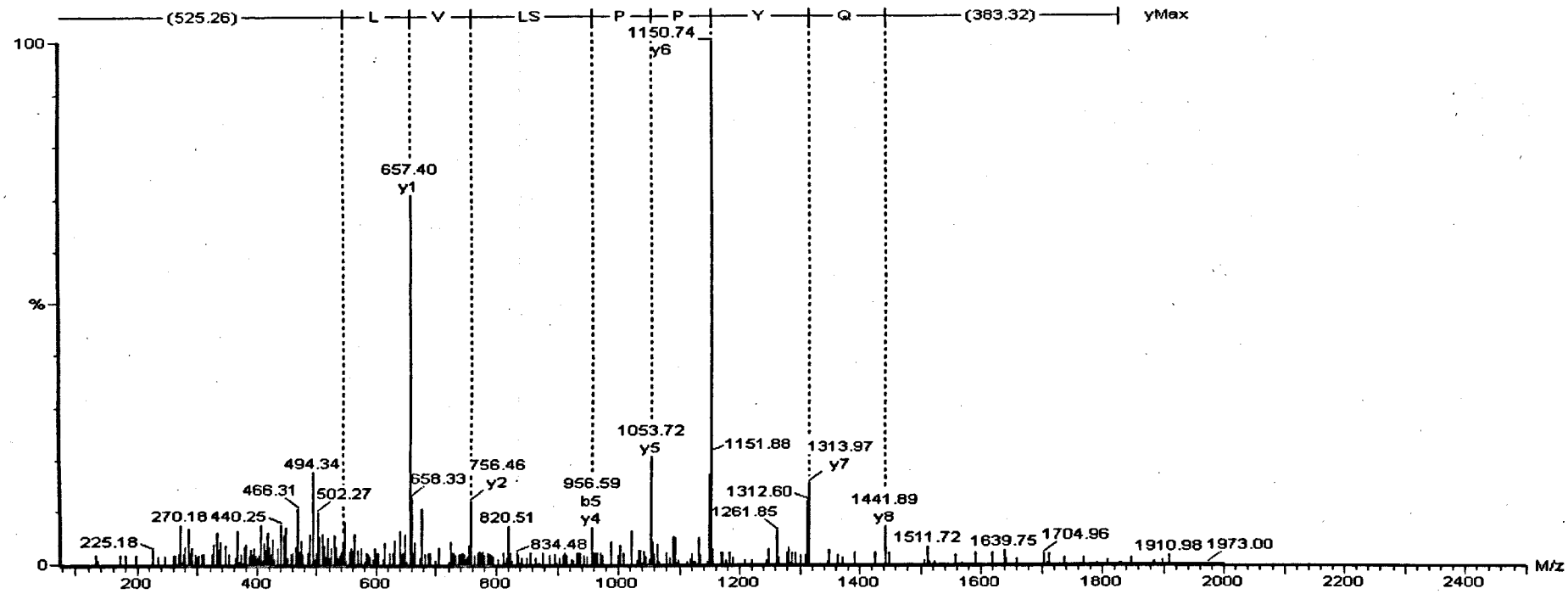

Sequence alignments

```
                    Query:      1   QYPPSL   6
                                    ||||||
Hypothetical protein XP_243178:  151   QYPPSL   156

                    Query:      3   PPSLVL   8
                                    ||||||
          Olfactory receptor:   143   PPSLVL   148
```

MS/MS spectrum for precursor ion 1601.9113

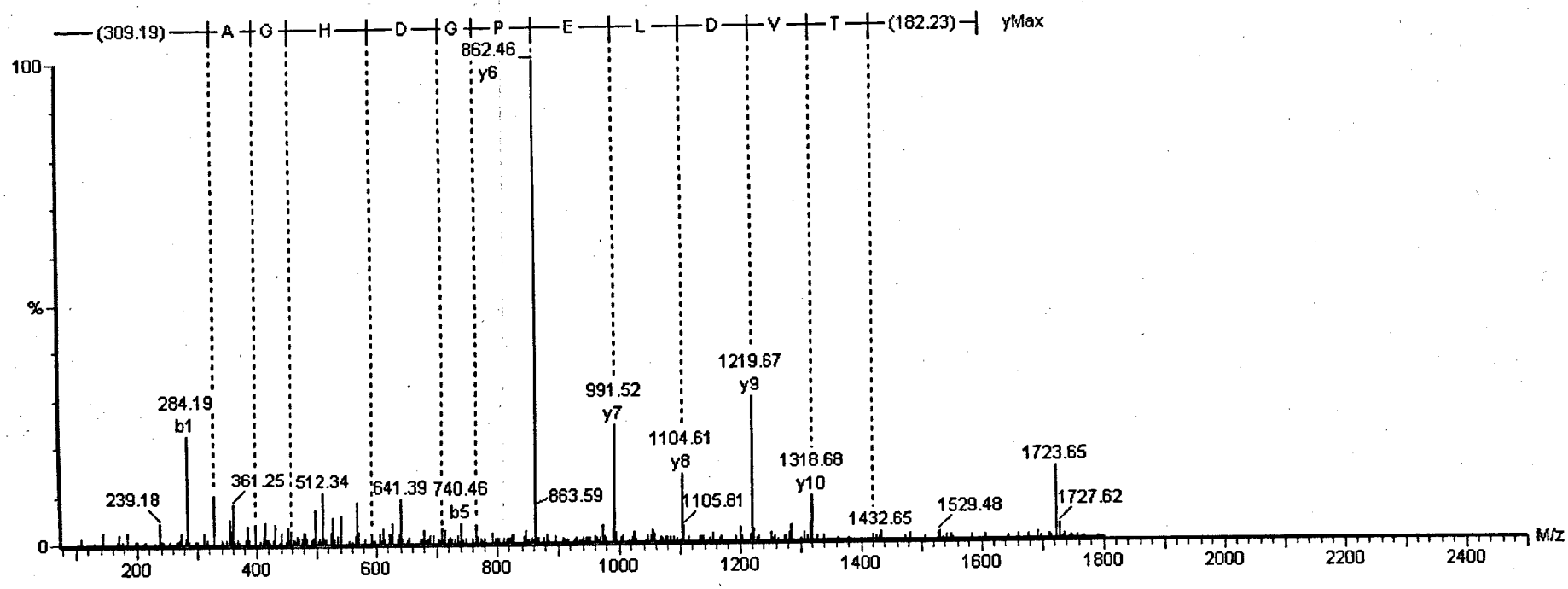

Sequence alignments

```
                    Query:   1   NVDLEP   6
                             ||||||
D-3-phosphoglycerate dehydrogenase:  34   NVDLEP   39

                    Query:   2   VDLEPG   7
                             ||||||
                β-tubulin:   66   VDLEPG   71
```

MS/MS spectrum for precursor ion 1701.962

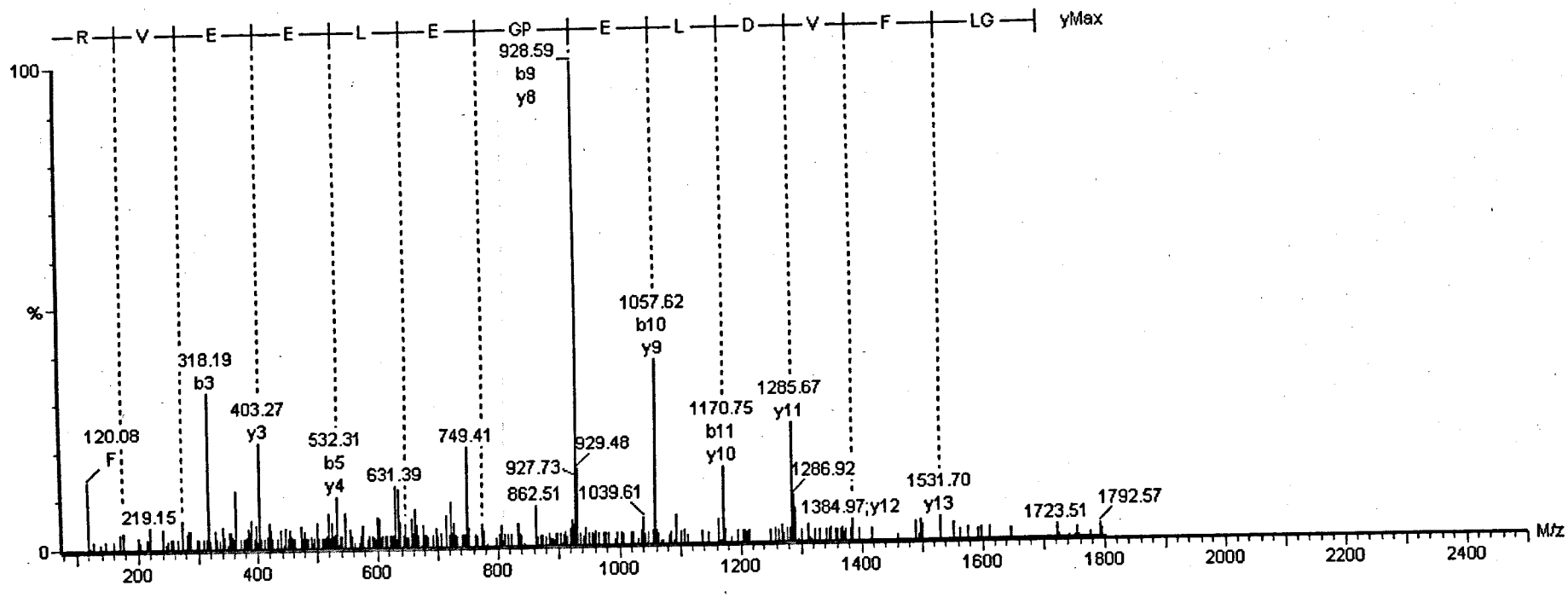

Sequence alignments

```
Query:   3   FVDLEPGELEEVR   15
             ||||||  ++|||
Similar to tubulin, α6: 131   FVDLEPTGIDEVR   143
```

MS/MS spectrum for precursor ion 1825.2113

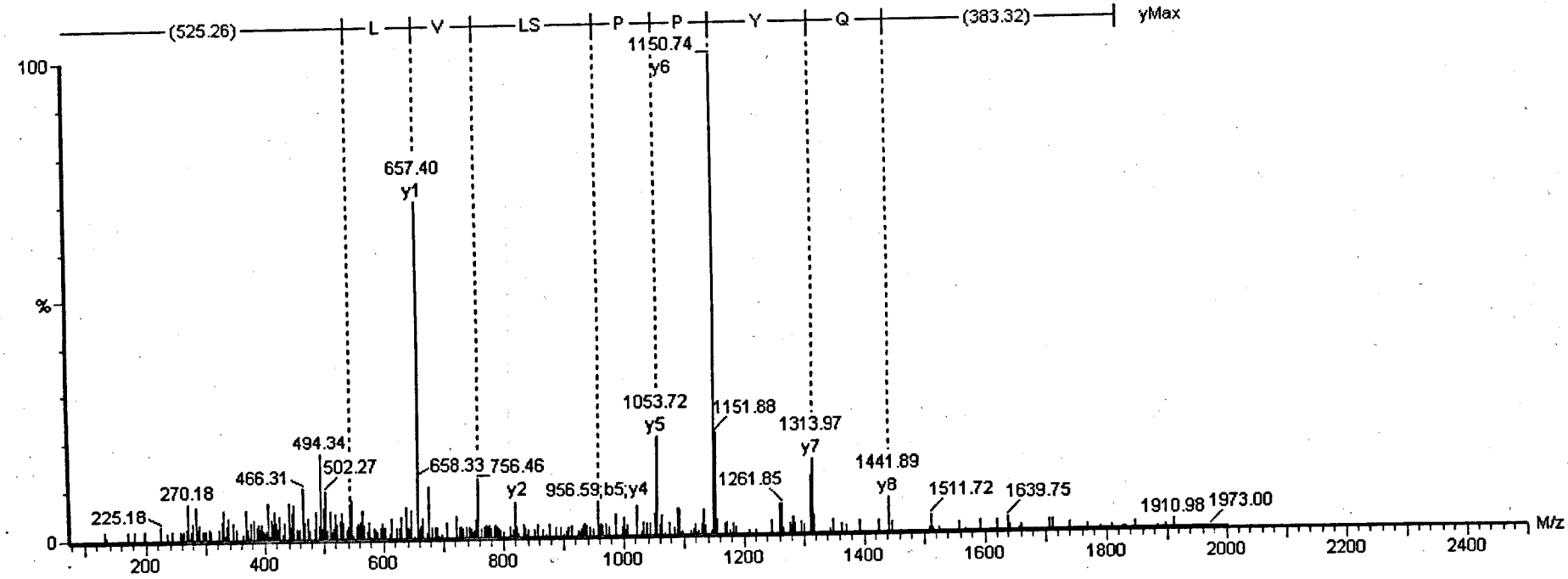

Sequence alignments

```
Query:                          1   QYPPSL   6
                                    ||||||
Hypothetical protein XP_243178:   151   QYPPSL   156

Query:                          3   PPSLVL   8
                                    ||||||
Olfactory receptor:             143   PPSLVL   148
```

Function 2

		BLAST Identifications				
Precursor ion	**Sequence**	**Top hit**	**NCBI accession #**	**Species**	**Top score**	**Notes**
1329.1205	LNVYDAQ	Similar to G630039H03Rik protein	34869222	Rattus norvegicus	107	One hit for putative pheromone receptor in rat (E=1507)
1826.6313	YPWN	Epsilon-trimethyllysine 2-oxoglutarate dioxygenas	15529963	Mus musculus	465	Haemoglobin beta chain also hit
2202.8076	not interpretable					
1144.0433	ALVNMVNGVAR	Glutathione S-transferase, pi	34861005	Rattus norvegicus	4.2	Multiple good hits for olfactory receptor-like proteins (E=18)
	or ALVNMVPAVAR	Stonin	33391898	Rattus norvegicus	4.2	Multiple hits for putative pheromone receptors, olfactory receptor-like proteins (E=18) and B-tubulin (E=80)
1230.0216	LSEQF(AT)MFR	Tubulin beta chain	7441369	Homo sapiens	0.44	
1039.9573	VANT	No significant sequence similarity				
1616.4003	not interpretable					
2009.5671	SFNTFFSETGQK	Similar to tubulin alpha-1 chain	27664758	Rattus norvegicus	0.023	Multiple hits to vomeronasal 1 receptors (E=27) and a hit for olfactory receptor MOR202-33 (E=212)
	or SFNTFFSETGAGK	Similar to tubulin alpha-1 chain	27664758	Rattus norvegicus	9e-05	Hits to vomeronasal 1 receptors (E=20), putative pheromone receptor VN2 (E=117) and olfactory receptor MOR202-33 (E=211)
1794.5667	NEQA	Unnamed protein product	26333209		131101	Sequence to short to get any significant results
1438.3416	LASALAQLPQK	Glucuronosyltransferase UGT2B13 precursor	539778	Oryctolagus cuniculus	0.14	
	or LASALAQIPQK	Olfactory UDP glucuronosyltransferase	10441350	Mus musculus	0.1	
1702.4697	LVDLEM	Cystatin TE-1	24308502	Rattus norvegicus	66	Multiple hits to aldehyde dehydrogenase (E=385)

Function 3

		BLAST Identifications				
Precursor ion	**Sequence**	**Top hit**	**NCBI accession #**	**Species**	**Top score**	**Notes**
2281.9956	GNFVDLE	Microtubule-actin crosslinking factor 1, isoform 4	30316105	Homo sapiens	159	Top hit not found in brain or kidney. Multiple hits to alpha tubulin (E=929)

Table 4.3.8 LC-MS/MS analysis of tryptic in-gel digestion products derived from 55kDa protein in rat olfactory cilia preparations

The peptide sequences gained from LC-MS/MS data analysis were searched against the non-redundant NCBI protein database using the "short, nearly exact sequences" BLAST tool with the following default search parameters: expect 20000, wordsize 2, matrix PAM30 and gap costs existence9 extension1. The function numbers assigned to each section of the table denote different acquisition functions which allow the collection of MS/MS data from simultaneously eluting peptides.

Figure 4.3.18 MS/MS spectra provide evidence that the 55kDa band present in rat cilia preparations contains tubulin proteins and additional proteins potentially similar to olfactory receptors
LC-MS/MS spectra are shown with sequence annotation derived from the y ion series. The alignment between the predicted peptide sequence and the putative identifications are also provided.

MS/MS spectrum for precursor ion 1329.1205

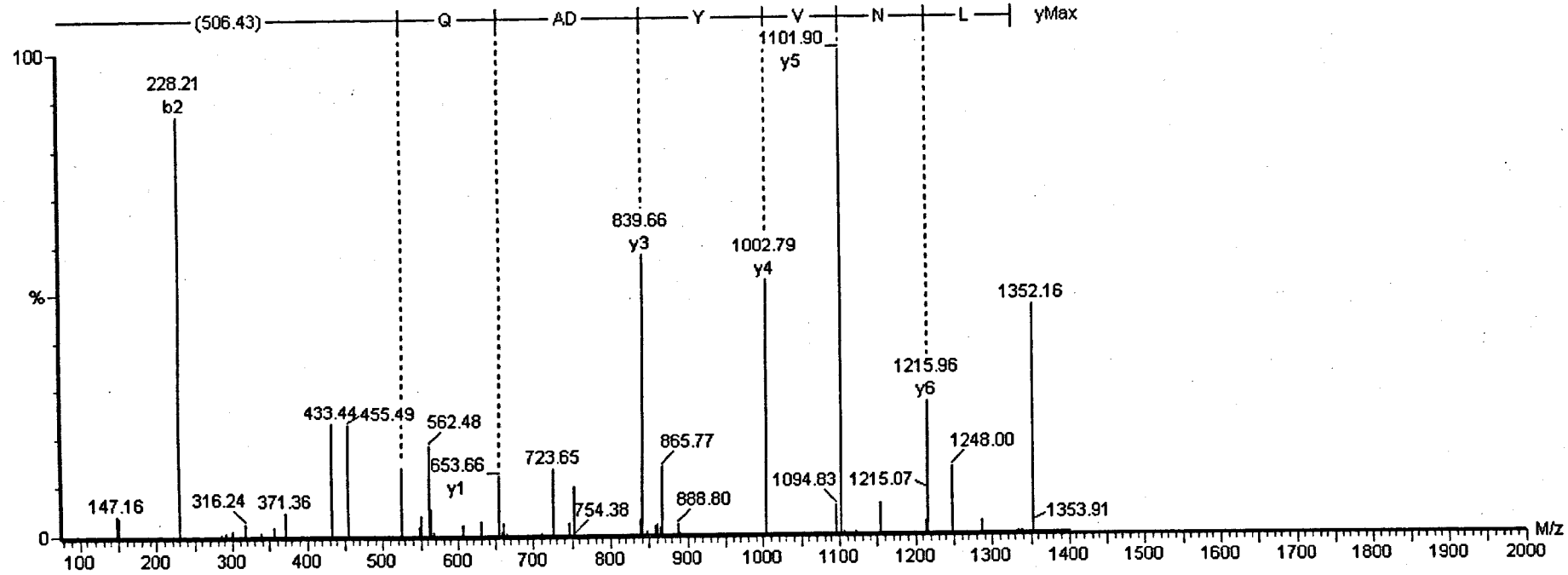

Sequence alignments

```
                                Query:    1   LNVYDAQ   7
                                            |||||  |
Similar to G630039H03Rik protein:    26   LNVYDQQ   32

                                Query:    1   LNVYDAQ   7
                                            ||+||
Similar to putative pheromone receptor:    6   LNIYDLT   143
```

MS/MS spectrum for precursor ion 1144.0433

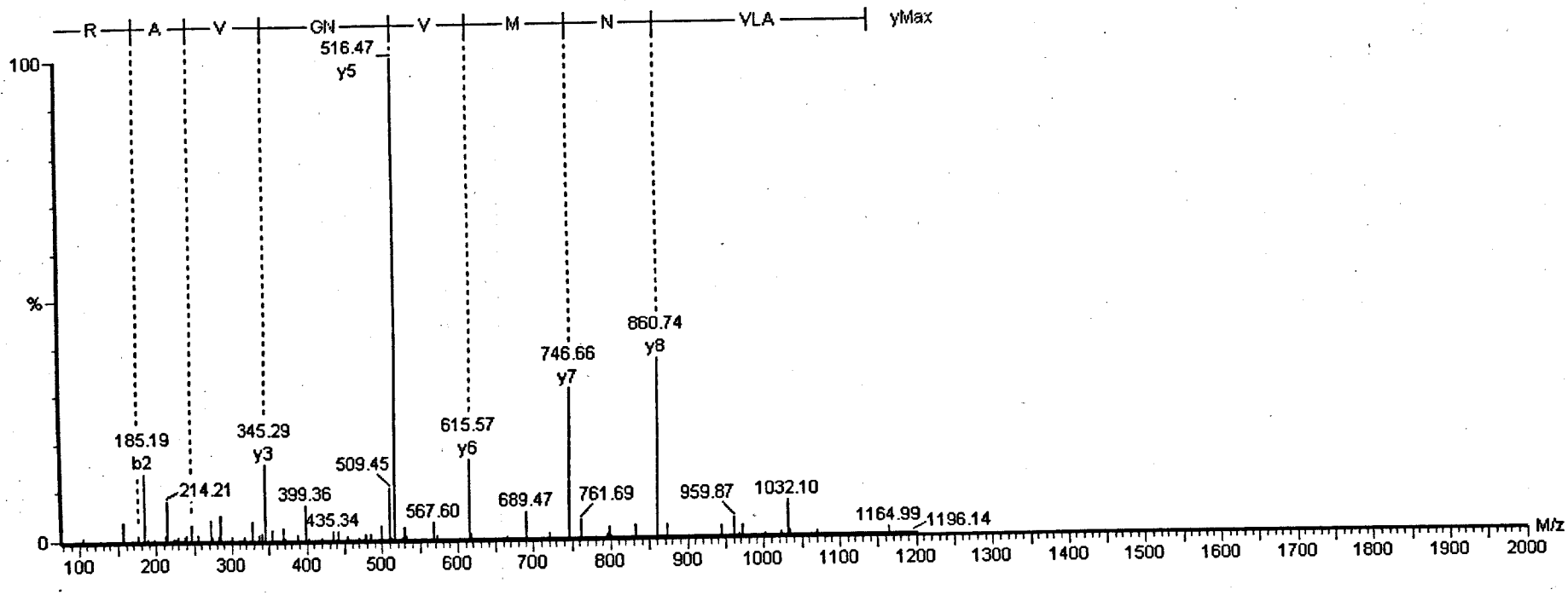

Sequence alignments

```
                Query:    1  ALVNMVN-GV  9
                             |||+|||  ||
Glutathione S-transferase, pi:  69  ALVDMVNDGV  78

                Query:    1  ALVNMV  6
                             ||||||
Olfactory receptor-like protein:  281  ALVNMV  286
```

MS/MS spectrum for precursor ion 1330.0314

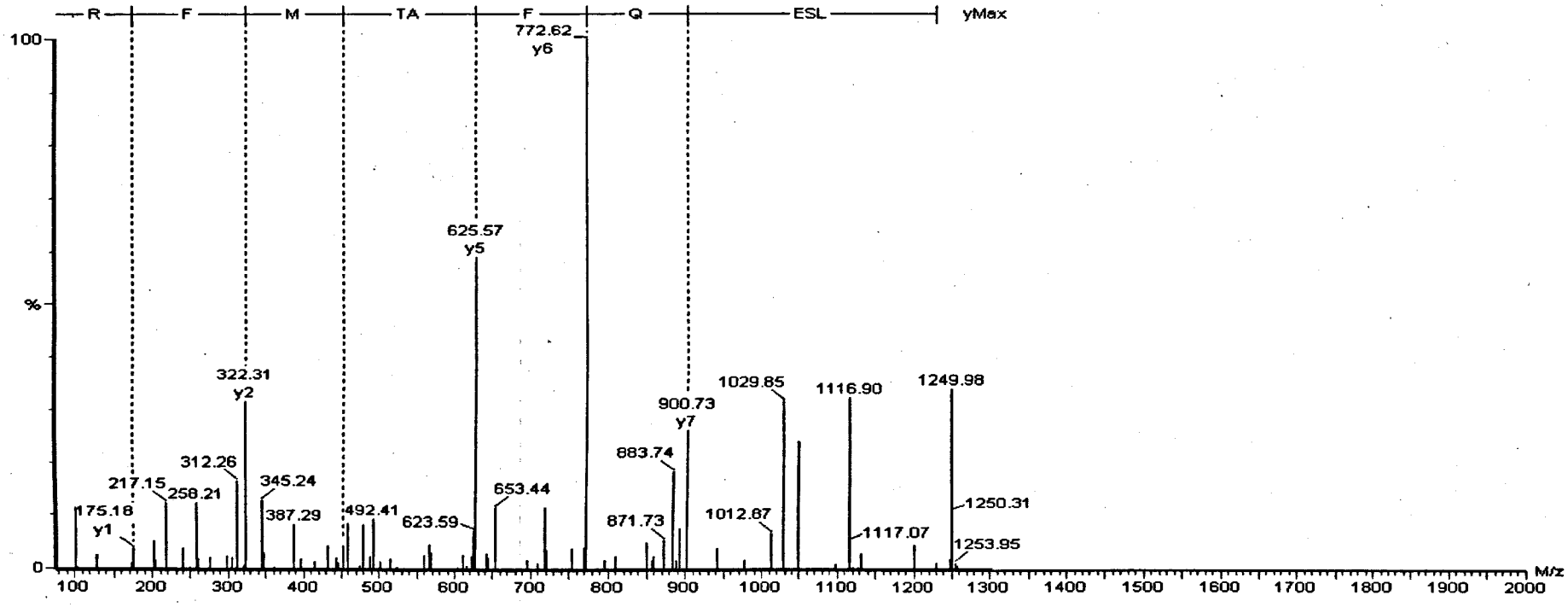

Sequence alignments

```
Query:              2   SEQFATMFR
                        ||||  ||||
Tubulin beta chain:   382   SEQFTTMFR
```

MS/MS spectrum for precursor ion 2009.5671

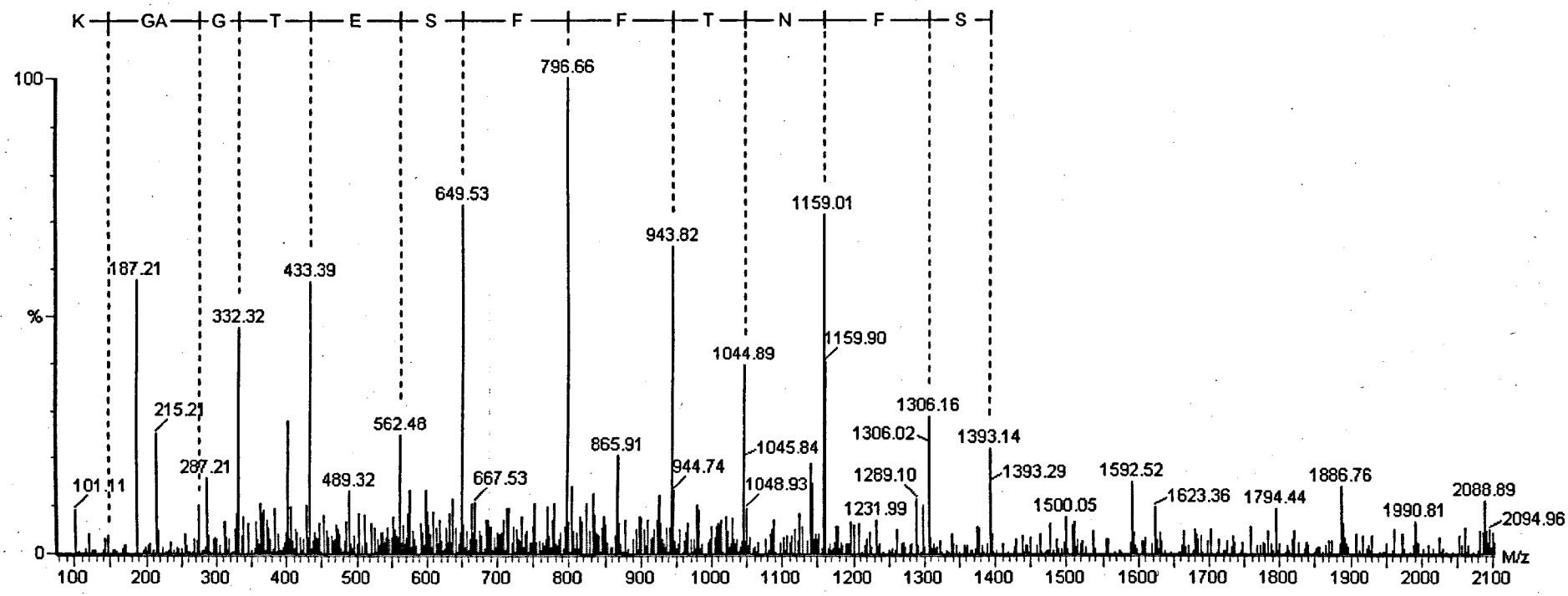

Sequence alignments

```
                    Query:     1   SFNTFFSETGAGK   13
                               ||||||||||||||
Similar to tubulin α,1 chain:  50   SFNTFFSETGAGK   62

                    Query:     3   NTFFSETGAG   12
                               ||||||  | |
Vomeronasal 1 receptor, A9:    31  NTFFSEIGIG   40
```

however in neither preparation were the E values significant (E=0.44 and 219 for rat and mouse peptides respectively).

4.4 Discussion

4.4.1 Species-specific I-LC-biotin labelling of olfactory cilia proteins in mouse, rat and sheep: 2D-PAGE analysis

The 2D biotinylation profiles of olfactory cilia proteins differed between the mouse, rat and sheep preparations studied, with the only proteins with common labelling patterns across the three model species being the highly conserved cytoskeletal proteins. There were demonstrably fewer I-LC-biotin labelled proteins in rat olfactory cilia in comparison to mouse and sheep cilia preparations. This could be explained by major differences in proteomes, reactivity of the cysteine residues or reagent diffusion rates through the cilia membrane in the three species. The first of these possibilities was discounted as the 2D-PAGE olfactory cilia protein profiles of mouse and rat were very comparable (Section 3.3.1) and would therefore be expected to contain similar proteins. The hypothesis that alternative isoforms with fewer/less reactive exposed cysteine residues are expressed in rat tissue is plausible, yet the cytoskeletal proteins and aldehyde dehydrogenase enzymes common to rat and sheep olfactory cilia were also biotinylated in both. However, this explanation cannot be entirely discounted for proteins with less well conserved primary sequences. The final possibility, that the rat olfactory cilia membrane imposes greater restrictions upon the transmembrane diffusion of I-LC-biotin was addressed during the comparison of rat olfactory and respiratory biotinylation profiles. Ultimately, the reduced levels of biotinylation and therefore exposed, reactive cysteine residues may represent a species-specific adaptation of the rat olfactory system.

4.4.2 I-LC-biotin labelling profiles of olfactory and respiratory cilia in the rat: 2D-PAGE analysis

The I-LC-biotin labelling profile of rat olfactory cilia contained markedly fewer proteins than comparable preparations of respiratory cilia. As described above, there are three main explanations for this: differing cilia proteomes, the presence of alternative isoforms/subtypes of proteins and significantly lower diffusion rates of I-LC-biotin through the olfactory cilia membrane. The 2D-protein profiles of rat olfactory and respiratory cilia preparations exhibited high levels of similarity and therefore the proteomes are likely to be similar. The consistent comparability of the 2D-profiles across all regions of the gel also suggests that the levels of proteins present in alternative isoforms/subtypes is minimal, as sequence modifications are likely to lead to alterations in the final migration point of a protein. The final possibility was addressed by labelling experiments using increased levels of I-LC-biotin during labelling procedures.

Exposure to an increased concentration of I-LC-biotin led to labelling of additional proteins in the rat olfactory and respiratory cilia Cilia samples derived from olfactory and respiratory tissue both showed an increase in the number of labelled proteins following treatment with 24nmol/mg tissue I-LC-biotin. However, the abundance /levels of biotinylation of these additional proteins differed greatly between olfactory and respiratory preparations. Following the treatment of nasal tissue with 24nmol/mg tissue I-LC-biotin, the biotinylation profile of respiratory cilia was predominantly unchanged with the addition of a few extra, poorly defined proteins in the central region of the gel. By contrast the labelling profile of the olfactory cilia preparation is dramatically changed by the addition of new heavily labelled proteins. This change is unlikely to be due to protein denaturation in the

presence of increased I-LC-biotin as the proteins that were labelled during 12nmol/mg tissue I-LC-biotin treatment maintained consistent levels of biotinylation (relative to other labelled proteins) following exposure to the higher level of reagent. Should denaturation be occurring it is likely that many more proteins from all regions of the gel would be labelled as biotinylation would no longer be dependent on cysteine residues being exposed on the surface of a native protein. The reactivity of cysteine residues is highly dependent upon the immediate protein environment *e.g.* the substitution of a neighbouring negatively charged amino acid in an alternative protein isoform could reduce cysteine reactivity (Torchinsky, 1981). However such substitutions are likely to be accompanied by a shift in the migration characteristics of the protein, particularly in the first dimension of 2D-PAGE. Given the extensive similarity of the protein profiles and significant differences between the biotinylation patterns of olfactory and respiratory cilia preparations, the presence of alternative protein isoforms is unlikely to be the major causal factor of the observed labelling differences. Moreover, the biotinylation pattern of rat respiratory cilia bore a greater resemblance to the profile obtained from mouse rather than rat olfactory tissue, implying that the profile differences may be species-specific in addition to sensory organ-specific. Six of the seven additional proteins labelled after treatment with the increased final concentration of I-LC-biotin were intracellular proteins, suggesting an increase in the number of proteins accessible to I-LC-biotin. It is therefore concluded that a significant proportion of the differential labelling of proteins in the rat olfactory cilia preparations is due to greater restrictions upon the diffusion of the reagent into the cell. Although it is conceded that this is unlikely to be the only factor as the biotinylation patterns for the olfactory and respiratory cilia preparations are not equivalent even at increased reagent levels.

Discussion of the biotinylation profiles thus far has assumed that the olfactory and respiratory preparations are, save a shared anatomical location, entirely unrelated. This is not the case however, as approximately one-third of the proteins in the respiratory cilia preparation are of olfactory tissue origin (Section 3.3.2). Therefore the significant labelling differences between olfactory and respiratory cilia not only suggest sensory *versus* non-sensory adaptation in membrane permeability/cysteine reactivity but also indicate fundamental differences between the olfactory epithelia lining the nasal turbinates and septum. The septum lining has two regions of olfactory tissue (not including the vomeronasal organ, which is part of the accessory rather than main olfactory system and therefore not comparable to the nasal turbinate olfactory epithelium), a large region approximately covering the caudal third of the septum and the much smaller septal organ, located in a ventral position relative to the main section of olfactory epithelium (Farbman, 1992). Whilst the septal organ has been predicted to have unique functions in olfaction (Marshall and Maruniak, 1986; reviewed Farbman, 1992; Weiler and Farbman, 2003) it only constitutes a small percentage of the sensory regions of the septum and it is unlikely that the olfactory cilia within respiratory preparations were solely derived from this region. The labelling profile differences between olfactory and respiratory cilia preparations therefore suggest that the main section of olfactory epithelium lining the nasal septum may also be adapted to fulfil a distinct functional role.

Repetition of the olfactory and respiratory tissue labelling experiments at two different concentrations, using an alternative reagent with different chemical group specificity *e.g.* targeting amine groups, would test the conclusion that the differing labelling profiles are a direct consequence of membrane permeability restrictions. If reagent diffusion rates do differ between olfactory and respiratory surface

membranes, the activity of this second reagent should mirror the changes in labelling patterns obtained with I-LC-biotin. If however the reactivity of cysteine residues is the main determinant of the observed profile changes, the results of a second, non-sulphydryl targeting reagent should show no differences between the olfactory and respiratory cilia preparations at both reagent concentrations. Comparisons between the I-LC-biotin labelling of olfactory and respiratory cilia should also be repeated both with rat (to confirm reproducibility) and with other species such as cows or sheep to assess the species-specificity of the labelling differences. In addition, the use of larger animals may permit the reproducible dissection of the nasal septum to investigate the I-LC-biotin labelling profiles of the olfactory and non-sensory regions individually.

Whatever the primary cause of the differential biotinylation pattern of olfactory and respiratory cilia, these experiments indicated that the olfactory system of the rat may be specifically adapted to reduce uptake of external chemicals; a property that is potentially both species and sensory-cilia specific.

Metabolic enzymes are labelled with I-LC-biotin in olfactory and respiratory cilia

The labelling of proteins such as creatine kinase, enolase 1α and aldehyde dehydrogenase in the olfactory and respiratory preparations studied may provide evidence for a putative secondary role for these proteins.

Aldehyde dehydrogenase is a well-characterised xenobiotic-metabolising enzyme present in species including rats, rabbits, mice and dogs (reviewed in Thornton-Manning and Dahl, 1997). The aldehyde dehydrogenase subtype over-expressed in the cornea - ALDH3 (Cuthbertson *et al.*, 1992; Bilgihan *et al.*, 1998) was also found in respiratory cilia preparations and unlike the subtypes *e.g.* ALDH1A1 observed in olfactory cilia, was not labelled during I-LC-biotin treatment.

This difference may represent part of the functional adaptation of aldehyde dehydrogenase subtypes involving the exposure of reactive cysteine residues on the protein surface.

The importance of maintenance of steady redox conditions under oxidative stress was briefly reviewed in the Discussion section of Chapter 3, where the importance of thiol groups to the olfactory system and the high levels of antioxidant proteins were discussed. The main damage resulting from oxidative stress is the loss of glutathione, which forms mixed disulphide bonds with proteins bearing exposed cysteine residues. This glutathione can be recovered by thiol transferase enzymes, which specifically reduce these mixed disulphide bonds (Balijepalli *et al.*, 1999). However the derivatisation of functionally important cysteine residues could have serious implications for the cell *e.g.* the inhibition/loss of function in a key enzyme. If the formation of the mixed disulphides by glutathione is entirely based on proximity of available cysteine residues, the specific recruitment of proteins bearing exposed cysteine residues that are functionally less vital than *e.g.* signal transduction proteins may constitute a mechanism to reduce the potential for oxidative stress damage. Therefore the overexpression/specific localisation of primarily metabolic proteins containing exposed cysteine residues (such as creatine kinase, enolase 1α and aldehyde dehydrogenase) in the olfactory and respiratory cilia may limit the effects of oxidative stress by providing cysteine residues that can be reversibly-derivatised by glutathione without causing significant cell trauma. This provides a secondary role for these proteins in addition to their metabolic roles and may be one explanation for their expression levels apparently exceeding those necessary for metabolism alone.

4.4.3 Species-specific labelling of olfactory cilia proteins in mouse, rat and sheep: SDS-PAGE analysis

As discussed previously the analysis of proteins using 2D-PAGE introduces unequal representation of cellular proteins and primarily a bias against poorly soluble species. This bias means that membrane proteins are likely to be significantly underrepresented during the above 2D-PAGE-based analyses. Therefore comparisons of the I-LC-biotin labelling profiles between mouse, rat and sheep were also undertaken using SDS-PAGE protein separation.

Three major bands were labelled by I-LC-biotin in the olfactory cilia of mouse, rat and sheep: 40kDa, 55kDa and 70kDa SDS-PAGE analysis of I-LC-biotin labelled proteins present in olfactory cilia preparations indicated the conservation of three, strongly labelled bands across the model species. These bands were at slightly varying positions in the three species, with approximate masses of 40kDa, 55kDa and 70kDa.

As demonstrated using unlabelled cilia preparations and tissue washes, the 70kDa band is non-specifically visualised during biotin detection. This could be due to strong, non-specific interactions between the proteins within this band and the streptavidin-alkaline conjugate but could also represent the detection of endogeneous biotin-containing enzymes *e.g.* the 75kDa biotin-containing subunit of mitochondrial propionyl-CoA carboxylase (Kirkeby *et al.*, 1993). These possibilities could be distinguished by the use of a streptavidin conjugate pre-incubated with biotin to detect labelled proteins.

The 40kDa biotinylated protein band in the rat olfactory cilia preparation was identified as beta/gamma actin by peptide mass fingerprinting (subtypes indistinguishable using the data obtained). However attempts to identify the 55kDa

protein band by MALDI-ToF mass spectrometry were unsuccessful, therefore tandem mass spectrometry (MS/MS) was used.

Potential significance of the 55kDa band Further protein labelling and SDS-PAGE characterisation work was undertaken on the olfactory cilia preparations of the mouse, rat and sheep and also in rat respiratory cilia. Use of the membrane-impermeable reagent LYIA indicated that the only bands containing proteins with extracellular cysteine residues in all three model species had an approximate mass of 55kDa.

Experiments comparing the I-LC-biotin labelling profiles of rat olfactory and respiratory cilia preparations resolved by SDS-PAGE demonstrated that the labelled band at ~55kDa was detected with greater intensity in cilia derived from sensory rather than non-sensory epithelia. This comparison of olfactory cilia prepared from the nasal turbinates and cilia derived from rostral regions of the septum should be repeated, using tissue from rats and larger mammals with clearer demarcation of sensory and non-sensory regions (Nef *et al.*, 1989). The results of these initial experiments however, indicated that the 55kDa band contains proteins predominantly localised to sensory cilia that bear exposed cysteine residues, a number of which are extracellular and therefore directly available for putative interactions with thiol odorants.

Identification of the proteins within the 55kDa protein band Tandem mass spectrometry (MS/MS) was employed in the identification of the proteins in the 55kDa bands of mouse, rat and sheep olfactory cilia preparations. The specific technique used was liquid chromatography-tandem mass spectrometry (LC-MS/MS), in which the peptides resulting from an in-gel trypsin digest were concentrated on a reverse-phase chromatography column and eluted directly into a Q-ToF mass

spectrometer (see Section 2.11/2.14 for further details). The peptide sequence data obtained from the LC-MS/MS analysis of tryptic digestions failed to conclusively identify the proteins within the 55kDa band in mouse, rat and sheep olfactory cilia. Whilst significant evidence was provided for the presence of α-tubulin and additional data suggested β-tubulin was also present, these proteins would not account for the external cysteine residues associated with proteins of the 55kDa band. In addition tubulin proteins are highly conserved across both species and cilia types and due to identical structural roles are unlikely to show the adaptation implied by the specific enrichment of selected protein species within this band in olfactory cilia.

There were no further significant matches between the LC-MS/MS peptide sequences and known proteins in the database searched. The results taken cumulatively however, are suggestive of the presence of G-protein coupled receptors (GPCRs) and potentially chemoreceptors. Although peptide alignments with GPCRs were never significant *i.e.* the E values were consistently greater than the 0.05 significance threshold, the number of alignments to GPCRs found in mouse, rat and sheep olfactory cilia - 4/5, 4/10 and 13/19 peptides respectively (excluding peptides known to be trypsin/keratin and therefore not searched against the database) - was strongly suggestive that the 55kDa band does indeed contain this type of protein receptor. As many of these peptide sequences aligned to putative chemoreceptors and selected proteins within the 55kDa band of rat olfactory cilia were shown to be localised to olfactory cilia; it is concluded that in addition to containing tubulin proteins, the 55kDa band also contains olfactory receptors.

Supporting evidence for the putative identification of olfactory receptors in the 55kDa The conclusion that the band at ~55kDa may contain olfactory receptors is

supported in the available literature on olfactory receptor proteins. The lectin concanavalin A (ConA) differentially inhibits odorant responses in the rat olfactory epithelium (Shirley *et al.*, 1987b; Kirner *et al.*, 1999) and Western blots probed using ConA detected a protein ~55kDa in rat olfactory tissue only faintly present in the rat respiratory preparation (Henderson *et al.*, 1992). This 55kDa glycoprotein was also detected in the olfactory cilia of pigs and frogs (Chen and Lancet *et al.*, 1984; Henderson *et al.*, 1992). In addition, studies of rat olfactory tissue indicated that a protein of ~50kDa (as stated previously the 55kDa band has a mass 50-55kDa in the mammalian species studied), is phosphorylated in a transient, odorant-dependent manner consistent with the role of phosphorylation in the termination of the olfactory response (Boekhoff *et al.*, 1992). Finally an olfactory-receptor specific antibody recognised a polypeptide ~50kDa (Nekrasova *et al.*, 1996). The exact mass of olfactory receptors may alter slightly between species and locations (potentially due to differential glycosylation) hence the slightly different masses for the precise location between 50-55kDa of the putative olfactory receptor-containing proteins bands in the model species used during this study (Nekrasova *et al.*, 1996). Furthermore none of the above papers presented SDS-PAGE gels with a 50kDa marker and therefore the stated protein mass figures are estimates and potentially more similar than their predicted masses imply.

4.4.4 The identification of proteins by tandem mass spectrometry

The identification of proteins by peptide sequence tags is theoretically far more accurate and sensitive than peptide mass fingerprinting. Amino acid sequences can distinguish between different peptides of the same mass and can provide sufficient data from a single peptide to identify a protein (Poutanen *et al.*, 2001). The high level

of information obtainable from a single peptide is due to the high levels of potential sequence permutations. A peptide containing 6 amino acids could theoretically have any one of the 20 naturally occurring amino acids in each position. This gives a potential number of permutations of 20^6. Therefore each hexapeptide sequence is only likely to occur in a small number of homologous proteins. In a peptide containing 10 amino acid residues the number of permutations dramatically increases with the probability of a randomly occurring complete sequence match of 1 in 1.034×10^{13}. Therefore a conclusive identification of the protein can be made from a single peptide sequence of ten amino acids. This theory does not entirely hold for real proteins as secondary structure elements are governed by patterns of amino acid chemical properties *e.g.* in α-helices there is often a conserved pattern of side chains alternating between mainly hydrophobic and mainly hydrophilic every 3-4 residues and the transmembrane regions of proteins predominantly containing hydrophobic residues (Branden and Tooze, 1999), which restricts the likelihood of certain amino acids being found in adjacent positions. In addition the relative abundance of amino acids also influences the incorporation frequency of selected residues in a protein. Despite these issues sequences from individual peptides still provide extremely valuable data and have been used for protein identification in a large number of proteomic surveys; particularly those relating to organisms with unsequenced genomes where proteins can be identified by their sequence homology to a known protein rather than relying on peptide mass fingerprint match to few (if any) published protein sequences/theoretical protein sequences (Verrills *et al.*, 2000; Shevchenko *et al.*, 2001).

Potential problems with the identification of unknown, low abundance proteins by LC-MS/MS During this work the success rate of identifications from single peptides

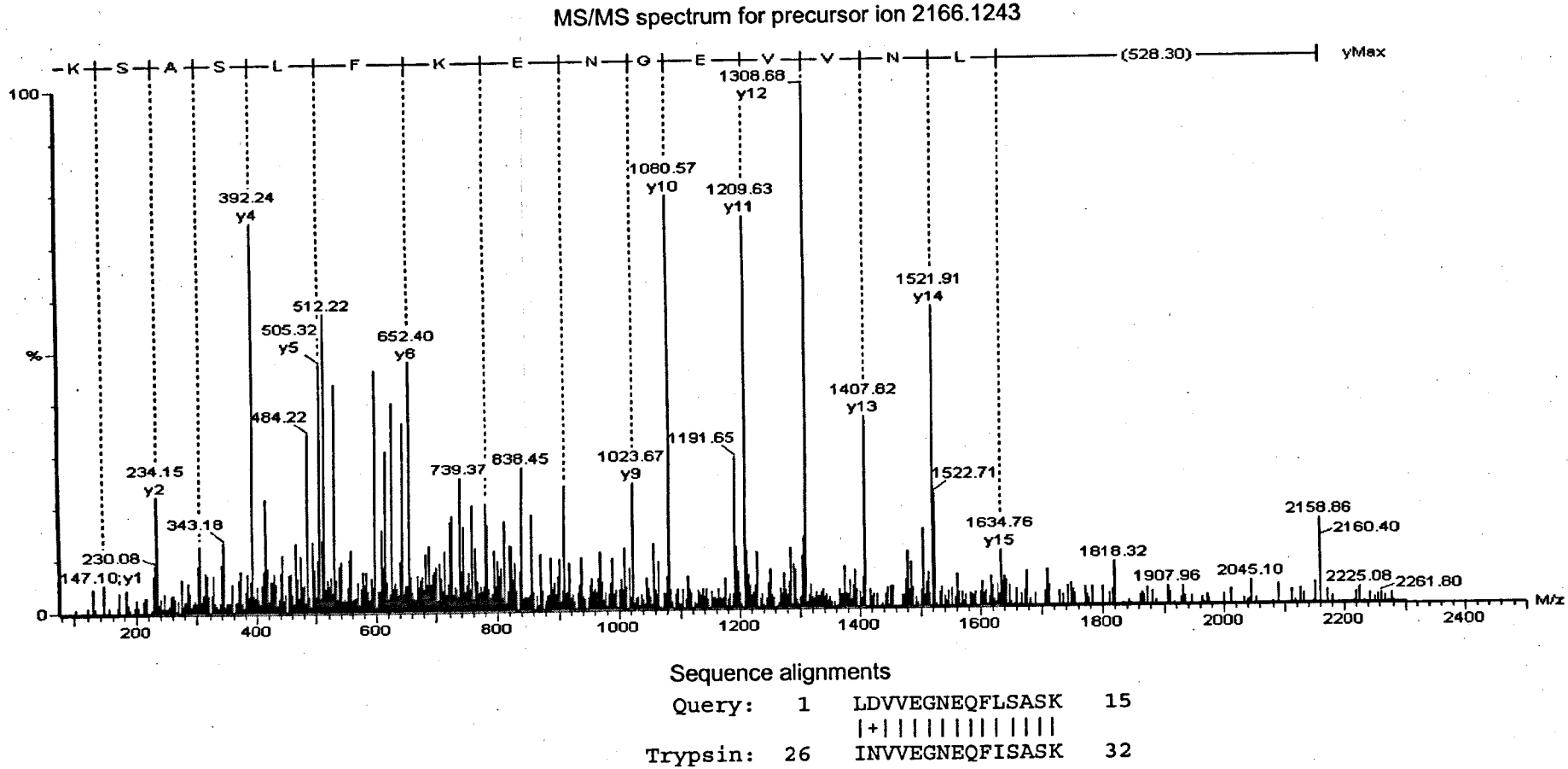

Sequence alignments

```
Query:    1   LDVVEGNEQFLSASK   15
              |+|||||||||||||
Trypsin:  26  INVVEGNEQFISASK   32
```

Figure 4.4.1 Manually sequences MS/MS spectra of trypsin (*bos taurus*) and keratin (*homo sapiens*) peptides from the mouse 55kDa band analysis correspond precisely to the known amino acid sequences

Leucine and isoleucine are considered to be equivalent as these cannot be distinguished by MS/MS spectra and the peptide sequencing software (MassLynx) includes leucine residues by default.

MS/MS spectrum for precursor ion 1065.4764

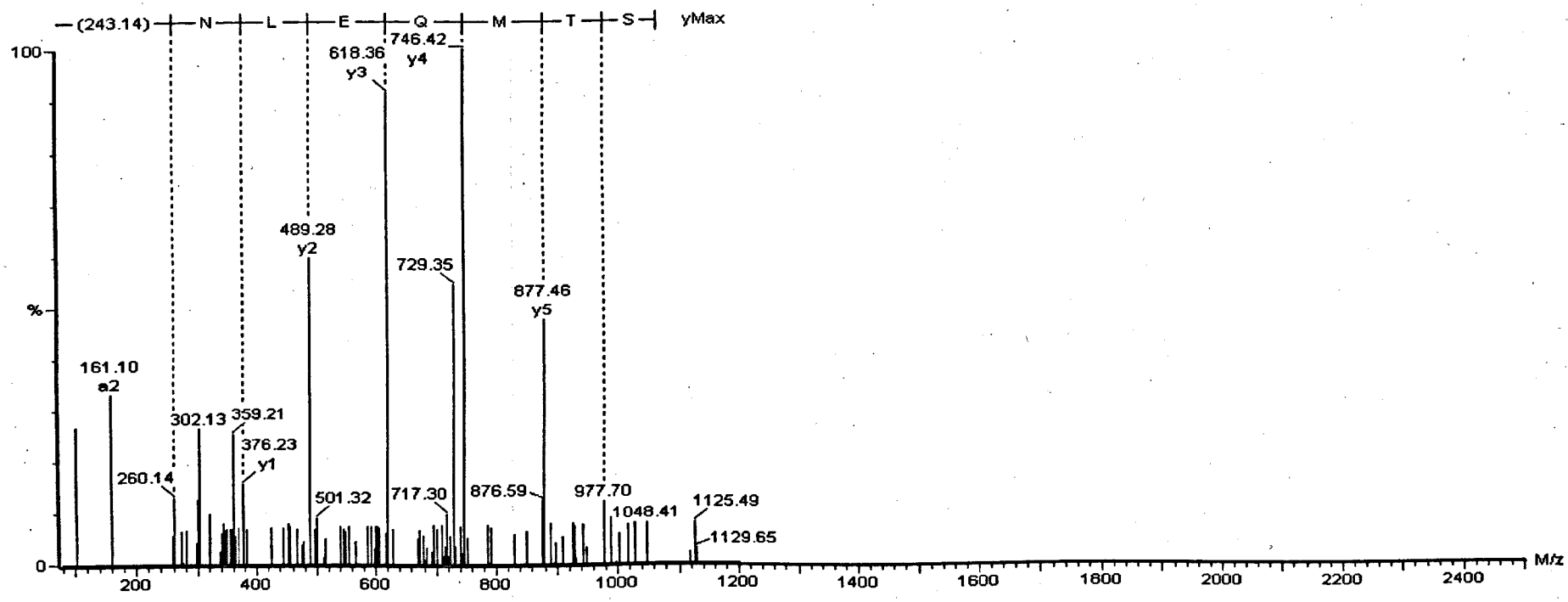

Sequence alignments

```
Query:      1   STMQELN   7
                  |||||||
Keratin 9:  154   STMQELN   160
```

(Figure 4.4.1)

was extremely low (only a single sequence provided a conclusive, statistically significant identification). There are two main explanations for this: sequencing errors or MS/MS spectra from low concentrations of peptides that provide ambiguous sequence data *i.e.* spectra that could be interpreted in many different ways. Manual *de novo* peptide sequencing was competent to the point of predicting the precise sequences of trypsin and keratin contaminant peptides (Figure 4.4.1). There remains however significant scope for improving the method of application of samples to the tandem mass spectrometer in order to improve the detection and sequencing of the peptides present in the tryptic digestions.

LC-MS/MS methodology, involving the use of an on-line chromatography system eluting directly into the mass spectrometer, was utilised during these studies to concentrate tryptic peptides and therefore maximise the levels of an individual peptide entering the mass spectrometer at a given timepoint (Poutanen *et al.*, 2001). This approach was taken to compensate for the low concentration of the starting sample – the olfactory cilia preparations commonly required visualisation by silver nitrate staining. The use of an on-line chromatography system however does have inherent problems. Despite the use of a nano-flow LC system, the flow of peptides into the mass spectrometer is still over ten times higher than that for static injection/infusion of samples at 20nL/min (nano-electrospray ionisation – nanoESI, Kast *et al.*, 2003) and the direct flow of chromatographic fractions into the mass spectrometer restricts the time available for peptide analysis before further peptides elute from the column. In summary there are numerous opportunities for the loss of peptides/limited analysis of peptides with this method. The use of data-dependent switching to MS/MS mode also poses problems. Peptides at low concentrations may not be detected in the single MS mode and yet if the mass spectrometer is manually

programmed to focus on a known mass previously undetected there can be sufficient levels of that peptide to allow sequencing (Kast *et al.*, 2003). To improve the number and quality of the MS/MS spectra obtained from the tryptic digestions of the 55kDa bands, peptides may be analysed by nano-ESI-MS/MS with the instrument targeted to acquire sequence data from known peptide masses determined by prior analysis of the digest sample by MALDI-ToF mass spectrometry. This procedure termed MALDI-directed nano-ESI-MS/MS provides effectively greater instrument sensitivity both in model peptides and for the identification of unknown proteins (Kast *et al.*, 2003).

It is acknowledged that GPCRs are one of the largest gene families in the mammalian genome and this certainly true of olfactory receptors. This introduces the potential for peptide sequences to hit GPCRs more often than other proteins by the sheer number of sequences available in the protein databases rather than by true homology. Conversely however, as these proteins are integral membrane proteins with seven-transmembrane spanning domains they are likely to be subject to more sequence constraints, reducing the likelihood of purely random sequence alignments. In addition where as 7/19 peptide sequences from the analysis of the 55kDa band in sheep olfactory cilia showed alignments to chemoreceptors in the nasal cavity, in the inconclusive data provided during the LC-MS/MS analysis of the 70kDa biotinylated band (raw data provided in Appendix) only 5/39 peptide sequences showed any sequence homology to any GPCRs. This indicated that the recurrent, low E value sequence alignments observed during the analyses of the 55kDa band may be significant rather than an artefact resulting from the sheer number of GPCR sequences available.

4.4.5 Evidence for the role of cysteine residues in odorant detection

Thiol groups have been shown to play a major role in the mammalian olfactory system and are required to some extent for the detection of the wide variety of odorants (Menevse *et al.*, 1978; Shirley *et al.*, 1983). Cysteine residues were shown to be involved in specific detection mechanisms during experiments where selected odorants protected the receptors for related odorants from sulphydryl-targeted mersalyl derivatisation (Menevse *et al.*, 1978). The use of a membrane-impermeable reagent such as mersalyl reinforces the importance of extracellular thiol groups in the olfactory process and this thesis presents further evidence for the presence of external cysteine residues on olfactory receptors in the mouse, rat and sheep.

The role played by cysteine residues in the detection of thiol odorants remains open to debate. Certainly these residues are not the only requirement for thiol detection as derivatisation of cysteine residues (again using mersalyl) had a lesser impact on the electroolfactogram (EOG) generated during thiol exposure than on the control odorant amyl acetate (Shirley *et al.*, 1983). These experiments were conducted using wide-ranging concentrations of odorants to ensure that the EOG generated in response to exposure to each odorant was approximately the same in all cases, octanethiol being used at the joint lowest concentration. This means that the thiol response in these experiments is not being investigated at its lowest detection threshold. As a wider number of receptors become stimulated at higher concentrations additional factors other than the property instilling the initial sensitivity of thiol detection may assume greater importance. These results may also be explained by any potential bias of the olfactory system towards lower carbon number compounds. Certainly in the case of thiol compounds, odorants with chains of 2-4 carbon atoms smell much fouler than larger straight chain thiols including

octanethiol (Node *et al.*, 2001) suggesting that the mechanism of thiol detection and aversion is biased towards a defined size of odorant molecule. Therefore the relative importance of molecule size and sulphydryl group interactions in the apparent sensitivity of the mammalian olfactory system to thiol compounds cannot at present be determined.

One potential method to study the relative importance of these two factors is to repeat the electrophysiological experiments of Shirley *et al.* (1983) using thiol concentration ranges starting at the absolute detection threshold for these compounds and then introducing the chemical derivatisation of cysteine residues. This experiment could also utilise multiple straight chain thiol compounds to address the relative importance of the functional group (primary determinant - Uchida *et al.*, 2000), the size of the carbon chain and whether this is concentration dependent.

If cysteine residues do govern olfactory sensitivity to thiol odorants, the reduced levels of labelling following tissue treatment with both LYIA and I-LC-biotin suggests that rats are less sensitive to thiols than other mammals such as mice and sheep. This potentially means that the rat may not be a suitable model for studies on the sensitivity/aversive properties of thiol compounds. Further work on the detection thresholds for thiol compounds using electrophysiology techniques and/or behavioural tests in the mouse, rat and sheep would determine whether this is actually the case and could also confirm or refute the hypothesis that exposed cysteine residues are required for the observed sensitivity/aversion to thiol compounds. Such behavioural experiments may also be used to investigate the relationship if any, between odorant sensitivity and aversion.

If thiol detection/aversive properties are dependent on non-receptor mediated pathways mediated by proteins bearing exposed cysteine residues, the only candidate

proteins conserved across the model species are the cytoskeletal proteins actin and tubulin. As reviewed in the introductory chapter of this volume, changes in the cytoskeletal structure of a cell can influence the activity of plasma membrane ion channels, thus providing a potential mechanism for membrane depolarisation. However in order to interact with cytoskeletal proteins a thiol odorant would be required to cross the cilia membrane. Here again the rat may be an unsuitable model, as the dual concentration I-LC-biotin experiments suggested greater restrictions on the movement of molecules through the olfactory cilia membrane of the rat in comparison to the mouse and sheep tissue. Therefore the rat would exhibit lower levels of cytoskeletal protein-dependent sensitivity and/or aversion to thiol compounds than the mouse and sheep.

Chapter 5

METALLOPROTEIN HYPOTHESIS OF OLFACTORY RECEPTOR FUNCTION

5.1 Introduction

Olfactory receptor proteins convert the specific binding of odorants into a membrane depolarisation event *via* a G protein activated signal transduction cascade. G protein-coupled receptors (GPCRs) of which olfactory receptors are one example make up one of the largest and most diverse receptor superfamilies, with known sequences numbering in several hundreds even before the addition of the multitude of olfactory receptor sequences now available (Strader *et al.*, 1989; Gudermann *et al.*, 1997). Key questions remain for olfactory receptors and GPCRs as a whole regarding the identity of both the ligand-binding residues/domains and the mechanism behind G protein activation. One hypothesis placing a metal ion at the heart of the mechanisms governing odorant binding by olfactory receptors and the subsequent activation of the G protein transduction cascade has recently been proposed (Wang *et al*, 2003a).

5.1.1 Metal ions in proteins

Metal ions may have been incorporated into early cells to help maintain cell integrity under osmotic pressure and to assist in the catalytic function of enzymes (Hay, 1984). Whatever the origins, it has been estimated that approximately 30% of all known enzymes require metal ions for their activity (Hirose and Kidani, 1990). The use of metal ions can often supplement the chemical reactivities provided by amino acids and improve the efficiency of selected reactions e.g. electron transfer reactions. Alternatively, metal ions may also be incorporated to stabilise the tertiary structure of a given protein e.g. the DNA-binding domain of zinc finger transcription factors

(Branden and Tooze, 1999). The specific ion in these metalloproteins is related to the properties of the individual metal ion and the protein function e.g. sodium ions form weak complexes with proteins and are therefore commonly involved in charge transfer, iron atoms form strong complexes and tend to participate in redox reactions. Of specific relevance to the metalloprotein hypothesis for olfactory receptor function, copper and zinc ions also form strong complexes, with nitrogen and sulphur as their preferred protein ligands (Hay, 1984).

5.1.2 The Metalloprotein Hypothesis

The metalloprotein hypothesis provides a model for odorant reception and G protein activation involving structural changes induced by the co-ordination of a metal cation and exchanges in the co-ordinating ligands.

Figure 5.1.1 shows the predicted secondary structure of the human olfactory receptor hOR o2d2 based on hydrophobicity measurements and homology with the well-characterised GPCR bovine rhodopsin (Floriano *et al.*, 2000; Singer *et al.*, 2000; Wang *et al.*, 2003a). It has seven transmembrane-spanning regions (TM1-7), three extracellular loops exposed to the olfactory mucus (EC1-3) and three intracellular loops (IC1-3) projecting into the cytosol of the ORN. The protein inserts into the membrane so that the N-terminal tail is extracellular (glycosylation motifs are commonly found within this region) and the C-terminal tail projects into the cytoplasm of the cell.

According to the metalloprotein hypothesis the structure shown in Figure 5.1.1, Figure 5.1.2a is the inactive form of the olfactory receptor. It adopts its active conformation upon the co-ordinate binding of a metal ion by selected residues in the EC2 domain, specifically by the amine, sulphydryl and carboxyl groups of the

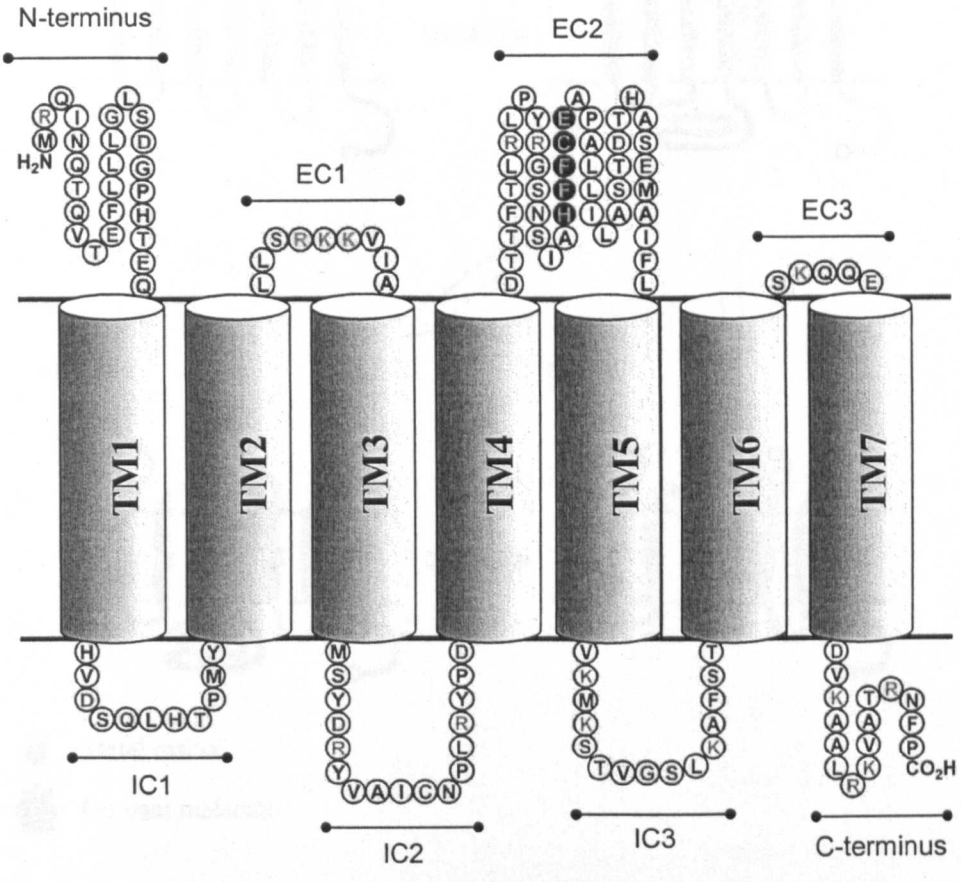

Figure 5.1.1 The secondary structure of the human olfactory receptor hOR o2d2.

Olfactory receptors are predicted to have seven transmembrane-spanning regions (TM1-7), four extracellular regions including the N-terminal domain (EC1-4) and four intracellular domains including the C-terminus (IC1-4). The shaded residues in EC3 are the five residues that form the putative metal-binding site.

Source: modified from Wang *et al.* (2003a)

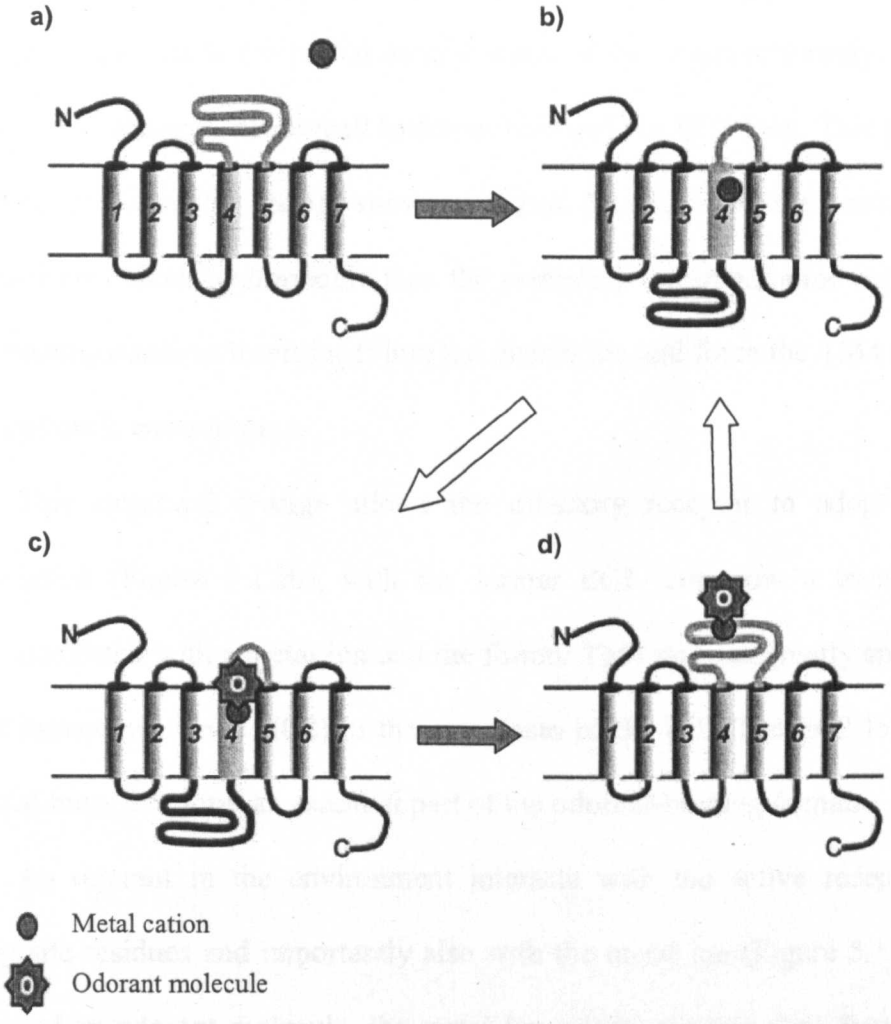

Figure 5.1.2 Olfactory receptors may alter their conformation upon the binding of a metal ion and interactions with odorant molecules

a) Olfactory receptors without an associated have a large EC3 loop exposed to the extracellular environment.

b) The co-ordination of a metal cation by a key aspartate/glutamate residue neutralises the charge on the EC3 domain. This domain becomes more hydrophobic than the preceding transmembrane segment (TM4) and inserts into the membrane bilayer displacing TM4.

c) An odorant molecule interacts with the olfactory receptor and its co-ordinated metal ion

d) Interactions between the odorant and metal ion cause a change in charge distribution around the metal centre resulting in the EC3 domain becoming less hydrophobic and being ejected out of the membrane.

Source: Wang *et al.* (2003a)

histidine (H), cysteine (C) and aspartate or glutamate (D or E respectively) amino acids that form the binding motif (Wang *et al.*, 2003a). An important outcome of this metal ion interaction is the partial neutralisation of the negatively charged carboxyl group, which increases the overall hydrophobicity of the EC2 loop. This precipitates the radical conformation change shown in Figure 5.1.2b, where the neutralised EC2 domain is now more hydrophobic than the preceding transmembrane region (TM4) and is therefore able to insert itself into the membrane and force the TM4 region into the cytoplasmic environment.

This structural change allows the olfactory receptor to adopt its active conformation (Figure 5.1.2b), with the former EC2 loop now a transmembrane region associated with a metal ion and the former TM4 domain greatly enlarging the second intracellular loop (IC2) in the cytoplasm of the cell. The EC2 loop and co-ordinated metal ion form an essential part of the odorant-binding domain.

An odorant in the environment interacts with the active receptor *via* its binding site residues and importantly also with the metal ion (Figure 5.1.2c). In the absence of an odorant molecule, the metal ion adopts a tetrahedral formation with three co-ordinate bonds to the three residues of the metal ion-binding motif (H, C and D/E) and a water molecule as the final ligand. When an odorant enters the olfactory receptor-binding site there is a switch whereby it displaces the water molecule as the fourth ligand. This ligand change results in alterations of the electron distribution around the metal centre such that the previously partially neutralised carboxyl group regains some of its charged character thus decreasing the net hydrophobicity of the EC2 domain. As a result, the TM4 region originally forced into the cytoplasm upon metal ion binding displaces the EC2 domain forcing it to return to its extracellular

position and the olfactory receptor back into its inactive conformation (Figure 5.1.2d).

After the odorant-induced ejection of the EC2 domain from the transmembrane region, the odorant leaves the receptor (potentially due to the loss of additional contacts with amino acid residues in the binding site). The fourth co-ordinate ligand position around the metal ion is taken up by a water molecule and the olfactory receptor reforms its active conformation (Figure 5.1.2b) in readiness for the next odorant interaction.

Crucially, this "shuttlecock" movement also involves large shifts in the cytoplasmic side of the receptor where the IC2 domain enlarged during the initial metal ion binding, shrinks back to its original size. This movement could potentially hold the key to activation of the G protein signal transduction cascade.

Supporting evidence: metal ions in the olfactory system Anatomical analysis of the central nervous system has shown that Cu^{2+} and Zn^{2+} ions are present in relatively high concentrations in specific regions of the rat brain including the olfactory bulb (Kofod, 1970; Donaldson *et al.*, 1973) and levels of Zn^{2+} were also reported to be high in ORNs (Horning and Trombley, 2001). This means that these ions, amongst the most commonly found in metalloproteins, are found in the necessary locations for incorporation into olfactory receptor proteins.

Supporting evidence: Genetic analysis of human olfactory receptor sequences The co-ordination of zinc and copper ions in a putative receptor would require amino acid residue binding motifs incorporating nitrogen and sulphur-containing sidechains. Sequence analysis of the human olfactory receptor genome demonstrates that 70% of human olfactory receptors listed in the SWISS-PROT database contain the metal-binding motif HxxCD/E previously found in known metalloproteins such as the plant

protease papain (Friedman, 1973; Wang *et al.*, 2003a). Such a high rate of conservation in a microsmatic mammal such as humans, by comparison to the >40% sequence conservation that defines a receptor family lends credence to the idea that this motif does play a role in odorant detection.

Supporting evidence: synthetic peptides The potential impact of metal ion binding on the secondary/tertiary structure of the olfactory receptor was highlighted by peptide chemistry and computational analysis of the comparative hydrophobicity of receptor domains.

Assignment of putative transmembrane regions based on the primary sequence of a protein is performed by computational analysis of the overall hydrophobicity of a given stretch of amino acids using the hidden Markov model predictive algorithm. Analysis of the human olfactory receptor hOR o2d2 yields a hydrophobicity plot showing seven regions with sufficient hydrophobicity to be assigned as putative transmembrane-spanning domains (Figure 5.1.3). The analysis of some receptor sequences e.g. hOR o2d2 revealed that although the hydrophobicity values of TM4 > EC2 suggesting that TM4 is indeed the transmembrane region, the values are very close (Table 5.1.1). The relative values change however upon the neutralisation of a glutamate residue found in EC2. The hydrophobicity of the EC2 domain becomes greater than the hydrophobicity of TM4, potentially providing the favourable energetic conditions for the insertion of EC2 into the transmembrane region and displacement of TM4 (Wang *et al.*, 2003a).

In the above scenario, neutralisation of the glutamate residue was performed *in silico via* the sequence mutation E180V. However experimental evidence using larger peptides supports the theoretical possibility of charge neutralisation leading to conformation change and membrane insertion of protein domains. Studies into the

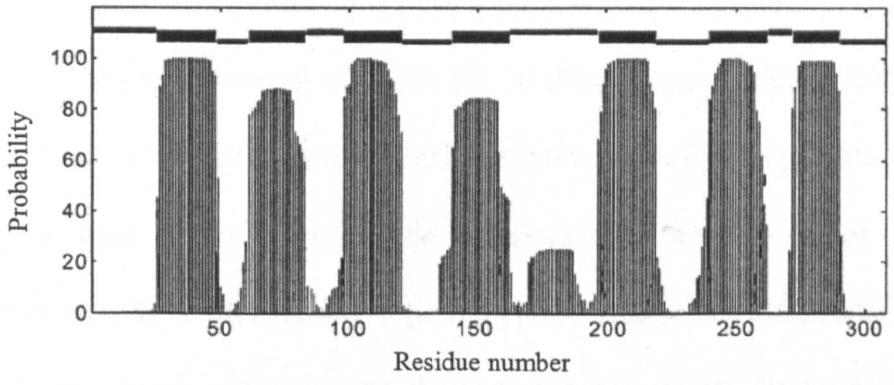

Figure 5.1.3 Hydropathy plot illustrating the probability of each amino acid being in a transmembrane region

This hydropathy plot predicts that the native human olfactory receptor hOR o2d2 adopts a seven transmembrane spanning conformation.

Source: Wang *et al.* (2003a)

Receptor region	Residues	Hydrophobicity scores	
		Charged E180	*Neutralised E180*
TM4	140-162	21.9	21.9
EC2	170-192	21.1	24.3
TM5	197-219	39.9	39.9

Table 5.1.1 The EC2 region of the human olfactory receptor hOR o2d2 becomes more hydrophobic than the preceding transmembrane domain TM4 if the charge on its glutamate residue is neutralised

Hydrophobicity scores given are on the Kyte-Doolittle scale.

Data source: Wang *et al.* (2003a)

mechanism of spontaneous insertion of α-helices into lipid bilayers were performed using a 36-residue peptide corresponding to residues in the third transmembrane-spanning region of the bacterial sensory receptor bacteriorhodopsin (Hunt *et al.*, 1997). In these experiments one of the aspartate residues present in the peptide was neutralised by the lowering of buffer pH. In the presence of lipids this lead to both the adoption of a well-ordered α-helical conformation by the peptide and insertion into the lipid phase. The peptide therefore was able to adopt an α-helical conformation in a pH-dependant (thus peptide charge state-dependant) and lipid-dependant manner and overcome the energy requirements for lipid insertion. The formation of the α-helical structure is particularly significant for membrane insertions as theoretically this may be the most energetically favourable conformation for a hydrophobic stretch of amino acids to cross a membrane bilayer (Engelman and Steitz, 1981).

Although this synthetic peptide had a sequence derived from a non-GPCR protein, experiments have also been performed on the synthetic pentapeptide HAKCE, a soluble form of the putative metal binding motif from olfactory receptors (Wang *et al.*, 2003a). Circular dichroism measurements demonstrated that in the presence of Cu^{2+}, Zn^{2+} and Ni^{2+} the peptide assumed an α-helical structure not previously observed in a such a short peptide. This suggests that the IC2 loop containing the metal binding motif may be capable of forming an α-helical structure upon metal co-ordination. Furthermore the addition of the cation may also act as a neutralising agent, the equivalent of a lower pH in the aspartate receptor peptide example above, allowing the region to become more closely associated with the lipid membrane and potentially spontaneously insert into it.

Supporting evidence: odorant thresholds The metalloprotein hypothesis can be applied to data on the relative human olfactory thresholds for alkane, alcohol, amine and thiol odorants. The range of olfactory sensitivities to thiol-containing compounds in comparison with similar structure alcohols and alkane odorants (detection thresholds for methylthiol = 1 ppb versus methanol detection at levels >100 ppm and methane undetectable at 10^6 ppm) may be better explained by the metal-ion binding properties of these molecules than the invocation of van der Waal's interactions and hydrogen bond potential (Wang *et al.*, 2003a). The specific properties in question govern the Lewis basicity of a compound; how readily it will donate one of its electrons to form a co-ordinate bond with a metal cation. The greater the basic character, the more readily a compound forms co-ordinate bonds with a metal ion and thus according to the metalloprotein hypothesis, the greater the sensitivity of a metal incorporating olfactory receptor to the given odorant. This provides a plausible explanation for the significantly increased sensitivity of the mammalian olfactory system to thiol odorants (Wang *et al.*, 2003a).

Lewis basicity not only explains thiol sensitivity but also the observation that α-substitution of thiols decreases the detection threshold of the odorant whereas an identical substitution with alcohol compounds increases the threshold. The threshold change could be the result of increased steric hindrance. This explains the result with alcohol odorants but also necessitates the involvement of an alternative receptor interaction mechanism capable of negating the steric effects to some degree in order to explain the thiol odorant observations. The additional sensitivity to α-substituted thiol compounds can be explained in terms of increasing Lewis base character, where the structural change results in a greater potential for donation of electrons to a metal ion and therefore lower thresholds of detection (Wang *et al.*, 2003a).

Supporting evidence: G protein-coupled receptor mutagenesis experiments In addition to suggesting a putative mechanism for odorant sensitivity, the metalloprotein also provides an intrinsic method of G protein activation involving the IC2 domain, which is significantly modified by the ejection/re-insertion of the TM4 region.

Mutagenesis experiments with bovine rhodopsin, a protein often used to model the 3D structure of olfactory receptors (Floriano *et al.*, 2000; Singer *et al.*, 2000) implicates the 2nd cytoplasmic loop alongside the 3rd cytoplasmic loop in G protein activation and binding (Franke *et al.*, 1992; Hedin *et al.*, 1993). Studies on the more distantly related β-adrenergic receptor have also provided evidence that individual residues in the second cytoplasmic loop may be involved in G protein activation (O'Dowd *et al.*, 1988).

5.1.3 Dual reagent protein labelling strategy

The selective labelling and crosslinking of cysteine residues has been used previously to characterise membrane-bound receptor proteins. Many of these experiments involved the artificial introduction of cysteine residues into putative sites on a receptor protein and have yielded information on the variable oligomeristation states of bacterial chemoreceptors (Milligan and Koshland, 1988), the secondary/tertiary structure of proteins (Kalomiris and Coller, 1985; Falke *et al.*, 1988; Fujinaga *et al.*, 1999) and has also shown that activation of signal transduction pathways by bacterial chemoreceptors requires the movement of two helices within subunits of a homodimer (Lee *et al.*, 1995). The putative identification of proteins within the 55kDa band as olfactory receptor proteins and the extensive and well-conserved labelling of the band by both I-LC-biotin and LYIA reagents (see Chapter

4, results section) provides the opportunity to use this mode of structural analysis to investigate whether or not a conformational change occurs with olfactory receptors in response to the presence of divalent metal cations.

The dual reagent protein labelling strategy is illustrated in Figures 5.1.4 and 5.1.5. Figure 5.1.4 illustrates the sequential labelling of a hypothetical olfactory receptor using the membrane-impermeable sulphydryl-targetting reagent LYIA to derivatise free, exposed extracellular cysteine residues. This initial labelling step is followed up by the use of I-LC-biotin, a membrane-permeable reagent that attaches a biotin tag to any remaining exposed cysteine residues whether they are intracellular or in a hydrophobic i.e. transmembrane environment. If the dual reagent labelling experiments are performed in buffers with and without the metal-chelating agent EDTA it allows the detection of any conformation change in an olfactory receptor resulting from the availability of divalent metal cations in the environment (Figure 5.1.5).

The hypothetical olfactory receptor in its non-metal bound state has two extracellular cysteine residues on the N-terminal tail and the second extracellular loop (EC2), one cysteine residue within the transmembrane region and a fourth cysteine residue in the first cytoplasmic loop (IC1). Under these conditions/this conformation, two residues are available for LYIA-labelling and the remaining two are accessible only to the membrane-permeable I-LC-biotin reagent.

According to the metalloprotein hypothesis, if divalent metal cations are present in the environment, this hypothetical olfactory receptor (which contains the putative metal binding motif) will bind the ion and adopt the metal-bound conformation illustrated in Figure 5.1.5. The adoption of this alternative state changes the distribution of the cysteine residues and their accessibility to the

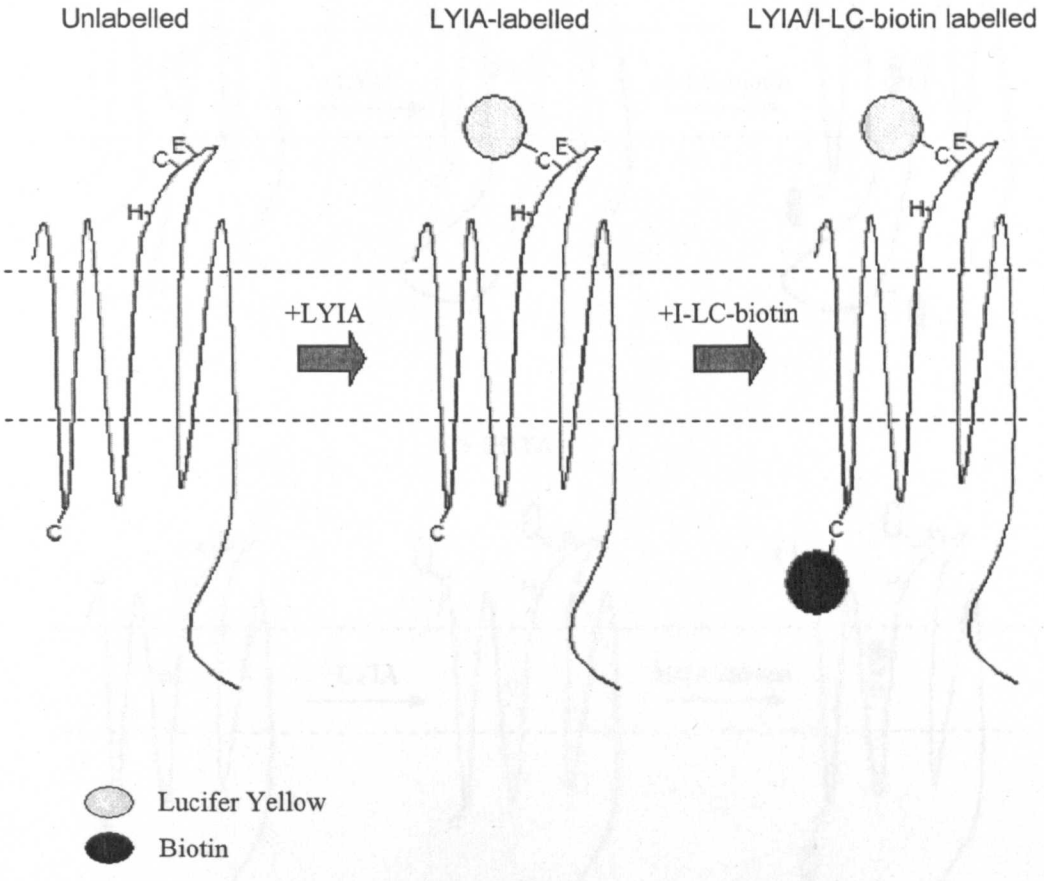

Figure 5.1.4 Dual reagent labelling of a hypothetical olfactory receptor

The hypothetical olfactory receptor is a seven transmembrane-spanning protein with one is intracellular and one extracellular cysteine residues. Treatment of the receptor with the membrane-impermeable reagent Lucifer-Yellow Iodoacetamide (LYIA) attaches a fluorescent group to the external cysteine residue. Subsequent treatment with a membrane-permeable reagent Iodoacetyl-long chain-biotin (I-LC-biotin) attaches a biotin tag to the remaining exposed cysteine residue.

The dashed line indicates the borders of the lipid bilayer, the top line representing the extracellular face of the membrane.

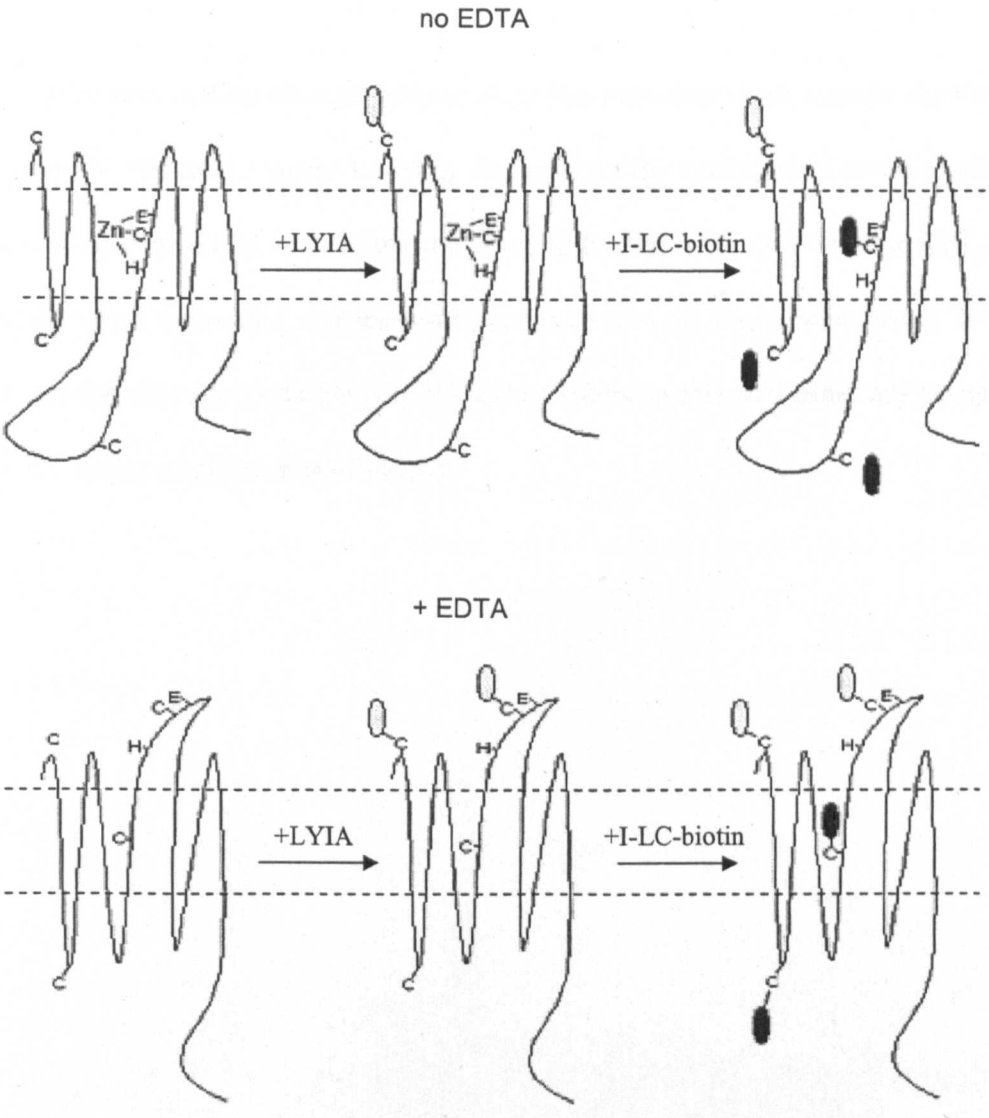

Figure 5.1.5 The predicted results of dual reagent labelling of a hypothetical putative metal-binding olfactory receptor in buffers containing EDTA

The dual reagent strategy can be used to detect the different conformations adopted by olfactory receptors by using cysteine-targeting reagents in the presence/absence of EDTA and thus the effects of divalent metal ions on receptor structure.

The dashed line indicates the borders of the lipid bilayer, the top line representing the extracellular face of the membrane. This receptor structure is hypothetical except for the positions of the cysteine residues in TM4 and EC2 regions, which are highly conserved across olfactory receptors (Buck and Axel, 1991; Chess *et al.*, 1992)

labelling reagents. In this conformation, only one cysteine residue is now accessible to the membrane-impermeable LYIA reagent and three will be labelled by I-LC-biotin.

The conformation change proposed by the metalloprotein hypothesis should be observed in this dual reagent labelling strategy *via* the comparison of the extent of chemical modification by each of the reagents, in buffers with and without EDTA. If the fluorescence decreases and biotinylation increases in the 55kDa band, it will support the hypothesis the binding of divalent cations to selected olfactory receptors results in a major conformational change.

5.2 Method Development

For the successful application of the dual reagent strategy to conformational studies of olfactory receptors three main criteria have to be fulfilled. Firstly the activity of the reagents should not be heavily influenced by their use in alternative buffers. The label detection scheme must be sufficiently sensitive to allow any differences between samples to be detected and quantified. Finally the use of reagents consecutively and alternative reaction buffers should not lead to tissue damage specific to either reagent or buffer conditions.

As PBS/EDTA buffer has been used previously in both Lucifer Yellow Iodoacetamide (LYIA) and Iodoacetyl-long chain-biotin (I-LC-biotin) reactions it was decided that PBS/EDTA, alongside an identical PBS buffer without the addition of 2mM EDTA, would be used as the buffers during the dual reagent labelling experiments (see Section 2.1 for buffer recipes). The labelling efficiency of both LYIA and I-LC-biotin in the two buffers were tested during time course experiments.

5.2.1 Time course experiments

Time course experiments were conducted using bovine serum albumin (BSA) as the protein substrate for LYIA and I-LC-biotin. All samples were kept in the dark where possible. Protein labelling was assessed by SDS-PAGE analysis (Figure 5.2.1). LYIA labelling was visualized by UV imaging of the unstained gel. A second gel was run and the resolved proteins blotted onto nitrocellulose. Biotin tags from I-LC-biotin were then detected using a streptavidin-AP conjugate as described in Section 2.9.

The results of these time course experiments indicate that the efficiency of the LYIA labelling reaction is very similar in PBS and PBS/EDTA buffers. The

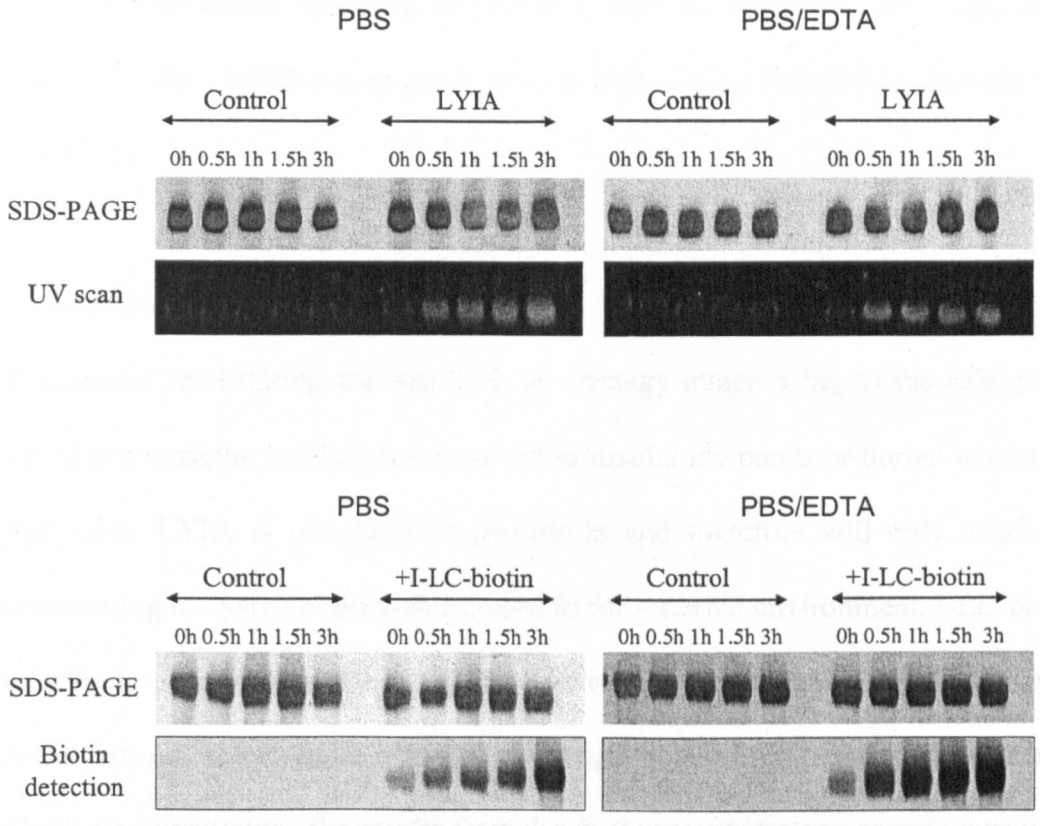

Figure 5.2.1 Sulphydryl targetting reagents show similar reaction rates in PBS buffers with or without added EDTA

Reaction mixtures consisted of added to 500µl PBS or PBS/EDTA buffer containing 50µg BSA to which 15µl I-LC-biotin or 25µl LYIA stocks were added. Mixtures were briefly vortexed and incubated in the dark at room temperature with agitation on a rotary wheel. Reactions were terminated at time points 0h, 0.5h, 1h, 1.5h and 3h, by the addition of 500µl 200mM DTT prepared in an identical buffer to that used during the labelling procedure. Samples were then vortex mixed and excess reagent removed by desalting using 0.5ml Vivaspin® columns (10000Da Mw cut-off point, polyethersulphone membrane, purchased from Vivascience, Surrey, UK). The Vivaspin® column desalting procedure was performed according to the manufacturer's instructions.

analysis of I-LC-biotin labelling again suggested sufficient similarity of reaction rates in the two buffers for their use in these experiments. The difference observed may also have been a property of the model protein used as analysis of the buffers from subsequent tissue labelling experiments gave no indication of a significant difference in the I-LC-biotin reaction rates in PBS versus PBS/EDTA buffers (see Figure 5.2.2).

5.2.2 Detection of protein tags

Both reagents used during the dual reagent strategy attach a tag to the sulphydryl group of any cysteine residues not involved in disulphide bonds or buried within the protein core. LYIA is membrane-impermeable and therefore will only attach its fluorescent tag to cysteine residues exposed to the external environment. I-LC-biotin is membrane-permeable and can therefore derivatise free cysteine residues of both extracellular and intracellular proteins. Although both of these tags are detectable and both are quantitative, the results from the dual reagent strategy experiments were based upon the detection of the biotin tag. This was for two reasons, first the biotin detection signal was considered to be more stable than a fluorescent tag and secondly the method of biotin detection involves the enzyme activity of alkaline phosphatase which provides intrinsic amplification of a signal *i.e.* the greater the length of time allowed for enzyme activity/blot development, the stronger the signal becomes. This means that the detection of biotin tags, whilst remaining quantitative was considered likely to be the more sensitive method of label detection.

An additional advantage of basing the results on biotin tag detection is that the effects on I-LC-biotin labelling with and without prior LYIA exposure allows the

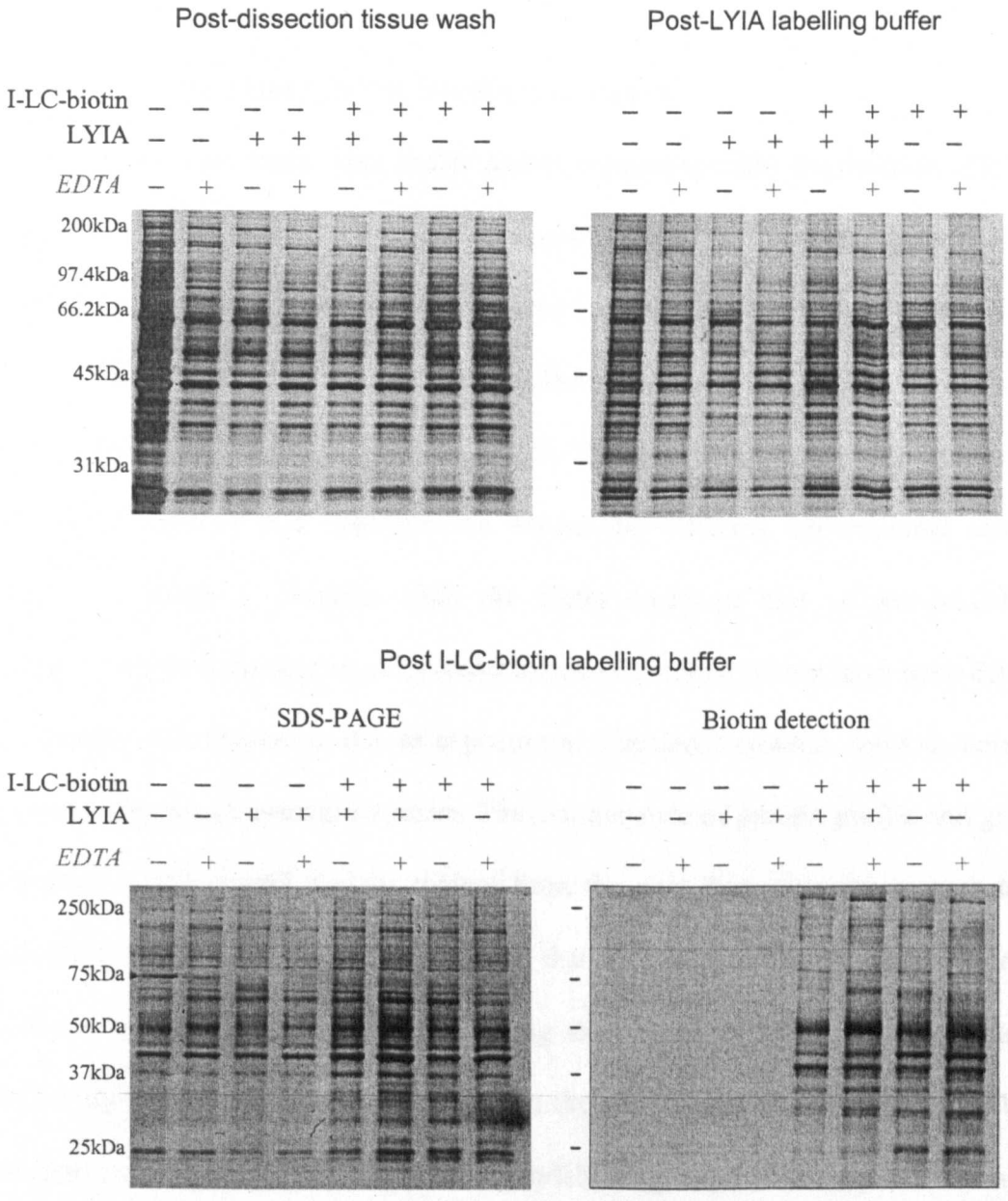

Figure 5.2.2 Analysis of tissue wash/post-labelling tissue buffers shows no evidence of buffer/reagent specific tissue damage or protein denaturation

The post-dissection tissue wash is the buffer used to wash the tissue immediately prior to the LYIA labelling procedure. The post-LYIA treatment buffer consisted of the labelling buffer used for the LYIA reaction. The post-I-LC-biotin treatment buffer was the buffer used for the I-LC-biotin reaction and was again also used to verify reagent activity.

Gel lanes contain equal loading volumes from each experiment.

detection of proteins modified by LYIA as these sites will no longer be accessible to I-LC-biotin.

5.2.3 Tissue degradation during labelling procedures

To verify whether there were buffer and/or reagent-specific degradation effects on the olfactory turbinates during the dual reagent labelling procedures, tissue wash and post-labelling reaction buffers were analysed by SDS-PAGE (Figure 5.2.2).

SDS-PAGE analysis indicated that there were no differences in tissue damage across the control and experimental groups. This can be seen from the similarity of the protein profile and concentration across the different experimental samples. Further evidence is obtained from the biotin detection blot of post-I-LC-biotin samples, where denaturation of proteins exposed to LYIA would have been detected by increased biotinylation due to exposure of additional cysteine residues normally buried in the native protein structure. The maintenance of protein profile and gradual decrease in the overall protein content from the post-dissection tissue wash to the post-I-LC-biotin labelling buffer suggests that the proteins present in the buffer are either a result of tissue damage occurring as a result of non-specific mechanical tissue breakage or are derived mainly from the lower layer of olfactory mucus being washed away during the subsequent wash/labelling steps. This explanation is also supported by the similarity in protein profile of all final olfactory cilia samples prepared during this work (Figure 5.3.1 and Figure 5.3.2).

5.2.4 Dual reagent labelling protocol

Tissue samples were washed using Krebs-Ringer or Krebs-Ringer/EDTA according to whether the samples were to be labelled in PBS or PBS/EDTA. Krebs-

Ringer/EDTA is used in the deciliation protocol described in Section 2.3 to remove extracellular mucus. The presence of EDTA ensured that as many of the free metal ions/ions associated with olfactory proteins were removed as possible in the metal ion labelling experiments. In experiments where the ions associated with the olfactory system were not chelated during the labelling reactions, Krebs-Ringer buffer lacking EDTA was used to ensure minimal removal of ions during tissue washes and labelling experiments.

LYIA-labelling was performed with dissected and washed tissue samples as described in Section 2.10. After the 30 min labelling period, the tissue was pelleted by a brief centrifugation 1000g, 3min before being resuspended in 1ml PBS/EDTA. The second reagent, I-LC-biotin was added to the resuspended tissue as described in Section 2.9. After the completion of all labelling reactions, enriched fractions of olfactory cilia were prepared as described in Section 2.3 and subsequently analysed by SDS-PAGE and biotin detection from a Western blot.

5.3 Results

5.3.1 Analysis methods

The results of these experiments were determined by the analysis of the SDS-PAGE gels and corresponding biotin detection blots by densitometry. The use of densitometry allowed the analysis of the biotinylation of individual bands of interest. The intensity of biotin detection was divided by the intensity of the staining of the corresponding band in the SDS-PAGE gel to give the degree of biotinylation of a given protein band. The values for degree of biotinylation are therefore corrected for protein concentration. Alongside determination of the degree of biotinylation for each sample, the ratio of biotinylation relative to other samples in the same experiment was also calculated. This provides figures for the relative changes in I-LC-biotin in samples pre-treated with LYIA and labelled under different buffer conditions.

During the densitometric analysis both the detection of biotin tags and silver staining intensity were assumed to be linear. The enzymatic process that produces the insoluble, coloured precipitate requires two chemicals (BCIP and NBT), which are present in excess in the development solution, therefore the intensity of the precipitant following biotin detection is dependant on the concentration of the alkaline-phosphatase in a given region. Silver staining has significant linearity problems when observing samples containing different proteins but as all comparisons are made from identical bands from olfactory cilia preparations this was not considered to be a problem during data analysis.

The changes in ion concentration of the buffers in the presence of EDTA is unlikely to result in major protein modifications as it represents an increase in ionic

strength of 11mM in Krebs-Ringer/EDTA and 5.5mM in PBS/EDTA in buffers that already contain ~150mM and 170mM inorganic salts respectively.

5.3.2 First dual reagent differential labelling experiment

The SDS-PAGE replica gel and biotin detection blot are shown in Figure 5.3.1, the densitometry results are provided in Table 5.3.1. The biotin detection blot shows two intensely stained bands. The first band at approximately 50-55kDa (referred to subsequently as the 55kDa band) was putatively identified in Chapter 4 as containing tubulin proteins and also olfactory receptor proteins. As tubulin is a cytoskeletal protein with well-established intracellular localisation, any changes in the biotinylation intensities between samples pre-treated with LYIA (dual reagent experiments) and those labelled with I-LC-biotin alone (single reagent experiments) are likely to be solely due to effects on the receptor proteins.

The second protein band has an approximate mass of 40kDa and was identified in Chapter 4 as coincident with actin isoforms. Additional tandem mass spectrometry experiments suggested that there are some peptides that may be derived from olfactory receptor like proteins, however where as the peptide mass fingerprints indicate the actin identification is statistically significant the peptide sequence data is far from conclusive (for further discussion see Chapter 4).

5.3.3 I-LC-biotin labelling of the 55kDa band

Labelling in PBS v PBS/EDTA There is a difference in relative biotinylation in buffers with and without EDTA and therefore limited free divalent cations. This supports the idea that the presence of free metal ions in the receptor environment can influence the conformation of the receptor proteins. Contrary to the metalloprotein

Full-view rat olfactory cilia labelling analysis

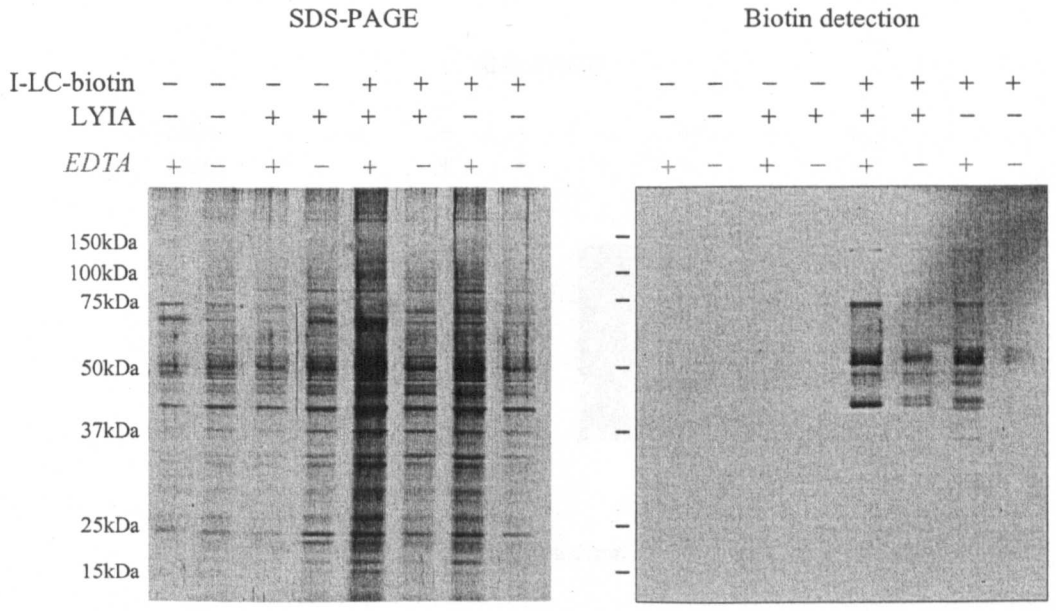

Figure 5.3.1 Dual reagent labelling of rat olfactory cilia proteins
Freshly dissected turbinates were washed using Krebs-Ringer or Krebs-Ringer/EDTA and resuspended in lml PBS or PBS/EDTA. Tissue samples were then treated with LYIA (50µl 6.5mg/ml stock), the labelling reaction performed as described in Section 2.10. Tissue samples were then centrifuged and resuspended in 1ml fresh PBS or PBS/EDTA to which 30µl I-LC-biotin was added. The I-LC-biotin reaction proceeded over 1h, before the labelling buffer was removed and enriched cilia fractions were prepared according to the protocol described in Section 2.3. Cilia preparations were resolved on a large-format SDS-PAGE gel and blotted onto a nitrocellulose membrane for biotin detection.

An enlarged view of the 35-60kDa region of both the biotin detection blot and corresponding gel is provided overleaf.

Enlarged view of 35-60kDa region

SDS-PAGE

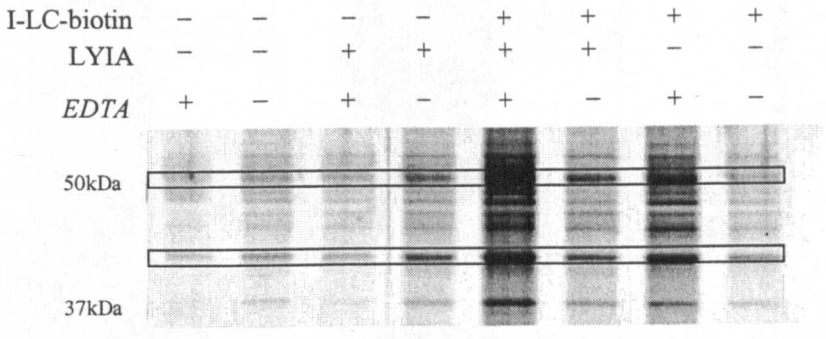

Biotin detection

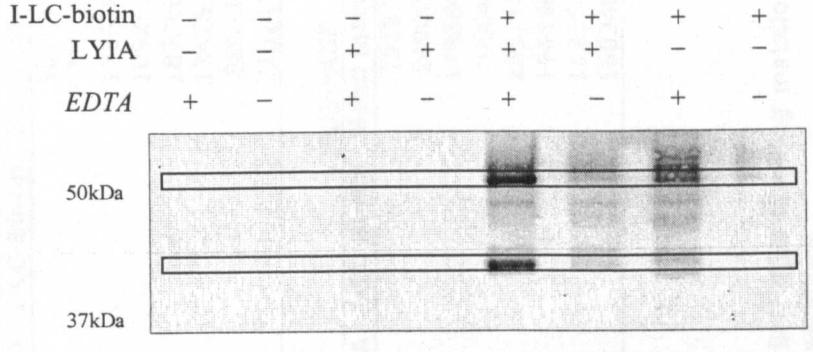

				SDS-PAGE	*Biotin detection*		
Band	**Labelling buffer**	**LYIA**	**I-LC-Biotin**	**Band intensity**	**Band intensity**	**Degree of biotinylation**	**Relative biotinylation**
55kDa	PBS			107048			
	PBS/EDTA			72802			
	PBS	+		173678			
	PBS/EDTA	+		109291			
	PBS	+	+	182260	19548	0.11	1.00
	PBS/EDTA	+	+	134259	143696	1.07	9.98
	PBS		+	88683	10410	0.12	1.09
	PBS/EDTA		+	215244	73840	0.34	3.20

				SDS-PAGE	*Biotin detection*		
Band	**Labelling buffer**	**LYIA**	**I-LC-Biotin**	**Band intensity**	**Band intensity**	**Degree of biotinylation**	**Relative biotinylation**
40kDa	PBS			73197			
	PBS/EDTA			24902			
	PBS	+		148584			
	PBS/EDTA	+		49004			
	PBS	+	+	155714	7135	0.05	2.19
	PBS/EDTA	+	+	194398	161856	0.83	39.85
	PBS		+	112554	13543	0.12	5.76
	PBS/EDTA		+	160340	3350	0.02	1.00

Table 5.3.1 Analysis of the first dual labelling metalloprotein experiment by reveals differential biotinylation of two major proteins in olfactory cilia preparations

The ratio of biotinylation for the 55kDa band shows an increase in biotinylation in the presence of EDTA and a further increase in biotinylation when pre-treated with LYIA.

The ratio of biotinylation for the 40kDa band shows the highest levels of biotinylation when pre-treated with LYIA in the presence of EDTA. Interestingly it also showed a 5-fold increase in relative biotinylation when labelled with I-LC-biotin only, in PBS without any added EDTA.

hypothesis discussed however, the increased levels of biotinylation observed in EDTA-containing buffers suggest that cysteine residues are more likely to be in a transmembrane or intracellular environment in the absence rather than presence of divalent metal cations.

Potential increase in cysteine reactivity The increase in biotinylation between 55kDa proteins labelled in PBS/EDTA *versus* PBS is maintained in both the dual reagent and I-LC-biotin alone reactions. This suggests that the accessibility of the cysteine residues may not be the only factor in determining I-LC-biotin labelling intensity. The intensities of the I-LC-biotin labelled bands should be largely unaffected by the conformational switch of a cysteine residue from an external to transmembrane domain, as this is unlikely to affect its accessibility to I-LC-biotin and further, there has been no pre-treatment with LYIA. This means that biotin detection intensities should be approximately equal as there should be an identical limited number of accessible cysteine residues in the receptors accessible for labelling in both samples. That intensity still increases even without prior LYIA treatment is consistent with the conformational change occurring in response to the lack of free metal ions also results in the increased reactivity of selected cysteine residues.

An increase in cysteine reactivity is defined as changes in the environment of a cysteine residue that leads to its sulphydryl group being more likely to react with the targeted labelling reagents within the time period allowed for labelling reactions to occur. The labelling experiments do not differentiate between increases in cysteine reactivity due to increased numbers of cysteine residues physically exposed or influences on their intrinsic reactivity. Therefore cysteine reactivity can effectively be altered by modification of the immediate chemical environment of the residue *e.g.*

during intracellular tertiary structure re-arrangements (sulphydryl groups become more reactive when positioned close to polar and/or charged groups - Friedman, 1973), or structural changes exposing additional cysteine residues to I-LC-biotin.

Effects of extracellular cysteine residue derivatisation In samples labelled in PBS buffer, biotinylation was lower in the LYIA/I-LC-biotin experiment than by I-LC-biotin alone. This supports the existence of an extracellular cysteine residue in at least some receptors. This result is not mirrored by the results of labelling experiments performed in PBS/EDTA buffer. The biotin detection intensity of the LYIA/I-LC-biotin samples is just over 3-fold greater than the corresponding sample labelled only with I-LC-Biotin. An increase in cysteine reactivity during a conformational change in response to the absence of co-ordinated/free metal ions as discussed above, accounts for part of the increase relative to PBS labelling samples but these results also suggest a structural impact of the derivatisation of external cysteine residues. One explanation is that there are multiple co-operating methods of increasing cysteine reagent reactivity. Structural changes occur in receptors exposed to EDTA that increase the reactivity of intracellular cysteine residues (intracellular/transmembrane as not blocked by LYIA) as shown by the single I-LC-biotin labelling experiments. A second tertiary structure change resulting from the derivatisation of an external cysteine residue may in addition lead to the exposure of previously inaccessible sites. This could be the result of denaturation however as no proteins in the post-I-LC-biotin labelling buffer samples showed signs of denaturation by heavily increased biotin labelling (Figure 5.2.2) this explanation is unlikely. It is perhaps more plausible that protein packing has altered in the intracellular domains of the receptor (again intracellular/transmembrane as these are not blocked by LYIA treatment). The internalisation of cysteine residues in response

to derivatisation/absence of metal ions that would otherwise be blocked by LYIA treatment increases the number of cysteine residues available for biotinylation however this would not increase levels of biotinylation above those observed for single reagent experiments as the number of sites available for labelling has not changed unless these residues also increased in their reactivity.

In summary, the results of the initial dual labelling experiment to determine whether the putative olfactory receptors identified in the 55kDa band of olfactory cilia preparations are metalloproteins support the hypothesis that receptor structure is mutable via the presence/absence of divalent cations in the environment. They do however point to a different mechanism than that proposed by Wang *et al* (2003a) as they suggest that less rather than more cysteine residues are exposed to the olfactory mucus environment in the presence of divalent cations.

5.3.4 I-LC-biotin labelling of the 40kDa band

The major fluctuation in biotinylation of the 40kDa band, under different conditions was unexpected. Relative biotinylation of the 40kDa band peaked at a 40-fold difference between dual and single reagent labelling in PBS/EDTA, suggesting that the derivatisation of external cysteine residues in the tissue has had a major impact upon the structure of the protein. As this protein band appears (from MALDI spectra of 40kDa band in sheep and rat olfactory cilia samples) to be dominated by isoforms of actin *i.e.* intracellular proteins, it is likely that LYIA derivatisation is acting indirectly on proteins within this band *via* other LYIA-sensitive proteins. There is also limited evidence that there are olfactory receptor-like proteins in this band. In order to achieve this great a difference in biotinylation these would have to potentially represent a subclass of receptors that respond to the absence of metal ions

and derivatisation of its external cysteine residues in a much greater manner than those in the 55kDa band, a possibility that cannot be discounted. A third explanation to account for such a large increase is that a combination of the above factors is occurring *i.e.* the structure of the receptors is being directly affected by the derivatisation in an identical manner to that observed in the 55kDa band and also the structure of actin is being influenced indirectly by these receptor proteins or others sensitive to the derivatisation of external residues. Verification of the significance of these findings requires confirmation by a replicate dual labelling experiment.

5.3.5 Second dual reagent differential labelling experiment

The results from the second dual labelling experiments also suggested that the presence or absence of EDTA in the labelling buffer may have an effect on the structure of the proteins present in the 55kDa and 40kDa bands of a SDS-PAGE gel. However these results show differences on a much smaller scale than the first experiment and do not unequivocally support the hypothesis of olfactory receptors being metalloproteins. It must be noted that although the experimental results appear to implicate metal ions involvement in protein structure, as observed via cysteine residue exposure they do not provide evidence for the shuttlecock mechanism of receptor motion proposed by the metalloprotein hypothesis (Wang *et al.*, 2003a).

The biotin detection blot and replica SDS-PAGE gel are shown in Figure 5.3.2. The results of the densitometry analysis of the dual reagent protein labelling are given in Table 5.3.2. The relative biotinylation levels for both the 55kDa and 40kDa bands are much reduced by comparison to the results from the previous experiment. This is unlikely to be the result of a reduction in reagent activity as shown by the sustained biotinylation in all samples.

Full-view rat olfactory cilia labelling analysis

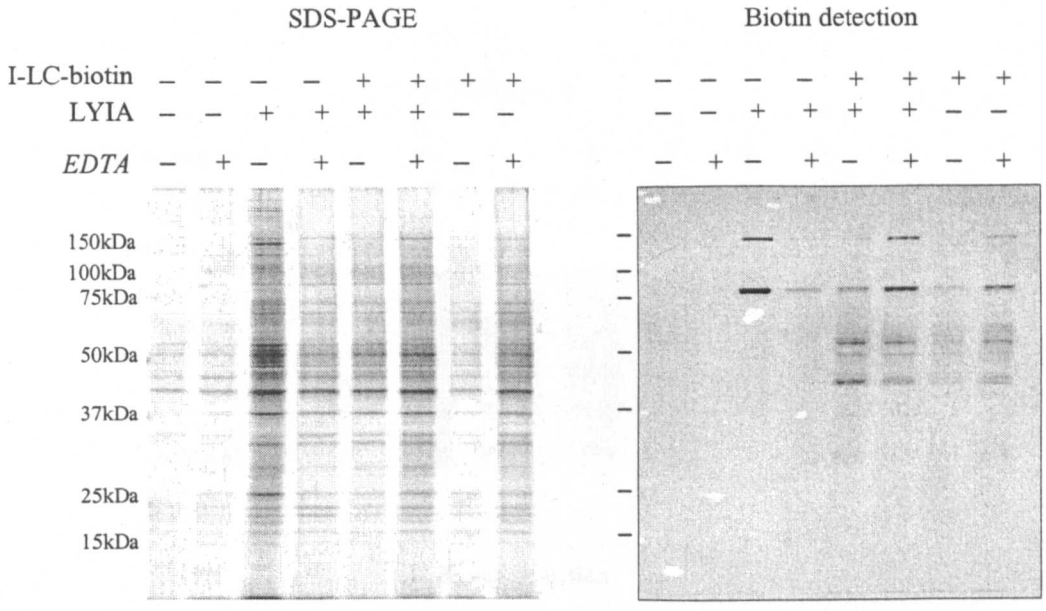

Figure 5.3.2 Second dual reagent labelling experiment performed using rat olfactory cilia proteins

Freshly dissected turbinates were washed using Krebs-Ringer or Krebs-Ringer/EDTA and resuspended in lml PBS or PBS/EDTA. Tissue samples were then treated with LYIA (50µl 6.5mg/ml stock), the labelling reaction performed as described in Section 2.10. Tissue samples were then centrifuged and resuspended in 1ml fresh PBS or PBS/EDTA to which 30µl I-LC-biotin was added. The I-LC-biotin reaction proceeded over 1h, before the labelling buffer was removed and enriched cilia fractions were prepared according to the protocol described in Section 2.3. Cilia preparations were resolved on a large-format SDS-PAGE gel and blotted onto a nitrocellulose membrane for biotin detection.

An enlarged view of the 35-60kDa region of both the biotin detection blot and corresponding gel is provided overleaf.

Enlarged view of 35-60kDa region

SDS-PAGE

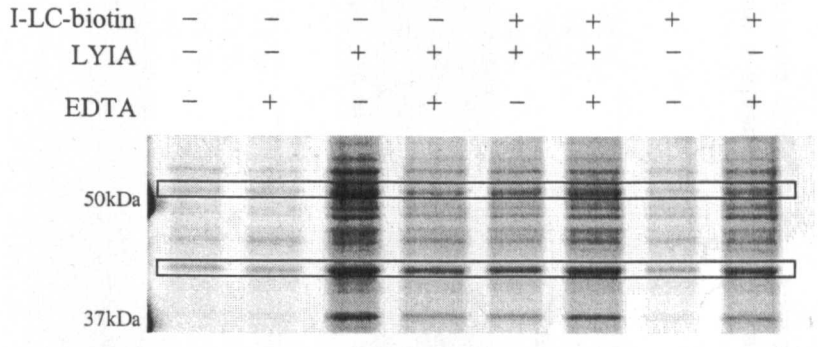

Biotin detection

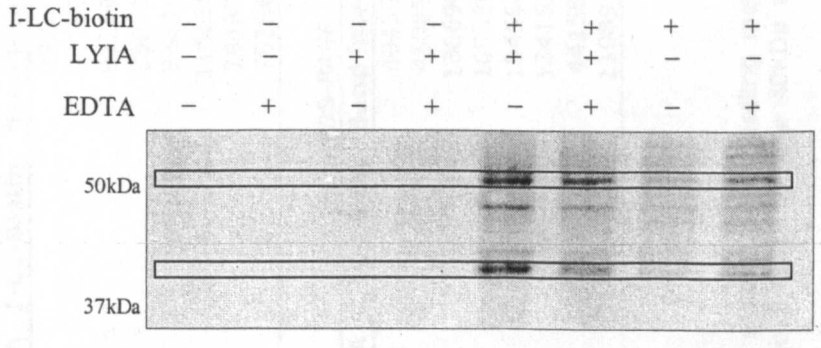

				SDS-PAGE	*Biotin detection*		
Band	**Labelling buffer**	**LYIA**	**I-LC-Biotin**	**Band intensity**	**Band intensity**	**Degree of biotinylation**	**Relative biotinylation**
55kDa	PBS			29267			
	PBS/EDTA			32389			
	PBS	+		91219			
	PBS/EDTA	+		85006			
	PBS	+	+	94483	91104	0.96	1.62
	PBS/EDTA	+	+	115098	68607	0.60	1.00
	PBS		+	28487	32271	1.13	1.90
	PBS/EDTA		+	75264	52225	0.69	1.16

				SDS-PAGE	*Biotin detection*		
Band	**Labelling buffer**	**LYIA**	**I-LC-Biotin**	**Band intensity**	**Band intensity**	**Degree of biotinylation**	**Relative biotinylation**
40kDa	PBS			40430			
	PBS/EDTA			45085			
	PBS	+		136690			
	PBS/EDTA	+		109530			
	PBS	+	+	104560	91339	0.87	3.75
	PBS/EDTA	+	+	134153	56332	0.42	1.80
	PBS		+	44158	10287	0.23	1.00
	PBS/EDTA		+	110891	29971	0.27	1.16

Table 5.3.2 Analysis of the second dual labelling metalloprotein experiment suggests a much smaller scale of differential biotinylation with and without EDTA of the 40kDa and 55kDa bands and directly contradicts the results from the first experiment.

5.3.6 Replicate labelling experiment: 55kDa band

The relative biotinylation for protein labelling conducted in PBS and PBS/EDTA both show increased values in the I-LC-biotin only experiments. This supports the observation that selected proteins in the 55kDa band have external cysteine residues that are blocked from I-LC-biotin labelling by pre-treatment with LYIA. The consistency of this pattern in both PBS and PBS/EDTA experiments suggests that there are no major structural changes caused by derivatisation of external cysteine residues under either buffering conditions that affect the total number of cysteine residues available for reactions with the labelling reagents.

A comparison of the differences in biotin detection intensity during labelling procedures conducted in PBS and PBS/EDTA show a decrease in relative biotinylation of the 55kDa band in the latter buffer. This might be interpreted as an increase in cysteine residues accessible to the membrane-impermeable reagent LYIA. This result appears to directly contradict the findings of the previous experiments however if the results are looked at more closely: biotin intensity in both buffers appears to increase by very similar percentages, 17% and 16% in the PBS and PBS/EDTA experiments respectively. This suggests that differences between the buffers in these experiments originate from total numbers of cysteine residues accessible to both reagents rather than differential exposure of residues under different conditions of divalent cation availability in the receptor environment.

This could arise from experimental procedures influencing the accessibility of labelling reagents to the target proteins *e.g.* the differential removal of mucus by the buffers with and without EDTA. Alternatively the presence/absence of metal ions in the environment may influence protein structure by resulting in changes in the packing of extracellular loops of olfactory receptors. This structural rearrangement

could bury cysteine residues within to centre of a globular structure therefore removing those cysteine residues from the pool that are accessible to either reagent. In this manner, the experiments may provide evidence of a mutable receptor structure dependant on the presence or absence of metal ions in the environment however this would only be one possible interpretation of the data and therefore no conclusions can be made.

5.3.7 Replicate labelling experiment: 40kDa band

Analysis of the relative biotinylation of the 40kDa band in the second dual labelling experiment reveals that one set of conditions (PBS buffer, LYIA derivatisation) gives a markedly increased biotin detection signal as observed during the first differential labelling experiment. This result also mirrors the data from the first experiment in that the maximal level of biotinylation was achieved in a dual reagent-labelling sample *i.e.* was a combined result of the buffer conditions and the direct or indirect effects of the derivatisation of external cysteine residues.

The data differs however in that the highest intensity of biotinylation was observed in the PBS rather than PBS/EDTA. This hints at connectivity of the biotinylation states of the 55kDa and 40kDa bands. During the first experiment, the highest levels of biotinylation in 55kDa band were observed in the LYIA/I-LC-biotin experiment in PBS/EDTA buffer and these conditions also provided maximal biotinylation in the 40kDa band. In the second experiment the highest levels of biotinylation were attained during the use of both labelling reagents and despite being in PBS rather than PBS/EDTA, were again found in the same buffer for both 55kDa and 40kDa bands.

5.4 Discussion

5.4.1 Defining the role of metal ions in olfactory receptor structure/function

The first experiment clearly suggests that divalent metal cations *i.e.* metal ions able to be chelated by EDTA, have an impact on the intracellular/extracellular distribution of cysteine residues and the accessibility and reactivity of their exposed sulphydryl groups. The manner in which the distribution and reactivities appear to be altered however, directly contradict the metalloprotein hypothesis as explained in Section 5.1 of this chapter. According to the mechanism proposed in Wang *et al.* (2003a), these results (if replicated) would imply that instead of being a crucial part of odorant-receptor interactions, the role of metal ions in the primary events of olfaction is an inhibitory one.

The results from the second experiment argue against the findings of the first. In this case, the presence of metal ions leads to an increase in the accessibility of cysteine residues/sulphydryl group reactivity. This is seemingly supportive of the metalloprotein hypothesis and yet gives no indication of the changes in intracellular/extracellular distribution of cysteine residues that form the proposed mechanism by which the sequestration of metal ions by olfactory receptors leads to activated receptors and G proteins.

The purpose of the dual reagent labelling experiments was to provide evidence for the structural impact the presence/absence of metal ions may have on the structure of olfactory receptors and therefore on their function. In this aim these experiments must be considered as pilot studies. For accurate conclusions to be made the dual labelling studies must be replicated and issues of variability in the experimental process must be addressed. Further investigations into the protein species in the 40kDa band may confirm the presence of additional proteins other than

actin, which could potentially explain the LYIA-induced changes in the biotinylation intensity.

There are two main areas of potential variability in these experiments, the labelling reagents and the tissue samples. The impact of any deterioration of reagents during this work is considered negligible as the activity of reagents can be monitored by the continual comparison of the I-LC-biotin protein labelling of soluble proteins present in the labelling buffer. During each experiment the SDS-PAGE and biotin detection analyses were conducted on two gels with all the labelled olfactory cilia samples from that experiment loaded. This limits variability due to development and staining processes within a single experiment and although slight variability may between different experiments this is unlikely to be the major causal factor of the contradiction observed in this work. Experiments could be repeated with increased levels of proteins. This would enable the use of Colloidal Coomassie Blue, which would reduce any slight analytical biases caused by the use of silver staining techniques. The author's personal observation is that there is a limit on how many tissue samples should be deciliated in a single batch to ensure consistent protein profiles across all cilia preparations. Therefore, bulking up preparations carries a trade-off between protein concentration and efficient cilia isolation and enrichment.

Another potential source of experimental variability are the tissue samples and any differential effects that the buffers used during this study may have. The animals utilised were female Wistar rats approximately 200g. The animals came from two different sources and although this is unlikely to have any major impact upon the comparative health status of the animals, different feeding regimes may have an effect upon the levels of trace elements such as zinc in the olfactory mucus (anosmia is one symptom of zinc deficiency, Wang *et al.*, 2003a). No metal ions are

artificially introduced during these experiments so any metalloprotein effects would only be seen in the presence of sufficient levels of metal ions in the olfactory environment not removed during dissection and subsequent tissue washes. Specific responses to the presence of metal ions may be more obvious if an external solution of *e.g.* 1mM $ZnCl_2$ was introduced prior to labelling so that each sample has at least this level of metal ions and thus sufficient levels for a minimum number of olfactory receptor proteins that bind metal ions to respond to the absence/presence of EDTA in a manner observable by the dual reagent strategy. Care must be taken to differentiate between metal ion binding effects and any general ionic effects when introducing external ions however low level introduction into ionic buffers such as PBS would be unlikely to cause major ionic strength-related problems.

Levels of metal ions in the overlying mucus as a source of variation is also potentially compounded by the differential use of wash buffers containing EDTA, which may enhance the removal of mucus from tissue samples exposed to it. Experiments were performed using Krebs-Ringer or Krebs-Ringer/EDTA to ensure that as much of the free metal ions or those associated with olfactory proteins was removed as possible. In repeated experiments the pre-labelling tissue wash could be performed using the same buffer to investigate the influence of this source of variability.

One final issue with EDTA is the range of metals that it is capable of chelating. The use of EDTA means that both Zn^{2+} and Cu^{2+} ions are efficiently chelated, however other ions such as Ca^{2+} and Mg^{2+} are also sequestered from free solution (dissociation constants $Mg^{2+}<Ca^{2+}<Zn^{2+}<Ni^{2+}<Cu^{2+}$ - Perrin and Dempsey, 1974). Although these ions are not proposed to have any effect on olfactory receptor

structure they may influence protein stability via indirect effects on cilia membrane stability.

5.4.2 The metalloprotein hypothesis

The metalloprotein hypothesis has been investigated further during this work using cysteine residues as structural markers. It can also be analysed further by looking at olfactory receptor sequences, specifically the evidence of mutational analyses and individual amino acid conservation levels. Wang *et al.* (2003a) reported 70% human olfactory receptor sequences contained the putative metal binding motif. Whilst this statistic lends credence to the metalloprotein hypothesis by suggesting high levels of conservation of this motif, the data leaves two important criteria unaddressed.

First, the use of genomic sequences for this analysis results in the inclusion of pseudogenes *i.e.* sequences that are not expressed and therefore not constrained by the evolutionary selection of useful sequences. This may not have a major impact in mammalian species such as mouse, with an estimated 20% of olfactory receptor sequences thought to be pseudogenes (Young and Trask, 2002) however analysis of human sequences has estimated pseudogene levels of 40-70% (Sharon *et al.*, 1999; Rouquier *et al.*, 2000; Fuchs *et al.*, 2001; Young and Trask, 2002). Therefore, of the 70% quoted as possessing the metal ion binding motif, a significant number are likely to be pseudogenes unless there is selection pressure for the maintenance of this sequence in functional olfactory receptors.

Sequences of olfactory receptors from human chromosome six were acquired from the HORDE database (http://bioinformatics.weizman.ac.il/HORDE), which annotates sequences as pseudogenes or intact sequences according to the occurrence of any in-frame stop codons. The genes from chromosome six were selected for

analysis as this cluster contains a mixture of intact receptor sequences and pseudogenes, with sequences derived from multiple human olfactory receptor (hOR) families and subfamilies. The sequences were analysed for the presence of the putative metal binding motif. If metal binding is an integral part of olfactory receptor function the frequency of this motif in intact genes should be much greater than in pseudogenes, reflecting the high levels of selective pressure to maintain the binding site. The distribution of the motif in intact genes and pseudogenes is shown in Table 5.4.1. There does not appear to be great selection pressure on the maintenance of this motif. Whilst 62% of intact genes contain the metal-binding motif the frequency of the motif in pseudogenes is only 5% lower showing no major selection of the motif in functional sequences. Non-functional receptors are more likely to acquire deleterious mutations and become pseudogenes (Freitag *et al.*, 1999) therefore if the metal binding motif is of major importance in the olfactory process it should have an exaggerated conservation in microsmatic organisms such as humans but should also have a much lower incidence amongst pseudogenes. Studying the pseudogene sequences on chromosome six show that the ratio of sequences with the motif to those without is 1.3:1, much less than would be predicted for residues involved in a key process of odorant reception. The lack of major bias between the frequencies of the metal binding motif in intact genes versus pseudogenes and also within pseudogenes alone suggests that this motif is not under strong selection pressure. This brings into question the importance of metal binding in the primary events of olfaction.

Another key argument to be addressed in the discussion of the metalloprotein hypothesis is that the presence of a metal-binding site is not the only requirement for the shuttlecock mechanism of metal-binding and G protein activation; the

	OR sequences	+ HxxCD/E	- HxxCD/E
Intact genes	35	22	13
Pseudogenes	23	13	10

Table 5.4.1 Analysis of the occurence of the metal binding motif in olfactory receptor sequences from human chromosome six

Human olfactory receptor sequences listed in the on-line HORDE database (http://bioinformatics.weizman.ac.il/HORDE) were examined for the presence of the putative metal ion binding motif. This analysis failed to show any major bias in the occurrence of the putative metal ion binding motif in intact genes *versus* pseudogenes in the 58 olfactory receptor sequences found.on chromosome six.

mechanism is also reliant upon the hydrophobicity values of TM4 and EC2 being similar. In the original paper hydropathy plots were provided for the human olfactory receptor hOR o2d2 and showed that with the single mutation of a glutamate residue to valine (E180V) the EC2 region became more hydrophobic than the preceding transmembrane section (TM4) and at least as likely to adopt a transmembrane position as TM4. The hydropathy plot is reproduced in Figure 5.4.1, the asterisks indicating the changes in hydrophobicity of the TM4 region (remaining constant - left-hand asterisk) and the EC2 loop (hydrophobicity increases - right-hand asterisk) following the E180V *in silico* mutation. Identical analysis of an olfactory receptor sequence from the same subfamily - hOR o2d3 (Figure 5.4.2), indicated that despite this receptor sharing the metal binding motif and at least 60% homology with hOR o2d2, it does not respond similarly to the E180V mutation. This is due to the surrounding amino acids in EC2 showing sufficient variation to no longer have the required levels of hydrophobicity. Subsequent analyses of four members of the olfactory receptor subfamily hOR o2b (Figure 5.4.1), which all contain the HxxCD/E motif, reinforced the notion that this motif may increase the likelihood of interactions between olfactory receptors and metal ions but that this does not mean that the shuttlecock mechanism of G protein activation is automatically applicable to these receptors.

A BLAST search of the hOR o2d2 sequence produced olfactory receptors/fragments of receptors and seven-transmembrane helix receptor, the top four of which did share the E180V structural changes (Figure 5.4.2). However this does not refute a flaw in the statistics of potential metalloprotein receptors where the 70% estimation was arrived at by the analysis of the presence of the putative binding motif.

Figure 5.4.1 Hydropathy plots of different olfactory receptors show that not all proteins containing the putative metal ion binding motif show the same response to the neutralisation of the EC2 glutamate residue

Native sequences: Olfactory receptor sequences were obtained from the HORDE database (http://bioinformatics.weizman.ac.il/HORDE) and analysed using the TMHMM topology prediction tool (www.expasy.org). Receptor sequences analysed are from OR2 D2 (a putative metal binding receptor identified by Wang *et al.*, 2003), OR2 D3 (a member of the same subfamily of human olfactory receptors and four members of the OR2 receptor family but a different subfamily to OR2 D2 (OR2 B2/B9, OR2 B3, OR2 B6, OR2 B8).

E-V Substitutions: Each sequence was mutated *in silico* by an amino acid substitution of the putative metal binding glutamate (E) residue with the uncharged residue valine (V) and re-analysed to observe the effects of glutamate neutralisation on the predicted topology of the receptor proteins.

* Marks the putative TM4 and EC2 regions of the olfactory receptor sequences

Native sequences

E-V substitutions

OR2 D2

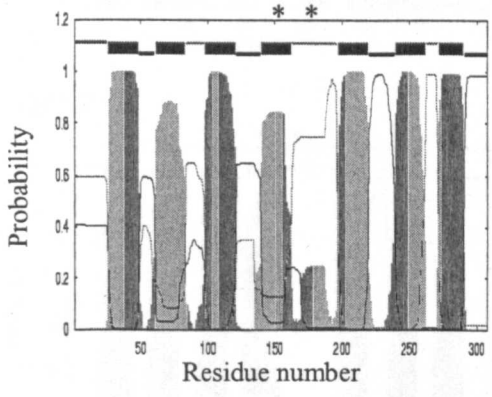

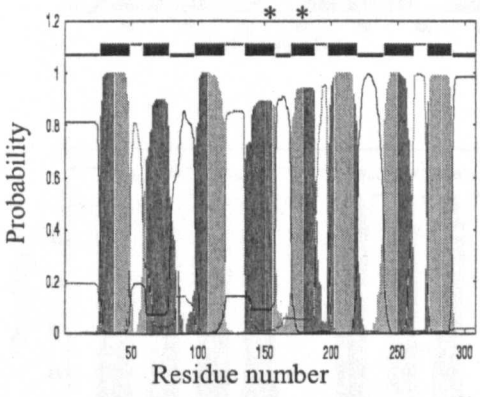

OR2 D3

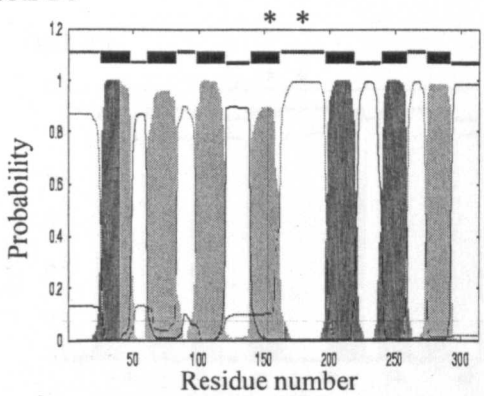

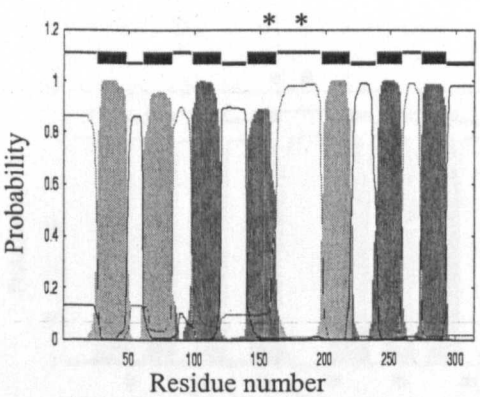

Native sequences

E-V substitutions

OR2 B2/B9

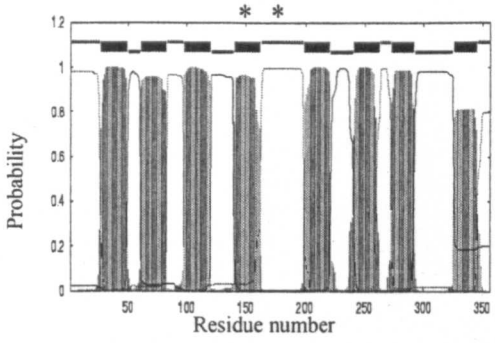

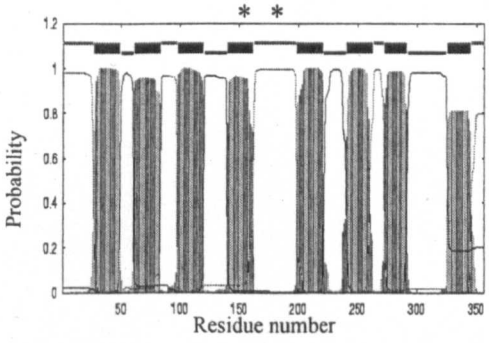

OR2 B3

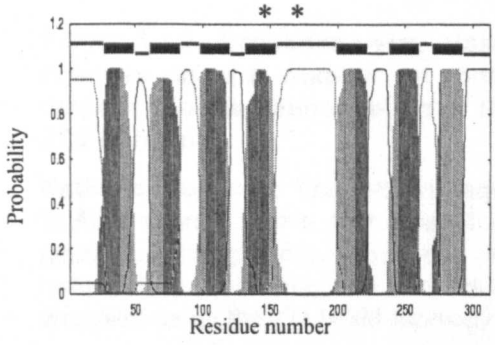

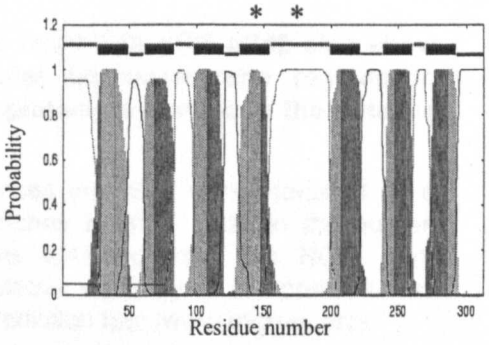

OR2 B6

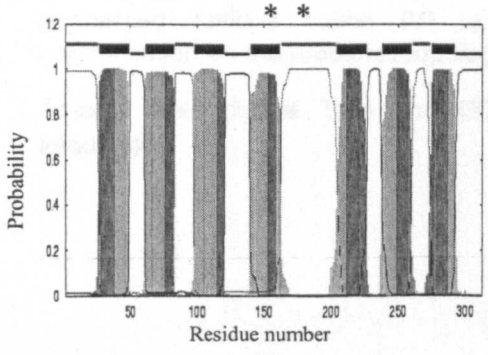

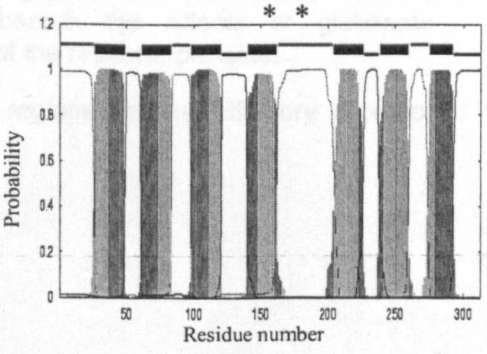

OR2 B8

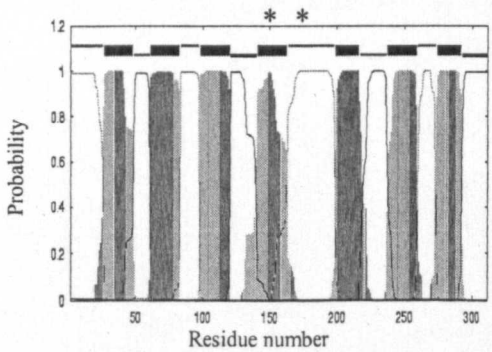

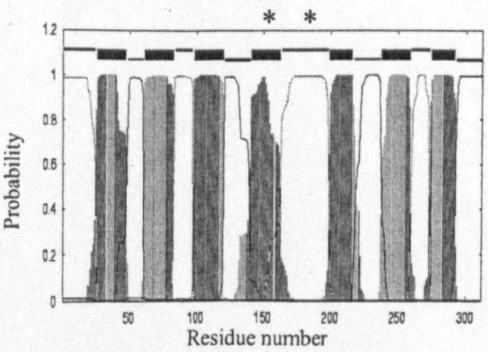

Figure 5.4.2 Sequences very closely related to hOR o2d2 also show changes in the number of potential transmembrane regions in response to the neutralisation of the glutamate residue in the putative EC2 domain

Native sequences: The protein sequences analysed were identified by a BLAST search as the four closest matches to hOR o2d2 in the human genome. The protein sequences were obtained from the NCBI non-redundant protein database and the putative topology of the proteins was analysed using the TM HMM topology prediction tool (www.expasy.org)

E-V Substitutions: Each sequence was then reanalysed with an amino acid substitution of the putative metal binding glutamate (E) residue with the uncharged residue valine (V) to observe the effects of glutamate neutralisation on the predicted topology of the receptor proteins.

*marks the putative TM4 and EC2 regions of the olfactory receptor sequences

Native sequences

E-V substitutions

OR hB2 (NCBI accession: 12007434)

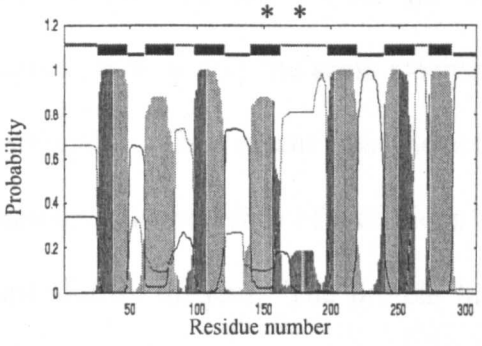

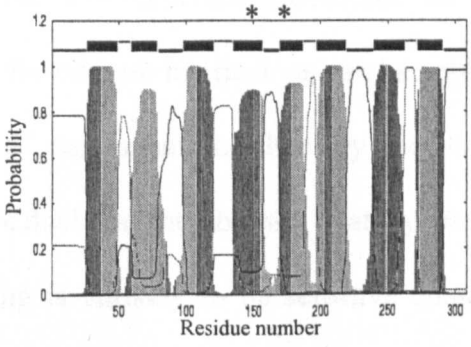

Similar to seven transmembrane helix receptor (NCBI accession: 18605327)

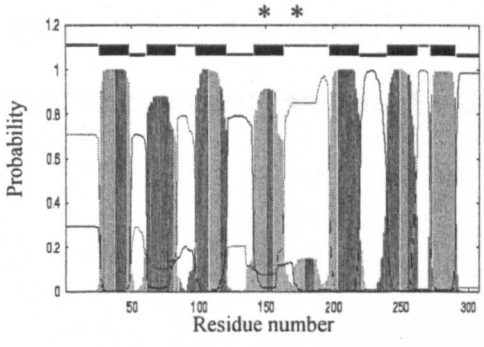

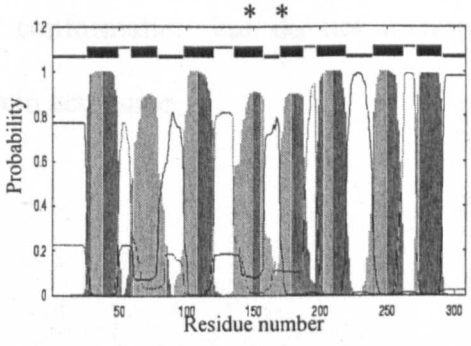

Olfactory receptor (NCBI accession: 3831619)

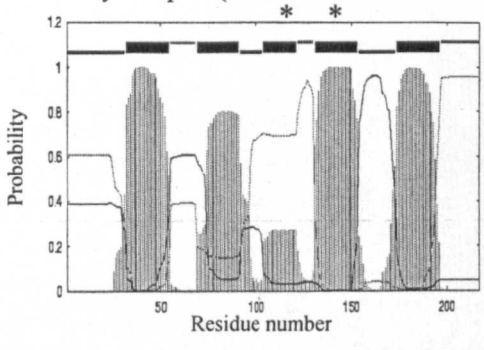

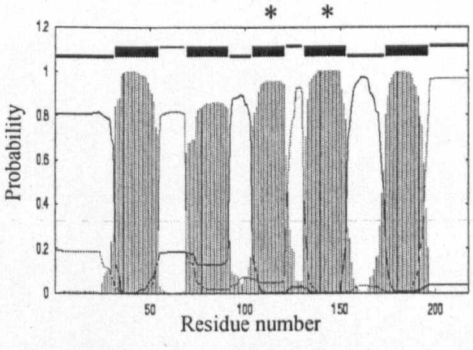

Olfactory receptor (NCBI accession: 1529376)

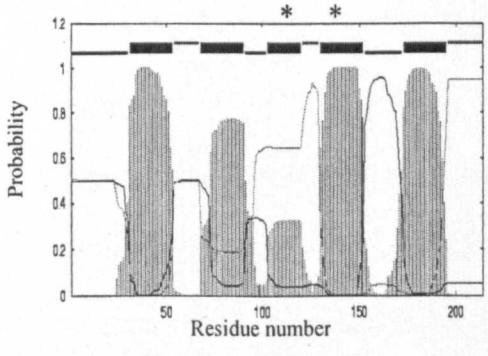

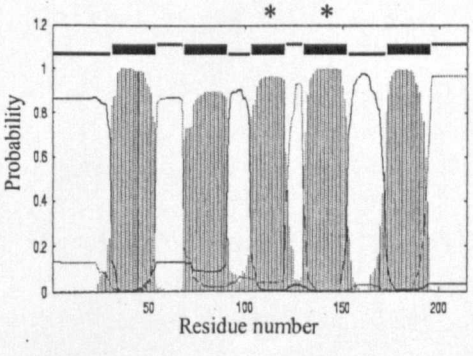

The above arguments call into question the extent and the mechanism by which metal ions may be involved in the primary reception of odorants. Whilst a small number of receptors using metal ions to increase sensitivity to odorants such as thiols would still account for the observed low detection thresholds for these odorants, how widely the same mechanism for odorant interactions can be applied is questionable. This means that detection of movement in olfactory receptors in response to the presence of metal ions by the dual reagent labelling strategy would be tremendously difficult. The protein labelling is unlikely to be sensitive enough to pick up changes in a subset of receptors below the masking effect of the majority of receptors, which may change in tertiary conformation but do not undergo the shuttlecock mechanism proposed for G protein activation.

Chapter 6

GENERAL DISCUSSION AND FURTHER WORK

6.1 Characterisation of the olfactory cilia proteomes of mouse, rat and sheep

Two of the key criteria for a putative thiol sensor protein are localisation to the olfactory cilia and conservation across different mammalian species. The search for thiol sensor candidates reported in this thesis therefore commenced with the characterisation of the olfactory cilia proteomes of three mammalian species, *Mus musculus*, *Rattus norvegicus* and *Ovis aries*. The primary requirement for this study was a reliable method for isolating an enriched cilia fraction from olfactory tissue of the chosen model species. The ability to derive such a preparation from mouse, rat and sheep was established at the beginning of Section 3.3 and the enrichment of cilia proteins was demonstrated using a combination of electron microscopy, biochemical techniques and protein profile comparisons.

The similarities between the olfactory cilia proteomes of the mouse, rat and sheep were assessed in two ways. The first was by comparison of the protein profiles derived from SDS-PAGE and 2D-PAGE separation of cilia preparations. This provided evidence of the major similarities between the protein complements of mouse and rat olfactory cilia, in addition to one area of significant difference. In contrast, the sheep olfactory cilia proteome exhibited little profile similarity with the rat and mouse. These results were as expected given the evolutionary relationships between the species. A continuation of these comparisons was the investigation of the extent of individual protein conservation in olfactory cilia preparations from each of the model species. This thesis reports the only study to date that has addressed the composition of olfactory cilia in terms of its entire protein complement rather than its surface characteristics and investigated the levels of individual protein conservation

across distantly related mammalian species. This study also provided an insight into the main groups of proteins that are required for the maintenance of viable olfactory cilia.

The use of mass spectrometry to identify unknown proteins was applied to observe the similarities and differences in the nature of proteins associated with the olfactory cilia of the model species. Large-scale characterisation of olfactory cilia proteins was not undertaken using mouse tissue due to the low protein yields of cilia preparations. In addition the pronounced profile similarity between the mouse and rat olfactory cilia preparations implied high levels of protein conservation between the two species. Therefore the analysis of protein conservation across the olfactory cilia proteomes of mammalian model species was undertaken using sheep and rat olfactory samples. Identification of individual proteins indicated that the enriched cilia fractions were composed of axonemal proteins, proteins of the cilia cytoplasm and also protein species associated with the external surfaces of the cilia membrane.

6.1.1 Cytoskeletal, cellular detoxification and metabolic proteins dominate the olfactory cilia proteomes of rat and sheep

The significant differences observed between the 2D-PAGE profiles of rat and sheep olfactory cilia were reflected in the protein identifications made during the proteome characterisation study. Less than 50% of proteins identified in rat olfactory cilia were found in the sheep preparation, a figure including proteins present in alternative subtypes. Despite the differences in absolute protein identities in the olfactory cilia proteomes of rat and sheep, the classes of proteins identified in both species did share some similarities. The olfactory cilia proteome was dominated by proteins forming

or associated with the cytoskeleton, cellular stress/detoxification proteins and more surprisingly, metabolic proteins.

The dominance of cytoskeletal proteins was easily predicted by the nature of the cilia preparation *i.e.* an enriched fraction of a cell surface feature reliant upon its internal microtubular axoneme for its physical structure. This preponderance of cytoskeletal proteins in cilia preparations was also demonstrated in a proteomic survey of human bronchial cilia (Ostrowski *et al.*, 2002). This survey of the bronchial cilia proteome also revealed the association of heat shock proteins (HSPs) with the axoneme, in agreement with this study, which indicated the localisation of multiple types of HSPs to the olfactory cilia. The biotransformation and antioxidant machinery/capacity of the olfactory system has been well characterised previously (Nef *et al.*, 1989; Ben-Arie *et al.*, 1993; Reed *et al.*, 2003). Therefore the identification of the second major group of proteins common to rat and sheep olfactory preparations: proteins involved in responses to cellular stress and cell detoxification, was also in line with the current literature. The third group of proteins dominating the olfactory cilia proteomes of rat and sheep provided a much greater surprise – this group of proteins were all primarily involved in cellular metabolism.

Potential secondary roles for the metabolic proteins identified in cilia proteomes

Many of the metabolic proteins identified during the olfactory cilia proteome characterisation are involved in cellular metabolism including glycolysis (enolase), the TCA cycle (malate dehydrogenase) and metabolism of aldehyde compounds. These proteins are certainly not olfactory cilia-specific as were also observed, along with proteins such as transketolase and aldehyde dehydrogenase 3 in rat respiratory cilia preparations. The reason for their abundance in cilia preparations is not yet

clear. From an energy metabolism perspective it is easy to suggest that these proteins are highly expressed in cilia to maximise the production of co-factors required by cellular stress/detoxification proteins *e.g.* ATP and NADH. However, in the cases of enolase and malate dehydrogenase, these enzymes are not the key regulatory sites for their respective pathways and therefore increased levels of these proteins (such that they are detected and identified during 2D-PAGE whilst other enzymes of the same pathway are not) would not lead to an increase the overall energy production capacity. In addition, none of the metabolic proteins identified are directly involved in the production of ATP or NADH (Mathews and van Holde, 1996). In summary, the metabolic capacity of these proteins may not explain their presence in cilia preparations.

The localisation of metabolic enzymes to both rat and sheep olfactory cilia and rat respiratory cilia preparations as indicated by this study suggested secondary roles for these proteins. Two putative secondary roles for these proteins are proposed from comparisons to proteins of the cornea and lens and by the cysteine-labelling experiments described in Chapter 4. The first potential role for the metabolic proteins is to utilise their structural properties in generating a high, stable protein concentration in the cilia and/or applying their catalytic properties to detoxification roles *e.g.* aldehyde dehydrogenase 3 (Cuthbertson *et al.*, 1992; Bilgihan *et al.*, 1998; Pappa *et al.*, 2003). The second proposal stemmed from the observation that enolase, creatine kinase and the non-class 3 aldehyde dehydrogenase subtypes all have exposed cysteine residues derivatised by I-LC-biotin. Given that glutathione forms a major part of the antioxidant capacity of the olfactory cilia and forms mixed disulphide bonds with exposed cysteine residues of local proteins during oxidative stress. It is proposed that these metabolic proteins are localised to the olfactory cilia

to ensure that the glutathione conjugation during oxidative stress does not inhibit the activity of key enzymes *e.g.* those involved in signal transduction, and instead forms disulphide bonds with proteins of less immediate functional importance.

There remains the possibility that these proteins were present in cilia preparations as a result of cytosolic contamination. This issue could be addressed using immunohistochemical techniques to confirm or refute ciliary localisation of these metabolic proteins.

6.2 Cross-species adaptation of mammalian olfactory cilia

During the analyses of mouse, rat and sheep olfactory cilia there were key similarities between the groups of proteins identified but also potentially significant differences. These include the high levels of abundance of annexins in sheep olfactory cilia and a cluster of proteins exclusively observed in mouse olfactory cilia preparations.

Annexin subtypes I, II and V were identified in sheep olfactory cilia preparations. Furthermore the resolution of annexins I and II into multiple distinct proteins spots on a 2D-gel, indicated that they are also present in multiple isoforms. Yet despite the high levels of abundance and presence of multiple subtypes and isoforms in the sheep olfactory cilia, neither annexin I or II were identified in rat olfactory cilia. The presence of annexin I in an enriched cilia preparation is supported by a previous immunohistochemical study in rabbit tracheal epithelium (Mayran *et al.*, 1996). Their presence/absence in sheep and rat preparations indicated a species-specific adaptation of sheep olfactory cilia. Although annexins are known to bind phospholipids in a Ca^{2+}-dependant manner (Burgoyne and Clague, 1994; Schnitzer *et al.*, 1995) and are capable of interactions with actin (Hamre *et al.*, 1995)

the major role of these proteins remains unclear. However from proposed functions for these proteins, the differential localisation/expression of annexins I and II in rat and sheep olfactory cilia could indicate alternative systems for vesicle trafficking and/or endocytosis (Schnitzer *et al.*, 1995; Benz and Hofmann, 1997). In addition, as annexins bind to and are regulated by the Ca^{2+} ions the abundance of these proteins may also be indicative of extra roles/alternative mechanisms for Ca^{2+} homeostasis and Ca^{2+}-mediated odorant adaptation mechanisms in the olfactory cilia (Zufall and Leinders-Zufall, 2000).

The second major species-specific adaptation observed during the analyses of olfactory cilia proteomes from the model species was a cluster of proteins at 75kDa, observed exclusively in mouse olfactory cilia preparations. Two of the spots within this cluster were identified by peptide mass fingerprinting as RIKEN cDNA 5430413K10 (NCBI accession 31982543) and Similar to RIKEN cDNA 5430413K10 (NCBI accession 38075198). The primary sequences of these proteins exhibited extensive homology to two putative pheromone binding proteins RYF3 and vomeromodulin (68% and 71% sequence identity respectively, see Figure 3.3.21) and were therefore defined as members of a novel pheromone binding family of secretory proteins. The presence of highly abundant pheromone binding proteins in close association with the main olfactory system in mice suggested that pheromones play a greater role in the behavioural ecology of mice compared to rats. One possibility is that the efficient detection of pheromones by both the vomeronasal organ and the main olfactory system allows multiple sets of information to be gained from pheromones, creating both hormonal responses (*via* the vomeronasal organ) and conscious behavioural responses (*via* main olfactory system).

6.3 Sensory adaptation of rat olfactory cilia

An additional requirement for putative thiol sensor proteins is that they are specific to the olfactory cilia. Previous studies addressing the sensory adaptation of cilia have utilised monoclonal antibodies (Chen *et al.*, 1986a; Anholt *et al.*, 1990) and various lectins (Chen and Lancet, 1984; Anholt *et al.*, 1986) to highlight protein species present in olfactory but not respiratory cilia. Theses studies tended to utilise amphibian tissue for their comparisons and commonly identified glycosylated proteins at 55kDa and 95kDa. A later immunohistochemical study indicated that 6 out of the 9 lectins used to monitor differential expression of glycoproteins in olfactory *versus* respiratory epithelia (including the commonly used lectins concanavalin A and wheatgerm agglutinin) exhibited no specificity in distribution between the sensory and non-sensory epithelia of the rat nasal cavity (Menco, 1992). The lectin-based approach to the study of sensory adaptation was therefore not pursued during this study. Instead, the comparison of sensory and non-sensory cilia proteomes was performed using gel electrophoresis separation of olfactory and respiratory cilia preparations and protein identification by peptide mass fingerprinting.

The respiratory cilia preparation utilised during these studies was derived from the epithelial lining of the nasal septum. The septal epithelium contains both olfactory and respiratory regions however this preparation was utilised due to its capacity to control for proteins specifically associated with the maintenance of cilia structure in the nasal cavity environment. The use of rat tissue for the sensory/non-sensory cilia comparisons was based upon the ease of dissection and the tissue availability throughout the second year of this work, during which the Foot and Mouth crisis in the UK prohibited the acquisition/dissection of sheep nasal tissue.

6.3.1 Analysis of the rat olfactory and respiratory cilia proteomes

Analysis by 2D-PAGE protein profile comparisons indicated a great deal of similarity between the two cilia preparations, clearly exceeding the percentage of olfactory cilia in the designated respiratory cilia preparations. Therefore in terms of the proteins resolved by 2D-PAGE, the vast majority of proteins associated with olfactory cilia were not specifically involved in sensory processes. This conclusion was reinforced during the identification of proteins from the 2D-PAGE cilia protein separations. The majority of proteins conclusively identified in rat respiratory cilia preparations fell into the same major categories as for the olfactory cilia preparations, once again being dominated by cytoskeletal, cellular stress response and metabolic proteins.

OBPs were consistently detected in respiratory cilia preparations One finding of potential significance was the consistent presence of an odorant binding protein subtype (OBP 1F) associated with respiratory cilia preparations. OBPs are low molecular weight proteins produced in both the Bowman's glands of the lamina propria (underlying the main olfactory epithelium) and the lateral nasal glands (Pevsner *et al.*, 1986). Therefore these proteins are present in the mucus covering both olfactory and respiratory epithelial surfaces (Schultz, 1960; Khew-Goodall *et al.*, 1991). The recurrent isolation of OBPs during cilia enrichment protocols strongly suggested an increased level of interactions between these proteins and the ciliated surface of the respiratory cilia. This observation has implications for the proposed functions of OBPs, which have been attributed various roles including co-stimulation of olfactory receptors, odorant sequestration and removal, facilitating passage of hydrophobic odorants across the mucosal layer (Breer *et al.*, 1994; Pes and Pelosi, 1995; Boudjelal *et al.*, 1996). If OBPs have a greater association with respiratory

cilia than olfactory cilia it implies a non-sensory role for these proteins *i.e.* an odorant clearance function rather than aiding the olfactory detection of selected odorants. Such a non-sensory role was also implied by findings indicating the specific binding of OBP to the respiratory but not olfactory epithelia of the nasal cavity (Boudjelal *et al.*, 1996). However this non-sensory role may be restricted to selected OBP subtypes and a putative role in olfactory reception cannot be ruled out for other OBPs. It is also plausible that this non-sensory role is specific to OBPs in rats. The non-sensory role may also be restricted to the main olfactory system as OBPs may have a volatile binding role in the accessory olfactory system of the vomeronasal organ (VNO). Certainly it is known from gene expression analyses and protein studies that OBPs are synthesised in the VNO glands of the pig (Guiradie *et al.*, 2003).

6.3.2 I-LC-biotin labelling of exposed cysteine residues of the rat olfactory and respiratory cilia

Iodoacetyl-long chain-biotin (I-LC-biotin) is a sulphydryl-targeting reagent that attaches a biotin moiety to any cysteine residues exposed on the surface of a protein and not involved in disulphide linkages. This reagent is membrane-permeable and therefore can pass through the cilia membrane and derivatise intracellular proteins bearing exposed cysteine residues. This was vital for an unbiased search for putative thiol sensor proteins as many thiol odorants are lipophilic and therefore able to cross a membrane to influence intracellular activities. Epithelial tissue was treated with I-LC-biotin and the analysis of biotinylated proteins restricted post-labelling preparation of enriched cilia fractions. Exposure of a protein blot from SDS-

PAGE/2D-PAGE separations using a streptavidin-alkaline phosphatase conjugate subsequently allowed the visualisation of biotin-tagged proteins.

From 2D-PAGE separation of I-LC-biotin labelled cilia preparations of the rat, mouse and sheep two observations were made. The first was that the biotinylation profiles were, with the exception of the cytoskeletal proteins, species-specific and the second was that rat olfactory cilia exhibited markedly fewer cysteine-containing targets for the reagent. This second observation was also true during comparisons of the biotinylation profiles of rat olfactory and rat respiratory cilia preparations. These observations suggested either differential restrictions on the activity of I-LC-biotin or a sensory adaptation of rat olfactory cilia proteins to limit the number of exposed sulphydryl groups. The use of increased levels of I-LC-biotin during the labelling reaction was used to examine these possibilities. The results from these experiments indicated that there were indeed restrictions placed upon I-LC-biotin permeation through the membrane. Most interestingly, the labelling profiles of rat olfactory and respiratory cilia did not share greater overall profile similarity at higher concentrations of I-LC-biotin. This indicated that whilst membrane-permeability may have been a significant factor in the reduced labelling of rat olfactory cilia preparations, the cilia proteins also exhibit differential reactivity to I-LC-biotin. Therefore rat olfactory cilia proteins exhibited sensory adaptation in the number of proteins bearing exposed and reactive cysteine residues. Further work investigating levels of proteins bearing exposed residues in olfactory and respiratory cilia of rat and sheep would allow assessment of the reproducibility and species-specificity of these results.

The final implication of the differential I-LC-biotin labelling patterns observed related to the levels of olfactory cilia contamination in respiratory cilia

preparations. Up to one third of proteins found in cilia preparations derived from the nasal septum originated from regions of olfactory epithelium (see Section 3.3.2). Therefore the differential increase in numbers of labelled proteins and intensity of labelling observed in olfactory cilia preparations following treatment with an increased level of I-LC-biotin indicated two types of adaptation: a non-sensory *versus* sensory adaptation of olfactory cilia proteins compared to respiratory cilia and an adaptation of sensory epithelia located on the nasal turbinates *versus* nasal septum.

Future studies of mammalian olfactory and respiratory cilia should ideally however be pursued using larger mammals such as sheep or cows, which have more clearly demarcated regions of sensory and non-sensory regions of the nasal septum (Nef *et al.*, 1989). This would also allow further investigations into any potential adaptation of the olfactory epithelium located on the nasal septum. Use of larger mammals would also increase the protein yields of individual preparations, aiding protein identification by mass spectrometry. During the characterisation work undertaken in this study, many of the identifications were made from low concentration cilia preparations. Although this did adversely affect the identification of proteins by mass spectrometry, a personal decision was made at the start of this project to minimise the number of animals used and optimise the sensitivity of the mass spectrometry techniques.

6.4 Further requirements for effective characterisation and comparison of olfactory cilia proteomes

The study using I-LC-biotin highlighted a key failing in the methodology employed during the characterisation of olfactory cilia from the model species and rat

respiratory cilia. 2D-PAGE provides an extra dimension for protein separation by gel electrophoresis however it also imposes restrictions upon the representation of certain classes of proteins including membrane proteins (Herbert, 1999). During 2D-PAGE cilia proteome work, no integral plasma membrane proteins were identified, including the notable absence of olfactory receptors in both the rat and sheep olfactory cilia preparations.

One of the major follow-up requirements of this work is the detailed comparison of membrane-associated proteins in olfactory and respiratory cilia as it is here that the primary events of olfaction occur and thus where adaptations of the sensory cilia proteomes are likely to be found. The use of 2D-PAGE ensured maximal protein separation so that identifications could be made by peptide mass fingerprinting – a method that does not tolerate the presence of peptides from multiple proteins. An alternative technique of protein identification is tandem mass spectrometry. Identifications by tandem mass spectrometry are based on the sequences of peptides, rather than the specific combination of peptide masses, making this technique far more applicable to identifications of protein mixtures.

The specific enrichment of membrane proteins by techniques such as sodium carbonate precipitation or detergent partitioning (Bordier *et al.*, 1981; Molloy *et al.*, 2000; Wissing *et al.*, 2000) would simplify the protein preparations by the removal of many of the highly soluble, cytosolic protein, thereby allowing the use of SDS-PAGE. Tandem mass spectrometry allows the analysis of cilia preparations separated by one-dimensional SDS-PAGE, samples that are therefore more likely to contain mixtures of proteins within a single tryptic digest and a greater proportion of membrane proteins than equivalent 2D-PAGE gels. An alternative approach bypassing gel electrophoresis altogether, would involve the tandem mass

spectrometry analysis of direct tryptic digestion of enriched membrane preparations isolated by the above techniques (Blonder *et al.*, 2002).

6.4.1 SDS-PAGE analysis of I-LC-biotin labelled proteins identified olfactory receptors as bearing exposed cysteine residues

SDS-PAGE analysis was applied to I-LC-biotin labelled olfactory cilia preparations and revealed three bands of proteins at 40kDa, 55kDa and 70kDa, common to rat, mouse and sheep. The 70kDa band was comprised of endogeneous biotin-containing proteins/protein subunits and was therefore excluded from further investigation. The 40kDa band was identified by peptide mass fingerprinting as containing beta and gamma subtypes of actin.

The 55kDa band was of key interest as it was the only one of the three conserved bands bearing an external cysteine residue in all the model species. One heavily-biotinylated area of the protein band was also found to be specific to cilia derived from a tissue containing a significant proportion of olfactory epithelia. The 55kDa band, only identified using tandem mass spectrometry contained a mixture of the cytoskeletal proteins α- and β-tubulin and olfactory receptors. This key result was in line with the proposals of a 55kDa species as an olfactory receptor (Fesenko *et al.*, 1988; Boekhoff *et al.*, 1992; Henderson *et al.*, 1992; Nekrasova *et al.*, 1996) and consistent with the involvement of reactive cysteine residues in the odorant binding sites of receptors (Singer *et al.*, 1975; Menevse *et al.*, 1978; Shirley *et al.*, 1983, Wang *et al.*, 2003a). The identification of accessible and potentially reactive cysteine residues on olfactory receptors also means that if the detection of thiol odorants is governed by sulphydryl group interactions it is likely that this involves the traditional receptor-mediated odorant detection mechanism. The identification

and labelling of a protein band containing olfactory receptors also allowed a brief investigation into the metalloprotein hypothesis of olfactory receptor function.

6.5 Are olfactory receptors metalloproteins?

If cysteine residues are involved in the detection of thiol compounds is it as part of a putative metal-binding site (Wang *et al.*, 2003a)? The proposal that olfactory receptors are metalloproteins was addressed in this study, using a combination of membrane-permeable (I-LC-biotin) and impermeable (Lucifer yellow iodoacetamide) reagents to monitor changes in cysteine residue distribution in the presence/absence of divalent metal cations. The results of this investigation were suggestive of an influence of divalent cations on the olfactory receptor structure however the limited experiments performed gave contradictory results and therefore neither confirm nor refute the metalloprotein hypothesis (Wang *et al.*, 2003a). Both experiments however provided evidence of a tentative link between the cysteine labelling of the olfactory receptors and the 40kDa band, identified as containing actin. Such a link may represent evidence of the derivatisation of external cysteine residues of olfactory receptors directly influencing the structure of actin, providing a protein-based mechanism for the putative role of olfactory receptors in neuronal pathfinding (Mombaerts, 1996; Cutforth *et al.*, 2003).

Bioinformatics analysis of the occurrence of the putative metal-binding domains in olfactory receptor proteins questions the extent to which the proposed mechanism of metalloprotein receptor activation would occur *in vivo*. However, as many properties of olfactory signal transduction *e.g.* use of cGMP, expression of multiple olfactory receptors, are restricted to a subset of neurons (Juilfs *et al.*, 1997;

Meyer *et al.*, 2000; Rawson *et al.*, 2000), this does not rule out the possibility that some olfactory receptors require metal ions for odorant binding and activation.

Further studies of the metalloprotein hypothesis would benefit from the cloning and overexpression of olfactory receptors that have the putative metal binding site *e.g.* human olfactory receptor o2d2 (Zhao *et al.*, 1998; Wang *et al.*, 2003a). Experiments monitoring changes in cysteine residue distribution would be more likely to give reproducible results if performed using a single, overexpressed olfactory receptor rather than the mixed population labelled during direct treatment of olfactory tissue.

6.6 The molecular basis of thiol odorant detection in the mammalian olfactory system

The application of proteomics techniques to the investigation of potential mechanisms for the thiol odorant sensitivity observed in mammalian species permitted a relatively unbiased survey of cilia-associated proteins. There were however defined requirements for putative thiol sensor proteins: conservation across the mammalian species investigated, exposed cysteine residues available for high affinity sulphydryl group interactions, specific localisation to the olfactory cilia and a mechanism by which the protein can generate sufficient membrane depolarisation to initiate an action potential in an olfactory receptor neuron (ORN).

The model species used in these experiments provided two degrees of evolutionary relatedness, comparing the olfactory cilia proteomes of the closely related mouse and rat to olfactory cilia preparations from the more distantly related sheep. Of the conserved proteins bearing exposed cysteine residues, aldehyde dehydrogenase was discounted as a putative odorant sensor as it was difficult to

envisage a mechanism for membrane depolarisation following thiol odorant interactions. Cytoskeletal proteins and their exposed cysteine residues were also conserved across the model species. These proteins can influence ion channel activity, therefore they provide a potential mechanism for membrane depolarisation and although they are obviously not specific to sensory cilia, the effects of their derivatisation may be (Maguire *et al.*, 1998). The only other proteins to obey all of the requirements for putative thiol sensor proteins are the traditional olfactory receptors.

The putative roles of non-receptor mediated *versus* receptor-mediated detection of thiol odorants can be addressed by monitoring the stimulation of regions of the olfactory bulb. If thiol odorant detection were receptor-mediated, a defined region of the olfactory bulb would consistently be stimulated during thiol odorant exposure. If however the detection of thiol odorants is non-receptor mediated and therefore governed by a less specific mechanism (*e.g.* involving cytoskeletal proteins), the regions of the olfactory bulb stimulated by thiol odorants may be much wider and less consistent.

The electrophysiology experiments performed by Shirley *et al.* (1983) demonstrated that extracellular cysteine residues are involved in the response to thiol odorants. As the 55kDa band contains the only proteins with external cysteine residues in all model species this study concludes that the most likely protein candidates for thiol odorant detection mediated by cysteine residues are olfactory receptors.

The potential involvement of cysteine residues via formation of putative metal-binding sites has been discussed previously. However it is the author's opinion that protein-based experiments are highly unlikely to identify the individual olfactory

receptor(s) involved in the thiol detection. These specific receptors could however be identified using genetic-based methods. The process would start by the selective isolation/enrichment of ORNs that exhibit measurable electrical responses to thiol odorant exposure. Once multiple thiol-responsive ORNs were obtained, the mRNA from these cells could be harvested. The specific receptors expressed could then be identified by reverse-transcriptase polymerase chain reaction (RT-PCR) using degenerate primers for the highly conserved second and seventh transmembrane regions of olfactory receptor proteins (Buck and Axel, 1991).

6.7 Odorant sensitivity and aversion

If traditional olfactory receptor-mediated pathways are responsible for the detection of thiol odorant compounds, how are the high levels of sensitivity and the aversive responses brought about? One system for increasing odorant sensitivity would be to raise the affinity of the odorant-receptor interaction, increasing the likelihood of an interaction between odorant and receptor even at low concentrations. This could be achieved in the olfactory system using sulphydryl group interactions (between the thiol odorant and an exposed cysteine residue on an olfactory receptor) or by indirect interactions *via* co-ordinate bond formation with a divalent cation bound to an olfactory receptor. An alternative approach to increasing olfactory sensitivity to a given odorant is to increase the number of receptors that can respond to it (Cleland and Linster, 1999; Yee and Wycoski, 2001). If the precise mRNA sequences of thiol-responsive olfactory receptors were obtained, this possibility could be assessed using *in situ* hybridisation to determine the cell-type specificity and expression levels of these proteins.

A crucial requirement for further odorant sensitivity studies is behavioural data on multiple mammalian species specifically indicating thiol detection thresholds and any subsequent threshold for an aversive response. Behavioural experiments could initially investigate the relationship between sensitivity and aversion to a given compound. With respect to thiol odorants, behavioural data on rats and mice could then be related back to the comparative levels of olfactory receptors bearing exposed cysteine residues; allowing the observation of any putative relationships between the levels of these olfactory receptors and differential responses to thiol compounds. A positive, linear correlation between thiol sensitivity and expression levels of putative thiol-responsive olfactory receptors would suggest that thiol odorant sensitivity is governed by the stimulation of increased numbers of olfactory receptors and potentially ORNs. If however, there was no relationship between expression levels of thiol-responsive receptors and thiol sensitivity, it would indicate that sensitivity is the result of increased affinity between the odorant and its receptor.

The causes of odorant aversion are more difficult to assess. Any possible link between odorant sensitivity and aversion could be investigated using behaviour experiments. If the two were linked it would implicate the involvement of the primary events of olfaction in the generation of an aversive response. However it is also possible that the aversive response is significantly modulated by, if not solely a result of higher processing of olfactory signals *e.g.* the targeting of axonal processes from distinct regions of the olfactory bulb to specific regions of the brain such as the hippocampus (Carpenter, 1996). Higher processing of the olfactory signals in the mammalian brain was shown to influence odorant aversion in rats, where studies indicated that animals infected with the parasite *Toxoplasma gondii*, which form parasitic cysts in the brain, lose their innate aversion to predator odour (Berdoy *et al.*,

2000). This hypothesis applied to thiol odorant aversion implies that the conservation of an aversive response across mammalian species confers an evolutionary advantage that can be fully maintained by neuronal processing and therefore may not be related to intrinsic odorant sensitivity.

6.8 Further questions in olfaction research

There are key unanswered questions remaining in the study of olfaction, many of which are broadly applicable to other fields. These include the precise mechanism for the activation of the G protein-coupled signal transduction cascade following odorant binding and the axonal pathfinding mechanism allowing individual ORNs to synapse with predetermined glomeruli.

A volume of research on G protein-coupled receptor (GPCR) function has been performed using deletion mutants and site-directed/oligonucleotide-directed mutagenesis (O'Dowd *et al.*, 1988; Strader *et al.*, 1989; Franke *et al.*, 1992). Additional work has involved cross-linking artificially introduced cysteine residues to restrict intra- or inter-subunit movements (Lee *et al.*, 1995). These techniques could all be applied to the study of olfactory receptor activation and are likely to be most effective if applied to a homogeneous population of cells to maximise the reproducibility of results. Therefore many of the initial experiments are perhaps better performed *in vitro*, before returning to *in situ* ORNs to test any hypotheses/conclusions. In addition to the application of the techniques described above, the use of targeted reagents to monitor changes in the internal and external distribution of selected amino acids such as cysteine could also be used to investigate molecular movements in the presence/absence of metal ions and odorants.

Appendix1 Raw LC-MS/MS data acquired during the analysis of the 70kDa biotinylated band in sheep olfactory cilia preparations

Precursor Ion	Spectra combined	Sequence	*BLAST Identifications* Top hit	PubMed Accession code	Top score	Notes
1132.6434	32:41	LSAADDDVVK	similar to ribosomal protein S10	27662934	22/161	multiple hits for cadherins, neurofibromatosis proteins, olfactory CNG channel and caveolins
1169.6179	42:54	EVHPMNPMSK	similar to brain specific membrane-anchored protein precursor (rat)	27668992	25/21	
1135.5078	78:87	(L)VTYTEAHK	Sfrs4 protein (mouse)	22268151	23/90	
1236.4918	92:97	VNELYDTER	hypothetical protein MGC24132 (human)	22748845	25/28	multiple hits for glutamate receptors (score=24/67)
1199.5458	100:112	(Y)VDGEASK or YVDGHSYR	hypothetical protein XP_288338 (mouse)	28549256	24/67	best hit from the first sequence given
1152.5643	141:147	(PN)HPMNNNSK	hypothetical protein XP_240889 (rat)	27682337	24/37	multiple hits for ATP-binding cassette proteins
977.5031	148:163	EFAGDDAPR	actin (beta or gamma) (human)	4501887	28/206	*multiple hits for actin, mostly beta and gamma isoforms*
1094.5781	171:178	YEELL	voltage-dependant calcium channel alpha 1G subunit isofrom aef (human)	7159263	20/702	multiple hits for calcium channel subunits and isoforms
1164.6105	222:229	LCSELCQR or SESELCQR	*RIKEN cDNA 1300017K07 (mouse)*	27229133	23/90	similar to odorant receptor M3 hit (21/390)
1021.5625	232:241	LLSDSSCK	trypsin (bovine)	18158714	24/37	trypsin autolysis peak
1236.572	251:255	GYAWLLNEPK	mannosidase, alpha, class 1A (human)	24497519	24/67	multiple hits for alpha actinin (rat and human, score=23/89)
1116.5474	256:263	SGSLVQEALGR	Map4k2 (MapKKKK2) (mouse)	6678800	24/49	hits for ATP-binding cassette proteins - mitochondrial membrane proteins
851.6336	264:287	LQLALR	epsin 3 (human)	8923678	21/291	*multiple hits for soluble guanylate cyclase isoforms, protein-tyrosine-phosphatases and Protein P3*
1343.6378	288:298	VEVDEVGAEALGR	haemoglobin beta-A chain (sheep)	70420	37/0.005	haemoglobin definitely present but at 70kDa on gel!!!
1154.5763	304:336	FWSYPDVLK	trypsin chain-A (bovine)	18158714	26/15	hits for vomeronasal receptors (21/390) and a similar to olfactory receptor MOR14-2 (21/523)
1162.6157	337:347	QDTALAPSTMK	actin (beta or gamma) (species including sheep)	11191964	31/0.45	*actin isoform definitely present but at 70kDa on gel?!!*
1138.6066	358:371	(CN)YSVYVYK	similar to histone H2B (mouse/rat)/similar to lysosomal trafficking factor	20874851/20889715	27/4.7	nearly all hits are histone H2B isoforms. Joint top hit also for similar to lysosomal trafficking regulator
1215.5647	372:383	DELFPEQQR	sarcoendoplasmic reticulum Ca2+ ATPase SERCA3a	1438541	25/28	mcf.2 transforming also hit - GEF found in neurons
1199.5984	384:401	NGFNQFMLTK	similar to immunoglobin-like transcript 8 (human/rat)/*hypothetical protein (Macaca fascicularis)*	*27675758/16041082*	*24/37*	*multiple hits for natural killer cell immunoglobin receptor - and p70 killer cell inhibitory receptor*
1181.6221	402:416	LSGLLVYSHK	hypothetical protein XP_297065	29742498	24/50	hits for different olfactory receptors and also serum albumin
1696.3148	417:427	WFGLTNYLR	hypothetical protein XP_297322	29728273	26/15	multiple hits for solute carrier family proteins
945.6148	428:446	QNQFPVGR	similar to histone H2A.1 (rat)	27686403	23/120	region of homology is in transcription repressor domain
1145.7119	447:454	SGLDQMNHLK	actinin alpha 2 (human)/unnamed protein product (mouse)	4501893/12834317	24/37	sequence matched is not in the spectrin repeats region
937.5974	455:461	ELTGFWGK	haemoglobin beta-A chain (sheep)	70420	24/67	additional multiple hits for voltage-gated potassium channels and ATP-binding cassette family proteins
1150.6829	462:468	FAQK				sequence too short to yield information
1192.6381	469:481	(NS)LLYPDGWK	similar to RIKEN cDNA 9330179015 (mouse/rat)	27704778	24/37	
1322.6757	482:494	D/NPQSGVLLPK	hypothetical protein XP_162321 (mouse)	20846327	24/50	carboxylesterase enzymes (both score=21/390)
954.6752	495:521	QVLPGELAK	similar to histone H2B 291B (mouse)	20874851	24/50	hits to similar to lysosomal trafficking factor - score 24/50, same sequence match
1041.6384	522:525	AGLAFTK	Tumor necrosis factor ligand superfamily member 15	21362994	21/390	*multiple hits for voltage-gated sodium channels*
1514.543	526:529	CWGQLDLPLNLSR	unnamed protein product (mouse)	26329551	27/8.4	multiple hits for endothelin receptor subtype B (score=26/15) - very messy spectrum
2164.3538	530:535	LDLLEWFLSASK	hypothetical protein XP_163190 (mouse)	20825982	26/11	no good alignments found - major gap in sequence for top hit
1280.6476	540:564	(NF)ANVSTVLTSK	haemoglobin alpha-1 chain (water buffalo)	*477890*	*36/0.013*	*Globin family proteins - any alternative functions?*
1380.5767	565:574	VSFELNEFAVPK	similar to alpha-macroglobulin (human)	30157920	26/15	multiple hits for peptidyl-prolyl cis-trans isomerase A (score=25/20)
1517.2335	575:600	LNDNLMLLK	peptidase homolog (human)	2653781	25/21	multiple hits for trypsin (scores start at 24/37) - not top score due to I/L substitutions
1499.538	601:611	SNSFMPSNSLFLR	1,3,4,5,6-pentakisphosphate 2-kinase (human)	20548344	27/4.7	multiple hits for solute carrier family proteins
1072.5782	612:637	MFLSFSVLK	hypothetical protein XP_096912 (human)	27483748	24/37	multiple hits for putative pheromone receptor and similar to olfactory receptor (scores from 22/161)
1110.6676	641:645	NEPTF(F)__R	golgi coiled-coil 1 (human)	22208850	24/50	multiple hits for cytochrome P450 family proteins (scores from 21/523)
1509.4938	653:661	HLQGMPANLLFLR	*similar to hypothetical protein MGC28611 (mouse)*/G protein-coupled receptor 43 (human)	27731101/4885333	25/20	joint top hits for putative GPCRs (human) and multiple hits for A-kinase anchor protein (scores from 24/
1094.6033	666:681	ASFLDGVVK	cytoskeletal-associated protein tyrosine phosphatase (human)	18104986	22/217	region of PTP hit is the FERM domain (band 4.1 family of cytoskeletal proteins including ezrin)
1563.457	682:692	TNPMDGNGCSTLWR	similar to peptidylprolyl isomerase D (mouse)	28489567	25/27	hits include macroglobulin proteins
1275.6519	693:732	QVVVYPDYHR	similar to Eukaryotic translation initiation factor 3 subunit 6 interacting protein 6 (human)	17477074	26/11	multiple hits for membrane metalloendopeptidase (scores from 21/389)
1311.6338	737:760	MDVVYALK	Histone H4	32097	30/0.81	multiple hits to GPCRs (scores from 22/161)

REFERENCES

Altschul, S. F., Madden, T. L., Schaffer, A. A., Zhang, J., Zhang, Z., Miller, W., and Lipman, D. J. (1997). Gapped BLAST and PSI-BLAST: a new generation of protein database search programs. Nucleic Acids Res *25*, 3389-3402.

Andersen, K. K., and Bernstein, D. T. (1975). Some chemical constituents of the scent of the striped skunk (*Mephitis mephitis*). J Chem Ecol *1*, 496-499.

Anholt, R. R., Aebi, U., and Snyder, S. H. (1986). A partially purified preparation of isolated chemosensory cilia from the olfactory epithelium of the bullfrog, Rana catesbeiana. J Neurosci *6*, 1962-1969.

Anholt, R. R., Mumby, S. M., Stoffers, D. A., Girard, P. R., Kuo, J. F., and Snyder, S. H. (1987). Transduction proteins of olfactory receptor cells: identification of guanine nucleotide binding proteins and protein kinase C. Biochemistry *26*, 788-795.

Anholt, R. R., Petro, A. E., and Rivers, A. M. (1990). Identification of a group of novel membrane proteins unique to chemosensory cilia of olfactory receptor cells. Biochemistry *29*, 3366-3373.

Archer, J. R., Badakere, S. S., Macey, M. G., and Whelan, M. A. (1995). Use of lucifer yellow iodoacetamide in a flow cytometric assay to measure cell surface free thiol. Biochem Soc Trans *23*, 38S.

Arner, E. J. S., and Holmgren, A. (2000). Physiological functions of thioredoxin and thioredoxin reductase. Eur J Biochem *267*, 6102-6109.

Balijepalli, S., Tirumalai, P. S., Swamy, K. V., Boyd, M. R., Mieyal, J. J., and Ravindranath, V. (1999). Rat brain thioltranferase: regional distribution, immunological characterisation, and localization by fluorescent in situ hybridisation. J Neurochem *72*, 1170-1178.

Banerjee, A., Roach, M. C., Trcka, P., and Luduena, R. F. (1992). Preparation of a monoclonal antibody specific for the class IV isotype of beta-tubulin. Purification and assembly of alpha beta II, alpha beta III, and alpha beta IV tubulin dimers from bovine brain. J Biol Chem *267*, 5625-5630.

Banerjee, A., Roach, M. C., Wall, K. A., Lopata, M. A., Cleveland, D. W., and Luduena, R. F. (1988). A monoclonal antibody against the type II isotype of beta-tubulin. Preparation of isotypically altered tubulin. J Biol Chem *263*, 3029-3034.

Bargmann, C. I. (1997). Olfactory receptors, vomeronasal receptors, and the organization of olfactory information. Cell *90*, 585-587.

Bargmann, C. I., Hartwieg, E., and Horvitz, H. R. (1993). Odorant-selective genes and neurons mediate olfaction in C. elegans. Cell *74*, 515-527.

Bear, M. F., Connors, B. W., and Paradiso, M. A. (2001). Neuroscience - exploring the brain, Second edn (Baltimore, Lippincott Williams and Wilkins).

Becker, W. M., Kleinsmith, L. J., and Hardin, J. (2000). The world of the cell, Addison Wesley LOngman Inc.).

Ben-Arie, N., Khen, M., and Lancet, D. (1993). Glutathione S-transferases in rat olfactory epithelium: purification, molecular properties and odorant biotransformation. Biochem J *292 (Pt 2)*, 379-384.

Benz, J., and Hofmann, A. (1997). Annexins: from structure to function. Biol Chem *378*, 177-183.

Berdoy, M., Webster, J. P., and Macdonald, D. W. (2000). Fatal attraction in rats infected with Toxoplasma gondii. Proc R Soc Lond B Biol Sci *267*, 1591-1594.

Berryman, M., Franck, Z., and Bretscher, A. (1993). Ezrin is concentrated in the apical micorvilli of a wide variety of epithelial cells whereas moesin is found primarily in endothelial cells. J Cell Sci *105*, 1025-1043.

Bignetti E, Cavaggioni A, Pelosi P, Persaud KC, Sorbi RT, Tirindelli R. (1985). Purification and characterisation of an odorant-binding protein from cow nasal tissue. Eur J Biochem *149*, 227-231.

Bilgihan, K., Bilgihan, A., Hasanreisoglu, B., and Turkozkan, N. (1998). Corneal aldehyde dehydrogenase and glutathione S-transferase activity after excimer laser keratectomy in guinea pigs. Br J Opthalmol *82*, 300-302.

Blonder, J., Goshe, M. B., Moore, R. J., Pasa-Tolic, L., Masselon, C. D., Lipton, M. S., and Smith, R. D. (2002). Enrichment of integral membrane proteins for proteomic analysis using liquid chromatography-tandem mass spectrometry. J Proteome Res *1*, 351-360.

Boekhoff, I., Schleicher, S., Strotmann, J., and Breer, H. (1992). Odor-induced phosphorylation of olfactory cilia proteins. Proc Natl Acad Sci U S A *89*, 11983-11987.

Boekhoff, I., Tareilus, E., Strotmann, J., and Breer, H. (1990). Rapid activation of alternative second messenger pathways in olfactory cilia from rats by different odorants. Embo J *9*, 2453-2458.

Boekhoff, I., Touhara, K., Danner, S., Inglese, J., Lohse, M. J., Breer, H., and Lefkowitz, R. J. (1997). Phosducin, potential role in modulation of olfactory signaling. J Biol Chem *272*, 4606-4612.

Bollag, D. M., and Edelstein, S. J. (1991). Protein methods (New York, Wiley-Liss).
Bordier, C. (1981). Phase separation of integral membrane proteins in Triton X-114 solution. J Biol Chem *256*, 1604-1607.

Boudjelal, M., Sivaprasadarao, A., and Findlay, J. B. (1996). Membrane receptor for odour-binding proteins. Biochem J *317 (Pt 1)*, 23-27.

Boyle, A. G., Park, Y. S., Huque, T., and Bruch, R. C. (1987). Properties of phospholipase C in isolated olfactory cilia from the channel catfish (Ictalurus punctatus). Comp Biochem Physiol B *88*, 767-775.

Branden, C., and Tooze, J. (1999). Introduction to protein structure, Second edn (New
York, Garland Publishing Inc).

Breer, H. (1994). Odor recognition and second messenger signaling in olfactory receptor neurons. Semin Cell Biol *5*, 25-32.

Breer, H., Raming, K., and Krieger, J. (1994). Signal recognition and transduction in olfactory neurons. Biochim Biophys Acta *1224*, 277-287.

Broillet, M. C. (2002). Cysteine-nitric oxide interaction and olfactory function. Methods Enzymol *353*, 209-219.

Buck, L., and Axel, R. (1991). A novel multigene family may encode odorant receptors: a molecular basis for odor recognition. Cell *65*, 175-187.

Burden, R. H., Gill, V., and Rice Evans, C. (1990). Active oxygen species and heat shock protein induction. In Stress proteins - induction and function, M. J. Schlesinger,
M. G. Santoro, and E. Garaci, eds. (Berlin, Springer-Verlag).

Burgoyne, R. D., and Clague, M. J. (1994). Annexins in the endocytotic pathway. Trends Biochem Sci *19*, 231-232.

Bustamante, M., Roger, F., Bochaton-Piallat, M.-L., Gabbiani, G., Martin, P.-Y., and Feraille, E. (2003). Regulatory volume increase is associated with p38 kinase-dependant actin cytoskeleton remodelling in rat kidney MTAL. Am J Physiol *285*, F336-F347.

Cao, Y., Oh, B. C., and Stryer, L. (1998). Cloning and localization of two multigene receptor families in goldfish olfactory epithelium. Proc Natl Acad Sci U S A *95*, 11987-11992.

Carpenter, R. H. S. (1996). Neurophysiology, Third edn (London, Arnold).

Carr, V. M., Menco, B. P., Yankova, M. P., Morimoto, R. I., and Farbman, A. I. (2001). Odorants as cell-type specific activators of a heat shock response in the rat olfactory mucosa. J Comp Neurol *432*, 425-439.

Chalansonnet, M., and Chaput, M. A. (1998). Olfactory bulb output cell temporal response patterns to increasing odor concentrations in freely breathing rats. Chem Senses *23*, 1-9.

Chang, L., and Barnett, S. C. (2003). Differentiation potential of the olfactory epithelium in culture. British Neurosci Assoc Abstr *17*, 28.

Chazot, P. L., and Strange, P. G. (1992). Importance of thiol groups in ligand binding to D_2 dopamine receptors from brain and anterior pituitary gland. Biochem J *281*, 377-380.

Chen, Z., and Lancet, D. (1984). Membrane proteins unique to vertebrate olfactory cilia: candidates for sensory receptor molecules. Proc Natl Acad Sci U S A *81*, 1859-1863.

Chen, Z., Ophir, D., and Lancet, D. (1986b). Monoclonal antibodies to ciliary glycoproteins of frog olfactory neurons. Brain Res *368*, 329-338.

Chen, Z., Pace, U., Heldman, J., Shapira, A., and Lancet, D. (1986a). Isolated frog olfactory cilia: a preparation of dendritic membranes from chemosensory neurons. J Neurosci *6*, 2146-2154.

Chen, Z., Pace, U., Ronen, D., and Lancet, D. (1986c). Polypeptide gp95. A unique glycoprotein of olfactory cilia with transmembrane receptor properties. J Biol Chem *261*, 1299-1305.

Chess, A., Simon, I., Cedar, H., and Axel, R. (1994). Allelic inactivation regulates olfactory receptor gene expression. Cell *78*, 823-834.

Clayden, J., Greeves, N., Warren, S., and Wothers, P. (2001). Organic chemistry (Oxford, Oxford University Press).

Cleland, T. A., and Linster, C. (1999). Concentration tuning mediated by spare receptor capacity in olfactory sensory neurons: A theoretical study. Neural Comput *11*, 1673-1690.

Cromarty, S. I., and Derby, C. D. (1997). Multiple excitatory receptor types on individual olfactory neurons: implications for coding of mixtures in the spiny lobster. J Comp Physiol [A] *180*, 481-491.

Cunningham, A. M., Ryugo, D. K., Sharp, A. H., Reed, R. R., Snyder, S. H., and Ronnett, G. V. (1993). Neuronal inositol 1,4,5-trisphosphate receptor localized to the plasma membrane of olfactory cilia. Neuroscience *57*, 339-352.

Cutforth, T., Moring, L., Mendelsohn, M., Nemes, A., Shah, N. M., Kim, M. M., Frisen, J., and Axel, R. (2003). Axonal ephrin-As and odorant receptors: coordinate determination of the olfactory sensory map. Cell *114*, 311-322.

Cuthbertson, R. A., Tomarev, S. I., and Piatigorsky, J. (1992). Taxon-specific recruitment of enzymes as major soluble proteins in the corneal epithelium of three mammals, chicken, and squid. PNAS *89*, 4004-4008.

Dear, T. N., Boehm, T., Keverne, E. B., and Rabbitts, T. H. (1991). Novel genes for potential ligand-binding proteins in subregions of the olfactory mucosa. Embo J *10*, 2813-2819.

Donaldson, J., Pierre, T. S., Minnich, J. L., and Barbeau, A. (1973). Determination of Na + , K + , Mg 2+ , Cu 2+ , Zn 2+ , and Mn 2+ in rat brain regions. Can J Biochem *51*, 87-92.

Duchamp-Viret, P., Duchamp, A., and Chaput, M. A. (2000). Peripheral odor coding in the rat and frog: quality and intensity specification. J Neurosci *20*, 2383-2390.

Duchamp-Viret, P., Duchamp, A., and Chaput, M. A. (2003). Single olfactory sensory neurons simultaneously integrate the components of an odour mixture. Eur J Neurosci *18*, 2690-2696.

Duchamp-Viret, P., Duchamp, A., and Sicard, G. (1990). Olfactory discrimination over a wide concentration range. Comparison of receptor cell and bulb neuron abilities. Brain Res *517*, 256-262.

Dwyer, N. D., Troemel, E. R., Sengupta, P., and Bargmann, C. I. (1998). Odorant receptor localization to olfactory cilia is mediated by ODR-4, a novel membrane-associated protein. Cell *93*, 455-466.

Eisthen, H. L. (2002). Why are olfactory systems of different animals so similar? Brain Behav Evol *59*, 273-293.

Engelman, D. M., and Steitz, T. A. (1981). The spontaneous insertion of proteins into and across membranes: the helical hairpin hypothesis. Cell *23*, 411-422.

Fabbri, E., Ferretti, M. E., Buzzi, M., Cavallaro, R., Vesce, G., and Biondi, C. (1995). Olfactory transduction mechanisms in sheep. Neurochem Res *20*, 719-725.

Falke, J. J., Dernburg, A. F., Sternberg, D. A., Zalkin, N., Milligan, D. L., and Koshland, D. E., Jr. (1988). Structure of a bacterial sensory receptor. A site-directed sulfhydryl study. J Biol Chem *263*, 14850-14858.

Farbman, A. I. (1992). Cell biology of olfaction (Cambridge, Cambridge University Press).

Fatma, N., Singh, D. P., Shinohara, T., and Chylack Jr, L. T. (2001). Transcriptional regulation of the antioxidant protein 2 gene, a thiol-specific antioxidant, by lens

epithelium-derived growth factor to protect cells from oxidative stress. J Biol Chem *276*, 48899-48907.

Feron, F., Mackay-Sim, A., Andrieu, J. L., Matthaei, K. I., Holley, A., and Sicard, G. (1999). Stress induces neurogenesis in non-neuronal cell cultures of adult olfactory epithelium. Neuroscience *88*, 571-583.

Fesenko, E. E., Novoselov, V. I., and Bystrova, M. F. (1988). Properties of odour-binding glycoproteins from rat olfactory epithelium. Biochim Biophys Acta *937*, 369-378.

Finger, T. E., Bottger, B., Hansen, A., Anderson, K. T., Alimohammadi, H., and Silver, W. L. (2003). Solitary chemoreceptor cells in the nasal cavity serve as sentinels of respiration. PNAS *100*, 8981-8986.

Floriano, W. B., Vaidehi, N., Goddard, W. A., 3rd, Singer, M. S., and Shepherd, G. M. (2000). Molecular mechanisms underlying differential odor responses of a mouse olfactory receptor. Proc Natl Acad Sci U S A *97*, 10712-10716.

Fountoulakis, M., and Takacs, B. (2001). Effect of strong detergents and chaotropes on the detection of proteins in two-dimensional gels. Electrophoresis *22*, 1593-1602.

Franke, R. R., Sakmar, T. P., Graham, R. M., and Khorana, H. G. (1992). Structure and function in rhodopsin. Studies of the interaction between the rhodopsin cytoplasmic domain and transducin. J Biol Chem *267*, 14767-14774.

Freitag, J., Beck, A., Ludwig, G., von Buchholtz, L., and Breer, H. (1999). On the origin of the olfactory receptor family: receptor genes of the jawless fish (Lampetra fluviatilis). Gene *226*, 165-174.

Freitag, J., Krieger, J., Strotmann, J., and Breer, H. (1995). Two classes of olfactory receptors in Xenopus laevis. Neuron *15*, 1383-1392.

Friedman, M. (1973). The chemistry and biochemistry of the sulphydryl group in amino acids, peptides and proteins (Oxford, Pergamon Press).

Fuchs, T., Glusman, G., Horn-Saban, S., Lancet, D., and Pilpel, Y. (2001). The human olfactory subgenome: from sequence to structure and evolution. Hum Genet *108*, 1-13.

Fujinaga, J., Tang, X. B., and Casey, J. R. (1999). Topology of the membrane domain of human erythrocyte anion exchange protein, AE1. J Biol Chem *274*, 6626-6633.

Gesteland, R. C., Yancey, R. A., and Farbman, A. I. (1982). Development of olfactory receptor neuron selectivity in the rat fetus. Neuroscience *7*, 3127-3136.

Gibson, A. D., and Garbers, D. L. (2000). Guanylyl cyclases as a family of putative odorant receptors. Annu Rev Neurosci *23*, 417-439.

Gilad, Y., Segre, D., Skorecki, K., Nachman, M. W., Lancet, D., and Sharon, D. (2000). Dichotomy of single-nucleotide polymorphism haplotypes in olfactory receptor genes and pseudogenes. Nat Genet *26*, 221-224.

Giusti, L., Taddei, S., Ceccarelli, F., Chericoni, S., Bigini, G., Lucacchini, A., and Mazzoni, M. R. (2003). Alkylation of sulfhydryl groups on Galpha(s/olf) subunits by N-ethylmaleimide: regulation by guanine nucleotides. Biochim Biophys Acta *1613*, 7-14.

Grill, R. J., Jr., and Pixley, S. K. (1993). 2-Mercaptoethanol is a survival factor for olfactory, cortical and hippocampal neurons in short-term dissociated cell culture. Brain Res *613*, 168-172.

Gudermann, T., Schoneberg, T., and Schultz, G. (1997). Functional and structural complexity of signal transduction via G-protein-coupled receptors. Annu Rev Neurosci *20*, 399-427.

Guiraudie, G., Pageat, P., Cain A-H, Madec, I., and Nagnan-Le Meillour, P. (2003). Functional characterisation of olfactory binding proteins for appeasing compounds and molecular cloning in the vomeronasal organ of pre-pubertal pigs. Chem Senses *28*, 609-619.

Hamre, K. M., Chepenik, K. P., and Goldowitz, D. (1995). The annexins: specific markers of midline structures and sensory neurons in the developing murine central nervous system. J Comp Neurol *352*, 421-435.

Hay, R. W. (1984). Bio-Inorganic Chemistry (Chicester, Ellis Horwood).

Hedin, K. E., Duerson, K., and Clapham, D. E. (1993). Specificity of receptor-G protein interactions: searching for the structure behind the signal. Cell Signal *5*, 505-518.

Henderson, T., Kraevskaya, M., Gregson, N., Gower, D. B., and Bannister, L. H. (1992). Biochemical and ultrastructural characterisation of olfactory receptor membranes of rat and pig, using a novel method of cilium separation. Biochem Soc Trans *20*, 352S.

Herbert, B. (1999). Advances in protein solubilisation for two-dimensional electrophoresis. Electrophoresis *20*, 660-663.

Hildebrand, J. G., and Shepherd, G. M. (1997). Mechanisms of olfactory discrimination: converging evidence for common principles across phyla. Annu Rev Neurosci *20*, 595-631.

Hirose, J., and Kidani, Y. (1990). Thermodynamic and kinetic aspects of metalloenzymes and metalloproteins. In Bioco-ordination chemistry: co-ordination equilibria in biologically-active systems, K. Burger, ed. (New York, Ellis Horwood Ltd.).

Horning, M. S., and Trombley, P. Q. (2001). Zinc and copper influence excitability of rat olfactory bulb neurons by multiple mechanisms. J Neurophysiol *86*, 1652-1660.

Hunt, J. F., Rath, P., Rothschild, K. J., and Engelman, D. M. (1997). Spontaneous, pH-dependent membrane insertion of a transbilayer alpha-helix. Biochemistry *36*, 15177-15192.

Imamura, K., Mataga, N., and Mori, K. (1992). Coding of odor molecules by mitral/tufted cells in rabbit olfactory bulb. I. Aliphatic compounds. J Neurophysiol *68*, 1986-2002.

Juilfs, D. M., Fulle, H. J., Zhao, A. Z., Houslay, M. D., Garbers, D. L., and Beavo, J. A. (1997). A subset of olfactory neurons that selectively express cGMP-stimulated phosphodiesterase (PDE2) and guanylyl cyclase-D define a unique olfactory signal transduction pathway. Proc Natl Acad Sci U S A *94*, 3388-3395.

Kabakov, A. E., and Gabai, V. L. (1997). Heat shock proteins and cryoprotection: ATP-derived mammalian cells (Heidelberg, Springer-Verlag).

Kalomiris, E. L., and Coller, B. S. (1985). Thiol-specific probes indicate that the beta-chain of platelet glycoprotein Ib is a transmembrane protein with a reactive endofacial sulfhydryl group. Biochemistry *24*, 5430-5436.

Kashiwayanagi, M., and Kurihara, K. (1985). Evidence for non-receptor odor discrimination using neuroblastoma cells as a model for olfactory cells. Brain Res *359*, 97-103.

Kast, J., Parker, C. E., van der Drift, K., Dial, J. M., Milgram, S. L., Wilm, M., Howell, M., and Borchers, C. H. (2003). Matrix-assisted laser desorption/ionisation directed nano-electrospray ionization tandem mass spectrometric analysis for protein identification. Rapid commun mass spectrom *17*, 1825-1834.

Katayama, H., Nagasu, T., and Oda, Y. (2001). Improvement of in-gel digestion protocol for peptide mass fingerprinting by matrix-assisted laser desorption/ionization time-of-flight mass spectrometry. Rapid Commun Mass Spectrom *15*, 1416-1421.

Kawai, F. (1999). Odorant suppression of delayed rectifier potassium current in newt olfactory receptor cells. Neurosci Lett *269*, 45-48.

Kawai, J., Shinagawa, A., K., S., Yoshino, M., Itoh, M., Ishii, Y., Arakawa, T., Hara, A., Fukunishi, Y., Konno, H. (2001). Functional annotation of a full-length mouse cDNA collection. Nature *409*, 685-690.

Keller, A., and Margolis, F. L. (1975). Immunological studies of the rat olfactory marker protein. J Neurochem *24*, 1101-1106.

Khew-Goodall, Y., Grillo, M., Getchell, M. L., Danho, W., Getchell, T. V., and Margolis, F. L. (1991). Vomeromodulin, a putative pheromone transporter: cloning, characterization, and cellular localization of a novel glycoprotein of lateral nasal gland. Faseb J *5*, 2976-2982.

Kirkeby, S., Moe, D., Bog-Hansen, T. C., and van Noorden, C. J. (1993). Biotin carboxylases in mitochondria and the cytosol from skeletal and cardiac muscle as detected by avidin binding. Histochemistry *100*, 415-421.

Kirner, A., Deutsch, S., Weiler, E., Polak, E. H., and Apfelbach, R. (2003). Concanavalin A application to the olfactory epithelium reveals different sensory neuron populations for the odour pair D- and L-carvone. Behav Brain Res *138*, 201-206.

Klose, J., Nock, C., Herrmann, M., Stuhler, K., Marcus, K., Bluggel, M., Krause, E., Schalkwyk, L. C., Rastan, S., Brown, S. D. M. (2002). Genetic analysis of the mouse brain proteome. Nat Genet *30*, 385-393.

Kofod, B. (1970). Iron, copper, and zinc in rat brain. Eur J Pharmacol *13*, 40-45.

Kraft, P., Mills, J., and Dratz, E. (2001). Mass spectrometric analysis of cyanogen bromide fragments of integral membrane proteins at the picomole level: application to rhodopsin. Anal Biochem *292*, 76-86.

Krautwurst, D., Yau, K. W., and Reed, R. R. (1998). Identification of ligands for olfactory receptors by functional expression of a receptor library. Cell *95*, 917-926.

Krishna, N. S., Getchell, M. L., Margolis, F. L., and Getchell, T. V. (1995) Differential expression of vomeromodulin and odorant-binding protein, putative pheromone and odorant transporters, in the developing rat nasal chemosensory mucosae. J Neurosci Res *40*, 54-71.

Lancet, D. (1986). Vertebrate olfactory reception. Annu Rev Neurosci *9*, 329-355.

Lane Brown, R., Snow, S. D., and Haley, T. L. (1998). Movement of gating machinery during the activation of rod cyclic nucleotide-gated channels. Biophys J *75*, 825-833.

Lazard, D., Barak, Y., and Lancet, D. (1989). Bovine olfactory cilia preparation: thiol-modulated odorant-sensitive adenylyl cyclase. Biochim Biophys Acta *1013*, 68-72.

Lee, G. F., Lebert, M. R., Lilly, A. A., and Hazelbauer, G. L. (1995). Transmembrane signaling characterized in bacterial chemoreceptors by using sulfhydryl cross-linking in vivo. Proc Natl Acad Sci U S A *92*, 3391-3395.

Levisohn Getchell, M., and Gesteland, R. C. (1972). The chemistry of olfactory reception: stimulus-specific protection from sulphydryl reagent inhibition. PNAS *69*, 1494-1498.

Lindquist, S., and Craig, E. A. (1988). The heat shock proteins. Ann Rev Genetics *22*, 631-677.

Maguire, G., Connaughton, V., Prat, A. G., Jackson, G. R., Jr., and Cantiello, H. F. (1998). Actin cytoskeleton regulates ion channel activity in retinal neurons. Neuroreport *9*, 665-670.

Malnic, B., Hirono, J., Sato, T., and Buck, L. B. (1999). Combinatorial receptor codes for odors. Cell *96*, 713-723.

Margolis, F. L. (1972). A brain protein unique to the olfactory bulb. Proc Natl Acad Sci U S A *69*, 1221-1224.

Marshall, D. A., and Maruniak, J. A. (1986). Masera's organ responds to odorants. Brain Res *366*, 329-332.

Masukawa, L. M., Kauer, J. S., and Shepherd, G. M. (1983). Intracellular recordings from two cell types in an in vitro preparation of the salamander olfactory epithelium. Neurosci Lett *35*, 59-64.

Mathews, C. K., and van Holde, K. E. (1996). Biochemistry, Second edn (Menlo Park, The Benjamin/Cummings Publishing Company, Inc.).

Mayran, N., Traverso, V., Maroux, S., and Massey-Harroche, D. (1996). Cellular and subcellular localizations of annexins I, IV, and VI in lung epithelia. Am J Physiol *270*, L863-L871.

McLean, J. H., and Shipley, M. T. (1992). Neuroanatomical Substrates of Olfaction. In Science of Olfaction, M. J. Serby, and K. L. Chobor, eds. (New York, Springer-Verlag), pp. 126-171.

Meister, A. (1995). Glutathione metabolism. Methods Enzymol *251*, 3-7.

Menco, B. P. (1992). Lectins bind differentially to cilia and microvilli of major and minor cell populations in olfactory and nasal respiratory epithelia. Microsc Res Tech *23*, 181-199.

Menco, B. P., and Farbman, A. I. (1987). Genesis of cilia and microvilli of rat nasal epithelia during prenatal development. III. Respiratory epithelium surface, including a comparison with the surface of the olfactory epithelium. J Anat *152*, 145-160.

Menco, B. P., and Farbman, A. I. (1992). Ultrastructural evidence for multiple mucous domains in frog olfactory epithelium. Cell Tissue Res *270*, 47-56.

Menevse, A., Dodd, G., and Poynder, T. M. (1978). A chemical-modification approach to the olfactory code. Studies with a thiol-specific reagent. Biochem J *176*, 845-854.

Meyer, M. R., Angele, A., Kremmer, E., Kaupp, U. B., and Muller, F. (2000). A cGMP-signaling pathway in a subset of olfactory sensory neurons. Proc Natl Acad Sci U S A *97*, 10595-10600.

Milligan, D. L., and Koshland, D. E., Jr. (1988). Site-directed cross-linking. Establishing the dimeric structure of the aspartate receptor of bacterial chemotaxis. J Biol Chem *263*, 6268-6275.

Molloy, M. P., Herbert, B. R., Slade, M. B., Rabilloud, T., Nouwens, A. S., Williams, K. L., and Gooley, A. A. (2000). Proteomic analysis of the Escherichia coli outer membrane. Eur J Biochem *267*, 2871-2881.

Molloy, M. P., Herbert, B. R., Walsh, B. J., Tyler, M. I., Traini, M., Sanchez, J.-C., Hochstrasser, D. F., Williams, K. L., and Gooley, A. A. (1998). Extraction of membrane proteins by differential solubilization for separation using two-dimensional gel electrophoresis. Electrophoresis *19*, 837-844.

Mombaerts, P. (1999). Seven-transmembrane proteins as odorant and chemosensory receptors. Science *286*, 707-711.

Mombaerts, P., Wang, F., Dulac, C., Chao, S. K., Nemes, A., Mendelsohn, M., Edmondson, J., and Axel, R. (1996). Visualizing an olfactory sensory map. Cell *87*, 675-686.

Mori, K., Nagao, H., and Yoshihara, Y. (1999). The olfactory bulb: coding and processing of odor molecule information. Science *286*, 711-715.

Munger, S. D., Gleeson, R. A., Aldrich, H. C., Rust, N. C., Ache, B. W., and Greenberg, R. M. (2000). Characterization of a phosphoinositide-mediated odor transduction pathway reveals plasma membrane localization of an inositol 1,4, 5-trisphosphate receptor in lobster olfactory receptor neurons. J Biol Chem *275*, 20450-20457.

Nagao, H., Yamaguchi, M., Takahash, Y., and Mori, K. (2002). Grouping and representation of odorant receptors in domains of the olfactory bulb sensory map. Microsc Res Tech *58*, 168-175.

Nef, P., Heldman, J., Lazard, D., Margalit, T., Jaye, M., Hanukoglu, I., and Lancet, D. (1989). Olfactory-specific cytochrome P-450. cDNA cloning of a novel neuroepithelial enzyme possibly involved in chemoreception. J Biol Chem *264*, 6780-6785.

Nekrasova, E., Sosinskaya, A., Natochin, M., Lancet, D., and Gat, U. (1996). Overexpression, solubilization and purification of rat and human olfactory receptors. Eur J Biochem *238*, 28-37.

Ngai, J., Chess, A., Dowling, M. M., Necles, N., Macagno, E. R., and Axel, R. (1993a). Coding of olfactory information: topography of odorant receptor expression in the catfish olfactory epithelium. Cell *72*, 667-680.

Ngai, J., Dowling, M. M., Buck, L., Axel, R., and Chess, A. (1993b). The family of genes encoding odorant receptors in the channel catfish. Cell *72*, 657-666.

Nickell, W. T., and Shipley, M. T. (1992). Neurophysiology of the olfactory bulb. In Science of Olfaction, M. J. Serby, and K. L. Chobor, eds. (New York, Springer-Verlag), pp. 172-212.

Node, M., Kumar, K., Nishide, K., Ohsugi, S., and Miyamoto, T. (2001). Odorless substitutes for foul-smelling thiols: syntheses and applications. Tetrahedron Lett *42*, 9207-9210.

Nomura, T., and Kurihara, K. (1987). Liposomes as a model for olfactory cells: changes in membrane potential in response to various odorants. Biochemistry *26*, 6135-6140.

Nover, L., Neumann, D., and Scharf, K.-D. (1991). Intracellular localisation and related functions of heat shock proteins. In Heat shock proteins, L. Nover, ed. (CRC Press Inc).

Novoselov, S. V., Peshenko, I. V., Popov, V. I., Novoselov, V. I., Bystrova, M. F., Evdokimov, V. J., Kamzalov, S. S., Merkulova, M. I., Shuvaeva, T. M., Lipkin, V. M., and Fesenko, E. E. (1999). Localization of 28-kDa peroxredoxin in rat epithelial tissues and its antioxidant properties. Cell Tissue Res *298*, 471-480.

O'Dowd, B. F., Hnatowich, M., Regan, J. W., Leader, W. M., Caron, M. G., and Lefkowitz, R. J. (1988). Site-directed mutagenesis of the cytoplasmic domains of the human beta 2-adrenergic receptor. Localization of regions involved in G protein-receptor coupling. J Biol Chem *263*, 15985-15992.

Olivieri, E., Herbert, B., and Righetti, P. G. (2001). The effect of protease inhibitors on the two-dimensional electrophoresis pattern of red blood cell membranes. Electrophoresis *22*, 560-565.

Onoda, N. (1992). Odor-induced fos-like immunoreactivity in the rat olfactory bulb. Neurosci Lett *137*, 157-160.

Ostrowski, L. E., Blackburn, K., Radde, K. M., Moyer, M. B., Schlatzer, D. M., Moseley, A., and Boucher, R. C. (2002). A proteomic analysis of human cilia. Mol Cell Proteomics *1*, 451-465.

Pace, U., Hanski, E., Salomon, Y., and Lancet, D. (1985). Odorant-sensitive adenylate cyclase may mediate olfactory reception. Nature *316*, 255-258.

Pappa, A., Estey, T., Manzer, R., Brown, D., and Vasiliou, V. (2003). Human aldehyde dehydrogenase 3A1 (ALDH3A1): biochemical characterization and immunohistochemical localization in the cornes. Biochem J *376*, 615-623.

Pasquali, C., Fialka, I., and Huber, L. A. (1997). Preparative two-dimensional gel electrophoresis of membrane proteins. Electrophoresis *18*, 2573-2581.

Pause, B. M., Sojka, B., and Ferstl, R. (1997). Central processing of odor concentration is a temporal phenomenon as revealed by chemosensory event-related potentials. Chem Senses *22*, 9-26.

Pelosi, P., Baldaccini, N. E., and Pisanelli, A. M. (1982). Identification of a specific olfactory receptor for 2-isobutyl-3-methoxypyrazine. Biochem J *201*, 245-248.

Pes, D., and Pelosi, P. (1995). Odorant-binding proteins of the mouse. Comp Biochem Physiol B Biochem Mol Biol *112*, 471-479.

Peshenko, I. V., Novoselov, V. I., Evdokimov, V. A., Nikolaev, Y. V., Kamzalov, S. S., Shuvaeva, T. M., Lipkin, V. M., and Fesenko, E. E. (1998). Identification of a 28 kDa secretory protein from rat olfactory epithelium as a thiol-specific antioxidant. Free Radic Biol Med *25*, 654-659.

Pevsner, J., Sklar, P. B., Hwang, P. M., and Snyder, S. H. (1989). Odorant binding protein: sequence analysis and localization suggest an odorant transport function. In Chemical Senses: Receptor Events and Transduction in Taste and Olfaction, J. G. Brand, J. H. Teeter, R. H. Cagan, and M. R. Kare, eds.

Pevsner, J., Sklar, P. B., and Snyder, S. H. (1986). Odorant-binding protein: localization to nasal glands and secretions. Proc Natl Acad Sci U S A *83*, 4942-4946.

Pevsner, J., Trifiletti, R. R., Strittmatter, S. M., and Snyder, S. H. (1985). Isolation and characterization of an olfactory receptor protein for odorant pyrazines. Proc Natl Acad Sci U S A *82*, 3050-3054.

Pilpel, Y., and Lancet, D. (1999). The variable and conserved interfaces of modeled olfactory receptor proteins. Protein Sci *8*, 969-977.

Poutanen, M., Salusjarvi, L., Ruohonen, L., Penttila, M., and Kalkkinen, N. (2001). Use of matrix-assisted laser desorption/ionization time-of-flight mass mapping and nanospray liquid chromatography/electrospray ioinization tandem mass spectrometry sequence tag analysis for high sensitivity identification of yeast proteins separated by two-dimensional gel electrophoresis. Rapid commun mass spectrom *15*, 1685-1692.

Rabilloud, T., Blisnick, T., Heller, M., Luche, S., Aebersold, R., Lunardi, J., and Braun-Breton, C. (1999). Analysis of membrane proteins by two-dimensional electrophoresis: comparison of the proteins extracted from normal or *Plasmodium falciparum*-infected erythrocyte ghosts. Electrophoresis *20*, 3603-3610.

Raming, K., Krieger, J., Strotmann, J., Boekhoff, I., Kubick, S., Baumstark, C., and Breer, H. (1993). Cloning and expression of odorant receptors. Nature *361*, 353-356.
Rankin, M. L., Alvania, R. S., Gleason, E. L., and Bruch, R. C. (1999). Internalization of G protein-coupled receptors in single olfactory receptor neurons. J Neurochem *72*, 541-548.

Rawson, N. E., Eberwine, J., Dotson, R., Jackson, J., Ulrich, P., and Restrepo, D. (2000). Expression of mRNAs encoding for two different olfactory receptors in a subset of olfactory receptor neurons. J Neurochem *75*, 185-195.

Rawson, N. E., and Gomez, G. (2002). Cell and molecular biology of human olfaction. Microsc Res Tech *58*, 142-151.

Reed, C. J., Robinson, D. A., and Lock, E. A. (2003). Antioxidant status of the rat nasal cavity. Free Radic Biol Med *34*, 607-615.

Reed, R. R. (1992). Mechanisms of sensitivity and specificity in olfaction. Cold Spring Harb Symp Quant Biol *57*, 501-504.

Reisert, J., and Matthews, H. R. (2001). Response properties of isolated mouse olfactory receptor cells. J Physiol *530*, 113-122.

Ressler, K. J., Sullivan, S. L., and Buck, L. B. (1994). Information coding in the olfactory system: evidence for a stereotyped and highly organized epitope map in the olfactory bulb. Cell *79*, 1245-1255.

Rhein, L. D., and Cagan, R. H. (1980). Biochemical studies of olfaction: isolation, characterization, and odorant binding activity of cilia from rainbow trout olfactory rosettes. Proc Natl Acad Sci U S A *77*, 4412-4416.

Rhodin, J. A. G. (1974). Histology: a text and atlas (Oxford, Oxford University Press).

Ronnett, G. V., Cho, H., Hester, L. D., Wood, S. F., and Snyder, S. H. (1993). Odorants differentially enhance phosphoinositide turnover and adenylyl cyclase in olfactory receptor neuronal cultures. J Neurosci *13*, 1751-1758.

Rouquier, S., Blancher, A., and Giorgi, D. (2000). The olfactory receptor gene repertoire in primates and mouse: evidence for reduction of the functional fraction in primates. Proc Natl Acad Sci U S A *97*, 2870-2874.

Royal, S. J., and Key, B. (1999). Development of P2 olfactory glomeruli in P2-internal ribosome entry site-tau-LacZ transgenic mice. J Neurosci *19*, 9856-9864.

Rubin, B. D., and Katz, L. C. (1999). Optical imaging of odorant representations in the mammalian olfactory bulb. Neuron *23*, 499-511.

Sanhueza, M., and Bacigalupo, J. (1999). Odor suppression of voltage-gated currents contributes to the odor-induced response in olfactory neurons. Am J Physiol *277*, C1086-1099.

Sanhueza, M., Schmachtenberg, O., and Bacigalupo, J. (2000). Excitation, inhibition, and suppression by odors in isolated toad and rat olfactory receptor neurons. Am J Physiol Cell Physiol *279*, C31-39.

Santoni, V., Molloy, M., and Rabilloud, T. (2000). Membrane proteins and proteomics: un amour impossible? Electrophoresis *21*, 1054-1070.

Sax, C. M., Salamon, C., Kays, W. T., Guo, J., Yu, F. X., Cuthbertson, R. A., and Piatigorsky, J. (1996). Transketolase is a major protein in the mouse cornea. J Biol Chem *271*, 33568-33574.

Schandar, M., Laugwitz, K. L., Boekhoff, I., Kroner, C., Gudermann, T., Schultz, G., and Breer, H. (1998). Odorants selectively activate distinct G protein subtypes in olfactory cilia. J Biol Chem *273*, 16669-16677.

Schild, D., and Restrepo, D. (1998). Transduction mechanisms in vertebrate olfactory receptor cells. Physiol Rev *78*, 429-466.

Schnitzer, J. E., Liu, J., and Oh, P. (1995). Endothelial caveolae have the molecular transport machinery for vesicle budding, docking, and fusion including VAMP, NSF, SNAP, annexins and GTPases. J Biol Chem *270*, 14399-14404.

Schreiber, S., Fleischer, J., Breer, H., and Boekhoff, I. (2000). A possible role for caveolin as a signaling organizer in olfactory sensory membranes. J Biol Chem *275*, 24115-24123.

Schultz, E. W. (1960). Repair of the olfactory mucosa with special reference to regeneration of olfactory cells (sensory neurons). Am J Pathol *37*, 1-19.

Schwartz Levey, M., Chikaraishi, D. M., and Kauer, J. S. (1991). Characterization of potential precursor populations in the mouse olfactory epithelium using immunocytochemistry and autoradiography. J Neurosci *11*, 3556-3564.

Schwob, J. E., Szumowski, K. E., and Stasky, A. A. (1992). Olfactory sensory neurons are trophically dependent on the olfactory bulb for their prolonged survival. J Neurosci *12*, 3896-3919.

Seebungkert, B., and Lynch, J. W. (2001). A common inhibitory binding site for zinc and odorants at the voltage-gated K(+) channel of rat olfactory receptor neurons. Eur J Neurosci *14*, 353-362.

Sharon, D., Glusman, G., Pilpel, Y., Khen, M., Gruetzner, F., Haaf, T., and Lancet, D. (1999). Primate evolution of an olfactory receptor cluster: diversification by gene conversion and recent emergence of pseudogenes. Genomics *61*, 24-36.

Shevchenko, A., Sunyaev, S., Loboda, A., Shevchenko, A., Bork, P., Ens, W., and Standing, K. G. (2001). Charting the proteomes of organisms with unsequenced genomes by MALDI-quadrupole time-of-flight mass spectrometry and BLAST homology searching. Anal Chem *73*, 1917-1926.

Shirley, S., Polak, E., and Dodd, G. H. (1983). Chemical-modification studies on rat olfactory mucosa using a thiol-specific reagent and enzymatic iodination. Eur J Biochem *132*, 485-494.

Shirley, S. G., Polak, E. H., Edwards, D. A., Wood, M. A., and Dodd, G. H. (1987a). The effect of concanavalin A on the rat electro-olfactogram at various odorant concentrations. Biochem J *245*, 185-189.

Shirley, S. G., Polak, E. H., Mather, R. A., and Dodd, G. H. (1987b). The effect of concanavalin A on the rat electro-olfactogram. Differential inhibition of odorant response. Biochem J *245*, 175-184.

Singer, G., Rozental, J. M., and Norris, D. M. (1975). Sulphydryl groups and the quinone receptor in insect olfaction and gustation. Nature *256*, 222-223.

Singer, M. S. (2000). Analysis of the molecular basis for octanal interactions in the expressed rat 17 olfactory receptor. Chem Senses *25*, 155-165.

Singer, M. S., Oliveira, L., Vriend, G., and Shepherd, G. M. (1995). Potential ligand-binding residues in rat olfactory receptors identified by correlated mutation analysis. Receptors Channels *3*, 89-95.

Singer, M. S., Weisinger-Lewin, Y., Lancet, D., and Shepherd, G. M. (1996). Positive selection moments identify potential functional residues in human olfactory receptors. Receptors Channels *4*, 141-147.

Sklar, P. B., Anholt, R. R., and Snyder, S. H. (1986). The odorant-sensitive adenylate cyclase of olfactory receptor cells. Differential stimulation by distinct classes of odorants. J Biol Chem *261*, 15538-15543.

Sleigh, M. A. (1962). The biology of cilia and flagella (Oxford, Pergamon).

Stein, J. F. (1982). An introduction to neurophysiology (Oxford, Blackwell Scientific).

Stewart, W. B., Kauer, J. S., and Shepherd, G. M. (1979). Functional organization of rat olfactory bulb analysed by the 2-deoxyglucose method. J Comp Neurol *185*, 715-734.

Strader, C. D., Sigal, I. S., and Dixon, R. A. (1989). Structural basis of beta-adrenergic receptor function. Faseb J *3*, 1825-1832.

Strausberg, R. L., Feingold, E. A., Grouse, L. H., Derge, J. G., Klausner, R. D., Collins, F. S., Wagner, L., Shenmen, C. M., Schuler, G. D., Altschul, S. F. (2002). Generation and initial analysis of more than 15,000 full-length human and mouse cDNA sequences. Proc Natl Acad Sci U S A *99*, 16899-16903.

Strotmann, J., Wanner, I., Helfrich, T., Beck, A., Meinken, C., Kubick, S., and Breer, H. (1994). Olfactory neurones expressing distinct odorant receptor subtypes are spatially segregated in the nasal neuroepithelium. Cell Tissue Res *276*, 429-438.

Sung, Y. K., Moon, C., Yoo, J. Y., Pearse, D., Pevsner, J., and Ronnett, G. V. (2002). Plunc, a member of the secretory gland protein family, is up-regulated in nasal respiratory epithelium after olfactory bulbectomy. J Biol Chem *277*, 12762-12769.

Suzuki, Y., Takeda, M., Obara, N., Suzuki, N., and Takeichi, N. (2000). Olfactory epithelium consisting of supporting cells and horizontal basal cells in the posterior nasal cavity of mice. Cell Tissue Res *299*, 313-325.

Tang, X. B., Fujinaga, J., Kopito, R., and Casey, J. R. (1998). Topology of the region surrounding Glu681 of human AE1 protein, the erythrocyte anion exchanger. J Biol Chem *273*, 22545-22553.

Tareilus, E., Noe, J., and Breer, H. (1995). Calcium signals in olfactory neurons. Biochim Biophys Acta *1269*, 129-138.

Theimer, E. T., Yoshida, T., and Klaiber, E. M. (1977). Olfaction and molecular shape. Chirality as a requisite for odor. J Agric Food Chem *25*, 1168-1177.
Thornton-Manning, J. R., and Dahl, A. R. (1997). Metabolic capacity of nasal tissue interspecies comparisons of xenobiotic-metabolizing enzymes. Mutation Res *380*, 43-59.

Torchinsky, Y. M. (1981). Sulfur in proteins (Oxford, Pergamon).

Turin, L. (1996). A spectroscopic mechanism for primary olfactory reception. Chem Senses *21*, 773-791.

Uchida, N., Takahashi, Y. K., Tanifuji, M., and Mori, K. (2000). Odor maps in the mammalian olfactory bulb: domain organization and odorant structural features. Nat Neurosci *3*, 1035-1043.

van Houten, J. (2000). Chemoreception in microorganisms. In The neurobiology of taste and smell, T. E. Finger, J. Silver, and D. Restrepo, eds. (New York, Wiley-Liss, Inc.).

van Montfort, B. A., Canas, B., Duurkens, R., Godovac-Zimmermann, J., and Robillard, G. T. (2002a). Improved in-gel approaches to generate peptide maps of integral membrane proteins with matrix-assisted laser desorption/ionization time-of-flight mass spectrometry. J Mass Spectrom *37*, 322-330.

van Montfort, B. A., Doeven, M. K., Canas, B., Veenhoff, L. M., Poolman, B., and Robillard, G. T. (2002b). Combined in-gel tryptic digestion and CNBr cleavage for the generation of peptide maps of an integral membrane protein with MALDI-TOF mass spectrometry. Biochim Biophys Acta *1555*, 111-115.

Vassar, R., Chao, S. K., Sitcheran, R., Nunez, J. M., Vosshall, L. B., and Axel, R. (1994). Topographic organization of sensory projections to the olfactory bulb. Cell *79*, 981-991.

Vassar, R., Ngai, J., and Axel, R. (1993). Spatial segregation of odorant receptor expression in the mammalian olfactory epithelium. Cell *74*, 309-318.

Verrills, N. M., Harry, J. H., Walsh, B. J., Hains, P. G., and Robinson, E. S. (2000). Cross-matching marsupial proteins with eutherian mammal databases: proteome analysis of cells from UV-induced skin tumours of an opposum (*Monodelphis domestica*). Electrophoresis *21*, 3810-3822.

Villet, R. H. (1974). Involvement of amino and sulphydryl groups in olfactory transduction in silk moths. Nature *248*, 707-709.

Wang, J., Luthey-Schulten, Z. A., and Suslick, K. S. (2003a). Is the olfactory receptor a metalloprotein? Proc Natl Acad Sci U S A *100*, 3035-3039.

Wang, X., Phelan, S. A., Forsman-Semb, K., Taylor, E. F., Petros, C., Brown, A., Lerner, C. P., and Paigen, B. (2003b). Mice with targeted mutation of peroxiredoxin 6 develop normally but are susceptible to oxidative stress. J Biol Chem *278*, 25179-25190.

Weiler, E., and Farbman, A. I. (2003). The septal organ of the rat during postnatal development. Chem Senses *28*, 581-593.

Weston, T. (1985). Atlas of anatomy (Marshall Cavendish Books Ltd.)

Williams, N. E., and Nelson, E. M. (1997). HSP70 and HSP90 homologs are associated with tubulin in hetero-oligomeric complexes, cilia and the cortex of *Tetrahymena*. J Cell Sci *110*, 1665-1672.

Wissing, J., Heim, S., Flohe, L., Bilitewski, U., and Frank, R. (2000). Enrichment of hydrophobic proteins via Triton X-114 phase partitioning and hydroxyapatite column chromatography for mass spectrometry. Electrophoresis *21*, 2589-2593.

Wong, S. T. (2000). Disruption of the Type II Adenylyl Cyclase Gene Leads to Peripheral and Behavioral Anosmia in Transgenic Mice. Neuron *27*, 487-497.

Woo, K., Jenson-Smith, H. C., Luduena, R. F., and Hallworth, R. (2002). Differential synthesis of beta-tubulin isotypes in gerbil nasal epithelia. Cell Tissue Res *309*, 331-335.

Wright, R. H. (1982). The sense of smell (Boca Raton, CRC Press Inc.).

Yee, K. K., and Wysocki, C. J. (2001). Odorant exposure increases olfactory sensitivity: olfactory epithelium is implicated. Physiol Behav *72*, 705-711.

Yokoi, M., Mori, K., and Nakanishi, S. (1995). Refinement of odor molecule tuning by dendrodendritic synaptic inhibition in the olfactory bulb. Proc Natl Acad Sci U S A *92*, 3371-3375.

Yoshihara, Y., and Mori, K. (1997). Basic principles and molecular mechanisms of olfactory axon pathfinding. Cell Tissue Res *290*, 457-463.

Young, J. M., and Trask, B. J. (2002). The sense of smell: genomics of vertebrate odorant receptors. Hum Mol Genet *11*, 1153-1160.

Zhang, Y., Chou, J. H., Bradley, J., Bargmann, C. I., and Zinn, K. (1997). The Caenorhabditis elegans seven-transmembrane protein ODR-10 functions as an odorant receptor in mammalian cells. Proc Natl Acad Sci U S A *94*, 12162-12167.

Zhao, H., Ivic, L., Otaki, J. M., Hashimoto, M., Mikoshiba, K., and Firestein, S. (1998). Functional expression of a mammalian odorant receptor. Science *279*, 237-242.

Zufall, F., and Leinders-Zufall, T. (2000). The cellular and molecular basis of odor adaptation. Chem Senses *25*, 473-481.

Zufall, F., and Munger, S. D. (2001). From odor and pheromone transduction to the organization of the sense of smell. Trends Neurosci *24*, 191-193.